Universidade de São Paulo
Instituto de Física

Estatística de calor e trabalho em modelos colisionais

Marcelo Janovitch Broinizi Pereira

Orientador: Prof. Dr. Gabriel Teixeira Landi

Dissertação de mestrado apresentada ao Instituto de Física da Universidade de São Paulo, como requisito parcial para a obtenção do título de Mestre em Ciências.

Banca Examinadora:
Prof. Dr. Gabriel Teixeira Landi - Instituto de Física da Universidade de São Paulo
Prof. Dr. Gabriel Horácio Aguilar - Instituto de Física da Universidade Federal do Rio de Janeiro
Prof. Dr. Rafael Chaves Souto Araujo - International Institute of Physics, Universidade Federal do Rio Grande do Norte

São Paulo
2020

University of São Paulo
Physics Institute

Statistics of heat and work in collisional models

Marcelo Janovitch Broinizi Pereira

Supervisor: Prof. Dr. Gabriel Teixeira Landi

Dissertation submitted to the Physics Institute of the University of São Paulo in partial fulfillment of the requirements for the degree of Master of Science.

Examining Committee:
Prof. Dr. Gabriel Teixeira Landi - Physics Institute of the University of São Paulo
Prof. Dr. Gabriel Horácio Aguilar- Physics Institue of the Federal University of Rio de Janeiro
Prof. Dr. Rafael Chaves Souto Araujo - International Institute of Physics, Federal University of Rio Grande do Norte

São Paulo
2020

DADOS PARA FICHA CATALOGRÁFICA DE TESES E DISSERTAÇÕES

Área do Conhecimento (CAPES): Ciencias Exatas e da Terra

(consulte: http://www.cnpq.br/documents/10157/186158/TabeladeAreasdoConhecimento.pdf)

Autor (nome completo): Marcelo Janovitch Broinizi Pereirs

e-mail: marcelobro.pera@gmail.com

Título da Tese: Statistics of heat and work in collisional models

Ano: 2021 **Mestrado:(** X **)** **Doutorado:(** **)**

Orientador(a): Prof. Gabriel Teixeiira Landi

Departamento: Fisica dos Materiais e Mecanica

Área de Concentração: Física - Termodinâmica Quântica

Unitermos(Assunto): Calor; Informação Quântica; Termodinâmica

(indique no mínimo 3 e no máximo 5 termos, consulte o vocabulário controlado em http://143.107.154.62/Vocab/Sibix652.dll/Index)

Instruções:

1. **Preencha o formulário acima e encaminhe-o para o e-mail bib@if.usp.br ou pessoalmente ao Serviço de Atendimento ao Usuário da Biblioteca do IFUSP;**

Após a normalização dos unitermos pela equipe da Biblioteca, de acordo com o vocabulário USP, a ficha será preparada e encaminhada ao solicitante por e-mail.

A ficha catalográfica deverá ser inserida no verso da página de rosto da tese ou dissertação.

2. **Encaminhe para o e-mail bib@if.usp.br o resumo e abstract em formato TXT.**

Para maiores informações consulte o Serviço de Atendimento ao Usuário no Serviço de Biblioteca e Informação do SBI/IFUSP pelo telefone 3091.6923

“Quanto ao século, os médicos que estavam presentes ao parto reconhecem que este é difícil, crendo uns que o que agora aparece é a cabeça do XX, outros que são os pés do XIX. Eu sou pela cabeça, como sabe”

— Machado de Assis.

Aos meus queridos pais...

Abstract

At the quantum scale, heat and work cannot be understood solely through their average values; fluctuations are prominent and are thus crucial in Quantum Thermodynamics. To fully comprehend fluctuating currents in quantum systems, one has to model environmental degrees of freedom, yet, these are commonly discarded in usual treatments of open quantum systems. Timely, collisional models render the possibility of restoring control over environments in a simple way. In this dissertation I extend statistics of heat and work to collisional models. In particular, I apply the formalism to autonomous heat engines, which operate in non-equilibrium steady-states (NESS). Using concepts from resource theory of coherence, I characterize NESS according this property, with particular interest in the three-level engine of Scovil and Schulz-DuBois. Yet, coherent states pose limitations in determining work distributions, since measurements often erase such property. Combining quantum Bayesian networks and insights from statistics, I develop a technique to predict work fluctuations while maintaining the system's coherence untouched.

Keywords: quantum thermodynamics; open quantum systems; nonequilibrium steady-states; collisional models; quantum coherence; full counting statistics; quantum work; quantum heat.

Resumo

Na escala quântica, calor e trabalho não podem ser compreendidos somente por seus valores médios; flutuações são significantes e portanto cruciais em Termodinâmica Quântica. Para descrever correntes que flutuam em sistemas quânticos, é preciso incluir na descrição os graus de liberdade do ambiente, que são usualmente descartados no tratamento usual de sistemas quânticos abertos. Em tempo, modelos colisionais possibilitam restaurar tais graus de liberdade de forma simples. Nesta dissertação, estendo a estatística de calor e de trabalho para o formalismo de modelos colisionais. Em particular, aplico esse formalismo a máquinas térmicas autônomas, que operam em estados estacionários fora do equilíbrio (NESS). Usando conceitos de teoria de recursos de coerência, caracterizo NESS de acordo com sua coerência, com particular interesse na máquina térmica de Scovil e Schulz-DuBois. Contudo, estados coerentes impõe limitações aos modelos de distribuições de trabalho, uma vez que medições comumente destroem coerência. Combinando redes Bayesianas quânticas e técnicas de estatística, desenvolvo um preditor para as flutuações do trabalho, mantendo a coerência do sistema intacta.

Palavras-chave: termodinâmica quântica; modelos colisionais; sistemas quânticos abertos; full counting statistics; previsão estatística; coerência quântica; trabalho quântico; calor quântico.

Agradecimentos

Primeiramente, agradeço à minha mãe, Paula, e ao meu pai, Maurício, as duas pessoas que mais amo nesse mundo. Vocês me deram todo o apoio e preparo necessários para que eu chegasse até aqui, em todos os sentidos. Desde cedo me ensinaram não só sobre a importância mas também sobre o prazer dos estudos. Também me ensinaram a trabalhar com empenho e não dispensar uma boa risada. Eu posso até ter errado a área, mas acho que aprendi parte das lições, rs.

Gostaria de deixar meus agradecimentos aos meus avós, Silvio e Antonieta. Apesar de não nos vermos tanto e, menos ainda durante esses tempos de pandemia, amo muito vocês. À minha querida avó Rachel, com quem tive a oportunidade de passar boa parte desses duros meses, também deixo meus agradecimentos; sua vontade de viver sempre será uma inspiração para mim.

Poxa Gabriel, você eu nem sei por onde começar. Talvez deva ser pela sua paciência comigo e com o respeito que sempre teve com meu processo de aprendizado. De alguma forma, você sempre me disse quando achava que eu não estava certo, mas sempre me incentivou a insistir nas minhas ideias e, no fim das contas (que não foram poucas), me ensinou a acreditar em mim mesmo. Durante esses meses trancado em casa, nos quais poucas coisas realmente me alegravam, eu encontrei algum refúgio na Física. Mesmo assim, em vários momentos eu vi meu ânimo minguar, mas sempre depois das nossas reuniões eu voltava a trabalhar animado. Além de um ótimo orientador e alguém que admiro, você é um cara muito gente boa e que eu espero encontrar bastante por aí! Te agradeço demais, por todas as oportunidades e aprendizados.

Meus amigos queridos, também sou grato a vocês. Sejam aqueles que, mesmo distantes físicamente, se fizeram presentes ou aqueles dos quais me distanciei nesses tempos mas basta uma oportunidade para eu dar um abraço e sentar numa mesinha de bar. Sinto muitas saudades de vocês! Deixo também um agradecimento especial ao Franklin e ao Jader, com quem tantas vezes tive o prazer de discutir.

Falando em amigos, isso inclui todos vocês do QT^2. Uma das coisas que eu mais senti falta ao longo da pandemia foi a nossa convivência; reuniões, cafés, almoços, discussões, congressos... O que foi, foi pouco, mas foi muito bom. Então, agradeço muito pela oportunidade e por me aguentarem hehe. Espero que nos encontremos muito pelo mundo!

Gostaria de agradecer também a todos os professores que fizeram parte da minha trajetória no IFUSP. Em especial, à Bárbara e ao Oscar. Também, agradeço os funcionários do IFUSP, em especial os da CPG.

Finalmente, agradeço aos membros da banca por aceitarem participar dela e pelas críticas ao meu trabalho.

O presente trabalho foi realizado com apoio da Coordenação de Aperfeiçoamento de Pessoal de Nível Superior – Brasil (CAPES) – Código de Financiamento 001 .

Contents

List of Figures

List of Tables

Symbols

ρ	state (density matrix)
H	Hamiltonian
H_0	Free Hamiltonian, sum of local Hamiltonians
V	pontential, interaction
U	unitary time evolution
$\mathcal{E}$	stroboscopic map
$\mathbb{D}$	dephasing operator w.r.t. generic basis
Δ	dephasing operator w.r.t. energy basis
$\mathcal{D}$	dissipator
$\mathsf{L}, \mathsf{M}, \mathsf{N}, ...$	generic Hilbert space operators
Π	projector
$\mathbb{1}$	identity operator
$\mathscr{H}$	Hilbert space
$\mathcal{L}(\mathscr{H})$	set of linear operators over $\mathscr{H}$
$\mathscr{T}$	set of states (traceclass, positive-semidefinite operators)
$\mathscr{I}$	set of incoherent states
$\mathcal{Q}$	average heat
$\mathcal{W}$	average work
w	stochastic work
σ	stochastic entropy production
$\langle\bullet\rangle$	quantum average
$\mathbb{E}[\bullet]$	statistical average
CPTP	completely positive and trace preserving
CM	collisional model
FCS	full counting statistics
GKSL	Gorini-Kossakowski-Surdashan-Lindblad
SEC	strictly energy conserving
SSDB	Scovil and Schulz-DuBois
(Q)MSP	(quantum) mean-square predictor
(Q)BN	(quantum) Bayesian network
γ-TPM	two-point measurement with outcomes γ
w.r.t.	with respect to
$A \equiv B$	A is defined as B
$\sum_a x_a$	$\sum_{a\in A} x_a$ where the set of indices A is clear from the context
$\{y_a\}_a$	$\{y_a\vert\ a \in A\}$ where the set of indices A is clear from the context.

Chapter 1

Introduction

The advancement of technology in the last few centuries has been driven by the construction of engines of all sort. Be them vapor engines or top-notch laser technologies, at the core of their designs lies efficiency. And thermodynamics is the physical theory of efficiency [1]. In spirit, heat encodes the energy flux from readily available resources, while work entails the desired task to be performed. Figure 1.1 represents the basic structure of a heat engine: two sources (A, B) at different temperatures $(T_A > T_B)$ are put in contact with a system of interest (S) which, if we wait long enough, settles a steady conversion of heat into work. This is the content of the first law, when S is at its steady-state

$$Q_A + Q_B = \mathcal{W}. \tag{1.1}$$

The efficiency of such device is measured by the ratio of work with respect to the hottest source's heat, $\eta = \mathcal{W}/Q_A$. The second law establishes that heat engines' efficiency is hindered by a quantity $\Sigma \geq 0$,

$$\eta = 1 - \frac{T_B}{T_A} - T_B \frac{\Sigma}{|Q_A|}, \tag{1.2}$$

where Σ, so-called entropy production, quantifies how irreversible a process is [2].

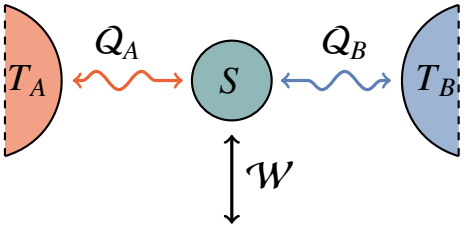

Figure 1.1: Prototypical autonomous heat engine. After a long while the system energy no longer changes and the mismatch between heat exchanged is constantly converted into work. Heat embodies energies fluxes from sources, which are inherently inefficient while work the energy flux associated to a task to be performed.

Nevertheless, Einstein taught us that fast systems are those close to speed of light, c, while Dirac that small energies are those of the order of $\hbar$ [3]; physics is a matter of scale. Thermodynamics was originally a phenomenological theory, which could effectively describe the operation of complicated systems in disregard of their microscopic (classical) model. Its connection with the underlying classical mechanics later culminated in the field of statistical mechanics [4]. At that point, it was reasonable to say that thermodynamics of single particle systems did not even made sense. In fact, even for systems with an intermediate scale — say, of the size of cells — the statistical interpretation of thermodynamics provided by (classical) statistical mechanics clarified that only for systems which were large enough would fluctuations be irrelevant. Only in this scenario the average quantities provided by statistical mechanics would correspond to the observed phenomenology and, further, agree with the laws of thermodynamics.

Quantum theory struck the 20th century with awe and ache, feelings which strive until the present days in the scientific community. Although its immense success in predicting the phenomena in the atomic scale, the hitherto most accepted interpretation of the theory predicts measurements which are fundamentally probabilistic [5, 6]. Such fluctuations are expected to appear regardless of the most carefully prepared experimental apparatus. At the time, the famous quote by Einstein ”God does not play dice“ represented the beliefs of many scientists, which did not consider the possibility that their conception of a deterministic reality was replete of physics which were only well-established in the macroscopic world.

It was then with von Neumann’s contributions [6] that thermodynamic considerations were formally brought to the quantum realm, extending entropy and statistical ensembles to quantum systems of *any* size. It was only through these considerations that quantum theory would be rigorously formulated. But important questions remained unanswered. What would distinguish and what would unify the classical and quantum uncertainty is, until today, one of the most

intriguing questions in the foundations of quantum theory. Later on, Jaynes made an enormous contribution to this puzzle; he saw a connection between quantum theory, statistical mechanics and probability: *information* [7, 8]. Followed by developments in open quantum systems in the following years [9–12], the field of quantum information started to gain relevance.

Quantum thermodynamics (QT) is the thrive to extend thermodynamics to finite size systems, non-equilibrium dynamics and include genuine quantum properties [13], largely based on quantum information principles. It is a young and fast growing field, pushed by nowadays' meticulous experimental control of devices which operate in the quantum regime [14–28]. The field is a patchwork of quantum information, non-equilibrium statistical mechanics, quantum optics, mesoscopic systems, quantum many-body systems and open quantum systems.

This dissertation is not about the whole field of QT, but navigates through a considerable number of its paradigms. Under the lens of a particular framework to approach open quantum systems, known as collisional models (CMs) [29, 30], I concentrate in the study of autonomous heat engines, as in Fig. 1.1. Collisional models are particularly compelling in situations in which book-keeping heat and work is non-trivial [30] and, more generally, due to their simplicity. Autonomous engines of finite size display considerable fluctuations in heat and work. In order to engineer such small devices, one has, for instance, to properly design them to endure such fluctuations. The first contribution of this dissertation is the application of full counting statistics (FCS) [31] to CMs, which provides formal prescriptions for distributions of thermodynamic currents and, thereby, enriches the study of quantum engines.

It is yet desirable to establish a prototypical heat engine to investigate such fluctuations. To this end, I revisit and extensively discuss the heat engine of Scovil and Schulz-DuBois (SSDB) [32], using the CM framework. This system is a minimal microscopic engine, associated to laser technologies. Before even discussing fluctuations, it will provide a concrete task associated to work and illustrate interesting questions at the level of averages. For instance, we will explore the role of energetic coherences in this model, a quantum feature of central thermodynamic importance [33]. To better understand coherence in non-equilibrium systems, I employ some tools from the resource theory of coherence [34–37]. The second contribution of this dissertation is the study of this particular example, which helps to draw a clearer picture of heat engines operating with genuine quantum resources and will be prepared for publication.

In classical non-equilibrium systems, the probability distributions of thermodynamic quantities encompass generalizations of the laws of thermodynamics, so-called fluctuation theorems

(FTs) [38–41]. Their generalizations to the quantum realm is yet trivial only in the absence of energetic coherences. To prescribe the statistics necessary to quantum FTs, one has to make reference to measurements, whose back-action is to erase coherence. For instance, quantum mechanics sets fundamental restrictions on work distributions [13, 42]. Recently, a framework to bypass some of these limitations has been established [43] based on Bayesian networks. This technique is here used to provide a model of work distributions in the presence of coherence. Such distribution is yet complicated to access experimentally. The final contribution of this dissertation is, borrowing insight from statistical prediction [44], to provide a predictor of work fluctuations, based only on the information available to the experimenter. The so-called quantum-mean square predictor of work estimates the work distribution based on heat measurements, leaving quantum coherence untouched. Moreover, it can be regarded as a stochastic formulation of the first law which includes the role of coherence in the thermodynamic process. This method culminated in a draft [45], which is currently in process of submission.

Below, I summarize the contents of each Chapter of this dissertation.

- Chapter 2 — settles notation and relevant concepts from quantum theory, quantum information and the standard approach to open quantum systems;
- Chapter 3 — presents the collisional model framework, with regards to non-equilibrium steady-states (NESS). Some results from resource theory of coherence are introduced and used to characterize NESS;
- Chapter 4 — heat, work and entropy production are introduced. An informational perspective on the laws of thermodynamics is provided;
- Chapter 5 — the heat engine of Scovil and Schulz-DuBois is studied in the CM framework. Its steady-state properties and the role of coherence are discussed;
- Chapter 6 — discusses simple quantum fluctuation theorems for heat, work and entropy production.
- Chapter 7 — full counting statistics framework for CMs. Also provides the graphical representation of quantum Bayesian networks. The framework is applied to minimal qubit examples and the SSDB engine;
- Chapter 8 — discusses the fundamental limitations of quantum work, the framework of

quantum Bayesian networks for initially coherent systems, its limitations and interpretation;

- Chapter 9 — discusses statistical prediction and then formulates the quantum mean-square predictor of work. The predictor of work is then studied in a minimal two-process qubit engine and in the SSDB heat engine.

- Appendix A — Few mathematical identities and derivations.

- Appendix B — Calculations concerning the SSDB engine; algebraic properties of the system's operators, symmetries, local master equation derivation.

All the numerical calculations and plots in this dissertation are done in Mathematica.

Chapter 2

Concepts in quantum mechanics

The goal of this chapter is to present some of the quantities and set the notation that will be used throughout this dissertation. I present relevant results from quantum channels, quantum information and open systems without venturing in discussions or derivations which do not cope with the narrative of this dissertation. All results discussed here can be found in the references [5, 6, 46–48].

2.1 Closed quantum systems

For simplicity, I consider finite dimensional quantum systems, described by a d-dimensional Hilbert space $\mathscr{H}$. A physical observable is a linear operator $\mathsf{A} : \mathscr{H} \to \mathscr{H}$ which is Hermitian; the set of linear operators operators on $\mathscr{H}$ is denoted $\mathcal{L}(\mathscr{H})$. The state describing the physical system $\rho \in \mathcal{L}(\mathscr{H})$ is such that $\mathrm{Tr}\,\rho = 1$, $\rho = \rho^\dagger$ and all its eigenvalues are positive or zero (positive semi-definite, $\rho \geq 0$ for short); the subset of $\mathcal{L}(\mathscr{H})$ containing only physical states is called $\mathscr{T}$.

The space $\mathscr{H}$ admits a basis of d orthonormal kets denoted $\{|\psi_a\rangle\}_{a\leq d}$. Outer products of such vectors define projectors in their respective subspaces $\Pi_a \equiv |\psi_a\rangle\langle\psi_a|$, which add to the identity:

$$\sum_{a=1}^{d} \Pi_a = \mathbb{1}. \tag{2.1}$$

A state ρ can be projected in an eigenspace of $|\psi_a\rangle$ through

$$\rho \to \rho_a = \frac{\Pi_a \rho \Pi_a}{\mathrm{Tr}(\Pi_a \rho)} = \Pi_a. \tag{2.2}$$

The term $\mathrm{Tr}\{\Pi_a\rho\}$ is the probability p_a associated to a projective measurement Π_a. This statement acquires more meaning if we choose $\{|\psi_a\rangle\}_a$[1] to be eigenvectors of A, with associated (non-degenerate and discrete) spectrum $\{a\}_a$. In such basis A assumes a spectral representation

$$\mathsf{A} = \sum_a a\Pi_a. \tag{2.3}$$

In this case, there are d different values which a measurement of A can yield, each occurring with a probability $p_a = \mathrm{Tr}(\Pi_a\rho)$ (Born's rule). Such probabilities are attained whenever we perfectly reproduce the experimental conditions producing the state ρ and again perform the projective measurement.

The quantum average value of the operator A is given by

$$\langle\mathsf{A}\rangle = \mathrm{Tr}(\mathsf{A}\rho). \tag{2.4}$$

If we represent the trace in the basis $\{|\psi_a\rangle\}_a$ we find that

$$\langle\mathsf{A}\rangle = \sum_a a p_a = \mathbb{E}[a]. \tag{2.5}$$

That is, the quantum average over the state ρ coincides with the statistical average of an ensemble of many copies of the system, measured with outcomes a. Note that $p_a = p_a(\rho)$, and we could say that "p_a is the probability of finding a given the system was in the state ρ". Yet, one never measures ρ, one can only measure an observable A, which is suited to determine ρ only in the case $[\mathsf{A}, \rho] = 0$.

The spectral representation of an Hermitian operator A also defines functions of operators $f(\mathsf{A})$. Let f be an analytic function of any element in the spectrum of A, then

$$f(\mathsf{A}) \equiv \sum_a f(a)\Pi_a. \tag{2.6}$$

In particular, using the above formula, I set $f(a) = a^2$ to establish the variance of A

$$\mathrm{var}\mathsf{A} = \left\langle\mathsf{A}^2\right\rangle - \langle\mathsf{A}\rangle^2 = \sum_a a^2 p_a - \left(\sum_a a p_a\right)^2 = \mathbb{E}[a^2] - \mathbb{E}[a]^2. \tag{2.7}$$

[1] **Notation**: as with the sums, I omit the set of values a is allowed to assume whenever it is clear from the context or previously mentioned.

The evolution of a state ρ is given, in the Schrödinger picture, by von Neumann's equation

$$\frac{d}{dt}\rho(t) = -i[\mathsf{H}(t), \rho(t)], \tag{2.8}$$

where I set $\hbar = 1$ and H is the Hamiltonian operator. The solution of von Neumann's equation is

$$\rho(t) = \mathsf{U}_t \rho(0) \mathsf{U}_t^\dagger, \tag{2.9}$$

with

$$\mathsf{U}_t = \mathcal{T} e^{-i\int_0^t ds \mathsf{H}(s)}; \tag{2.10}$$

the symbol $\mathcal{T}$ indicates time ordering, for $[\mathsf{H}(t_i), \mathsf{H}(t_j)] \neq 0$ in general. The operator U_t satisfies $\mathsf{U}_t \mathsf{U}_t^\dagger = \mathsf{U}_t \mathsf{U}_t^{-1} = \mathbb{1}$. If H is time independent it simplifies to $\mathsf{U}_t = e^{-it\mathsf{H}}$, as will often be the case in the forthcoming chapters. Any unitary operator is also an isometry in $\mathscr{H}$; it leaves the inner product unaltered $\langle\phi|\psi\rangle = \langle\phi|\,\mathsf{U}^\dagger\mathsf{U}\,|\psi\rangle$ and, thus, preserves the orthogonality between state-vectors.

In the Heisenberg picture, an operator $\mathsf{A}(t)$ satisfies

$$\frac{d}{dt}\mathsf{A}(t) = i[\mathsf{H}(t), \mathsf{A}(t)] + \partial_t \mathsf{A}(t), \tag{2.11}$$

and thus evolves as

$$\mathsf{A}(t) = \mathsf{U}_t^\dagger \mathsf{A}(0) \mathsf{U}_t. \tag{2.12}$$

Also, when H is time independent, $[\mathsf{H}, \mathsf{U}_t] = 0$ for all t. Hence, energy is a conserved quantity. Through the spectral resolution of $f(\mathsf{A}(t))$

$$\mathsf{U}_t^\dagger f(\mathsf{A}(0)) \mathsf{U}_t = f(\mathsf{U}_t^\dagger \mathsf{A}(0) \mathsf{U}_t), \tag{2.13}$$

which is in fact true not only for the time evolution but for any unitary operator.

Another fundamental quantity is the von Neumann entropy of a state

$$S(\rho) = -\operatorname{Tr}\{\rho \ln \rho\}. \tag{2.14}$$

I work in units in which $k_B = 1$ and will often refer to it simply as *entropy*. This quantity was derived in [6], by considering the statistical nature of ρ. Remarkably, it is also conserved under unitaries[2]. The density operator ρ can be written $\rho = \sum_\nu p_\nu \Pi_\nu$, with $p_\nu \in [0, 1]$ and $\sum_\nu p_\nu = 1$, in which case

$$S(\rho) = -\sum_\nu p_\nu \ln p_\nu, \tag{2.15}$$

and $0 \ln 0 \equiv 0$. From the normalization of ρ, we see that whenever some $p_\nu = 1$, the others are zero and thus $S(\rho) = 0$ for *pure states* which have the form Π_ν. The von Neumann entropy thus quantifies our ignorance about in which (pure) state the system is, with respect to its eigenbasis. In the spectral representation (2.15), it coincides with the Shannon entropy of a probability distribution p_ν. The Shannon entropy stems from information theory and it quantifies the amount of ignorance about a set of probabilities. It is maximal whenever each outcome is equally probable and zero if any event is deterministic.

2.2 Multipartite quantum systems

For simplicity I consider a bipartite quantum system, described by a Hilbert space $\mathscr{H} = \mathscr{H}_E \otimes \mathscr{H}_S$ where $\otimes$ is the tensor product. Let $\mathsf{E} \in \mathcal{L}(\mathscr{H}_E)$ and $\mathsf{S} \in \mathcal{L}(\mathscr{H}_S)$, then we can always form an operator $\mathsf{E} \otimes \mathsf{S} \in \mathcal{L}(\mathscr{H})$ — often, I omit the "$\otimes$" . We can choose to represent $\mathscr{H}$ in a basis formed of local vectors $\{|e_i\rangle \otimes |s_l\rangle\}_{i,l}$. In finite dimensions, the tensor product is implemented operationally through the Kroenecker product of matrices

$$\mathsf{E} \otimes \mathsf{S} = \sum_{ijlm} e_{ij} s_{lm} \left|e_i s_l\right\rangle\!\!\left\langle e_j s_m\right| = \begin{pmatrix} e_{11}\mathsf{S} & e_{12}\mathsf{S} & \dots e_{1d_E}\mathsf{S} \\ e_{21}\mathsf{S} & e_{22}\mathsf{S} & \dots e_{2d_E}\mathsf{S} \\ \vdots & \ddots & \dots e_{3d_E}\mathsf{S} \\ e_{d_E 1}\mathsf{S} & \dots & e_{d_E d_E}\mathsf{S} \end{pmatrix}, \tag{2.16}$$

[2] Setting $0 \ln 0 \equiv 0$ and noting that $\rho \geq 0$ and $\rho = \rho^\dagger$, $f(x) = x \ln x$ is analytic in the spectrum of ρ. Then, $f(\mathsf{U}_t \rho \mathsf{U}_t^\dagger) = \mathsf{U} f(\rho) \mathsf{U}^\dagger$ holds. Therefore, $S(\mathsf{U}_t \rho \mathsf{U}_t^\dagger) = S(\rho)$

where $[\mathsf{E}]_{ij} = \langle e_i | \mathsf{E} \left| e_j \right\rangle = e_{ij}$ and d_E is the dimension of $\mathscr{H}_E$. Yet, not every operator in H can be decomposed in local operators. In general, we can represent $\mathsf{G} \in \mathcal{L}(\mathscr{H})$ in the local basis as

$$\mathsf{G} = \sum_{ijlm} g_{ijlm} \left| e_i s_l \right\rangle\!\left\langle e_j s_m \right| . \tag{2.17}$$

That is, we cannot in general factor g_{ijlm} in two local parts.

Now, as $\mathscr{T} \subset \mathcal{L}(\mathscr{H})$, one would wonder whether the same reasoning holds for states. Indeed, this is true: if we have two states $\rho_E \in \mathscr{T}_E$ and $\rho_S \in \mathscr{T}_S$ then $\rho_E \otimes \rho_S \in \mathscr{T}$. Yet, this is only true because $\otimes$ preserves the trace normalization *and* the positive semi-definiteness.

We are now at the position to announce the most general class of maps that transform states into states. A so-called completely positive and trace preserving (CPTP) map is a map $\Lambda : \mathcal{L}(\mathscr{H}_S) \to \mathcal{L}(\mathscr{H}_S)$ such that, for any $\rho_S \in \mathscr{T}_S$, it produces a state: $\Lambda(\rho_S) \in \mathcal{L}(\mathscr{H}_S)$ such that $\mathrm{Tr}\,\Lambda(\rho_S) = 1$ (trace preserving) and $\Lambda(\rho_S) \geq 0$ (positivity). Further, the affix "complete" is added once every natural extension of the map $\mathbb{1}_E \otimes \Lambda : \mathcal{L}(\mathscr{H}_E) \otimes \mathcal{L}(\mathscr{H}_S) \to \mathcal{L}(\mathscr{H}_E) \otimes \mathcal{L}(\mathscr{H}_S)$ is required to be positive too.

Different from unitaries, CPTP maps do not generally leave the inner product invariant and may change von Neumann entropy.

Kraus' theorem asserts that a map is CPTP *iff* it disposes of a Kraus representation. That is, Λ is CPTP *iff* it can be written as

$$\Lambda(\rho) = \sum_{j=1}^{d^2} K_j^\dagger \rho K_j, \tag{2.18}$$

where K_j is a Kraus component and they satisfy $\sum_j K_j^\dagger K_j = \mathbb{1}$. Note that, assuming $\dim\mathscr{H} = d$, we have that $\dim \mathcal{L}(\mathscr{H}) = d^2$. Two relevant examples are the closed system time evolution $\mathcal{U}_t(\rho) = \mathsf{U}_t \rho \mathsf{U}_t^\dagger$, whose unitary representation is a Kraus representation $\mathsf{U}_t^\dagger \mathsf{U}_t = \mathbb{1}$ and the partial trace operation $\mathrm{Tr}_E : \mathcal{L}(\mathscr{H}_S) \otimes \mathcal{L}(\mathscr{H}_E) \to \mathcal{L}(\mathscr{H}_S)$. To see the Kraus form of Tr_E, I use the basis $\{|n_i\rangle \otimes \left| e_j \right\rangle\}_{ij}$:

$$\mathrm{Tr}_B \rho = \sum_j \underbrace{\left(\mathbb{1}_A \otimes \left\langle e_j \right|\right)}_{K_j} \rho \underbrace{\left(\mathbb{1}_A \otimes \left| e_j \right\rangle\right)}_{K_j^\dagger}, \tag{2.19}$$

$$\sum_k K_j^\dagger K_j = \mathbb{1}_S \otimes \mathbb{1}_E. \tag{2.20}$$

Once I have introduced multipartite systems, let me discuss again the von Neumann entropy. If $\rho = \rho_A \otimes \rho_B$ then we have

$$S(\rho_S \otimes \rho_E) = S(\rho_S) + S(\rho_E). \tag{2.21}$$

If ρ is not a product, it makes sense to quantify the amount of entropy due to the correlations between each system; in fact, we talk about the reciprocal quantity, the mutual information

$$\mathcal{I}_\rho(S : E) \equiv S(\rho_S) + S(\rho_E) - S(\rho), \tag{2.22}$$

where $\rho_S = \mathrm{Tr}_E \rho$ and $\rho_E = \mathrm{Tr}_S \rho$. Entropy can be regarded as a quantifier of disorder or ignorance, that is, lack of information.

The mutual information can also be written as

$$\mathcal{I}_\rho(S : E) = S(\rho \| \rho_S \otimes \rho_E), \tag{2.23}$$

where I have introduced the relative entropy $S(\alpha\|\beta) \equiv \mathrm{Tr}[\alpha(\ln\alpha - \ln\beta)] \geq 0$. The latter has the spirit of a norm, for it quantifies the entropic distance between two states. Yet, it is not a norm since it is not symmetric in $\alpha \leftrightarrow \beta$ and does not satisfy the triangle inequality. Moreover, once the relative entropy is always positive, $S(\rho)$ is subadditive:

$$S(\rho) \leq S(\rho_A) + S(\rho_B). \tag{2.24}$$

From the subadditivity property, Lindblad [10] derived an interesting result: the so-called *quantum data processing inequality*

$$S(\Lambda(\rho)\|\Lambda(\sigma)) \leq S(\rho\|\sigma), \tag{2.25}$$

where $\rho, \sigma \in \mathscr{T}$ and Λ is any CPTP map. That is, under any quantum channel Λ, the entropic distance between two states can only decrease.

2.3 Open quantum systems

As we have seen, CPTP maps are the most general transformations from states into states and they lead to the possibility of performing operations between different Hilbert spaces. Every theory of open quantum system begins with the splitting of a multipartite universe between a system S and an environment E. The system is chosen as it is the piece of interest and the environment, usually due to its complexity, is disregarded. Symbolically, we start with the von Neumann equation for the universe

$$\frac{d}{dt}\rho(t) = -i[\mathsf{H}(t), \rho(t)], \tag{2.26}$$

with $\rho(t), \mathsf{H}(t) \in \mathcal{L}(\mathscr{H}_E \otimes \mathscr{H}_S)$, and then perform the partial trace operation with respect to the environment

$$\frac{d}{dt}\rho_S(t) = -i\,\mathrm{Tr}_E[\mathsf{H}(t), \rho(t)] \equiv \mathscr{L}\rho. \tag{2.27}$$

In a similar fashion, the same procedure holds for the solutions

$$\rho_S(t) = \mathrm{Tr}_E(\mathsf{U}_t\rho(0)\mathsf{U}_t^\dagger) \equiv \mathcal{V}_t\rho(0). \tag{2.28}$$

I assume H to be time independent henceforth. From this point on, there are a series of methods that can be employed to manipulate this expression. Usually, they rely on approximations which make sense for specific models or limiting situations. In this dissertation, the tool I use to model an open system is the collisional model, which will be throughly discussed in Chapter 3. In the present Chapter, I outline the most common approach, the so-called Gorini-Kossakowski-Surdashan-Lidblad (GKSL) [9, 11] derivation for master equations. The following argument is found in [47].

The starting point is to consider the consequences of imposing the semigroup property

$$\mathcal{V}_{t_1}\mathcal{V}_{t_2} = \mathcal{V}_{t_1+t_2}, \quad \forall t_1, t_2 \in \mathbb{R}^+. \tag{2.29}$$

Physically, this is to say that there are no memory effects (Markovianity) concerning the interaction with the environment. For example, if the environment is a many-body system, we could assume that each of its pieces interact and then takes a time so long to interact again that the

effect of the first interaction was already mitigated. Indeed, every piece interacts at the same time, but, as a matter of scale, some interactions may decrease fast with distance and can be discarded at a fixed instant of time.

Remarkably, such property gives a very complete characterization of $\mathcal{V}_t$

$$\mathcal{V}_t = e^{t\mathscr{L}}, \tag{2.30}$$

where $\mathscr{L}$ is the infinitesimal generator of the dynamical semigroup. From there

$$\frac{d}{dt}\rho_S(t) = \mathscr{L}\rho_S(t). \tag{2.31}$$

This map somewhat resembles the unitary dynamics and indeed unitaries are a particular case. Yet, the spectral properties of $\mathcal{V}_t$ are very different from $\mathcal{U}_t$, since $\mathscr{L}$ is not anti-Hermitian as it is the case of $-i\mathsf{H}$.

I now set $\mathsf{U}_t = e^{-it\mathsf{H}}$ with $\mathsf{H} = \mathsf{H}_S + \mathsf{H}_E + \mathsf{V}$. Further, requiring that the initial global state is factorized as $\rho(0) = \rho_E(0) \otimes \rho_S(0)$ one can construct the Kraus decomposition of $\mathcal{V}_t$. For that sake, consider the spectral representation $\rho_E(0) = \sum_\alpha \lambda_\alpha |\psi_\alpha\rangle\langle\psi_\alpha|$ and let me represent the partial trace operation w.r.t. such basis:

$$\mathcal{V}_t(\rho_S(0)) = \sum_{\alpha\beta} \lambda_\alpha \left\langle \psi_\beta \right| \mathsf{U}_t \left| \psi_\alpha \right\rangle \rho_S(0) \left\langle \psi_\alpha \right| \mathsf{U}_t^\dagger \left| \psi_\beta \right\rangle \tag{2.32}$$

$$= \sum_{\alpha\beta} \mathsf{W}_{\alpha\beta}\rho_S(0)\mathsf{W}_{\alpha\beta}^\dagger, \tag{2.33}$$

where $\mathsf{W}_{\alpha\beta} = \sqrt{\lambda_\alpha}\left\langle \psi_\beta \right| \mathsf{U}_t \left| \psi_\alpha \right\rangle$, satisfying $\sum_{\alpha\beta} \mathsf{W}_{\alpha\beta}^\dagger \mathsf{W}_{\alpha\beta} = \mathbb{1}_S$.

Let me assume that $\dim\mathscr{H}_S = d$. In this case, the space $\mathcal{L}(\mathscr{H}_S)$ has dimension d^2 and hence there are d^2 operators which form a basis of it. Indeed, we can define an inner product of operators through

$$(\mathsf{A}, \mathsf{B}) \equiv \mathrm{Tr}\left(\mathsf{A}^\dagger \mathsf{B}\right), \tag{2.34}$$

according to which we can find d^2 orthogonal operators to form a basis of $\mathcal{L}(\mathscr{H}_S)$, *i.e.*,

$$(\mathsf{F}_i, \mathsf{F}_j) = \delta_{ij} \;\; i, j = 1, ..., d^2. \tag{2.35}$$

Further, we can choose $d^2 - 1$ operators to be traceless if we set $\mathsf{F}_{d^2} \equiv \mathbb{1}_S / \sqrt{d}$. With this basis we can choose to decompose each $\mathsf{W}_{\alpha\beta}$ in projections along F_i's:

$$\mathsf{W}_{\alpha\beta}(t) = \sum_{i=1}^{d^2} \mathsf{F}_i(\mathsf{F}_i, \mathsf{W}_{\alpha\beta}(t)), \tag{2.36}$$

with

$$\mathcal{V}_t(\rho_S(0)) = \sum_{i,j=1}^{d^2} c_{ij}(t)\mathsf{F}_i\rho_S(0)\mathsf{F}_j^\dagger, \tag{2.37}$$

$$c_{ij}(t) = \sum_{\alpha\beta}(\mathsf{F}_i, \mathsf{W}_{\alpha\beta})(\mathsf{F}_j, \mathsf{W}_{\alpha\beta})^*. \tag{2.38}$$

Now, one can use the above the structure of the generator to compute the small ϵ expansion in

$$\lim_{\epsilon\to 0} \frac{1}{\epsilon}\{\mathcal{V}_\epsilon\rho_S(0) - \rho_S(0)\}. \tag{2.39}$$

The details of the above calculation can be found in [47]. Through keeping the lower order terms in ϵ, it is found that

$$\mathscr{L}\rho_S = -i[\mathsf{H}_S^{\text{eff}}+, \rho_S] + \sum_{ij=1}^{d^2-1} a_{ij}\left(\mathsf{F}_i\rho_S\mathsf{F}_i^\dagger - \frac{1}{2}\left\{\mathsf{F}_j^\dagger\mathsf{F}_i, \rho_S\right\}\right), \tag{2.40}$$

where $\mathsf{H}_S^{\text{eff}} = \mathsf{H}_S + \mathsf{G}$, the original local Hamiltonia plus a unitary correction that may arise from tracing out the environment. At this point the precise form of G is unimportant, but can be found in [47]; its importance will be addressed in the framework of collisional models too. From the derivation, one also finds that a_{ij} can be diagonalized as $\text{diag}\{\gamma_1, ..., \gamma_{d^2-1}\}$, thus simplifying the above expression in terms of a new orthogonal basis of operators $\{\mathsf{A}_i\}_i$; this leads to the so-called GKSL master equation:

$$\mathscr{L}\rho_S = -i[\mathsf{H}_S^{\text{eff}}, \rho_S] + \sum_{i=1}^{d^2-1} \gamma_i\left(\mathsf{A}_i\rho_S\mathsf{A}_i^\dagger - \frac{1}{2}\left\{\mathsf{A}_i^\dagger\mathsf{A}_i, \rho_S\right\}\right). \tag{2.41}$$

If the system S is multipartite, say a spin-chain, one can think about an environment coupled to an end of the chain. In this case, if the system has local internal interactions (an XX-chain for example), to a good a approximation the environment interacts only with the first site of the chain and therefore the A_i's would be just local operators in this site. Such scenario is so-called

Local Master Equations (LMEs). Of course, in a more realistic case the interaction is Global, *i.e.*, the environment interacts with the whole system although the rates γ_i of more distant sites would be smaller for local interactions.

The formalism here presented is a remarkable formal accomplishment of quantum theory. The field of Open Quantum Systems has been thoroughly developed in the late 20th century, pushed by the development of laser technologies. The environments envisioned in such cases are mostly concerned with applications of quantum optics and also provided the theoretical background to experimentally access the phenomena of decoherence [49–52]. Curiously, the theory of (classical) irreversible thermodynamics also provided important insights to the realm of Open Quantum System; for instance, just after the seminal papers of GKSL [9, 11] (1975 and 1976), Spohn formulated a version of entropy production for Open Quantum Systems [12] (1977).

2.4 POVMs and measurement operators

In quantum theory, measurements and open systems are two faces of the same coin. In practice, isolated systems only exist while unmeasured, since the measurement apparatus should also be accounted in quantum mechanics. So far, I have discussed only projective measurements which are indeed an idealized situation. They are an effective description of a measurement apparatus which has interacted unitarily with the system of interest during a time frame much smaller than the time scale of interest and, therefore, have a built-in "instantaneous" structure. More generally, we consider *positive operator valued measures* (POVMs), which are given by a set of operators $\{\mathsf{E}_\gamma\}_\gamma$, with $\sum_\gamma \mathsf{E}_\gamma = \mathbb{1},\ \mathsf{E}_\gamma \geq 0\ \forall\gamma$ and

$$p_\alpha = \mathrm{Tr}(\mathsf{E}_\alpha \rho). \tag{2.42}$$

Yet, to provide the post measuremement state we need to work with *measurement operators* $\{\mathsf{M}_\alpha\}_\alpha$ whose associated probabilities are

$$p_\alpha = \mathrm{Tr}\left(\mathsf{M}_\alpha^\dagger \mathsf{M}_\alpha \rho\right), \tag{2.43}$$

and they add to identity as $\sum_\alpha \mathsf{M}_\alpha^\dagger \mathsf{M}_\alpha = \mathbb{1}$. Although M_α need not to be Hermitian, $\mathsf{M}_\alpha^\dagger \mathsf{M}_\alpha$ is Hermitian and $\mathsf{M}_\alpha^\dagger \mathsf{M}_\alpha \geq 0$. Then, setting $\mathsf{E}_\alpha \equiv \mathsf{M}_\alpha^\dagger \mathsf{M}_\alpha$ we have established a POVM.

The state of the system after a given measurement outcome α is given by

$$\rho'_\alpha = \frac{\mathsf{M}_\alpha \rho \mathsf{M}_\alpha^\dagger}{p_\alpha}. \tag{2.44}$$

If we combine all possible states after measurements according to their respective probabilities we always have a legit state, guaranteed by Kraus' theorem;

$$\sum_\alpha p_\alpha \rho'_\alpha = \sum_\alpha \mathsf{M}_\alpha \rho \mathsf{M}_\alpha^\dagger = \Lambda(\rho) = \rho'. \tag{2.45}$$

In general, there are multiple sets of measurement operators which can give rise to the same POVM [48]. That is, the precise measurement operator is associated to the apparatus we use but different apparatus can, ideally, lead to the same statistics. A reasonable take is to consider an auxiliary system, or ancilla, as the measurement apparatus and assume we have good control of this particular system and can perform even projective measurements in it, while in the system of interest we have some technical limitation. In this manner, we start with the system S and ancilla A in the state $\rho = \rho_A \otimes \rho_S$, evolve them unitarily during τ, U_τ, and projectively measure the ancilla with Π_α. For simplicity, I assume $\rho_A = |\phi\rangle\langle\phi|$. In the end, we then discard the ancilla to provide the state of the system after measurement. Symbolically

$$\rho_A \otimes \rho_S \to \mathrm{Tr}_A\{\Pi_\alpha \mathsf{U}(\rho_S \otimes \rho_A)\mathsf{U}^\dagger \Pi_\alpha\} = \langle\alpha|\,\mathsf{U}\,|\phi\rangle\,\rho_S\,\langle\phi|\,\mathsf{U}^\dagger\,|\alpha\rangle\,; \tag{2.46}$$

which, by identifying $\mathsf{M}_\alpha = \langle\alpha|\,\mathsf{U}\,|\phi\rangle \in \mathcal{L}(\mathscr{H}_S)$, satisfies $\sum_\alpha \mathsf{M}_\alpha^\dagger \mathsf{M}_\alpha = \langle\phi|\,\mathsf{U}\sum_\alpha \Pi_\alpha \mathsf{U}^\dagger\,|\phi\rangle = \mathbb{1}$, and thereby gives the updated system state $\rho'_{S|\alpha} = \mathsf{M}_\alpha \rho_S \mathsf{M}_\alpha^\dagger / \mathrm{Tr}\big(\mathsf{M}_\alpha \rho_S \mathsf{M}_\alpha^\dagger\big)$.

Chapter 3

Collisional models

The focus of this dissertation is on the fluctuations of heat and work in open quantum systems. The treatment of open systems is commonly done through continuous maps generated by GKSL master equations. As discussed in the previous Chapter, they are usually derived from the joint unitary dynamics of a system S and an environment E; the environment is assumed to be an infinitely large system whose degrees of freedom are constantly interacting with the system and is traced out to produce the reduced open dynamics of S. This procedure is usually followed by a series of approximations and assumptions which render the problem tractable.

In obtaining statistics of heat and work in the course of this dissertation, it will prove important to count the environmental quanta, but discarding the environment hinders such possibility. For this reason, the present Chapter introduces the framework of collisional models (CMs), also known as repeated interactions.

Instead of picturing all the interactions happening at the same time, CMs implement the bath as a sequence of little pieces (units or ancillae) which collide with the system and are then traced out to produce the system reduced dynamics. Such models have been largely explored recently [29, 30, 33, 53–70], with particular emphasis to the fact that they can recover local master equations (LMEs).

In this Chapter, we will not start with master equations. I will introduce the framework in its more general form; a time-discrete CPTP map applied sequentially. We will then understand how these models relate to thermalization and, more generally, to the process of stabilization in non-equilibrium situations. For this sake, I will employ some ideas from resource theories of coherence [34–37, 71–75], once the understanding of how the collisions process coherence and populations will be important in the future. Further, this dissertation mainly explores discrete-

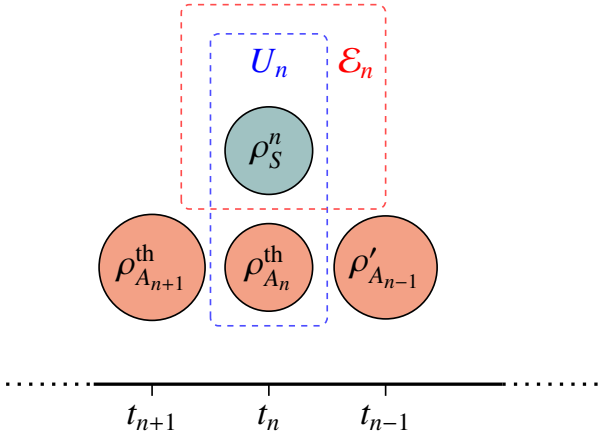

Figure 3.1: Each identically thermal ancilla interacts sequentially with the system and is then discarded. Formally, at time t_n the unitary interaction $\rho^{\text{th}}_{A_n} \otimes \rho_S \xrightarrow{\mathcal{U}_n} \rho'_n$, is followed by the partial trace $\rho'_n \xrightarrow{\text{Tr}_{A_n}} \rho_S^{n'} = \rho_S^{n+1}$, characterizing a single collision; then the process repeat generating the dynamics for an arbitrary time interval.

time maps in its applications; LMEs are treated as a limit case and are discussed in Section 3.3.

3.1 General framework

Picture two quantum systems, one named S for system and another E, for environment. This division is to some extent arbitrary, in the sense that whatever the system is, it will be the piece whose dynamics we are interested in. I assume E to be divided as smaller ancillae (or units) A_n, each given by a quantum system in its own right. The dynamics is then described by a series of sequential collisions, where the system only interacts with one unit at a time. Each collision lasts for a fixed time τ and afterwards, the ancilla is discarded and never participates again in the dynamics, as in Fig. 3.1.

Formally, consider at time $t = 0$ two quantum systems A_0 and S initialized at global state $\rho = \rho_S^0 \otimes \rho_{A_0}$; they are described by self-Hamiltonians H_{A_0} and H_S, and interact via V_0 during a time τ. The time-independent global Hamiltonian is then

$$\mathsf{H}^{(0)} = \mathsf{H}_S + \mathsf{H}_{A_0} + \mathsf{V}_0, \tag{3.1}$$

and, according to von Neumann's equation $\dot{\rho} = -i[\mathsf{H}, \rho]$, after a time τ the dynamics is resolved by the unitary $\mathsf{U}_0 = e^{-i\tau\mathsf{H}^{(0)}}$. That is, the global state is then given by $\rho' = \mathcal{U}_0(\rho) = \mathsf{U}_0\rho\mathsf{U}_0^\dagger$. The assumption of discarding the ancilla A_0 is implemented by the partial trace operation; it defines the first collision of our completely positive and trace preserving evolution by updating

the system's state with the local change after the unitary interaction:

$$\mathcal{E}_0(\rho_S^0) = \mathrm{Tr}_{A_0}\{\mathsf{U}_0(\rho_{A_0} \otimes \rho_S^0)\mathsf{U}_0^\dagger\} = \rho_S^1. \tag{3.2}$$

After this, we repeat the cycle with an ancilla A_1 and so forth. In general, we then have that

$$\mathcal{E}_n(\rho_S^n) = \mathrm{Tr}_{A_n}\{\mathsf{U}_n(\rho_{A_n} \otimes \rho_S^n)\mathsf{U}_n^\dagger\} = \rho_S^{n+1}. \tag{3.3}$$

I also assume that every ancilla is identical and identically prepared, that is, their respective Hilbert spaces are isomorphic and they are all at the same state before interacting with S. Under this umbrella, although each unitary $\mathcal{U}_n$ and partial trace Tr_{A_n} act on different spaces, we can simply think of the global dynamics in a bipartite space $\mathscr{H}_S \otimes \mathscr{H}_A$, where we reset the state of A by tracing it out and bringing a fresh one at the rate τ. In this manner, we can write, for the n-th application of the map

$$\mathcal{E}(\rho_S^n) = \mathrm{Tr}_A\{\mathsf{U}(\rho_A \otimes \rho_S^n)\mathsf{U}^\dagger\} = \mathcal{E}^n(\rho_S^0), \tag{3.4}$$

where $\mathsf{U} = e^{-i\tau\mathsf{H}}$ and $\mathsf{H} = \mathsf{H}_A + \mathsf{H}_S + \mathsf{V}$. Thereby, we see that the open-system dynamics is described by a stroboscopic (discrete-time) map, which only relies on the system and a single ancilla. This is a drastic simplification in contrast to ordinary open quantum system dynamics, which are derived from a system interacting with an infinite dimensional environment.

To solidify the framework used in this text, I list the assumptions which constrain my CMs of interest

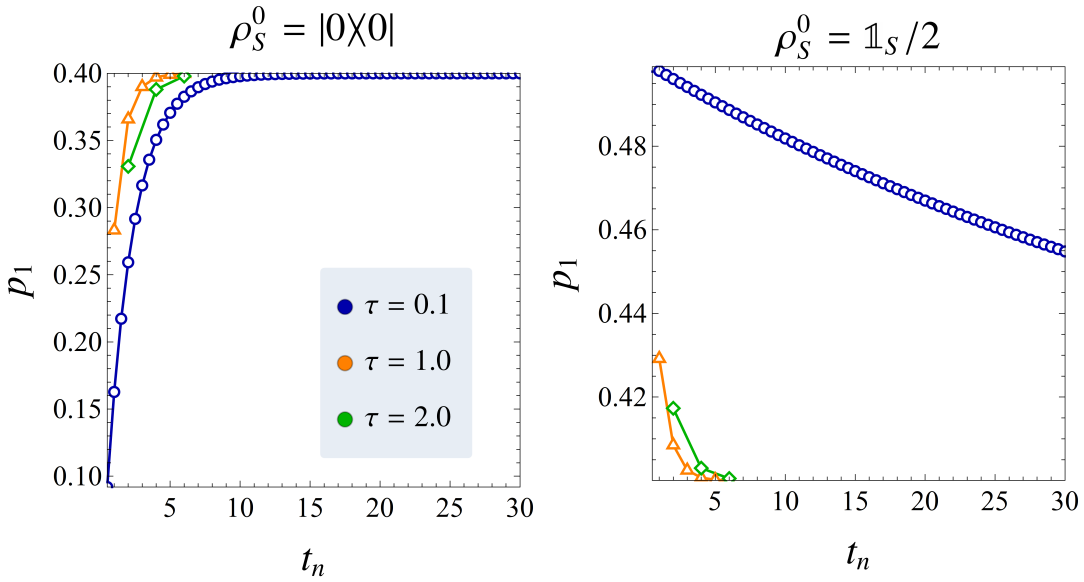

Figure 3.2: Both plots depict the change of the excited state population of a qubit system, p_1, upon sequential collisions with qubit ancillae. In each plot, the system is initialized in a different state. For each choice of collision rate τ and initial state, the system thermalizes; this is witnessed through p_1 which equates the excited state population of the qubit ancillae $\lambda_A = 0.4$. The other parameters are fixed as $g = \omega_A = \omega_S = 1$.

Assumptions (*Thermal Collisional Models*) — Let E label the bath and S the system. The bath is assumed to be such that:

- its Hilbert space is factorized in N identical subspaces $\mathscr{H}_E = \mathscr{H}_A^{\otimes N}$ where N is arbitrarily large;
- its state is factorized as Gibbs states $\rho_E = (\rho_A^{\text{th}})^{\otimes N}$ with $\rho_A^{\text{th}} = e^{-\beta \mathrm{H}_A} / \operatorname{Tr}\{e^{-\beta \mathrm{H}_A}\}$;
- each subsystem (or unit/ancilla) interacts sequentially, identically, once and for all with S for the same duration τ.

As a consequence, the evolution under sequential collisions is Markovian and the map is homogeneous for each rate τ.

Before proceeding on the formal results of CMs, I will introduce a minimal qubit example to illustrate how CMs work.

Example 3.1 (*Minimal qubit model*)**.** I consider a bath given by an assemblage of identical and identically prepared qubits interacting with the system, which is also a qubit. The Hamiltonian

at each collision writes

$$\mathsf{H} = \underbrace{\omega_A \sigma_A^z}_{\mathsf{H}_A} + \underbrace{\omega_S \sigma_S^z}_{\mathsf{H}_S} + \underbrace{g(\sigma_A^- \sigma_S^+ + \sigma_A^+ \sigma_S^-)}_{\mathsf{V}}, \tag{3.5}$$

where $\sigma' s$ are the usual Pauli spin operators. I assume that each ancilla interacts with the system for a fixed time τ and it is initially prepared in thermal state $\rho_A = e^{-\beta_A \omega_A \sigma_A^z}/Z_A$. The simplest way to write such state is in terms of the populations of the ground and excited states $|0\rangle, |1\rangle$, respectively. Defining λ_A as the population of $|1\rangle$, the population of $|0\rangle$ must me $1 - \lambda_A$, so ρ_A is parametrized[1] by

$$\rho_A = \begin{pmatrix} \lambda_A & 0 \\ 0 & 1 - \lambda_A \end{pmatrix}. \tag{3.6}$$

It is common to define the entry $(\rho_A)_{1,1}$ as the ground state's population of the qubit; here I will always set this entry to be the *excited state population* while the entry $(\rho_A)_{2,2}$ corresponds to the ground state's population.

For concreteness, suppose the system starts either at the ground state $|0\rangle\langle 0|$ or at the maximally mixed state $\mathbb{1}_S/2$ and, set $\omega_S = \omega_A = g = 1$. In Fig. 3.2 I plot the population p_1 of the state $|1\rangle\langle 1|$, for a fixed ancilla population $\lambda_A = 0.4$ (which plays the role of temperature). In both cases, the system eventually thermalizes to the temperature of the bath, that is, $p_1 \to \lambda_A$ as collisions accumulate; this situation will prove more general further ahead. For each choice of τ we see that the time to reach the steady-state changes, for very small τ the interactions are weak and the system needs many collisions to thermalize; in particular, at the blue plot for the system starting at $\mathbb{1}_S/2$ we cannot visualize equilibration at the chosen scale of time, for sufficiently large number of collisions.

3.2 Properties of the collisional map $\mathcal{E}$

In this section I discuss the relevant properties of the map $\mathcal{E}$. To understand in the future its thermodynamical properties we need to single out how populations and coherences are processed.

[1] One can solve for β_A, to find $\beta_A = \frac{1}{2\omega_A} \ln\left(\frac{1-\lambda_A}{\lambda_A}\right)$. Up to an energy scale ω_A, we see that temperature is dual to the probability of finding the ancilla at a given level. This shows that for a fixed Hamiltonian H_S every diagonal state with respect to such Hamiltonian can be written as a thermal state. This is a very special property of two-dimensional systems; in general, diagonal states need not to be thermal.

For that sake, some concepts and results from resource theory will be examined in the context of collisional models. They are organized in a mathematical structure for organization and future reference, but by no means intend to be rigorous.

3.2.1 Kraus decomposition

Any CPTP map disposes of a Kraus form. In what follows I derive such representation of $\mathcal{E}$. Consider the basis in which ρ_A is diagonal (non-degenerate), say $\rho_A = \sum_a p_a |a\rangle\langle a|$, and then write the partial trace with respect to such basis

$$\begin{aligned}\mathcal{E}(\rho_S) &= \sum_{aa'} p_a \mathbb{1}_S \otimes \langle a'| (\mathsf{U} |a\rangle\langle a| \otimes \rho_S \mathsf{U}^\dagger) \mathbb{1}_S \otimes |a'\rangle \\ &= \sum_{a,a'} \mathsf{K}_{a,a'} \rho_S \mathsf{K}_{a,a'}^\dagger,\end{aligned} \tag{3.7}$$

where I have defined the so-called Kraus operators $\mathsf{K}_{a,a'} = \sqrt{p_a}\,\langle a|\,\mathsf{U}\,|a'\rangle$, which add to identity $\sum_{aa'} \mathsf{K}_{a,a'}^\dagger \mathsf{K}_{a,a'} = \mathbb{1}_S$.

3.2.2 Steady-states

Through the course of this dissertation, I am mostly interested in the steady-state (SS) behaviour of S. Such state is nothing more than the fixed point of the stroboscopic map, $\mathcal{E}(\rho_S^*) = \rho_S^*$; that is, the state which no longer changes upon further interactions with ancillae

$$\rho_S^* = \mathrm{Tr}_A\{\mathsf{U}(\rho_A \otimes \rho_S^*)\mathsf{U}^\dagger\}. \tag{3.8}$$

Although mathematical results assuring the uniqueness of such states are rare and not always illuminating, all the applications we will be concerned fall under this conjecture and therefore I take it for granted henceforth.

As it is the case of uniqueness, the characterization of the fixed point is not an easy task; for this reason I divide the CPTP map $\mathcal{E}$ in less generic classes. Whichever perk the fixed point may have must be due to the map itself, for its very nature is that of a state reached regardless of the initial conditions. On this wise, there are two pieces of the map that must be observed; the environment states, which are expected to set a trend for the fixed point and the global Hamiltonian H, which can completely disregard such trend or resonate corroborate with

it. Since I have set the unit states to be thermal, if we take the inverse temperature $\beta_A = 1/T_A$ to be higher than that of the system - in the case it has a definite one - the trend shall be that of cooling, unless a very disruptive interaction takes place. Yet, to be able to give further details about ρ_S^* we first need to discuss sub-classes of the map $\mathcal{E}$. The properties of steady-states will follow as direct consequences of the characterizations of the map presented in this section.

3.2.3 Thermal operations

The most well-behaved yet interesting class of interaction is that which conserves the sum of local energies. That is, consider the global Hamiltonian split as

$$\mathsf{H} = \underbrace{\mathsf{H}_S + \mathsf{H}_A}_{\mathsf{H}_0} + \mathsf{V}, \tag{3.9}$$

with an associated unitary $\mathsf{U} = \exp\{-i\tau\mathsf{H}\}$. If we have that $[\mathsf{H}_0, \mathsf{U}] = 0$, meaning that H_0 is a conserved quantity. This is equivalent to $[\mathsf{H}_0, \mathsf{V}] = 0$ for time independent Hamiltonians. To show this, I first need the following formula (see Appendix A):

$$[A, e^B] = \int_0^1 ds e^{(1-s)B}[A, B]e^{sB}. \tag{3.10}$$

Using it in $[\mathsf{H}_0, \mathsf{U}]$

$$[\mathsf{H}_0, e^{-i\tau\mathsf{H}}] = \int_0^1 ds e^{-i\tau(1-s)\mathsf{H}}[\mathsf{H}_0, \mathsf{H}]e^{-i\tau s\mathsf{H}} = \int_0^1 ds e^{-i\tau(1-s)\mathsf{H}}[\mathsf{H}_0, \mathsf{V}]e^{-i\tau s\mathsf{H}}. \tag{3.11}$$

Of course, assuming $[\mathsf{H}_0, \mathsf{V}] = 0$, this is zero. Now let me argue in the opposite direction. Suppose that $[\mathsf{H}_0, \mathsf{U}] = 0$, hence

$$\int_0^1 ds e^{-i\tau(1-s)\mathsf{H}}[\mathsf{H}_0, \mathsf{V}]e^{-i\tau s\mathsf{H}} = 0; \tag{3.12}$$

noting that the commutator is constant and the s-dependent part is always positive[2], the integral over a positive interval is zero only in the case the commutator itself vanishes. So, we have that

> Assuming H is time independent, $[\mathsf{H}_0, \mathsf{U}] = 0 \Leftrightarrow [\mathsf{H}_0, \mathsf{V}] = 0$.

Regardless of the internal structure of S, this class of interactions provide the first set of

[2] More carefully, one uses the spectral decomposition of the exponentials to check the sign element-wise.

relevant results about fixed points. Together with the assumption of thermal environments $\rho_A = e^{-\beta_A \mathsf{H}_A}/Z_A$, we can directly check that the state $\rho_S^{\text{th}} = e^{-\beta_A \mathsf{H}_S}/Z_S$ satisfies $\mathcal{E}(\rho_S^{\text{th}}) = \rho_S^{\text{th}}$ [35], as follows from direct substitution

$$\mathcal{E}(\rho_S^{\text{th}}) = \text{Tr}_A\{\mathsf{U}\underbrace{e^{-\beta_A(\mathsf{H}_A+\mathsf{H}_S)}}_{F(\mathsf{H}_0)}\mathsf{U}^\dagger\}/(Z_A Z_B) = \text{Tr}_A\{e^{-\beta_A(\mathsf{H}_A+\mathsf{H}_S)}\}/(Z_A Z_B) = \rho_S^{\text{th}}, \tag{3.13}$$

where I have used that $[A, B] = 0 \Rightarrow [A, F(B)] = 0$. Then we have the following result:

Thermal fixed points — Consider the map $\mathcal{E}(\bullet) \equiv \text{Tr}_A\{\mathsf{U}(\rho_A^{\text{th}} \otimes \bullet)\mathsf{U}^\dagger\}$ with $\mathsf{U} = e^{-i\tau(\mathsf{H}_0+\mathsf{V})}$. If $[\mathsf{H}_0, \mathsf{V}] = 0$ then $\rho_S^* = \rho_S^{\text{th}}$ with the *same* temperature of ρ_A^{th}.

Another sound implication of thermal operations is energy conservation at the level of eigenvalues, which can be easily shown for non-degenerate spectra. Let us consider the tensor product of eigenbases of H_A and H_S, say $\{|a\rangle \otimes |n\rangle\}$. Now, considering the element $\langle an|\,\mathsf{H}_0\mathsf{U}\,|a'n'\rangle$, the commutator $[\mathsf{H}_0, \mathsf{U}] = 0$ guarantees that $\langle an|\,\mathsf{H}_0\mathsf{U}\,|n'a'\rangle = \langle an|\,\mathsf{U}\mathsf{H}_0\,|a'n'\rangle$ and, thus, $\langle an|\,\mathsf{U}\,|a'n'\rangle\,(a' + n' - a - n) = 0$, where I considered that $\mathsf{H}_0\,|an\rangle = (a+n)\,|an\rangle$. The interpretation of the condition $\langle na|\,\mathsf{U}\,|a'n'\rangle\,(a' + n' - a - n) = 0$ is that the transition $\langle an|\,\mathsf{U}\,|a'n'\rangle$ is only possible in the case that energy conservation holds at the level of eigenvalues $(a' + n' - a - n) = 0$. It then follows that:

Strict energy conservation — Assuming H_0 has a non-degenerate spectrum

$$[\mathsf{U}, \mathsf{H}_0] = 0 \Rightarrow \langle an|\,\mathsf{U}\,|a'n'\rangle \propto \delta(a' + n' - a - n). \tag{3.14}$$

As it is commonly found in quantum mechanics, a conserved quantity furnishes a selection rule for the transitions. This property has been used to understand a series of important thermodynamic phenomena of quantum systems [30, 35, 76] and it means that whatever energy that leaked from either of the parties A and S must have entered the other, at the level of eigenvalues.

Example 3.2. Consider again the minimal qubit model of Example 3.1. Now, we compute the commutator $[\mathsf{H}_0, \mathsf{V}]$ by using that $\mathsf{V} = g(\sigma_A^x\sigma_S^x + \sigma_A^y\sigma_S^y)/2$, and then the Pauli algebra. With that, we conclude

$$[\mathsf{H}_0, \mathsf{V}] = ig(\omega_A - \omega_S)(\sigma_A^y\sigma_S^x - \sigma_A^x\sigma_S^y), \tag{3.15}$$

from which we see that the condition to attain thermal operations is that the qubits are resonant

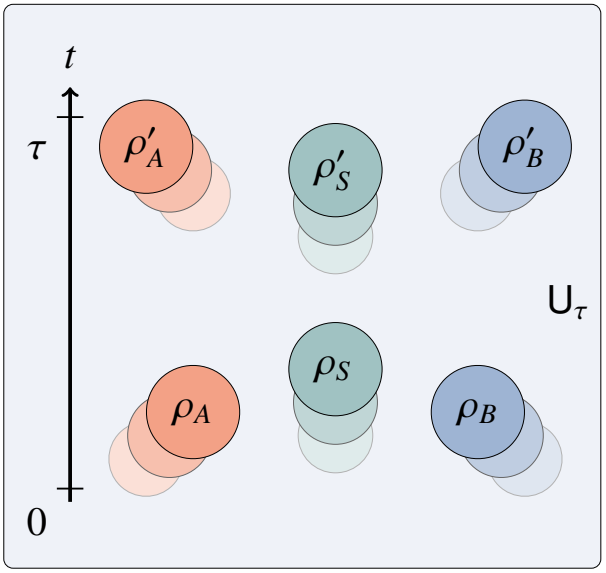

Figure 3.3: Within each time frame, during τ, a single collision accounting for two environments is given by bringing two fresh ancillae, one from bath A and another from bath B, interacting with the system through U_τ and then discarding both ancillae.

with each other. Noting that V is the exchange interaction, we can think about this condition in the following way; the frequencies regulate sizes of system and ancilla gaps and therefore how much energy they can exchange in each collision. Suppose that $\omega_A < \omega_S$; the ancilla would then need to borrow some extra energy from somewhere to provide such difference, the interaction V plays this role.

3.2.4 Two environments

I address now the extension of the strict energy conservation condition and the characterization of steady-states to two environments. Without loss of generality, the two-environment case represents a multiple environment scenario. The first step is to establish another stream of ancillae, say B. One could either choose alternating collisions, for example, setting even collisions between $S-A$ and odd ones between $S-B$, akin to [69]. We will not explore this possibility here. I assume that in each collision both $S-A$ and $S-B$ occur concomitantly; this enables all three parties to get correlated within each collision, although we shall always assume that A and B do not interact directly with each other.

The action of the stroboscopic map is depicted in Fig. 3.3 and redefined by

$$\mathcal{E}(\rho_S) = \mathrm{Tr}_{AB}\{\mathsf{U}(\rho_A^{\mathrm{th}} \otimes \rho_B^{\mathrm{th}} \otimes \rho_S)\mathsf{U}^\dagger\}, \tag{3.16}$$

where $\rho_B^{\text{th}} = e^{-\beta_B \mathsf{H}_B}/Z_B$ (with $\beta_B \neq \beta_A$, in general) and the Hamiltonian involved in U is

$$\mathsf{H} = \underbrace{\mathsf{H}_A + \mathsf{H}_B + \mathsf{H}_S}_{\mathsf{H}_0} + \mathsf{V}_{SA} + \mathsf{V}_{SB}. \tag{3.17}$$

Now, we can again look at the thermal operations regime $[\mathsf{U}, \mathsf{H}_0] = 0$. It is a straightforward generalisation of the single bath case to find

Strict energy conservation (SEC) — For H_0 with non-degenerate spectrum

$$[\mathsf{U}, \mathsf{H}_0] = 0 \Rightarrow \langle abn| \mathsf{U} |a'b'n'\rangle \propto \delta(a' + b' + n' - a - b - n). \tag{3.18}$$

However, this time the above condition does not give an obvious characterization of the steady-state. If you try to use the same thermal state *ansatz*, you can notice that whenever $\beta_A \neq \beta_B$ you cannot form a function of H_0 to follow the same trick used in Eq (3.13). A more modest take is to show that for this given class of maps the steady-state is incoherent, that is, the map $\mathcal{E}$ destroys any off-diagonal element with respect to the eigenbasis of H_S, once applied many times. For this sake we need some machinery concerning coherent processes, which will be discussed below. Note that this assumption is built in the thermal state *ansatz*, but since that worked and we assumed the steady-state to be unique, we did not remark that decoherence was required for thermalization.

Example 3.3. *(Incoherent qubit model)* Consider another bath coupled to the minimal qubit model, whose single-collision Hamiltonian writes

$$\mathsf{H} = \underbrace{\omega_A \sigma_A^z + \omega_B \sigma_B^z + \omega_S \sigma_S^z}_{\mathsf{H}_0} + \underbrace{g(\sigma_A^- \sigma_S^+ + \sigma_A^+ \sigma_S^- + \sigma_B^- \sigma_S^+ + \sigma_B^+ \sigma_S^-)}_{\mathsf{V}}. \tag{3.19}$$

Similar to the single environment case, we have the commutator

$$[\mathsf{H}_0, \mathsf{V}] = ig(\omega_A - \omega_S)(\sigma_A^y \sigma_S^x - \sigma_A^x \sigma_S^y) + ig(\omega_B - \omega_S) i(\sigma_B^y \sigma_S^x - \sigma_B^x \sigma_S^y), \tag{3.20}$$

from which I decide to stay, for now, on resonance, $\omega_A = \omega_B = \omega_S = 1$. Moreover, I set $\tau = 1 = g$ and start the system at the ground state $|0\rangle\langle 0|$. Again, let us look at the behaviour of p_1 as we choose different values of λ_A and λ_B in Fig. 3.4. We find that p_1 will stabilize at a number which corresponds to neither of the bath populations whenever a there is a temperature bias (blue).

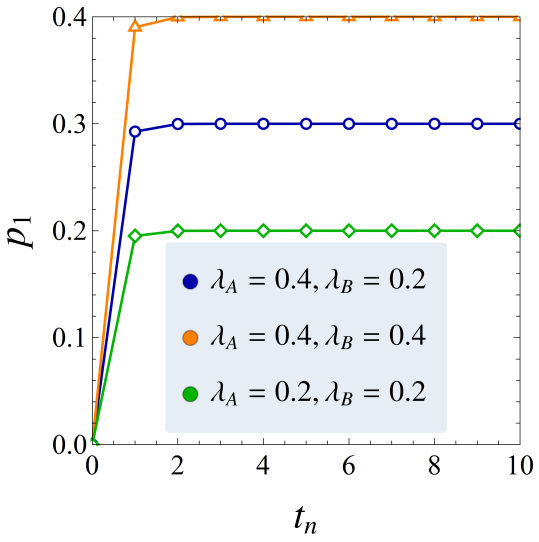

Figure 3.4: The excited state's population of a qubit system in terms of the discrete time steps ($t_n = \tau n$, where n is the number of collisions). The two situations in which both baths are set to equal temperatures (orange and green) lead to equilibrium, as in the one bath case. Yet, once a bias is set (blue), the system occupation does not agree with the occupations of neither of the baths.

3.2.5 Coherence processing

In the last example, we did not look at the dynamics of off-diagonal elements of the system state, yet the way to quantify them is non-trivial. Let me then dedicate some paper to introduce the tools from the resource theory of coherence which are particularly relevant. I follow [34–36], see especially [34] for a comprehensive exposition. In general, resource theories (RTs) concern a pair $(\mathcal{F}, \mathcal{O})$, in which $\mathcal{F}$ stands for free states and $\mathcal{O}$ for free operations. That is, it is all about a set of states which are not resources and operations which can transform between such states without any cost. In the case of coherence, there is a simple way to define free (incoherent) states but a large hierarchy[3] of types of incoherent maps. I will discuss a couple relevant ones, which will be used in the characterization of the stroboscopic map $\mathcal{E}$.

Consider a d-dimensional Hilbert space $\mathscr{H}$, and a Hamiltonian H with non-degenerate, discrete, spectral representation $\sum_n n\,|n\rangle\langle n|$. Let ρ be a state that is $\rho \in \mathscr{T}$ where $\mathscr{T} \subset \mathcal{L}(\mathscr{H})$. A state is said to be incoherent whenever $\rho = \sum_n p_n\,|n\rangle\langle n|$ with $p_n \geq 1$ and $\sum_n p_n = 1$ and whichever state satisfying this property pertains to a subset of states $\mathscr{I} \subset \mathscr{T}$, namely, the *set of incoherent states*.

Similar notions can be established for maps, as follows. I call a map Λ a *maximally incoherent operation* (MIO) if it maps incoherent states into incoherent states. That is, $\rho \in \mathscr{I} \Rightarrow$

[3] See [34, 73] for a complete accounting of incoherent maps.

$\Lambda(\rho) \in \mathscr{I}$. Consider now the *energy* decoherence operator $\Delta(\rho) = \sum_n \langle n|\rho|n\rangle |n\rangle\langle n|$, where $\{|n\rangle\}$ is the eigenbasis of H. Any state can be thought as the sum of a diagonal and off-diagonal parts, so we can always form a generic element of $\mathscr{I}$ by applying Δ to a generic state. Therefore it follows that

Decoherence preserving operations — If $\Lambda(\Delta(\bullet)) = \Delta(\Lambda(\bullet))$ then Λ is a MIO.

I also define an important subset of MIOs, the set of *incoherent operations* (IOs), as the CPTP maps $\Lambda : \mathcal{L}(\mathscr{H}) \to \mathcal{L}(\mathscr{H})$ which not just connect incoherent states to incoherent states, $\rho \in \mathscr{I} \to \Lambda(\rho) \in \mathscr{I}$ but whose arbitrary Kraus components do so. That is, I say that Λ is incoherent if for each j

$$\frac{K_j \rho K_j^\dagger}{\mathrm{Tr}\left\{K_j \rho K_j^\dagger\right\}} \in \mathscr{I}, \tag{3.21}$$

where $\Lambda(\rho) = \sum_j K_j \rho K_j^\dagger$ and $\sum_j K_j K_j^\dagger = \mathbb{1}$.

The sets of IOs and MIOs form a solid background to start introducing coherence quantifiers. For this, I now present a desiderata concerning such quantities. A coherence quantifier $C : \mathscr{T} \to \mathbb{R}$ is expected to satisfy the following properties [34, 36, 74]

1. *Nonnegativity* $C(\rho) \geq 0$, with equality *iff* $\rho \in \mathscr{I}$;
2. *Monotonicity* If Λ is a (M)IO , $C(\Lambda(\rho)) \leq C(\rho) \;\; \forall \rho \in \mathscr{T}$;
3. *Strong-monotonicity* $\sum_i q_i C(\sigma_i) \leq C(\rho)$, where $q_i = \mathrm{Tr}\left\{K_i \rho K_i^\dagger\right\}$ are probabilities associated to Kraus components of Λ and $\sigma_i = K_i \rho K_i^\dagger / q_i$ is are their associated states;
4. *Convexity* $\sum_i p_i C(\rho_i) \geq C\left(\sum_i p_i \rho_i\right)$.

The minimal requirements for a reasonable quantifier are 1 and 2. If C satisfies these, it is so-called a *coherence monotone*. I work with the *relative entropy of coherence*

$$C_{\mathrm{rel}}(\rho) \equiv S(\Delta(\rho)) - S(\rho), \tag{3.22}$$

where $S(\sigma) = -\mathrm{Tr}\{\sigma \ln \sigma\}$ is the von Neumann entropy. The reason is mainly due to its connection with thermodynamical quantities. For IOs it satisfies all four of the latter properties and for MIOs it satisfies all but 3 [34, 36]. From now I will thus reserve the notation $C \equiv C_{\mathrm{rel}}$ for it.

Employing these ideas to the framework of CMs, consider again the stroboscopic map for two baths $\mathcal{E}(\rho_S) = \mathrm{Tr}_{AB}\{\mathsf{U}(\rho_A^{\mathrm{th}}\otimes\rho_B^{\mathrm{th}}\otimes\rho_S)\mathsf{U}^\dagger\}$ and let me assume that $\rho_S \in \mathscr{I} \subset \mathcal{L}(\mathscr{H}_S)$. Note that we are working in the tensor product space spanned by the energy eigenbasis $\{|a\rangle\otimes|b\rangle\otimes|n\rangle\}_{a,b,n}$ but I am interested in coherence with respect to the local basis $\{|n\rangle\}_n$. In such basis, we can write the map in Kraus form

$$\mathcal{E}(\rho_S) = \sum_{aba'b'} p_a p_b \langle a'b'|\,\mathsf{U}\,|ab\rangle\,\rho_S\,\langle ab|\,\mathsf{U}^\dagger\,|a'b'\rangle \equiv \sum_\gamma K_\gamma \rho_S K_\gamma^\dagger, \tag{3.23}$$

where $\gamma = (a, b, a', b')$. If we then assume that the spectrum of H_0 is non-degenerate and $[\mathsf{H}_0, \mathsf{U}] = 0$, we can see that each Kraus component satisfies

$$\langle n'|\,K_\gamma\rho_S K_\gamma^\dagger\,|m'\rangle = p_a p_b p_n \langle a'b'n'|\,\mathsf{U}\,|abn\rangle\langle abn|\,\mathsf{U}^\dagger\,|abm'\rangle \tag{3.24}$$

$$\propto \delta(a'+b'+n'-a-b-n)\delta(a'+b'+m'-a-b-n), \tag{3.25}$$

where the deltas can only be mutually satisfied for $n' = m'$. Given $\rho_S \in \mathscr{I}$, each Kraus component of $\mathcal{E}$ thus produces an incoherent state $K_\gamma\rho_S K_\gamma^\dagger/\,\mathrm{Tr}\left\{K_\gamma\rho_S K_\gamma^\dagger\right\} \in \mathscr{I}$. Together with monotonicity under IOs and 3.2.4, this shows the following

SEC operations are IOs — Let $\mathcal{E}(\bullet) = \mathrm{Tr}_{AB}\{\mathsf{U}(\rho_A^{\mathrm{th}}\otimes\rho_B^{\mathrm{th}}\otimes\bullet)\mathsf{U}^\dagger\}$ be strictly energy preserving, *i.e.*, $[\mathsf{H}_0, \mathsf{U}] = 0$ and H_0 has a non-degenerate spectrum. Then $\mathcal{E}$ cannot increase coherences, that is

$$C(\mathcal{E}(\rho_S)) \leq C(\rho_S)\ \ \forall\rho_S\,. \tag{3.26}$$

This allow us to understand what this map does in terms of coherence processing in a single collision and thereby some properties inherited by the SS. Suppose now the fixed point is unique[4] and that we start subsequent applications of the map $\mathcal{E}$ at an incoherent state, *i.e.*, $C(\rho_S^0) = 0$; since coherence cannot increase, the steady-state must be incoherent. Moreover, should we start the evolution with a coherent state, it would have fully decohered since the fixed-point is unique.

The SS of SEC maps is incoherent — If $\mathcal{E}$ is strictly energy conserving, then its steady-state is incoherent, $\rho_S^* \in \mathscr{I}$.

[4]This will be the case for every case of interest in this dissertation.

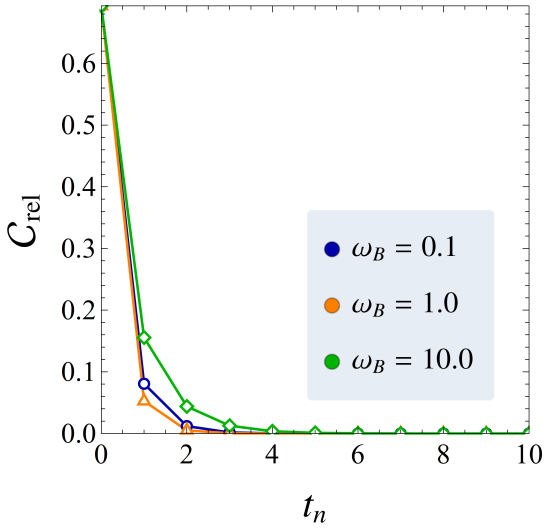

Figure 3.5: Relative entropy of coherence as a function of the time steps .Regardless of the chosen regime (ω_B) we see that coherence decreases very fast as soon as the collisions start.

Example 3.4. Consider again the Example 3.3 and let us study the coherence processing while the system reaches its NESS. I allow now ω's to assume any non-zero value and then, in general, $[\mathsf{H}_0, \mathsf{V}] \neq 0$. For concreteness, I will set $\omega_A = \omega_S = g = \tau = 1$ and the bath populations $\lambda_A = 0.4$ and $\lambda_B = 0.2$. We now observe the behaviour of the relative entropy of coherence in Fig. 3.5, in which I set an initial state manifestly coherent

$$\rho_S^0 = \frac{1}{2}\begin{pmatrix} 1 & 1 \\ 1 & 1 \end{pmatrix}, \tag{3.27}$$

and different choices of ω_B are allowed in the transient process. We see from Fig. 3.5 that coherences vanish whatsoever. Interestingly, for $\omega_B \neq 1$ the commutator $[\mathsf{H}_0, \mathsf{V}] \neq 0$ so we could expect that coherence would survive.

In the future, we will be looking at machines which operate in their steady-state, I would like to have coherence at our disposal at that point. To find a first toy model which displays a coherent steady-state I need to scrutinize the mechanism that prevents coherence to survive, even when energy is not stricly conserved.

The Hamiltonian of Example 3.3 is that of a XX chain with three sites and, remarkably, conserves the total z-spin profile: $[\mathsf{H}, \Sigma_Z] = 0$ with, $\Sigma_Z \equiv \sigma_A^z + \sigma_B^z + \sigma_S^z$ and, therefore, $[\mathsf{U}, \Sigma_Z] = 0$. By considering the *global* symmetry transformation $\mathcal{G}_k(\bullet) \equiv e^{-ik\Sigma_z} \bullet e^{ik\Sigma_z}$, let us see what we learn about $\mathcal{E}$ by transforming the initial state before evolving and tracing out. For this sake,

consider a generic state ρ_S and the modified map

$$\tilde{\mathcal{E}}(\rho_S) = \mathrm{Tr}_{AB}\{\mathcal{U}(\mathcal{G}_k(\rho))\} = \mathrm{Tr}_{AB}\{\mathsf{U}e^{-ik\Sigma_z}(\rho_A^{\mathrm{th}} \otimes \rho_B^{\mathrm{th}} \otimes \rho_S)e^{ik\Sigma_z}\mathsf{U}^\dagger\}. \tag{3.28}$$

Noting that all σ^z's in Σ_z commute with each other we have $e^{ik\Sigma_z} = e^{ik\sigma_A^z} \otimes e^{ik\sigma_A^z} \otimes e^{ik\sigma_S^z}$, and reminding that thermal states commute with these exponentials we conclude that

$$\tilde{\mathcal{E}}(\rho_S) = \mathrm{Tr}_{AB}\{\mathsf{U}(\rho_A^{\mathrm{th}} \otimes \rho_B^{\mathrm{th}} \otimes e^{-ik\sigma_S^z}\rho_S e^{ik\sigma_S^z})\mathsf{U}^\dagger\} = \mathcal{E}(e^{-ik\sigma_S^z}\rho_S e^{ik\sigma_S^z}), \tag{3.29}$$

which calls attention to the *local* symmetry map $\mathcal{Z}_k(\bullet) \equiv e^{-ik\sigma_S^z} \bullet e^{ik\sigma_S^z}$. Going back to Eq. 3.28, we can move the exponential outwards since $[\mathsf{U}, \Sigma_z] = 0$

$$\begin{aligned}
\tilde{\mathcal{E}}(\rho_S) &= \mathrm{Tr}_{AB}\{\mathcal{U}(\mathcal{G}_k(\rho))\} && (3.30)\\
&= \mathrm{Tr}_{AB}\{e^{-ik\Sigma_z}\mathsf{U}(\rho_A^{\mathrm{th}} \otimes \rho_B^{\mathrm{th}} \otimes \rho_S)\mathsf{U}^\dagger e^{ik\Sigma_z}\} && (3.31)\\
&= e^{-ik\sigma_S^z}\,\mathrm{Tr}_{AB}\{U\rho_A^{\mathrm{th}} \otimes \rho_B^{\mathrm{th}} \otimes \rho_S)U^\dagger\}e^{-ik\sigma_S^z} && (3.32)\\
&= e^{-ik\sigma_S^z}\mathcal{E}(\rho_S)e^{-ik\sigma_S^z}, && (3.33)
\end{aligned}$$

where I could use the partial cyclic property in A, B since the exponentials factorize. We have just concluded that $\mathcal{E}(\mathcal{Z}_k(\rho_S)) = \mathcal{Z}_k(\mathcal{E}(\rho_S)) \;\; \forall k \;\; \forall \rho_S$; that is, the global symmetry group $\mathcal{G}_k$ of the unitary $\mathcal{U}$ induces a local symmetry group $\mathcal{Z}_k$ of the CPTP map $\mathcal{E}$.

We can now understand why this map does not lead to a coherent steady-state. The generators of $\mathcal{Z}_k$ commute with the local Hamiltonian $\mathsf{H}_S = \omega_S\sigma_S^z$. The decoherence operator aforementioned, Δ, has a useful representation[5] in terms of the group average $\Delta(\bullet) = K^{-1}\int_0^K ds e^{-is\mathsf{H}_S} \bullet e^{is\mathsf{H}_S}$ with suitable $K \in \mathbb{R}$ [35, 75]. Using the symmetry of $\mathcal{E}$ with respect to $\mathcal{Z}_s$ we can conclude that $\mathcal{E}(\Delta(\rho_S)) = \Delta(\mathcal{E}(\rho_S)) \; \forall \rho_S$, so that decoherence is a symmetry of the map $\mathcal{E}$ and $\mathcal{E}$ is, through the box in pg. 28, a MIO. Fortunately, MIOs also enjoy monotonicity for C and we can understand now that the following holds

[5] To see it, let $e^{-i\mathsf{H}_S} = \sum_n e^{-in}|n\rangle\langle n|$. Then, write $\Delta(\rho_S) = K^{-1}\int_0^K ds \sum_{n,m} e^{-i(n-m)}\langle n|\rho_S|m\rangle|n\rangle\langle m|$. Now, considering the integral representation of the Kroenecker delta $\delta_{nm} = (2\pi)^{-1}\int_0^{2\pi} ds e^{-i(n-m)}$ we see that for $K = 2\pi$ we find $\Delta(\rho) = \sum_n \langle n|\rho_S|n\rangle|n\rangle\langle n|$.

Translationally invariant maps are MIOs — Consider a map $\mathcal{E}$, which disposes of the symmetry property[a] $\mathcal{E}(e^{-ikO_S} \bullet e^{ikO_S}) = e^{-ikO_S}\mathcal{E}(\bullet)e^{ikO_S}$, where $[O_S, \mathsf{H}_S] = 0$, k is arbitrary and H_S is non-degenerate. Then $\mathcal{E}$ is a MIO and, in particular, the relative entropy of coherence is non-increasing with respect to $\mathcal{E}$

$$C(\mathcal{E}(\rho_S)) \leq C(\rho_S)\ \forall \rho_S\,. \tag{3.34}$$

Therefore, under the same assumptions and if the steady-state of $\mathcal{E}$ is unique, such state must also be incoherent.

[a] In fact, this property defines another class of incoherent maps, the so-called *translationally invariant incoherent operations* (TIOs) [34]. Further, commuting with the decoherence operator also defines another class, DIOs [75].

In other words, we do not need SEC to find that the steady-state is incoherent, we just need to find a symmetry transformation which commutes with H_S and decoherence will be present.

We now understand the mechanism which prevents coherence to survive after many interactions. Then, we also know how to circumvent it in the qubit model: we break the σ_S^z symmetry by modifying $\mathsf{H}_S = \omega_S\sigma_S^z \to \omega_S\sigma_S^z + h\sigma_S^x$. In the present case this is rather artificial, but in the application considered Chapter 5 the addition of this kind of term will be physically motivated.

Example 3.5. As mentioned, I now work with the following Hamiltonian

$$\mathsf{H} = \underbrace{\omega_A\sigma_A^z + \omega_B\sigma_B^z + \omega_S\sigma_S^z + h\sigma_S^x}_{\mathsf{H}_0} + \underbrace{g(\sigma_A^-\sigma_S^+ + \sigma_A^+\sigma_S^- + \sigma_B^-\sigma_S^+ + \sigma_B^+\sigma_S^-)}_{\mathsf{V}}, \tag{3.35}$$

where I set the qubits to be resonant and $g = 1$, for simplicity. Let me plot the coherence quantifiers in Fig. 3.6, in which I study only the steady-state regime. At the left hand side we see that, for a fixed bias of $\lambda_A = 0.4$ and $\lambda_B = 0.1$ both coherence measures are zero only for $h = 0$, which corresponds to the the case in which the cummutator $[\mathsf{H}_0, \mathsf{V}] = ih\sigma_A^y\sigma_S^z$ vanishes. The choice of a lower temperature, associated to $\lambda_B = 0.1$ is depicted at the RHS, in which I fix the h so to stay in a possibly coherent regime; we learn that, in varying the bias through λ_B, the coherence tends to vanish. I illustrates that at least one bath at low temperature is an important ingredient to preserve coherences.

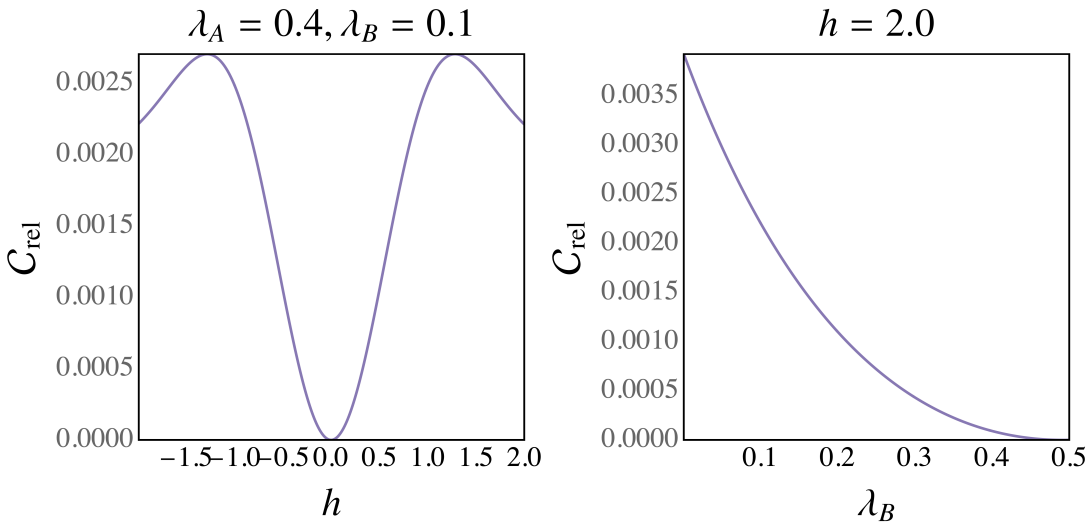

Figure 3.6: At the LHS we see the dependence of SS' coherence with h. At the RHS h is fixed and we see how higher temperatures (higher λ_B's) are detrimental to coherence, where again we observe the SS.

3.3 Local master equations

Finally let me discuss a particular case of collisional models, local master equations. This scenario is interesting for a lot of reasons and indeed remains relevant through the end of this text, since it represents a relevant physical limit of the phenomenology involved in the collisions. However, even when we talk about master equations one should keep in mind that the actual model is frequently not a continuous process, but a discrete number collisions that can be treated effectively as continuous. Indeed, very often other open systems approaches share the such spirit of effective descriptions.

For simplicity, let me start with a single bath. The Hamiltonian I consider is of the form

$$\mathsf{H} = \underbrace{\mathsf{H}_A + \mathsf{H}_S}_{\mathsf{H}_0} + g\mathsf{V}, \tag{3.36}$$

where I have factored out the overall scale of the interaction, g. Supposing that the global initial state is $\rho = \rho_A^{\text{th}} \otimes \rho_S$, and performing the Baker-Campbell-Hausdorff (BCH) expansion (see Appendix A) of the unitary evolution up to second order in time we have

$$e^{-it\mathsf{H}}\rho e^{it\mathsf{H}} \approx \rho - it[\mathsf{H}, \rho] - \frac{t^2}{2}[\mathsf{H}, [\mathsf{H}, \rho]]. \tag{3.37}$$

Tracing out the environment we see that

$$\begin{aligned}\rho_S(t) &\approx \rho_S - \mathrm{Tr}_A\left\{it[\mathsf{H},\rho] + \frac{t^2}{2}[\mathsf{H},[\mathsf{H},\rho]]\right\} \\ &= \rho_S - it[\mathsf{H}_S,\rho_S] - itg\,\mathrm{Tr}_A[\mathsf{V},\rho] - \frac{\tau^2}{2}\mathrm{Tr}_A\{[\mathsf{H}_0 + g\mathsf{V},[\mathsf{H}_0 + g\mathsf{V},\rho]]\},\end{aligned} \tag{3.38}$$

where I have used that $[\rho_A^{\mathrm{th}}, \mathsf{H}_A] = 0$. Let me concentrate for a moment in the term $\mathrm{Tr}_A[\mathsf{V},\rho]$; it is reasonable to assume it has a particular form such as $\mathsf{V} = \mathsf{A}^\dagger \otimes \mathsf{S} + \mathsf{A} \otimes \mathsf{S}^\dagger$, where $\mathsf{A} \in \mathcal{L}(\mathscr{H}_A)$ and $\mathsf{S} \in \mathcal{L}(\mathscr{H}_S)$. The operator A can be either diagonal or off-diagonal with respect to the eigenbasis of ρ_A, if it is off-diagonal the term vanishes once we perform the trace and if it is diagonal then $\mathrm{Tr}_A[\mathsf{V},\rho] = g[\mathsf{W},\rho_S]$, with $\mathsf{W} \equiv \left\langle \mathsf{A}^\dagger \right\rangle_{\mathrm{th}} \mathsf{S} + \langle \mathsf{A} \rangle_{\mathrm{th}} \mathsf{S}^\dagger$. If we now let each collision last $\tau << 1$, we set $t = \tau$. Passing ρ_S to the LHS dividing by τ and taking $\tau \to 0$ we have that

$$\dot{\rho}_S = -i\tau[\mathsf{H}_S + g\mathsf{W},\rho_S]. \tag{3.39}$$

This is the von Neumann equation for a (closed) evolution of S and it incorporates an additional unitary contribution due to W. Yet, it does not does not comprehend dissipation. To do that we need to make the interaction stronger, tuning g so that a piece of the second order term can be effectively of first order in τ. For this sake, I introduce an overall scale as $g \to g/\sqrt{\tau}$, so that

$$\rho_S(\tau) \approx \rho_S - \frac{ig}{\sqrt{\tau}}[\mathsf{W},\rho_S] - ig\tau[\mathsf{H}_S,\rho_S] - g^2\frac{\tau}{2}\mathrm{Tr}_A\{[\mathsf{V},[\mathsf{V},\rho]]\} + O(\tau^{3/2}).$$

Since dividing by τ and taking $\tau \to 0$ would lead to a term facotr $\tau^{-3/2}$ in the term proportional to $[\mathsf{W},\rho_S]$, there is a divergence in the continuum limit. To the best of my knowledge, there is no general way to wipe this divergence, but I shall make some observations about it. First, in a *lot* of cases it vanishes, for example, exchange interactions. Second, as I pointed out earlier, the continuum limit is not a physical situation for the CM, but an effective description; therefore, a divergence just indicates that it is not a good effective description in such case and one should stick with finite τ, while perturbation theory can still be used if τ is small but finite. Thirdly, there are ways to tune the W term so that it remains finite in the continuum limit, as in [33]. Ultimately, it is all a matter of scale.

A relevant case, thoroughly explored in [30][6], is that in which A are so-called eigenoperators

[6] In this reference they assume both S and A to eigenoperators of their respective local energies, but in the present case only the latter is necessary.

of H_A, that is, they satisfy $[\mathsf{A}, \mathsf{H}_A] = \alpha\mathsf{A}$, for some parameter α. If this is true, A has only off-diagonal elements with respect to H_A. Consequently it follows that $\mathsf{W} = 0$. As you can see, a remarkable class of interactions is safe from infinities and in these cases we can write the differential equation

$$\dot{\rho}_S = -i[\mathsf{H}_S, \rho_S] - \frac{g^2}{2}\,\mathrm{Tr}_A\{[\mathsf{V}, [\mathsf{V}, \rho]]\}. \tag{3.40}$$

Let me now explore a concrete example of such dynamics, from which a master equation in the GKSL form will emerge.

Example 3.6. Again, I recall the minimal qubit model with a single bath

$$\mathsf{H} = \underbrace{\omega_A\sigma_A^z + \omega_S\sigma_S^z}_{\mathsf{H}_0} + \frac{1}{\sqrt{\tau}}\underbrace{g(\sigma_A^-\sigma_S^+ + \sigma_A^+\sigma_S^-)}_{\mathsf{V}}, \tag{3.41}$$

where I also introduced the interaction scaling beforehand, as it is usually done in this kind of derivation.

The interaction V is composed of eigenoperators of A, for $[\sigma_A^+, \mathsf{H}_A] = -2\omega_A\sigma_A^+$. According to Eq. (3.40), we are left to work only the dissipative term $\mathcal{D}(\rho_S) = -\,\mathrm{Tr}_A[\mathsf{V}, [\mathsf{V}, \rho_A \otimes \rho_S]]/2$. This double commutator can be rewritten as $[\mathsf{V}, [\mathsf{V}, \rho]] = -2\mathsf{V}\rho\mathsf{V} + \{\mathsf{V}^2, \rho\}$, and we acquire some wisdom computing

$$\mathsf{V}^2 = g^2(\sigma_A^-\sigma_S^+ + \sigma_A^+\sigma_S^-)(\sigma_A^-\sigma_S^+ + \sigma_A^+\sigma_S^-) = g^2(\sigma_A^-\sigma_A^+\sigma_S^+\sigma_S^- + \sigma_A^+\sigma_A^-\sigma_S^-\sigma_S^+), \tag{3.42}$$

where I have used that $\sigma^\pm$ are nilpotent. Note that, in computing the partial trace of $\mathsf{V}^2\rho$, we find $\mathrm{Tr}\left(\sigma_A^+\sigma_A^-\rho_A^{\mathrm{th}}\right) = (1 + \exp\{2\beta_A\omega_A\})^{-1} = \lambda_A$ and, similarly, $\mathrm{Tr}\left(\sigma_A^-\sigma_A^+\rho_A^{\mathrm{th}}\right) = 1 - \lambda_A$. Hence, we obtain

$$\mathrm{Tr}_A\{\mathsf{V}^2, \rho\} = g^2(1 - \lambda_A)\{\sigma_S^+\sigma_S^-, \rho_S\} + g^2\lambda_A\{\sigma_S^-\sigma_S^+, \rho_S\}. \tag{3.43}$$

From hindsight, we can see that

$$\mathrm{Tr}_A\,\mathsf{V}\rho\mathsf{V} = g^2(1 - \lambda_A)\sigma_S^-\rho_S\sigma_S^+ + g^2\lambda_A\sigma_S^+\rho_S\sigma_S^-, \tag{3.44}$$

and, putting all together according to Eq. (3.40) we find

$$\dot{\rho} = -i[\mathsf{H}_S, \rho_S] + \mathcal{D}(\rho_S), \tag{3.45}$$

where $\mathcal{D}$ is a Lindblad dissipator given by

$$\mathcal{D}(\rho_S) = g^2 \left[(1-\lambda_A) \left(\sigma_S^- \rho_S \sigma_S^+ - \frac{1}{2}\{\sigma_S^+ \sigma_S^-, \rho_S\} \right) + \lambda_A \left(\sigma_S^+ \rho_S \sigma_S^- - \frac{1}{2}\{\sigma_S^- \sigma_S^+, \rho_S\} \right) \right].$$

Thereof we conclude that, under appropriate assumptions, the short-time limit of a collisional recovers a GKSL master equation, in accordance with pg. 14.

Beyond this example, it is also true that Eq. (3.40) can be always put in GKSL form. To do that, the recipe is similar to the derivation in Section 2.3: decompose V in a set of orthogonal system operators and then perform the partial trace with respect to the environment [2, 47].

3.4 What is a bath?

The choice of qubit models may raise questions about what kinds of quantum systems deserve the title of a "bath". Let me dedicate some considerations to this topic, in which I also put in perspective the hypotheses behind our CM for the bath (see pg. 20). In what follows, I start by paraphrasing a piece of heuristics, due to Landau [4].

Picture a closed classical system of s particles, described by the phase-space coordinates $(q, p) \equiv (q_1, ..., q_s, p_1, ..., p_s)$. If there are just a few number of particles, one can easily write and solve their equations of motion, provided their initial conditions. Although intrinsically possible, the solution is not virtually achievable in the many-body case; even if one manages to introduce an algorithm to solve the equations, she would still face the problem of knowing all the initial coordinates. The tractability of the few body case can be traced back to the amount of trivial symmetries, orbits, in the phase-space. Consider now the many-body scenario; interactions turn increasingly complex with the system size and a subsystem tends to travel less frequently through a given volume in the phase space $\Delta q \Delta p$. Consequently, it tends to access more sites outside of $\Delta q \Delta p$, to the extent that it loses sight of its initial state. Lest the many-body problem be solved, Landau advocates that the breakdown of these recurrences gives rise to two new kinds of symmetries, but at the level of the statistics.

To reformulate the problem, he resorts to the existence of a *macroscopic subsystem*, but

which is not closed since it is interacting with its vicinity. For concreteness, you can think about $s = 10^{24}$ particles that are divided in 10^{12} subsystems of 10^{12} particles. Such pieces interact in a very complex manner with their surroundings; although solving their reduced dynamics would require solving the global dynamic, if you observe the subsystem for a long time T, the probability of finding it in $\Delta q \Delta p$ can be formulated with respect to the time spent in such volume Δt as $w = \lim_{T\to\infty} \Delta t/T$ and then generalized to the probability density $\varrho(q, p)$ by considering an infinitesimal volume $dqdp$. Remarkably, the statistical ensemble ϱ is independent of the initial conditions. Any statistical average of a physical observable $f(q, p)$ can then be computed once ϱ is known through $\langle f \rangle = \int f(q, p)p(q, p)dpdq$ and this average must agree, by construction, with the time average $\langle f \rangle = \lim_{T\to\infty} T^{-1} \int_0^T f(t)dt$. The nature of such probabilities is extrinsic: they quantify *our* ignorance. This ergotic regime underlies his definition of equilibrium; the condition is established if you can find the observables of all those macroscopic subsystems to have the same mean values, that is, the macroscopic properties of the subsystems to scale with the number of subsystems.

At last, Landau introduces the notion of a system "closed" at the level of statistics. Let us think through weak interactions; suppose that each subsystem is a delimited cube, whose surface is interacting with the surrounding blocks. Then, imagine they are filled with 10^{12} (cubic) particles of unit volume; the ones at the surface represent $\approx 0.06\%$ of the total, hardly influencing the bulk of the subsystem by weakly interacting with other subsystems. On these grounds, Landau claims that such macroscopic subsystems are *quasi-closed*, that is, although interacting with the neighbours affects their deterministic trajectory, the probability distribution of the subsystem remains unaltered to a good extent. Therefore, it is reasonable to assume that each subsystem is statistically independent from the vicinity.

The two new kinds of "symmetries" indicated by Landau are built on the assumptions on page 20 which concern the preparation of the thermal collisional bath. First, the thermalization condition; it requires that the many-body system exhibits a degree of self-similarity, that is, a scaling of the local mean quantities with the system size, as do our locally identical thermal states. Second, the statistical independence condition; orignally introduced by Boltzmann's[7] *Stosszahlansatz* [77, 78], it translates to the CM as the factorization condition of the bath state.

Of course, in the case of quantum mechanics there are further considerations to be made. A deterministic view of the phase-space is even less plausible. Due to Heisenberg's principle,

[7] This name was coined by Paul Ehrenfest.

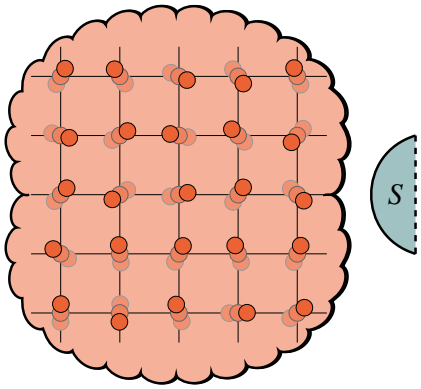

Figure 3.7: Snapshot of a common picture of a bath: a many-body system endowed with ergodicity. In a limiting situation, only the particle closer to S is interacting at a fixed time. In the CM picture, some common reasoning and approximations regarding a thermal bath are implemented *a priori*.

there are no points in phase space and *any* subsystem is eligible to a statistical description, namely a density matrix. Allowing for spin degrees of freedom, we can think of qubit models as effective descriptions in time of the spin degrees, while a sequence of scattering events[8] happens in the background grid of space. As in Fig. 3.7, a finite target[9] S selects only the closest particle of the bath to interact with for a fixed time, after interacting we can consider that the particle completely leaks out or bounces back to the bath to be re-thermalized.

Rather than constrain the applications of CMs, the discussion of Landau's reasoning illustrates one way of thinking about the hypotheses that underlie *thermal collisional baths*. Yet, if one wants to raise some of these requirements, repeated interactions are still suited and simple. Their primitive structure is that of a very general CPTP map and hence it has been used to explore a wealth of applications in the quantum regime. For instance, instead of assuming local equilibrium, the usage of CMs allows the investigation of coherent baths [33]. Further, CMs are also useful in the realm of non-Markovianity [54, 55, 79], in which one can attain such phenomenology by allowing ancillae to be correlated. Finally, CMs are just *a* way to implement baths and often just a means to an end. The choice of such technique is much more related to the theoretical clarity it can provide to thermodynamics, as we shall see in Chapter 4, than whether a bath is a bunch of sequential collisions or not.

[8] For an in-depth discussion of thermalization through sequential scattering see [66].
[9] In scattering problems it is common to assume that the interaction range is rapidly decaying with distance.

Chapter 4

Aspects of quantum thermodynamics

This chapter is concerned with a first conceptual background of Quantum Thermodynamics[1]. Strictly, what is relevant for us is the concept of heat, work and their statistics. Yet, this split of energy is intertwined with informational principles which underlie a central concept in thermodynamics: irreversibility. For this reason, I start the chapter with von Neumann's maximum entropy principle [6], whose informational content was advocated by Jaynes [7, 8]. Once the connection of Gibbs states and information is established, I will discuss the derivation of a generalized form of entropy production [2, 80, 81]; such derivation will provide techniques and ideas which are central to this dissertation, but it does not assume the environments to be in a Gibbs state. Joining these two pieces, I recover the usual statement of the second law and discuss why this suggests a splitting of energy into heat and work. I discuss a few simple examples using the CM framework of Chapter 3.

4.1 The maximum entropy principle

Following von Neumann [6], the so-called maximum entropy principle states that *given a Hamiltonian* H*, the state* ρ *which maximizes the von Neumann entropy* S *for a fixed average energy* $\mathrm{Tr}\{\mathsf{H}\rho\}$ *is a Gibbs state.*

Consider the spectral representation of ρ and H, $\rho = \sum_\nu p_\nu |\nu\rangle\langle\nu|$ and $\mathsf{H} = \sum_n n\,|n\rangle\langle n|$, both non-degenerate, for simplicity. Before I start, I argue that the maximum entropy state must be diagonal in the energy eigenbasis, as sustained in [6]. By contradiction, suppose that ρ is that state of maximum entropy with $E = \mathrm{Tr}\{\rho\mathsf{H}\}$ fixed and, in general, has non-vanishing off-

[1] For a comprehensive reference of the field, see [13].

diagonal elements in the energy eigenbasis; we can always establish a new ensemble $\Delta\rho$ by projectively measuring the energies[2]

$$\Delta\rho = \sum_n \langle n|\rho|n\rangle |n\rangle\langle n| = \sum_{n\nu} p_\nu |\langle \nu|n\rangle|^2 |n\rangle\langle n| . \tag{4.1}$$

Certainly, $\Delta\rho$ has the same average energy of ρ but if $\langle\nu|n\rangle \neq \delta_{\nu n}$, we have erased information about ρ in measuring it in another basis. Intuitively, the entropy S must have increased. Therefore, if ρ is the maximum entropy state for a fixed E it must be diagonal in the energy eigenbasis. In [6] this is shown explicitly for a particular quantum gas, but this reasoning is confirmed by considering the properties of coherence monotones discussed in Chapter 3, as follows. From the property $C_{\text{rel}}(\rho) \geq 0$ announced in pg. 28, we have that $S(\Delta\rho) \geq S(\rho)$ and therefore the decohered version of ρ is always more or equally entropic than ρ, with equality *iff* $\rho = \Delta\rho$. Thus, the maximally entropic state must be incoherent.

Now, let us find the exact structure of p_n such that the state $\rho = \sum_n p_n |n\rangle\langle n|$ maximizes S under the constraints (i) $E = \text{Tr}\{\mathsf{H}\rho\}$ and (ii) $\sum_n p_n = 1$. This is framed as a Lagrange multiplier problem, in which I aim to extremize $S - \lambda(\sum_n p_n - 1) - \beta(E - \text{Tr}(\mathsf{H}\rho))$ with Lagrange multipliers λ, β. We then find the extrema through

$$\frac{\partial}{\partial p_k}\left(-\sum_n p_n \ln p_n - \lambda\left(\sum_n p_n - 1\right) - \beta\left(\sum_n E_n p_n - 1\right)\right) = 0, \tag{4.2}$$

where I used that $S(\rho) = -\sum_n p_n \ln p_n$. Computing the derivatives we find that

$$\ln p_k = -\beta E_k - (\lambda + 1). \tag{4.3}$$

Solving for p_k, we conclude

$$p_k = \text{Const. } e^{-\beta E_k}, \tag{4.4}$$

the constant is fixed by normalization giving $1/Z$, with $Z = \sum_k e^{-\beta E_k}$. The value of β can be determined through theoretical considerations of a given system — for example, the theory of a quantum gas — or through experiments, given the energy E. Moreover, the constant β is, at our choice of units, the so-called inverse temperature of the system.

[2] This is the dephasing map considered in Subsection 3.2.5. It constitutes a CPTP map Λ whose Kraus components are projectors $\{\Pi_n\}_n$; see Section 2.4.

Hence, we concluded that the maximum entropy state is the Gibbs state

$$\rho^{\text{th}} = \frac{e^{-\beta \mathsf{H}}}{Z}, \tag{4.5}$$

in which $Z = \text{Tr}\left(e^{-\beta \mathsf{H}}\right)$ and the average energy can be recovered through $-Z^{-1}\partial_\beta Z = \langle \mathsf{H} \rangle$. Moreover, $F = -\beta \ln Z$ is the equilibrium free energy.

The informational essence of this procedure is the search for the least biased guess of the state of the system, provided scarce information about it [7, 8].

4.2 Irreversibility and generalized second laws

Although often called a theory of heat and work, thermodynamics can be regarded also as a theory of irreversibility. Ultimately, one wants to understand how much heat can be converted into work. As we will see, such work yield is hindered exactly by the amount of irreversibility of a given process. In this section I discuss a generalized formulation of the entropy production [2, 81], the quantifier of irreversibility of a quantum mechanical process. Remarkably, it can be formulated in purely information-theoretical terms, independent of the notions of heat and work.

Suppose there are two quantum systems, prepared in a product state $\rho = \rho_E \otimes \rho_S$, whose non-degenerate spectral representations are $\rho_E = \sum_a p_a \left|a\right\rangle\!\left\langle a\right|$ and $\rho_S = \sum_\nu p_\nu \left|\nu\right\rangle\!\left\langle \nu\right|$. The system is initially measured, undergoes unitary evolution and then it is measured again. Then, we seek to reverse the process and compare the probability distributions obtained for the forward and backward trajectories.

For that sake, I introduce the *two-point measurement* (TPM) protocol [82]. In particular, I perform measurements in both system and environment, the first measurement is at the beginning according to the projector $\Pi_{a\nu} \equiv \left|a\nu\right\rangle\!\left\langle a\nu\right|$ and the second, after unitary evolution U, at an arbitrary local basis $\Pi^*_{a'\nu'} = \left|\psi_{a'}\phi_{\nu'}\right\rangle\!\left\langle \psi_{a'}\phi_{\nu'}\right|$, schematically

$$\rho = \rho_E \otimes \rho_S \xrightarrow{\Pi_{a\nu}} \left|a\nu\right\rangle\!\left\langle a\nu\right| \xrightarrow{\mathsf{U}} \rho' \xrightarrow{\Pi^*_{a'\nu'}} \left|\psi_{a'}\phi_{\nu'}\right\rangle\!\left\langle \psi_{a'}\phi_{\nu'}\right|, \tag{4.6}$$

where $\rho' = \mathsf{U}\rho\mathsf{U}^\dagger$. The probability associated to this process is given by the Born rule

$$P[\gamma] = \text{Tr}\left(\mathsf{U}^\dagger \Pi^*_{a'\nu'} \mathsf{U} \Pi_{a\nu} \rho\right) = p_a p_\nu \left|\left\langle \psi_{a'}\phi_{\nu'}\right| \mathsf{U} \left|a\nu\right\rangle\right|^2, \tag{4.7}$$

in which I introduced the trajectory notation $\gamma = (a, \nu, a', \nu')$. It is noteworthy that the last factor of Eq. (4.7) satisfies all the requirements for a conditional probability $|\langle\psi_{a'}\phi_{\nu'}|\,\mathsf{U}\,|a\nu\rangle|^2 = p(a'\nu'|ab)$ and we can see the Bayes' rule $P[\gamma] = p_a p_\nu p(a', \nu'|a, \nu)$.

We now have to reverse this procedure. Note that the unitary evolution is invertible $\mathsf{U}\mathsf{U}^\dagger = \mathsf{U}\mathsf{U}^{-1} = \mathbb{1}$ and time reversal is equivalent to reversing the sign of time in U. Yet, the measurement process is not.

Any quantum process is composed of two fundamental interventions: measurements and unitary evolution [6]. Since the latter is reversible, measurements are the key to understand irreversibility. In particular, depending on what information we can access, that is, what choice we make about the basis $|\psi_{a'}\phi_{\nu'}\rangle\langle\psi_{a'}\phi_{\nu'}|$ we know more or less about the end of the process and, hence, we can dispose of more information on how to reverse it.

I now make a choice of measurement scheme, to be justified once its implications are established. Let the end-point measurement of the environment be made at the initial basis and for the system I choose the end-point measurement at the basis in which $\rho'_S = \mathrm{Tr}_E\{\mathsf{U}(\rho_E \otimes \rho_S)\mathsf{U}^\dagger\}$ is diagonal. That is, I assume $\Pi^*_{a'\nu'} = |a'\phi_{\nu'}\rangle\langle a'\phi_{\nu'}|$ with $\langle a'\phi_{\nu'}|a\nu\rangle = \delta_{aa'}\langle\phi_{\nu'}|\nu\rangle$. In that manner, I can only reverse the process based on the information acquired through it and then the reverse process begins at $\tilde{\rho} = \rho_E \otimes \rho'_S$[3]. Starting from this state, I perform the reverse TPM. Schematically

$$\tilde{\rho} = \rho_E \otimes \rho'_S \xrightarrow{\Pi^*_{a'\nu'}} |a'\phi_{\nu'}\rangle\langle a'\phi_{\nu'}| \xrightarrow{\mathsf{U}^\dagger} \tilde{\rho}' \xrightarrow{\Pi_{a\nu}} |a\nu\rangle\langle a\nu|\,, \tag{4.8}$$

whose associated probability is

$$\tilde{P}[\gamma] = p_{a'} p^*_{\nu'} |\langle a\nu|\,\mathsf{U}^\dagger\,|a'\phi_{\nu'}\rangle|^2. \tag{4.9}$$

To compare both processes, I introduce

$$\sigma[\gamma] \equiv \ln P[\gamma] - \ln \tilde{P}[\gamma] = \ln \frac{P[\gamma]}{\tilde{P}[\gamma]}. \tag{4.10}$$

This quantity is so-called *stochastic entropy production*; it quantifies the mismatch between a process and its reverse counterpart. Crucially, note that $|\langle a\nu|\,\mathsf{U}^\dagger\,|a'\phi_{\nu'}\rangle|^2 = |\langle\psi_{a'}\phi_{\nu'}|\,\mathsf{U}\,|a\nu\rangle|^2$ so

[3] In other words, the final state is the state produced by the CPTP map $\tilde{\rho} = \Lambda(\rho)$ whose Kraus components are measurement operators $\mathsf{M}_\gamma \equiv \Pi^*_{a'\nu'}\mathsf{U}\Pi_{a\nu}$

that

$$\sigma[\gamma] = \ln \frac{p_a p_\nu}{p_{a'} p^*_{\nu'}} \frac{p(a'\nu'|a\nu)}{\cancel{p(a\nu|a'\nu')}}^{1}. \tag{4.11}$$

We now perform the statistical average of this quantity $\Sigma \equiv \mathbb{E}[\sigma] = \sum_\gamma P[\gamma] \ln\Big(P[\gamma]/\tilde{P}[\gamma]\Big)$.

$$\Sigma = \sum_\gamma (\ln p_a p_\nu - \ln p_{a'} p^*_{\nu'}) p_a p_\nu |\langle \psi_{a'} \phi_{\nu'}| \mathsf{U} |a\nu\rangle|^2 \tag{4.12}$$

$$= \mathrm{Tr}(\rho_E \rho_S \ln \rho_E \rho_S) - \mathrm{Tr}(\rho' \ln \rho_E \rho'_S), \tag{4.13}$$

where $\rho' = \mathsf{U}(\rho_E \otimes \rho_S)\mathsf{U}^\dagger$, I used that $\rho'_S = \sum_{\nu'} p^*_{\nu'} |\phi_{\nu'}\rangle\langle\phi_{\nu'}|$ and $\rho_E = \sum_{a'} p_{a'} |a'\rangle\langle a'|$. Employing the definition of entropy (2.14) we can write

$$\Sigma = -S(\rho') + S(\rho'_S) - \mathrm{Tr}\, \rho'_E \ln \rho_E \pm (S(\rho'_E) + S(\rho'_S)), \tag{4.14}$$

Finally, this expression can be cast as

$$\Sigma = \mathcal{I}_{\rho'}(S : E) + S(\rho'_E || \rho_E), \tag{4.15}$$

where $\mathcal{I}_{\rho'}(S : E) = S(\rho'_S) + S(\rho'_E) - S(\rho')$ is the mutual information and $S(\rho'_E||\rho_E)$ the relative entropy, both introduced in pg. 11. The first term quantifies the informational loss in performing local measurements, *i.e.*, the destruction of correlations of SE state. The second term quantifies the change underwent by the environment, which we could not access due to our choice of basis in E. This formula was first presented in [80] and the above derivation comes originally from [81].

Let me discuss the meaning of our choice of basis. You can think, for example, that the environment is a collisional model and at the end of the process we either discarded the ancilla or it bounced back to the reservoir. In either case, information about the bath state would be hard to track and that is why we perform a measurement in a basis which only requires knowledge about the initial state. Performing the second measurement in the particular basis in which the end-point state is diagonal implies prior knowledge of such basis and, in general, this is an information we do not have about a bath. In practice, measuring in the end w.r.t. the initial basis formalizes formalizes our ignorance about the bath or, equivalently, implements the bath as a highly entropic entity.

More generally, one can also allow the environment to be multipartite, say $\rho_E = \rho_{E_1} \otimes ... \otimes \rho_{E_N}$; in this case we have

$$\Sigma = \mathcal{I}_{\rho' s}(S : E_1 : ... : E_N) + \sum_i S(\rho'_{E_i} \| \rho_{E_i}), \tag{4.16}$$

where $\mathcal{I}_{\rho' s}(S : E_1 : ... : E_N) = S(\rho'_S) + \sum_i S(\rho'_{E_i}) - S(\rho')$ [2].

The expression Σ in Eq. (4.15) is so-called a generalized second law of thermodynamics, once one realizes that both terms can be written as relative entropies (see pg. 11) and therefore are always positive

$$\Sigma \geq 0, \tag{4.17}$$

in which no mention was made to Gibbs states so far.

One may then find it peculiar that another choice of backward process could lead to a different second law. This is indeed the case, and these possibilities are explored in [81]. However, the specific choice I made is the one which treats the environments closer to a thermal bath and is thus suitable to make contact with the usual formulations of the second law, as follows.

First, Eq. (4.15) can be written in another form [2], which emphasizes the splitting between system and environment quantities. For this sake, I explicitly write Eq. (4.15) as

$$\Sigma = S(\rho'_S) + S(\rho'_E) - S(\rho') + \mathrm{Tr}(\rho'_E[\ln \rho'_E - \ln \rho_E]) \tag{4.18}$$

$$= S(\rho'_S) - S(\rho_S) - S(\rho_E) - \mathrm{Tr}(\rho'_E \ln \rho_E), \tag{4.19}$$

where I have considered that $S(\rho') = S(\rho = \rho_E \otimes \rho_S)$. Then, we can recognize that

$$\Sigma = \Delta S_S - \underbrace{\mathrm{Tr}\{(\rho'_E - \rho_E) \ln \rho_E\}}_{\Phi}, \tag{4.20}$$

where $\Delta S_S = S(\rho'_S) - S(\rho_S)$ and Φ is so-called entropy flux. At last, if we introduce the Gibbs state for the environment, we find that the last term writes

$$\Sigma = \Delta S_S + \beta \,\mathrm{Tr}\{\mathsf{H}_E(\rho'_E - \rho_E)\}, \tag{4.21}$$

where H_E is the local Hamiltonian of the environment. Assuming that the environment is at a

maximum entropy state thus renders a special way of entropy flux, proportional to the energy change in the environment. This motivates our definition of *heat*[4]

$$Q_E \equiv \mathrm{Tr}(\mathsf{H}_E(\rho'_E - \rho_E)), \tag{4.22}$$

the energy change in the environment. Therefore we can write the second law in the form

$$\Sigma = \Delta S_S + \beta Q_E \geq 0. \tag{4.23}$$

Notably, Gibbs states are a rather special in the sense that they define an entropy flux directly proportional to the energy flux $\Phi = \beta\,\mathrm{Tr}\{\mathsf{H}_E(\rho'_E - \rho_E)\}$. However, the derivation of Eq. (4.15) suggests that there are other ways to implement our ignorance about the environment and if one adopts our definition of heat with more information about the environment she could have an entropic flux which is not proportional to the energy flux in to the environment.

Equation 4.23 also generalizes to multiple environments [2]. For example, in the case of two environments

$$\Sigma = \Delta S_S + \beta_A Q_A + \beta_B Q_B. \tag{4.24}$$

4.3 The first law and various statements of the second law

I establish now the first law in the context of CMs [29, 30]. One should keep in mind that the reasoning here applied for a single collision is indeed valid for a generic interaction between a system of interest, that is, beyond the CM picture. Starting with a single bath the Hamiltonian reads

$$\mathsf{H}(t) = \mathsf{H}_S(t) + \mathsf{H}_A + \mathsf{V}, \tag{4.25}$$

and then $\mathsf{U} = \mathcal{T}_{>} e^{-i\int_0^\tau dt \mathsf{H}(t)}$, in which I consider a time dependent H_S to account for an external drive. The heat in a single collision is given by

$$Q_A \equiv \mathrm{Tr}\{\mathsf{H}_A(\rho'_A - \rho_A)\}, \tag{4.26}$$

[4]Note that I define heat as positive (negative) if the environment has gained (lost) energy.

where $\rho'_A = \mathrm{Tr}_S\{\mathsf{U}(\rho_A \otimes \rho_S)\mathsf{U}^\dagger\}$ and $\rho_A = \rho_A^{\mathrm{th}}$. Equivalently, heat can be cast in Heisenberg's picture considering the global dynamics

$$Q_A = \mathrm{Tr}\{(\mathsf{H}'_A - \mathsf{H}_A)\rho\}, \tag{4.27}$$

where $\mathsf{H}'_A = \mathsf{U}^\dagger \mathsf{H}_A \mathsf{U}$.

I now define the *internal energy variation* of the system in a similar fashion

$$\Delta U \equiv \mathrm{Tr}\{(\mathsf{H}_S(\tau)\rho' - \mathsf{H}_S\rho\}, \tag{4.28}$$

in which I consider the system Hamiltonian's time dependence evaluated at time zero and τ, $\mathsf{H}_S = \mathsf{H}_S(0)$ and $\mathsf{H}_S(\tau)$ respectively. Equivalently, in Heisenberg's picture

$$\Delta U \equiv \mathrm{Tr}\{(\mathsf{H}'_S - \mathsf{H}_S)\rho\}, \tag{4.29}$$

with $\mathsf{H}'_S = \mathsf{U}^\dagger \mathsf{H}_S(0)\mathsf{U}$. Consider now, in Schrödinger picture, that

$$\frac{d}{dt}\mathrm{Tr}\{\mathsf{H}(t)\rho(t)\} = \cancelto{0}{\mathrm{Tr}\left\{\mathsf{H}(t)\frac{d}{dt}\rho(t)\right\}} + \mathrm{Tr}\{\partial_t \mathsf{H}_S(t)\rho(t)\}, \tag{4.30}$$

where the cancellation comes from von Neumann's equation. That is, since the system is closed, the only average energy variation is due to the time dependence of H. Integrating over the collision duration, we have that

$$\mathrm{Tr}\{\mathsf{H}_A(\rho' - \rho)\} + \mathrm{Tr}\{\mathsf{H}_S(\tau)\rho' - \mathsf{H}_S\rho)\} = \int_0^\tau dt\, \mathrm{Tr}\{\partial_t \mathsf{H}(t)\rho(t)\} - \mathrm{Tr}(\mathsf{V}(\rho' - \rho)). \tag{4.31}$$

Identifying heat, Eq. (4.26), and internal energy, Eq. (4.28), we find

$$Q_A + \Delta U = \mathcal{W}, \tag{4.32}$$

in which work is attributed precisely to their mismatch $\mathcal{W} \equiv \int_0^\tau dt\, \mathrm{Tr}\{\partial_t \mathsf{H}(t)\rho(t)\} + \langle \mathsf{V} - \mathsf{V}(\tau)\rangle$. Whenever $\mathcal{W} > 0$, work has been *injected* into the system and when $\mathcal{W} < 0$ work has been *extracted* from it.

There are two sources of work in the first law, Eq. (4.32); the interaction $\mathcal{W}_{\mathrm{sw}} = \langle \mathsf{V} - \mathsf{V}(\tau)\rangle$, usually referred as the work needed to switch the interaction or drag the ancillae along the

system and another due to an external agent driving the system $\mathcal{W}_{\text{ext}} = \int_0^\tau dt\, \text{Tr}(\partial_t \mathsf{H}_S(t)\rho(t))$. Beyond their simplicity, CMs are useful in the derivation of LMEs also because they are able to spot the switching work and establish the correct energy balance, rendering the derivation consistent with thermodynamics [30]. The regime in which $\mathcal{W}_{\text{sw}} = 0$ is usually associated to weak coupling, and the condition $[\mathsf{H}_A + \mathsf{H}_S, \mathsf{U}] = 0$ can be seen as a way to implement weak coupling *a priori* [76]. Although a lot of applications in thermodynamics concentrate in the work $\mathcal{W}_{\text{ext}}$, in this dissertation I will mostly assume time independent Hamiltonians and therefore this term vanishes, while $\mathcal{W}_{\text{sw}}$ will be considered and mostly referred as just $\mathcal{W}$. I will set H time independent henceforth, unless mentioned.

Equation (4.32) can be combined with (4.24) giving

$$\Delta S_S - \beta(\Delta U - \mathcal{W}) \geq 0. \tag{4.33}$$

which, through dividing by β and introducing the non-equilibrium free energy $\mathcal{F} = \text{Tr}(\mathsf{H}_S\rho_S) - TS(\rho_S)$ gives another common form of the second law

$$\Sigma = \beta(\mathcal{W} - \Delta\mathcal{F}) \geq 0, \tag{4.34}$$

where $\Delta\mathcal{F} = \mathcal{F}(\rho_S') - \mathcal{F}(\rho_S)$.

In the case of multiple environments, one only needs to add more heats to upgrade the first law. For N thermal environments (in a single collision), we have that

$$\sum_i^N Q_i + \Delta U = \mathcal{W}. \tag{4.35}$$

At the steady-state $\rho_S' = \rho_S$ and therefrom $\Delta U = 0 = \Delta S_S$. For instance, in the two-bath case, a steady conversion of heat into work is established as

$$Q_A + Q_B = \mathcal{W}. \tag{4.36}$$

This setup embodies the simplest autonomous heat engine, as depicted in Fig. 4.1.

Now, we can substitute the Eq. (4.36) in the second law in the form of Eq. (4.24) and we

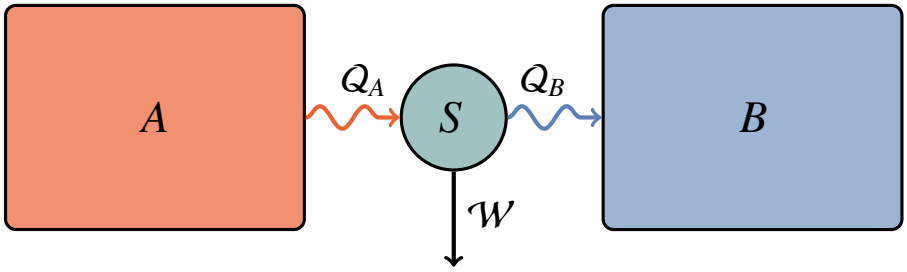

Figure 4.1: An autonomous heat engine exchanges heat with two reservoirs and outputs work at the same time, contrasting with stroke-based engines commonly studied in thermodynamics. Such engines operate in a steady-state, usually out of equilibrium. Heat flow is converted to extracted work ($\mathcal{W} < 0$). Conversely, injecting work ($\mathcal{W} > 0$) can lead to refrigeration.

obtain

$$\Sigma = \beta_A Q_A + \beta_B(\mathcal{W} - Q_A), \tag{4.37}$$

In the absence of work, this leads to Clausius' statement of the Second Law: In the absence of work, heat flows from hot to cold,

$$\left(\frac{1}{T_A} - \frac{1}{T_B}\right) Q_A \leq 0. \tag{4.38}$$

In the presence of work, Eq. (4.37) can be cast as

$$\mathcal{W} = \frac{\beta_B - \beta_B}{\beta_B} Q_A + \frac{1}{\beta_B}\Sigma. \tag{4.39}$$

For concreteness, let me fix $\beta_B \geq \beta_A$, that is, A is the hot bath. In this manner, we can talk about the efficiency $\eta = \mathcal{W}/Q_A$, thus

$$\eta = 1 - \frac{T_B}{T_A} + T_B \frac{\Sigma}{Q_A}. \tag{4.40}$$

According to my sign conventions, the hot bath A has negative Q_A whenever it provides heat to the system. In this manner, we see that the entropy production $\Sigma \geq 0$ is detrimental to the Carnot efficiency $\eta_{\text{Carnot}} = 1 - T_B/T_A$. This amounts to Carnot's statement of the second law: no engine can supersede Carnot's efficiency

$$\eta \leq \eta_{\text{Carnot}}. \tag{4.41}$$

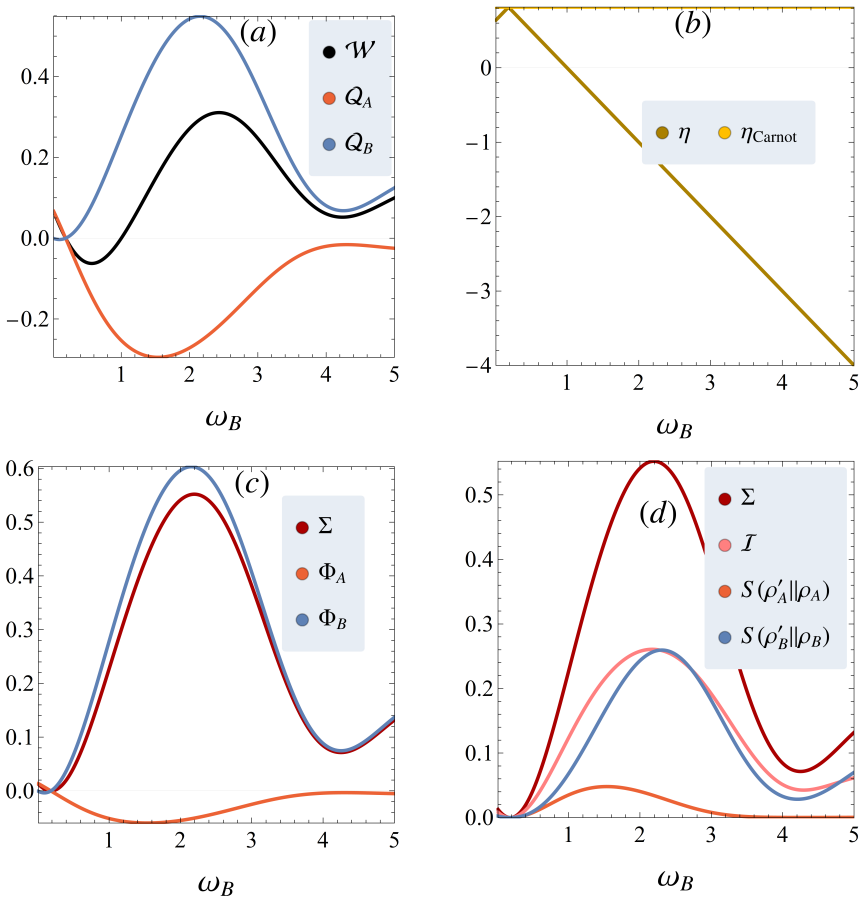

Figure 4.2: Thermodynamics of a minimal non-equilibrium incoherent system. The parameters are set $\omega_A = \omega_S = g = \tau = 1$, $\lambda_A = 0.4$, $\beta_B = \ln(9)/2$ and $\lambda_B = \lambda_B = (1 + e^{2\beta_B\omega_B})^{-1}$. (a) The interplay between heat and work in the steady-state; the system outputs work only when $\omega_B < 1$, further $Q_A \leq 0$ and $Q_B \geq 0$. (b) The efficiency of the machine is always upper bounded by the Carnot limit and deviates linearly from it. (c) Entropy production and its split in entropic fluxes to A and B. (d) The split of entropy production in the form 4.2.

Again, the awareness of the hypothesis underlying the bath is paramount in understanding why entropy production constrains efficiency. Think, for concreteness, of a single ancillary qubit in a thermal state within the CM framework $\rho_A = \text{diag}\{\lambda_A, 1 - \lambda_A\}$. The less we know about in what energy eigenstate the system is, the worst it is to use the energy of the ensemble to perform a specific task. Naturally, such ignorance must somehow restrict the amount of work yielded when using this unit as a an energetic resource.

Example 4.1 (*Qubit incoherent engine*)**.** Let me study the thermodynamics of the qubit model of Example 3.3, in its steady-state. I fix $\omega_A = \omega_S = g = 1$ and the population $\lambda_A = 0.4$. I study the model varying ω_B, while holding $\beta_B = \ln(9)/2$[5] fixed and therefore $\lambda_B = (1 + e^{2\beta_B\omega_B})^{-1}$. At Fig. 4.2 (a) we see the actual behaviour of the steady-state as an engine; the heat flows from

[5]This choice of temperature is such that, at $\omega_B = 1$, $\lambda_B = 0.1$.

hot A to cold B, so that $Q_A \leq 0$ and $Q_B \geq 0$ and whenever the ancillae B have smaller gaps than the system's gap $\omega_B < 1$ there's work being extracted $\mathcal{W} \leq 0$. In the contrary, the system consumes work to maintain the transport $\mathcal{W} \geq 0$.

Complementary, we can see at Fig. 4.2 (b) that Carnot's efficiency is reached only for $\omega_B = 0$, although at this point $\Sigma > 0$ as can be seen from Fig. 4.2 (c). The reason is that at $\omega_B = 0$ we have $T_B = 0$. In any other scenario we do not expect Carnot's efficiency to be reached, since there is always entropy production according to my parameter choices.

On the one hand, Fig. 4.2 (c) depicts Σ split in entropy fluxes. Comparing it with (a) we note that the shape of the cold (blue) heat curve and its corresponding entropic flux are closely related ($\beta_B \approx 1.1$), as they should for maximum entropy states. The same can be seen for the hot bath (orange), considering the prominence of the proportionality constant ($\beta_A \approx 0.2$). On the other hand Fig. 4.2 (d) witnesses the prominent role of global correlations (pink) in entropy production. Moreover, the entropic distances in (d) highlight that cold environments (blue) are much more sensible to the interaction with the system, while the hot one (orange) deviates much less with regards to its equilibrium state.

Now, let us look at an example which, as we saw in Chapter 3, involves a coherent steady-state.

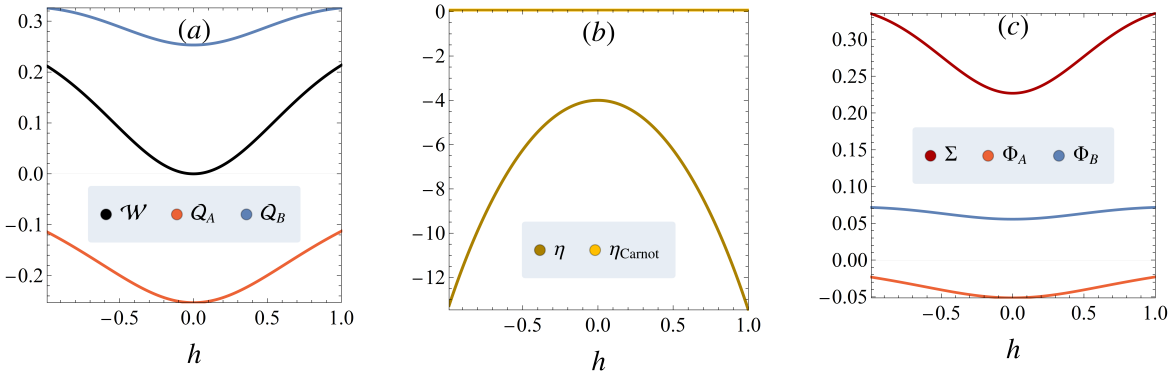

Figure 4.3: Thermodynamics of a minimal non-equilibrium incoherent system. The parameters are set $\omega_A = \omega_B = \omega_S = g = \tau = 1$, $\lambda_A = 0.4$ and $\lambda_B = 0.1$. (a) The average behaviour of heat is such that $Q_A < 0$ and $Q_B > 0$; yet in this case $\mathcal{W} > 0$ coherence thus consumes energy to establish a heat flow. (b) The efficiency is always far from Carnot and worsens as more coherence is introduced $|h| > 0$. (c) Correspondingly, entropy production is always high and bigger for bigger $|h|$.

Example 4.2 (*Qubit coherent engine*)**.** I now work with the same Hamiltonian of Example 3.5, setting $\omega_A = \omega_B = \omega_S = g = \tau = 1$, $\lambda_A = 0.4$ and $\lambda_B = 0.1$. Keep in mind the behaviour of coherence according to h, as depicted in Fig. 3.6 from the previous the Chapter.

The most important aspect of this simple system, according to Fig. 4.3 (a), is that coherence is always consuming work to allow heat to flow. This indicates that, in this setup, it leads to a bad quantum engine. Further, Fig. 4.3 (b) and (c) corroborate with this qualification; in (b) we see that efficiency is far from Carnot, and quadratically far as $|h|$ increases — should you compare it with Fig. 4.2 (b), you will see that the analogous relation is linear and Carnot efficiency is close for low temperature. In (c) we moreover see that entropy production is always high, gets higher as $|h|$ increases and is always above that of Fig. 4.2 (c).

Manipulation of quantum coherence is a primeval urge of Quantum Thermodynamics and although the previous example is useful as an illustration of the formalism, it is not a practical device. We shall go back to minimal qubit models often, but in Chapter 5 I will introduce an actual engine.

4.4 Thermodynamics in the LME limit

Since the discussion of the last sections was oriented towards finite time processes, I complement the general thermodynamic formalism by accounting for the limit of instantaneous processes.

Consider CMs in the limit of LMEs (see Section 3.3). For simplicity, I assume here the interaction between system and ancilla to be of the form $\mathcal{V} = \tau^{-1/2}\mathsf{V}$ with

$$\mathsf{V} = g(\mathsf{A}^\dagger\mathsf{S} + \mathsf{A}\mathsf{S}^\dagger), \tag{4.42}$$

where $[\mathsf{A}, \mathsf{H}_A] = -\omega_A \mathsf{H}_A$ (eigenoperators [30]). I now introduce the instantaneous state variation of a single thermal ancilla A

$$\dot{\rho}_A = -i \lim_{\tau\to 0} \frac{1}{\sqrt{\tau}}[s\mathsf{A}^\dagger + s\mathsf{A}, \rho_A] - i[\mathsf{H}_A, \rho_A] + \mathcal{D}(\rho_A), \tag{4.43}$$

where $s \equiv g\,\mathrm{Tr}(\mathsf{S}\rho_S)$ and $\bar{\mathcal{D}}(\rho_A) = -(1/2)\,\mathrm{Tr}_S\,[\mathsf{V}, [\mathsf{V}, \rho]]$ [6]. Despite the divergence, this expression can be used to define heat rates, since the divergent term will not contribute. This can be seen by considering the definition of heat in Eq. (4.26), diving it by τ and taking the limit

$$\dot{\mathcal{Q}}_A = \mathrm{Tr}(\mathsf{H}_A\dot{\rho}_A) = \mathrm{Tr}(\mathsf{H}_A\mathcal{D}(\rho_A)), \tag{4.44}$$

[6] The upper bar-hat in $\bar{\mathcal{D}}$ distinguishes the ancillae disspator from the system dissipator $\mathcal{D}$

where I have considered $\mathrm{Tr}([\mathsf{H}_A, \rho_A]) = 0$, since $\rho_A = \rho_A^{\mathrm{th}}$ the trace gives $\mathrm{Tr}(\mathsf{A}\rho_A) = 0$ and the total system was initialized in $\rho = \rho_A^{\mathrm{th}} \otimes \rho_S$.

We can now establish the first law at the level of rates, identifying the terms in Eq. (4.30), dividing by τ and taking $\tau \to 0$ we find

$$\dot{Q}_A + \dot{U} = \dot{\mathcal{W}}, \tag{4.45}$$

with $\dot{U} = d/dt\,\mathrm{Tr}(\mathsf{H}_S(t)\rho_S(t))$ and $\dot{\mathcal{W}} = \mathrm{Tr}(\partial_t \mathsf{H}_S(t)\rho_S(t)) - \mathrm{Tr}(\mathsf{V}\dot{\rho}(t))$, in which $\dot{\rho}_S$ is given by the LME for $\rho_S(t)$, as in Eq. (3.40), and $\dot{\rho}$ by the global unitary dynamics. The work rate associated to the interaction can be also written as [30]

$$\dot{\mathcal{W}}_{\mathrm{sw}} = \frac{1}{2}\,\mathrm{Tr}([\mathsf{V}, [\mathsf{V}, \mathsf{H}_A + \mathsf{H}_S\,]]\rho), \tag{4.46}$$

from which it becomes transparent the relation between $[\mathsf{V}, \mathsf{H}_0,] = [\mathsf{U}, \mathsf{H}_0]$[7] and $\mathcal{W}_{\mathrm{sw}}$.

Strict energy conservation guarantees that the energy which leaves the system is exactly the energy which enters the environments. Therefore, at the steady-state ρ_S^* we can compute heats directly from the *system* dissipators

$$\dot{Q}_X = -\,\mathrm{Tr}(\mathsf{H}_S \mathcal{D}_X(\rho_S)), \quad X = A, B, C, \tag{4.47}$$

where the minus sign is placed to convey with my definition of positive heat as energy absorbed by the bath. However, should $[\mathsf{H}_0, \mathsf{V}] \neq 0$, this approach would lead to thermodynamic inconsistencies, since the switching work is not properly book-kept [30]. Still, in the particular case that the *system* Hamiltonian can be decomposed as $\mathsf{H}_S = \mathsf{H}_S^0 + \mathsf{G}$, with $[\mathsf{H}_A + \mathsf{H}_S^0, \mathsf{V}] = 0$ the inconsistencies can be resolved by setting [2]

$$\dot{Q}_A = -\,\mathrm{Tr}\Big(\mathsf{H}_S^0 \mathcal{D}_A(\rho_S)\Big), \tag{4.48}$$

$$\dot{\mathcal{W}} = -\,\mathrm{Tr}(\mathsf{G}\mathcal{D}_A(\rho_S)). \tag{4.49}$$

$$\tag{4.50}$$

[7] Remember, from Chapter 3, that this equality holds for time-independent total Hamiltonians H

In the case of multiple baths, say A, B, we would have

$$\dot{Q}_A = -\mathrm{Tr}\Big(\mathsf{H}_S^0 \mathcal{D}_A(\rho_S)\Big), \tag{4.51}$$

$$\dot{Q}_B = -\mathrm{Tr}\Big(\mathsf{H}_S^0 \mathcal{D}_B(\rho_S)\Big), \tag{4.52}$$

$$\dot{\mathcal{W}} = -\mathrm{Tr}(\mathsf{G}[\mathcal{D}_A(\rho_S) + \mathcal{D}_B(\rho_S)]). \tag{4.53}$$

Entropy production can also be given a rate version. In particular, consider Eq. (4.24), from which

$$\Pi = \dot{S}_S + \beta_A \dot{Q}_A + \beta_B \dot{Q}_B, \tag{4.54}$$

where $\Pi = \dot{\Sigma}$ is the entropy production rate and the entropy variation of the system can be found through second order perturbation theory (see [33], for instance).

Chapter 5

The heat engine of Scovil and Schulz-DuBois

Quantum mechanics was born to explain phenomena in the atomic scale and, at the time of its conception, nobody expected that experimental finesse would reach nowadays' single atom precision. Still, in the mid 20th century a series of technologies based on quantum mechanical descriptions of matter were developed; in particular, the precursor of the laser, the so-called *maser*.

The acronym "maser" stands for *microwave amplification by stimulated emission of radiation*, and its inception is directly related to the manipulation of quantum states in the molecular scale. A simple example of such device is the ammonia maser [83]. Composed of three hydrogens and one nitrogen (NH_3), the molecule is structured in pyramid shape, with three hydrogens in the basis and it can be considered rotating around its tip, where the nitrogen atom lies (see Fig 5.1 (a)). In this configuration, there are two possible states of rotation of the molecule ($|1\rangle, |2\rangle$), which span the energy eigenstates of the molecule ($|\mathrm{I}\rangle, |\mathrm{II}\rangle$). A beam of a NH_3 gas, containing energy eigenstates, can be spatially separated; by passing it through a fast oscillating electric field (see Fig. 5.1 (b)), the excited states (II) are re-directed to another cavity, in which a time-dependent electric field is tuned close to resonance with the ammonia states. If the cavity's geometry is properly adjusted, most of the output molecules will now be in the ground state, having emitted microwave radiation inside the second cavity. Its experimental realization, by Townes, Basov and Prokhorov, culminated in the Nobel Prize of 1964.

The development of small scale devices yet demanded laws to comprehend their efficiency and, further, predict how thermal ensembles, ubiquitous in Nature, could be exploited. In 1959,

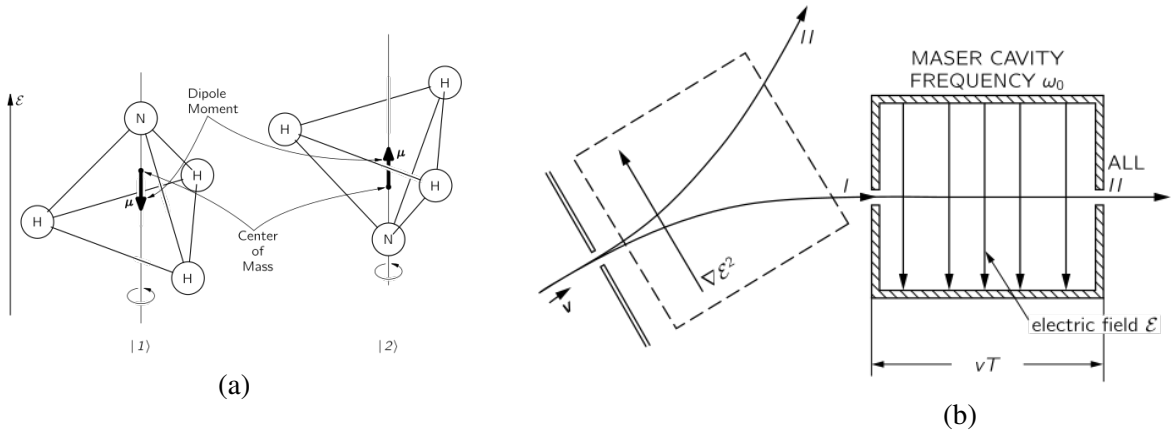

(a) (b)

Figure 5.1: (a) Two states of rotation of the ammonia molecule. Diagram taken from [83] (b) A beam of ammonia gas is passed through a first cavity, subjected to a fast oscillating field which selects excited states (I) . The excited beam interacts with a second cavity, with a time dependent electric field tuned to induce the transition I↔II. Taken from [83].

H. E. D. Scovil and E. O. Schulz-DuBois published a note in Physical Review Letters [32]; in this short document, they remark that a three-level maser could be understood as a heat engine, constrained by Carnot's efficiency. Different from the ammonia maser, in which one has to use a Stern-Gerlach apparatus to filter states which do not emit, their model was capable of operating with a noisy source of energy (heat bath). Furthermore, their thermodynamic analysis of this system singled out the possibility of reversing its operation to achieve refrigeration.

The Scovil and Schulz-DuBois (SSDB) model is considered one of the landmarks of Quantum Thermodynamics and has been largely revisited in recent years [84–92]. In this section, I present the model in fair detail, starting from a quasi-equilibrium analysis, as done originally by Scovil and Schulz-DuBois and then applying the theory of CMs to establish its open system dynamics. In this manner, I discuss the different regimes of operation of this machine and motivate the emergence of quantum coherence in this setup. Variations of this model will be used as prototypical applications of the framework developed in this dissertation, presented in Chapters 7, and 9. Finally, at the end of the Chapter, I discuss other approaches to this system found in the literature of quantum optics and pinpoint the relations with the CM framework.

5.1 Quasi-equilibrium analysis

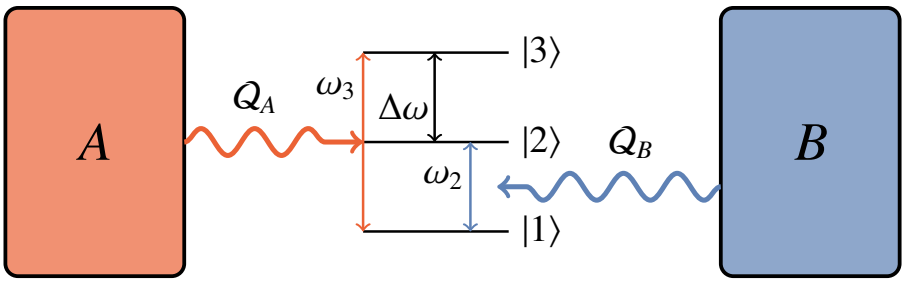

Figure 5.2: SSDB amplifier. The bath frequencies are filtered such that A can only exchange $\pm\omega_3$ quanta with the system and B only $\pm\omega_2$. According to SSDB's argument, if we wait long enough each bath would thermalize with the gap they interact with, leading to vanishing heat in this limit.

Consider a three-level system as in Fig. 5.2, whose levels are described in the basis $\{|i\rangle\}_{i=1,2,3}$. The gap $1 \leftrightarrow 3$ is set as ω_3, that of gap $1 \leftrightarrow 2$ as ω_2 and thus the gap $2 \leftrightarrow 3$ is $\Delta\omega = \omega_3 - \omega_2$. This system is connected to two thermal baths, one hot (A) and one cold (B), which couple to the gaps $1 \leftrightarrow 3$ and $1 \leftrightarrow 2$ respectively [1]. Following [32, 89], I assume there is a filter for the frequencies of each bath; the bath A only allows the exchange of energies $\pm\omega_3$ and, similarly, B only allows the exchange of $\pm\omega_2$. I refer to this assumption as *filtering condition* henceforth. As I will show in Section 5.2, this condition can be implemented using resonant collisional models.

I now look at the populations of each level, namely p_i, considering the coupling to each bath individually. The bath A is supposed to thermalize with the gap between $1 \leftrightarrow 3$, setting $p_3/p_1 = e^{-\beta_A\omega_3}$ and similarly for B, $p_2/p_1 = e^{-\beta_B\omega_2}$. This type of approach, designated *quasi-equilibrium*, bypasses the need to explicitly include thermalization dynamics, hugely simplifying the description. If we want this system to perform as an *engine* — in particular, producing a masing output — the baths must lead to population inversion in the remaining gap, $p_3/p_2 \geq 1$. In practice, a negative effective temperature is pursued. Accordingly, I write

$$\frac{p_3}{p_2} = \frac{p_3}{p_1}\frac{p_1}{p_2} = \frac{e^{-\beta_A\omega_3}}{e^{-\beta_B\omega_2}} = \exp\left\{\beta_B\omega_3\left(\underbrace{1-\frac{\beta_A}{\beta_B}}_{\eta_{\text{Carnot}}} - \frac{\Delta\omega}{\omega_3}\right)\right\}, \tag{5.1}$$

where we identify Carnot's efficiency and moreover $\eta_M \equiv \Delta\omega/\omega_3$ as the maser's efficiency. That is, the gap size of the remaining transition $\Delta\omega$ relative to the gap size of the hot bath ω_3

[1] In the original work of SSDB [32], the convention is slightly different but does not change the phenomenology. Our convention is based on recent works [86, 89].

quantifies the potential output relative to the heat input. Therefore, the masing condition is

$$\eta_M \leq \eta_{\text{Carnot}}. \tag{5.2}$$

Devoid of any dynamics, this simple reasoning predicts that if one manages to thermalize specific transitions of such three level system, the remaining transition is prone to emit. Of course, the actual emission relies on a coupling to a background field, which, in practice, can be assumed to embed the setup.

Conversely, this engine can be reversed, to operate as a refrigerator. Suppose that instead of emitting, we allow the masing transition to absorb quanta, *i.e.*, we pump the transition between 1 and 2 with photons. In this case, such sustained input would lead to refrigeration (bath A heats up and B cools downs), that is, the hot bath heats up and the cold bath cools down.

The above phenomenological discussion is insightful when it comes to applications and preceded techniques such as laser cooling. Yet, it leaves a lot of questions unanswered, such as: is the desired state which produces this effect physically achievable? How? That is, what dynamics leads to masing/refrigeration? We shall now focus on formulating the dynamics of this machine with regards to these questions.

5.2 Collisional model for the three-level maser

In this subsection I develop the dynamical description of the SSDB engine in terms of the CM. To the best of my knowledge, this particular description of the model is an original contribution of this dissertation.

To establish a heat engine based on SSDB's quasi-equilibrium analysis, I start with the system's Hamiltonian

$$\mathsf{H}_S = E_3 \left|3\rangle\langle 3\right| + E_2 \left|2\rangle\langle 2\right| + E_1 \left|1\rangle\langle 1\right|. \tag{5.3}$$

For simplicity I set once and for all $E_1 = 0$ and thus $\omega_2 = E_2$, $\omega_3 = E_3$ and $\Delta\omega = \omega_3 - \omega_2$ and we can then write

$$\mathsf{H}_S = \omega_3 \left|3\rangle\langle 3\right| + \omega_2 \left|2\rangle\langle 2\right|. \tag{5.4}$$

I also define associated ladder operators

$$\mathsf{A} = |1\rangle\langle 3|\,, \qquad \mathsf{A}^\dagger = |3\rangle\langle 1|\,, \mathsf{B} = |1\rangle\langle 2|\,, \qquad \mathsf{B}^\dagger = |2\rangle\langle 1|\,, \tag{5.5}$$

$$\mathsf{C} = |2\rangle\langle 3|\,, \qquad \mathsf{C}^\dagger = |3\rangle\langle 2|\,, \tag{5.6}$$

and a set of x, y components plus the projectors in each level

$$\mathsf{X}_x = \mathsf{X} + \mathsf{X}^\dagger, \tag{5.7}$$

$$\mathsf{X}_y = i(\mathsf{X} - \mathsf{X}^\dagger), \tag{5.8}$$

$$\mathsf{N}_1 = |1\rangle\langle 1| = \mathsf{B}\mathsf{B}^\dagger = \mathsf{A}\mathsf{A}^\dagger, \tag{5.9}$$

$$\mathsf{N}_2 = |2\rangle\langle 2| = \mathsf{C}\mathsf{C}^\dagger = \mathsf{B}^\dagger\mathsf{B}, \tag{5.10}$$

$$\mathsf{N}_3 = |3\rangle\langle 3| = \mathsf{A}^\dagger\mathsf{A} = \mathsf{C}^\dagger\mathsf{C}, \tag{5.11}$$

where $\mathsf{X} = \mathsf{A}, \mathsf{B}, \mathsf{C}$. Although inspired by the Pauli algebra these operators do not satisfy the properties of a Lie algebra (see Appendix B.1 for their algebraic properties).

Now, for the thermal baths, I define two sets of ancillae labeled A and B, associated to the baths as in Fig. 5.2, at thermal states $\rho_X = e^{-\beta_X \mathsf{H}_X}/Z_X$ and

$$\mathsf{H}_X = \frac{\omega_X}{2}\sigma_X^z, \tag{5.12}$$

where $X = A, B$.

For the interaction, it is clear from the quasi-equilibrium analysis that we need a bath A to couple with the gap $1 \leftrightarrow 3$ and the bath B with $1 \leftrightarrow 2$ and also that we do not want the baths to interact with each other, so that $\mathsf{V} = \mathsf{V}_A + \mathsf{V}_B$. Yet, the precise form of the potential which attain the desired phenomenology of an engine or refrigerator is unclear and we shall then start by a substantially general one. In spin chains, it is common to consider the XY interaction [93], given by

$$\mathsf{V}_{XY} = \sum_{i=1}^{N} \frac{1+\eta}{2}\sigma_i^x\sigma_{i+1}^x + \frac{1-\eta}{2}\sigma_i^y\sigma_{i+1}^y, \tag{5.13}$$

which generalizes the transverse field ising model (TFIM), $\eta = 1$, and the XX Hamiltonian $\eta = 0$ for a chain of N sites. Inspired by this quite general interaction structure, I start by

considering the interactions of the form

$$\mathsf{V}_X = g_X\left(\frac{1+\eta}{2}\sigma_X^x \mathsf{X}_x + \frac{1-\eta}{2}\sigma_y^x \mathsf{X}_y\right) \quad ,\mathsf{X} = \mathsf{A},\mathsf{B} \quad ,X = A,B. \tag{5.14}$$

We then have that

$$\mathsf{H} = \mathsf{H}_0 + \mathsf{V}, \tag{5.15}$$

$$\mathsf{H}_0 = \frac{\omega_A}{2}\sigma_A^z + \frac{\omega_B}{2}\sigma_B^z + \omega_3\mathsf{N}_3 + \omega_2\mathsf{N}_2, \tag{5.16}$$

$$\mathsf{V} = \frac{1+\eta}{2}\left(g_A\sigma_A^x\mathsf{A}_x + g_B\sigma_B^x\mathsf{B}_x\right) + \frac{1-\eta}{2}\left(g_A\sigma_A^y\mathsf{A}_y + g_B\sigma_B^y\mathsf{B}_y\right). \tag{5.17}$$

To understand the energetic balance of such system, it is illuminating to compute the commutator (see Appendix B.2 for details)

$$\begin{aligned}[\mathsf{H}_0,\mathsf{V}] = {} & ig_A\left[\left(\omega_3\frac{1+\eta}{2} - \omega_A\frac{1-\eta}{2}\right)\sigma_A^x\mathsf{A}_y - \left(\omega_3\frac{1-\eta}{2} - \omega_A\frac{1+\eta}{2}\right)\sigma_A^y\mathsf{A}_x\right] \\ & + ig_B\left[\left(\omega_2\frac{1+\eta}{2} - \omega_B\frac{1-\eta}{2}\right)\sigma_B^x\mathsf{B}_y - \left(\omega_2\frac{1-\eta}{2} - \omega_B\frac{1+\eta}{2}\right)\sigma_B^y\mathsf{B}_x\right].\end{aligned} \tag{5.18}$$

Setting $\eta = 0$ (XX), the resonance condition is such that $\omega_A = \omega_3$ and $\omega_B = \omega_3 - \omega_2$, in which case the interaction does not inject or extract work. It is indeed true that this is the only conservative case. To see this, it suffices to solve for the coefficients

$$\omega_3(1+\eta) = \omega_A(1-\eta), \tag{5.19}$$

$$\omega_3(1-\eta) = \omega_A(1-\eta), \tag{5.20}$$

which requires that

$$(1-\eta)^2 = (1+\eta)^2, \tag{5.21}$$

whose only solution is $\eta = 0$. The filtering condition suggested by SSDB's quasi-equilibrium analysis is translated here as the resonance condition $\omega_A = \omega_3$ and $\omega_B = \omega_3 - \omega_2$. Equation (5.19) also implies that, on resonance, any interaction with $\eta \neq 0$ may lead to $\mathcal{W} \neq 0$ once $[\mathsf{H}_0,\mathsf{V}] \neq 0$ implies that V is not conserved and $\mathcal{W} = \langle \mathsf{V} - \mathsf{V}(t)\rangle$, as discussed in Section 4.3.

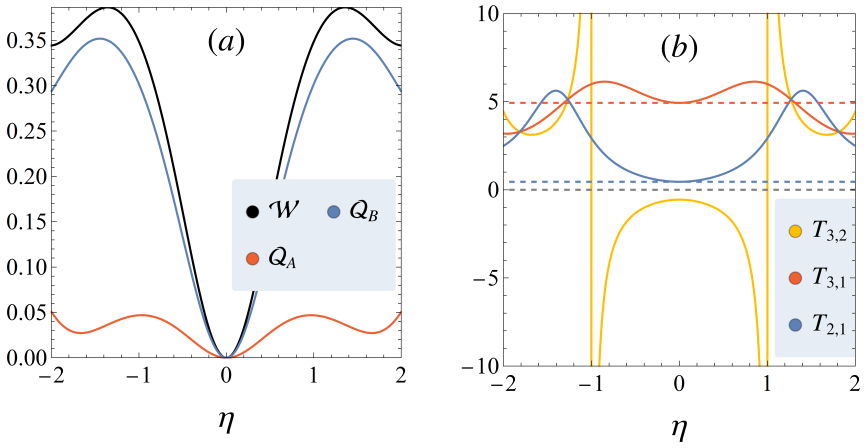

Figure 5.3: SSDB's heat engine, with $\lambda_A = 0.4$, $\lambda_B = 0.1$, $g_A = g_B = \tau = \omega_B = \omega_2 = 1$ and $\omega_3 = 2$. (a) The machine's operation, for $\eta = 0$ we see that indeed no current flows and work is zero, otherwise the interaction demands energy and ends up heating up both baths. (b) The effective temperature associated to each system gap ($T_{2,1} = \omega_2(\ln p_2/p_1)^{-1}, T_{3,1} = \omega_3(\ln p_3/p_1)^{-1}, T_{3,2} = (\omega_3-\omega_2)(\ln p_3/p_2)^{-1}$). The dashed lines represent the *bath* temperatures. We observe population inversion ($T_{3,2} < 0$) for every value $\eta \in (-1, 1)$ and it diverges before changing sign, at $\eta = -1, 1$.

What is still non-obvious from the above is whether such work can be extracted ($\mathcal{W} < 0$) or not, in which case I resort to Fig. 5.3 (a). In it, I set $\lambda_A = 0.4$, $\lambda_B = 0.1$, $g = \tau = \omega_B = \omega_2 = 1$ and $\omega_A = \omega_3 = 2$. We can see that for any choice of η the system consumes work to maintain its steady-state operation, except for $\eta = 0$.

Still for the same setup, Fig. 5.3 (b) shows the effective temperature associated to each system gap ($T_{2,1} = \omega_2(\ln p_2/p_1)^{-1}, T_{3,1} = \omega_3(\ln p_3/p_1)^{-1}, T_{3,2} = (\omega_3 - \omega_2)(\ln p_3/p_2)^{-1}$) as solid lines and, to check SSDB's quasi-equilibrium argument, dashed lines indicate the baths' temperatures. In accordance with SSDB's inspection, the system's levels which are coupled to the baths act as locally thermal, with always positive temperature while $T_{3,2}$ is inverted between $\eta = -1$ and $\eta = 1$. However, they are not always perfectly thermalized with the environments as assumed in the original paper [32]; the only case when $\mathcal{W} = 0 = \mathcal{Q}_A = \mathcal{Q}_B = 0$ (Fig. 5.3 (a)) is for $\eta = 0$ which coincides with the point in (b) where dashed lines meet solid lines. Remarkably, this shows that SSDB's static argument is much more than a phenomenological approximation: it is an *ansatz* for the steady-state precisely when $[\mathsf{H}_0, \mathsf{U}] = 0$. Now that I have discussed the role of η, I will fix $\eta = 0$ henceforth. That is

$$\mathsf{V}_X = \frac{g_X}{2}\left(\sigma_X^x \mathsf{X}_x + \sigma_y^y \mathsf{X}_X\right) = g_X(\sigma_X^- \mathsf{X}^\dagger + \sigma_X^+ \mathsf{X}), \quad \mathsf{X} = \mathsf{A}, \mathsf{B} \quad X = A, B. \tag{5.22}$$

Let me also elaborate on what I referred to as an steady-state ansatz. Consider again the

local Hamiltonian given by Eq. (5.16) and two thermal ancillae states $\rho_X^{\text{th}} = e^{-\beta_X \mathsf{H}_X}/Z_X$, $X = A, B$. They interact with the system through the interactions in Eq. (5.22), giving rise to

$$\mathcal{E}(\rho_S) = \text{Tr}_{AB}\{\mathsf{U}(\rho_A^{\text{th}} \otimes \rho_B^{\text{th}} \otimes \rho_S)\mathsf{U}^\dagger\}, \tag{5.23}$$

where $\mathsf{U} = e^{-i\tau\mathsf{H}}$ and $\mathsf{H} = \mathsf{H}_0 + \mathsf{V}$. Now, I define a candidate for steady-state based on SSDB's argument; this can be summarized by solving for p_1 the following equations

$$p_1 + p_2 + p_3 = 1, \tag{5.24}$$

$$p_3 = e^{-\beta_A \omega_3} p_1, \tag{5.25}$$

$$p_2 = e^{-\beta_B \omega_2} p_1, \tag{5.26}$$

where I set $p_i \equiv \langle i|\rho_S|i\rangle$. Under these conditions we find

$$\rho_S = \frac{1}{e^{-\beta_A\omega_3} + e^{-\beta_B\omega_2} + 1} \begin{pmatrix} 1 & 0 & 0 \\ 0 & e^{-\beta_B\omega_2} & 0 \\ 0 & 0 & e^{-\beta_A\omega_3} \end{pmatrix}, \tag{5.27}$$

where I have also used the fact that under strict energy conservation the steady-state is incoherent, and thus any candidate too. Since we have $[\mathsf{H}_0, \mathsf{V}] = 0$,

$$\mathcal{E}(\rho_S) = e^{-i\tau\omega\mathsf{H}_S}\,\text{Tr}_{AB}\{e^{-i\tau\mathsf{V}}(\rho_A^{\text{th}} \otimes \rho_B^{\text{th}} \otimes \rho_S)e^{+i\tau\mathsf{V}}\}e^{+i\tau\omega\mathsf{H}_S}, \tag{5.28}$$

where, for resonance, I set $\omega_A = \omega_B = \omega_S = \omega$. Each term in Eq. (5.28) can be solved analytically for τ, g_A, g_B arbitrary, even though the expressions are cumbersome. Direct substitution of the candidate in Eq. (5.27) inside Eq. (5.28) shows that this state is indeed invariant, $\mathcal{E}(\rho_S) = \rho_S$. Surprisingly, this is true for any τ and any coupling strengths g_A, g_B, which can be checked using Mathematica.

5.3 The role of photons: refrigeration and amplification

In this Section, I insert the SSDB amplifier studied in the last Section in an optical cavity. I will show how this leads to the creation of photons in the cavity, and, conversely, that if we initialize the cavity with a thermal ensemble we can consume it to achieve refrigeration in the case that

the cavity's temperature is higher than the hot bath's temperature. Moreover, I show that we need a coherent SS *in the amplifier* to achieve a coherent ensemble of light in the cavity, *i.e.*, actual maser light.

The complete maser is constituted by the three-level system *and* a cavity. I now include an optical cavity, with mode ω_C, which will prepare an ensemble of photons. The complete scenario can be visualized in Fig. 5.4.

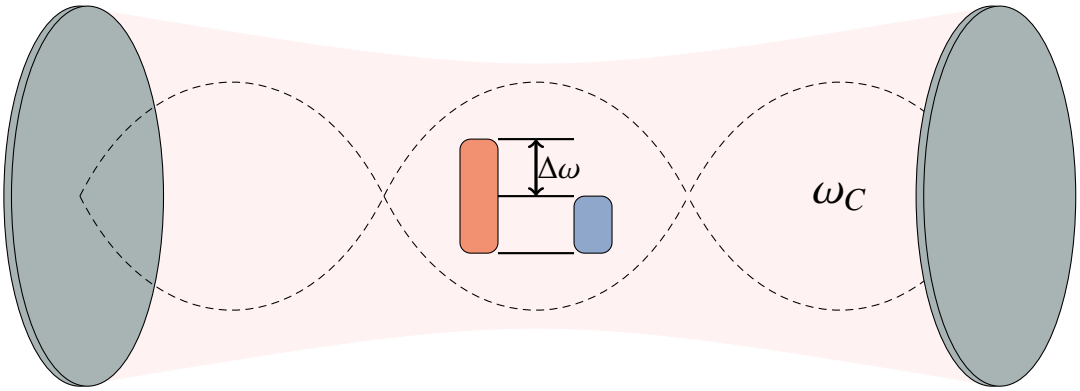

Figure 5.4: Physical implementation of the SSDB engine. The three-level engine is capable of emitting quanta to the cavity with frequency $\Delta\omega = \omega_3 - \omega_2$, if we tune the cavity to be resonant with that frequency the photons will be trapped inside it and the photon population will increase as heat flows through the atom. Eventually, the photons trapped inside the cavity can be leaked out by letting one of the mirrors be semi-transparent. Moreover, if we consider a high enough cavity temperature we can revert the operation of this engine, injecting quanta through the gap $2 \leftrightarrow 3$ and forcing heat to flow from the hot (orange) bath to the cold (blue) bath.

The cavity will be considered a stream of Gibbs states $\rho_C^{\text{th}} = \dfrac{e^{-\beta_C \mathsf{H}_C}}{Z_C}$, with a local Hamiltonian

$$\mathsf{H}_C = \omega_C a^\dagger a, \tag{5.29}$$

hence accounting for a possibly non-zero temperature inside the cavity. This description is in accordance with [94], in which a complete picture of quantum optics was built in the CM framework, by discretizing the electromagnetic field in times-bins; in this view, thermal radiation fields reduce to streams of bosonic Gibbs states. For simplicity, I will assume resonance conditions $\omega_A = \omega_3$ and $\omega_B = \omega_2$. At a first moment, I will look at the LME limit of the collisional model, once it is simpler to build thermodynamic insight on these grounds. The interaction with the cavity will also be an XX interaction, which I write in the form

$$\mathsf{V}_C = g_c(a^\dagger \mathsf{C} + a\mathsf{C}^\dagger), \tag{5.30}$$

analogous to the Jaynes-Cummings interaction.

You can expect from our discussion of the interaction that the resonance condition with the cavity is that $\omega_C = \Delta\omega$ and, thus, it will be fixed in that manner, I refer to B.2 for detailed calculations on the strict energy conservation. Under these conditions, we thus have $[\mathsf{H}_0, \mathsf{V}] = 0$, where now $\mathsf{V} = \mathsf{V}_A + \mathsf{V}_B + \mathsf{V}_C$. Re-scaling the interaction, $\mathsf{V} \to \tau^{-1/2}\mathsf{V}$, and initializing the evolution with $\rho = \rho_A^{\text{th}} \otimes \rho_B^{\text{th}} \otimes \rho_C^{\text{th}} \otimes \rho_S$, I consider the $\tau << 1$ expansion of $\delta\rho \equiv \mathsf{U}\rho\mathsf{U}^\dagger - \rho$ which gives

$$\delta\rho = -i\tau[\mathsf{H}_0 + \tau^{-1/2}\mathsf{V}, \rho] - \frac{\tau}{2}[\mathsf{V}, [\mathsf{V}, \rho]], \tag{5.31}$$

where $\mathsf{H}_0 = \mathsf{H}_A + \mathsf{H}_B + \mathsf{H}_C$ taking the trace w.r.t. A, B, C, since the environments are thermal, the divergence vanishes. The open system dynamics of S is then described by

$$\dot{\rho}_S = -i\tau[\mathsf{H}_S, \rho_S] - \frac{1}{2}\,\mathrm{Tr}_{ABC}([\mathsf{V}, [\mathsf{V}, \rho]]). \tag{5.32}$$

The calculation of the dissipative terms is not particularly illuminating and thus left to the appendix B.3; it renders the GKSL form

$$\dot{\rho}_S = -i[\mathsf{H}_S, \rho_S] + \mathcal{D}_A(\rho_S) + \mathcal{D}_B(\rho_S) + \mathcal{D}_C(\rho_S), \tag{5.33}$$

$$\mathcal{D}_A(\rho_S) = \gamma_A(1 - \lambda_A)L[\mathsf{A}] + \gamma_A\lambda_A L[\mathsf{A}^\dagger], \tag{5.34}$$

$$\mathcal{D}_B(\rho_S) = \gamma_B(1 - \lambda_B)L[\mathsf{B}] + \gamma_B\lambda_B L[\mathsf{B}^\dagger], \tag{5.35}$$

$$\mathcal{D}_C(\rho_S) = \gamma_C(\bar{n} + 1)L[\mathsf{C}] + \gamma_C\bar{n}L[\mathsf{C}^\dagger], \tag{5.36}$$

where $L[\mathsf{X}] \equiv \mathsf{X}\rho_S\mathsf{X}^\dagger - 1/2\{\mathsf{X}^\dagger\mathsf{X}, \rho_S\}$, λ_X is the excited population of qubit $X = A, B$ and $\bar{n} = (e^{\beta_C\omega_C} - 1)^{-1}$ is the Bose occupation of the cavity. Moreover, I set $\gamma_X = g_X^2, X = A, B, C$. Since $[\mathsf{H}_0, \mathsf{V}] = 0$ and the system is not driven externally, we have

$$\dot{U} = \dot{Q}_A + Q_B + Q_C, \tag{5.37}$$

and, in the steady-state

$$\dot{Q}_C = -(\dot{Q}_A + \dot{Q}_B). \tag{5.38}$$

The condition for creating photons in the cavity is that $\dot{Q}_C > 0$ and the condition for refrigeration

is that $\dot{Q}_B < 0$.

The refrigeration regime can now be spotted through a quasi-equilibrium analysis too. Following [89], suppose that the coupling to the cold bath is small, $\gamma_B \approx 0$. Then, we pretend the gaps are thermalized with the hot and cavity gaps, so that we can write

$$\frac{p_2}{p_1} = \frac{p_3 p_2}{p_1 p_3} = e^{-\beta_A \omega_A - \beta_C \omega_C} \equiv e^{-\beta_\nu \omega_B}, \tag{5.39}$$

which defines an effective temperature to the gap weakly coupled to the cold bath

$$T_\nu = \beta_\nu^{-1} = \frac{\omega_2}{\beta_A \omega_3 - \beta_C(\omega_3 - \omega_2)}. \tag{5.40}$$

To make heat flow from the cold bath to the system, we just need then to assure that this effective temperature is colder than the cold bath's temperature. It is a matter of choosing the parameter region correctly. The original SSDB's argument for the maser is the analogous, but assumes that the coupling to the *cavity* is negligible.

Let me then fix $\gamma_B = 0.1, \gamma_A = \gamma_C = 1.0, T_A = 5, T_B = 1, \omega_3 = 5, \omega_2 = 0.1$. Under these conditions, we have that

$$T_\nu \approx \frac{0.1}{1 - 5\beta_C}, \tag{5.41}$$

which for refrigeration has to be smaller than $T_B = 1$. It is exactly one when $T_C = 50/9$, and a sharp transition from negative to positive temperatures (T_ν) happens at $T_C = 5$. This transition drastically changes the heat current to the cavity, as we verify in Fig. 5.5.

We have now concluded that this device can indeed operate either emitting photons to the cavity (and hence functioning as a maser) or consuming cavity's thermal radiation to operate as a refrigerator. I shall focus henceforth in the masing regime, in which case we still have to understand what kind of light is produced. This can be verified by looking at the reduced dynamics of C. For that sake, I perform the partial trace of Eq. (5.31) w.r.t. A, B, S; this will then give us the reduced dynamics of the cavity only

$$\delta\rho_C = -i[\mathsf{G}_C, \rho_C] - i\tau[\mathsf{H}_C, \rho_C] - \frac{\tau}{2}\,\mathrm{Tr}_{ABS}[\mathsf{V}, [\mathsf{V}, \rho]], \tag{5.42}$$

where $\mathsf{G}_C = a^\dagger \,\mathrm{Tr}(\mathsf{C}\rho_S) + a^\dagger \,\mathrm{Tr}\big(\mathsf{C}^\dagger \rho_S\big)$. The dissipative term $[\mathsf{V}, [\mathsf{V}, \rho]]$ acts by modifying the diagonal elements of the density matrix (populations) and is thus unable to produce coherence.

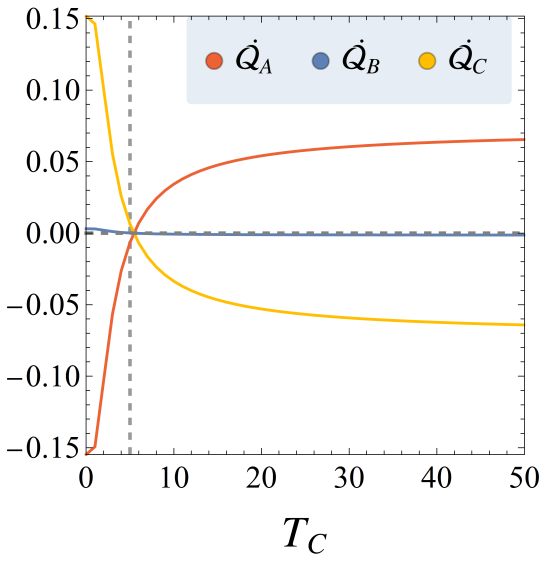

Figure 5.5: Steady-state operation of the SSDB engine for $\gamma_B = 0.1, \gamma_A = \gamma_C = 1.0, T_A = 5, T_B = 1, \omega_3 = 5, \omega_2 = 0.1$. The dashed vertical line is $T_C = 5$ and the dashed horizontal line is zero. We witness creation of photons for $T_C < 5$ ($\dot{Q}_C > 0$). As soon as $T_C > 5$, photons are consumed by the engine ($\dot{Q}_C < 0$) and it starts to behave as an refrigerator, with the hot bath heating up $\dot{Q}_A > 0$ and the cold one slightly cooling down $\dot{Q}_B < 0$.

Since the cavity is assumed to be in a thermal ensemble, the term $[\mathsf{H}_C, \rho_C]$ does not contribute too. The term $[\mathsf{G}_C, \rho_C]$ can generate coherences, but note that it is zero whenever the state ρ_S is incoherent. As we have discussed in Chapter 3, $[\mathsf{H}_0, \mathsf{V}] = 0$ implies an incoherent steady-state if H_0 is non-degenerate, and this is precisely the case. We thus reach the following important conclusion: a coherent steady-state in the *system* is essential to produce coherent light in the *cavity*. Further, the term which entails coherence is divergent in $\tau \to 0$ limit; to remedy this we can either work in a regime in which the interaction with the cavity is not scaled, that is, we can abdicate from dissipation to generate *only* coherent corrections, or we can work in a regime in which $q = \mathrm{Tr}(\mathsf{C}\rho_S) \propto \sqrt{\tau}$ [33]. In the first case, we would obtain the corrected von Neumann equation

$$\dot{\rho}_C = -i[\mathsf{G}_C, \rho_C], \tag{5.43}$$

which generates a unitary evolution, described by the time-propagator

$$\mathsf{U}_C = \exp\left\{-i\tau(a^\dagger q + a q^*)\right\} = \exp\left\{\xi a^\dagger - \xi^* a\right\} = D(\xi), \tag{5.44}$$

where q is the coherence of ρ_S given by $\mathrm{Tr}(\mathsf{C}\rho_S)$ and D denotes the displacement operator with

parameter $\xi = (-i\tau q)$. If the cavity was in the ground state $|0\rangle$ initially, it would then be in a (slightly) coherent state $|\xi\rangle = D(\xi)|0\rangle$ after interacting with the system. Of course, one has always to remember that τ is never zero, and then the coherence of ρ_C captures the interaction time, as a clock. So, even if we work with the scaled version without assuming $\mathrm{Tr}(\mathsf{C}\rho_S) \propto \sqrt{\tau}$ the outcome is not physically problematic; it just means that the output cavity state $\left|-i\sqrt{\tau}^{-1}q\right\rangle$ is a highly displaced state and thus oscillates very fast.

Let me now promote the discussion beyond the perturbative regime, that is, I now discuss the finite τ case. Even if we consider off-resonant qubits as the environments, it is possible to construct a quantity

$$\Omega_z = a^\dagger a + \sigma_A^z + \frac{\sigma_B^z}{2} + \mathsf{N}_3 - \mathsf{N}_1, \tag{5.45}$$

such that $[\Omega_z, \mathsf{H}_S] = 0 = [\Omega_z, \mathsf{V}]$ and therefore, as discussed in Chapter 3, this would also lead to an incoherent steady-state (see B.2 for calculations). To engineer a Hamiltonian which produces a coherent NESS, I resort to the same reasoning used for the minimal qubit model; we just need to add a term which is off-diagonal w.r.t. the original system's Hamiltonian. I then modify the Hamiltonian of the system to

$$\mathsf{H}_S \equiv \omega_3\mathsf{N}_3 + \omega_2\mathsf{N}_2 + h^*\mathsf{C} + h\mathsf{C}^\dagger, \tag{5.46}$$

whose added term is designed to yield a non-vanishing $\mathrm{Tr}\left(\mathsf{C}\rho_S^*\right)$. So far, it is clear that this modification is important in establishing a coherent masing output — at least based on the discussion of $\tau << 1$. Yet, the modification above comes at the cost of violating strict energy conservation (see B.2)

$$\begin{aligned}[\mathsf{H}_0, \mathsf{V}] = {} & g_A\frac{1}{2}\left(h^*\mathsf{B} - h\mathsf{B}^\dagger\right)\sigma_A^x - ig_A\frac{1}{2}\left(h^*\mathsf{B} + h\mathsf{B}^\dagger\right)\sigma_A^y \\ & - g_B\frac{1}{2}\left(h^*\mathsf{A} - h\mathsf{A}^\dagger\right)\sigma_B^x - ig_B\frac{1}{2}\left(h^*\mathsf{A} + h\mathsf{A}^\dagger\right)\sigma_B^y \\ & + g_C(ha - h^*a^\dagger)(\mathsf{N}_3 - \mathsf{N}_2),\end{aligned} \tag{5.47}$$

where $\mathsf{H}_0 = \mathsf{H}_S + \mathsf{H}_A + \mathsf{H}_B + \mathsf{H}_C$ (with the modified H_S). We can associate the energy expenditure of the interaction as the cost to produce a coherent state in the cavity.

Since the interaction time does not need to be small, in general, we do not have to care about scaling factors; every term in the expansion of U contributes. I now show that we still

need the modification in H_S to produce a coherent steady-state while using XX interactions, for arbitrary τ. Suppose we have not made any modification in H_S, in which case $[\mathsf{H}_0, \mathsf{V}] = 0$; in this manner we know that the SS is incoherent, even off-resonance, since Ω_z, Eq. (5.45), is conserved. Let me then examine the reduced dynamics of the *cavity*, which I initialize in a steady-state collision, $\rho = \rho_A^{\text{th}} \otimes \rho_B^{\text{th}} \otimes \rho_C^{\text{th}} \otimes \rho_C^{\text{th}} \otimes \rho_S^*$. In this case, the evolution map is

$$\mathcal{K}(\rho_C) = \text{Tr}_{ABS}(\mathsf{U}\rho\mathsf{U}^\dagger), \tag{5.48}$$

and I can then show that the decoherence operator, w.r.t. the cavity eigenbasis, commutes with this map

$$\begin{aligned}
\mathcal{K}(\Delta(\rho_C)) &= \frac{1}{K}\int_0^K ds\, \text{Tr}_{ABS}(\mathsf{U}e^{isa^\dagger a}\rho e^{-isa^\dagger a}\mathsf{U}^\dagger) && (5.49)\\
&= \frac{1}{K}\int_0^K ds\, \text{Tr}_{ABS}(\mathsf{U}e^{is\Omega_z}\rho e^{-is\Omega_z}\mathsf{U}^\dagger) && (5.50)\\
&= \frac{1}{K}\int_0^K ds\, \text{Tr}_{ABS}(e^{is\Omega_z}\mathsf{U}\rho\mathsf{U}^\dagger e^{-is\Omega_z}) && (5.51)\\
&= \Delta(\mathcal{K}(\rho_C)), && (5.52)
\end{aligned}$$

where I used that $[\Omega_z, \mathsf{U}] = 0$ and that, since the states are incoherent, the missing pieces of Ω_z can be inserted for free exploiting unitarity. Therefore, considering the discussion in 3.2.5, $\mathcal{K}$ is an incoherent operation and ρ_C can only decohere in the process. So, the autonomous operation of the machine in an incoherent steady-state will not create coherent photon states in the cavity, for any τ.

As we have seen, the device is composed of both cavity and the three-level system. In Fig. 5.6 I study the dynamics of the three level atom without including the dissipation to the cavity. This setup will be referred to as *SSDB amplifier*, since, once coupled to the cavity it will convert heat into light. The thermodynamic properties of the complete model mostly reside in this piece, and therefore this will be of particular interest. Its Hamiltonian is given by Eq. (5.46), but, for simplicity, I study the case of real h and include two thermals baths. That is the finite τ version of Eqs. (5.34) and (5.35), given by the stroboscopic map $\mathcal{E}(\rho_S) = \text{Tr}_{ABC}(\mathsf{U}\rho_A^{\text{th}} \otimes \rho_B^{\text{th}} \otimes \rho_S\mathsf{U}^\dagger)$.

In Fig. 5.6, I set $\lambda_A = 0.4, \lambda_B = 0.1, \omega_A = 2.0, \omega_B = \tau = g_A = g_B = 1.0$. (a) The engine behaviour for the averages. In (b) I give particular emphasis to the divergences in the effective temperature associated to the gap $3 \leftrightarrow 2$ may lead either to enhanced inversion or the opposite

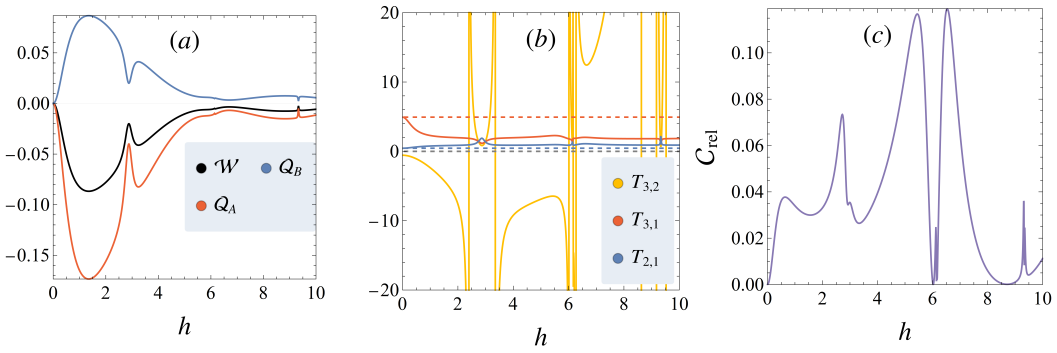

Figure 5.6: Coherent SSDB amplifier, for $\lambda_A = 0.4, \lambda_B = 0.1, \omega_A = 2.0, \omega_B = \tau = g_A = g_B = 1.0$. (a) The amplifier perform as an engine: for $h \neq 0$ heat flows from hot to cold ($Q_A < 0, Q_B > 0$) and work is extracted $\mathcal{W} < 0$. Moreover, no heat flows for $h = 0$. (b) The effective temperature associated to each system gap ($T_{2,1} = \omega_2(\ln p_2/p_1)^{-1}, T_{3,1} = \omega_3(\ln p_3/p_1)^{-1}, T_{3,2} = (\omega_3 - \omega_2)(\ln p_3/p_2)^{-1}$). The dashed lines represent the bath temperatures. (b) The relative entropy of coherence of the steady-state as h changes. All plots are symmetric for negative h.

depending on the values of h. Changing h drives the effective temperature $T_{3,2}$ across multiple sign changes, preceded by divergences. These abrupt changes coincide with oscillations in the currents in (a). In (c) we witness the behaviour of coherences as h is varied; it oscillates as h changes but it is never exactly vanishing again. As a general comment which pervades finite τ regimes, I point out oscillations; in LME scenarios most currents or coherences tend to be monotonic as only lower order terms contribute.

In Fig. 5.7 I again set $\lambda_A = 0.4, \lambda_B = 0.1, \omega_A = 2.0, \omega_B = \tau = g_A = g_B = 1.0$, but now I include the cavity,*i.e.*, $\mathcal{E}(\rho_S) = \text{Tr}_{ABC}(\text{U}\rho_A^{\text{th}} \otimes \rho_B^{\text{th}} \otimes \rho_C^{\text{th}} \otimes \rho_S \text{U}^\dagger)$, which is set in a thermal state with $T_C = 0.1$ and, thereof, $\bar{n} \approx 0.00005$. This is the complete SSDB engine (laser or maser). For comparision, the temperature of the baths are $T_A \approx 5.0, T_B \approx 0.5$. In Fig. 5.7 (a) we observe current Q_C filling the cavity with photons ($Q_C > 0$), with an optimal point close to $h = 1$, while the heat flows from hot to cold bath and work is injected to sustain the stimulated emission whenever $h \neq 0$. In (b) I again plot the effective temperatures of the system; they are still correlated with non-monotonic behaviour of the currents but, since the coupling to the cavity was established, the inversion is mostly destroyed. In (c) I now plot both steady-state coherence (system) $C(\rho_S^*)$ and the cavity's coherence *after* interacting with such steady-state ($C(\rho_C')$). As expected, for $h = 0$ cavity's coherence is zero and whenever $h \neq 0$ it is non-vanishing. Remarkably, for higher values of h, the steady-state coherence can still be small, while the cavity's acquired coherence remains significant.

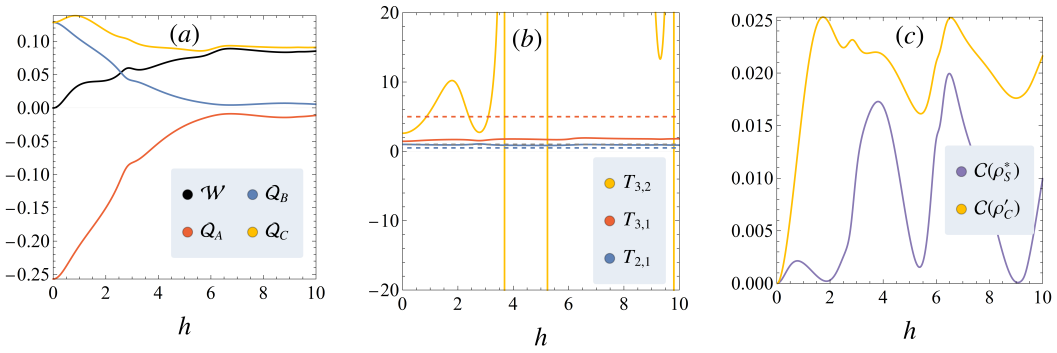

Figure 5.7: Complete SSDB engine in the masing regime, I set $\lambda_A = 0.4, \lambda_B = 0.1, \omega_A = 2.0, \omega_B = \tau = g_A = g_B = 1.0$, $T_A \approx 5.0, T_B \approx 0.5$ and $T_C = 0.1$. (a) The engine's average behaviour; photon creation is encoded in $Q_C > 0$, heat flows from hot to cold ($Q_A < 0, Q_B > 0$) and work is mostly injected $\mathcal{W} \geq 0$. (b) Abrupt effective temperature changes still occur, but they are mostly sustained at positive temperatures since energy is leaking out to the cavity. (c) The relative entropy of coherence of the steady-state of the system and of the bosonic mode after interacting with steady-state.

5.4 Masing equation for the SSDB engine

To bridge the gap between the CM framework here developed and the literature, in this Section I discuss part of the content of [86]. In this article, the authors work the statistics of the output of the cavity we have been studying, aiming a "full quantum description"; by which they mean beyond the mean-field approximation. I will focus only in the simpler mean-field analysis of the model, which provides insight on the origins of the non-conservative term introduced in Eq. (5.46).

The first marked difference is that they do not treat the cavity as an environment. Instead, their "system" is composed of the three-level atom plus the cavity, whose state I will denote by ρ. The 3-level atom is subjected, as before, to thermal dissipators which power the engine and the *cavity* is allowed to leak photons, that is, it contains a dissipator which only allows photons to leak out. I will show that, at the mean-field approximation this leads virtually to the same dynamics we have been studying, up to the cavity loss.

Consider, for now, the *closed* system $\rho = \rho_C \otimes \rho_S$ describing the cavity (C) and atom (S). But I consider that a laser device has a gas of N-atoms inside instead of a single atom, as in the ammonia maser, and each of these interact with the bosonic mode

$$\mathsf{H} = \sum_i \omega_3 \mathsf{N}_3^{(i)} + \omega_2 \mathsf{N}_2^{(i)} + \omega_C a^\dagger a + g \sum_i (a \mathsf{C}_i^\dagger + a^\dagger \mathsf{C}_i). \tag{5.53}$$

The trick is to modify this Hamiltonian, to allow the usage of the Hartree/mean field approx-

imation. For that, I map the single bosonic mode into an ensemble of bosons by setting, $a \to (\sqrt{N})^{-1}\sum_j a_j$, $a^\dagger a \to \sum_j a_j^\dagger a_j$ and reescaling the coupling $g \to g/\sqrt{N}$. This leads to

$$\mathsf{H} = \sum_i \omega_3 \mathsf{N}_3^{(i)} + \omega_2 \mathsf{N}_2^{(i)} + \sum_i \omega_C a_i^\dagger a_i + \frac{g}{N}\sum_{i\neq j}(a_i \mathsf{C}_i^\dagger + a_i^\dagger \mathsf{C}_i), \tag{5.54}$$

where the factor $1/N$ prevents over-counting interactions and, thus, $\langle \mathsf{H}\rangle \propto N$. The introduction of a many-body bosonic system is already in touch with the CM framework, since, in that context, we treated the bosonic system as an environment.

Now, the system plus cavity is initialized in $\rho_N = \rho^{\otimes N}$. The Hartree theorem guarantees that the evolution of ρ_N is a product state in the $N \to \infty$ limit, *i.e.*, $\rho_\infty(t) = \rho(t)^{\otimes\infty}$, where each $\rho(t)$ is the solution of the Hartree equation [47]

$$\dot{\rho} = -i\left[\omega_3 \mathsf{N}_3 + \omega_2 \mathsf{N}_2 + g\left(\mathrm{Tr}\{\mathsf{C}\rho(t))\}a^\dagger + \mathrm{Tr}\left\{\mathsf{C}^\dagger \rho(t)\right\}a\right) + g\left(\mathrm{Tr}\left\{a^\dagger \rho(t)\right\}\mathsf{C} + \mathrm{Tr}\{a\rho(t)\}\mathsf{C}^\dagger\right), \rho(t)\right]. \tag{5.55}$$

Before proceeding, note that if the cavity is traced out we obtain

$$\dot{\rho}_S = -i[\mathsf{H}_S, \rho_S], \tag{5.56}$$

where H_S is given precisely by Eq. (5.46) once we set $h \equiv g\,\mathrm{Tr}(a\rho)$. That is, the modification we forcibly made at H_S emerges naturally as the effect of the unitary interaction between cavity and atom in the many atoms limit. Further, we could trace out the atom and find the local cavity dynamics to resemble Eq. (5.43). In practice, we can interpret the breakdown of local energy conservation in the CM framework as an effective accounting of a persistent unitary interaction with the cavity.

Now let me proceed to find a so-called laser equation, following [86], in which case I include the heat baths and the photon leak. In the interaction picture, the LME reads

$$\dot{\rho} = -i[\rho, \mathsf{V}_{SC}] + \mathcal{D}_A(\rho) + \mathcal{D}_B(\rho) + \mathcal{D}_C(\rho), \tag{5.57}$$

where $\mathcal{D}_A, \mathcal{D}_B$ are the same given by Eqs. (5.34) and (5.35), the photonic dissipator is given by

$$\mathcal{D}_C(\rho) = \kappa\left(a\rho a^\dagger - \frac{1}{2}\left\{a^\dagger a, \rho\right\}\right), \tag{5.58}$$

and

$$\mathsf{V}_{SC} = g\left(\langle \mathsf{C}\rangle\, a^\dagger + \left\langle \mathsf{C}^\dagger\right\rangle a\right) + g\left(\left\langle a^\dagger\right\rangle \mathsf{C} + \langle a\rangle\, \mathsf{C}^\dagger\right). \tag{5.59}$$

With the cavity-atom master equation, we can also investigate the differential equations for some relevant quantities

$$\left\langle \dot{\mathsf{N}}_3\right\rangle = -ig\left\langle a^\dagger\right\rangle\langle \mathsf{C}\rangle - \langle a\rangle\left\langle \mathsf{C}^\dagger\right\rangle - \gamma_A(\lambda_A\langle \mathsf{N}_1\rangle - (1-\lambda_A)\langle \mathsf{N}_3\rangle), \tag{5.60}$$

$$\left\langle \dot{\mathsf{N}}_2\right\rangle = ig\left\langle a^\dagger\right\rangle\langle \mathsf{C}\rangle - \langle a\rangle\left\langle \mathsf{C}^\dagger\right\rangle - \gamma_B(\lambda_B\langle \mathsf{N}_1\rangle - (1-\lambda_B)\langle \mathsf{N}_2\rangle), \tag{5.61}$$

$$\left\langle \dot{\mathsf{C}}\right\rangle = -ig\langle a\rangle\langle \mathsf{N}_1 - \mathsf{N}_3\rangle - \frac{\langle \mathsf{C}\rangle}{2}(\gamma_A(1-\lambda_A) + \gamma_B(1-\lambda_B)) \tag{5.62}$$

$$\langle \dot{a}\rangle = -ig\langle \mathsf{C}\rangle - \frac{\kappa}{2}\langle a\rangle\,. \tag{5.63}$$

I now perform the adiabatic elimination of the atom degrees of freedom; *i.e.*, I assume that the atom has reached its steady-state whilst the cavity is still undergoing a transient. This renders $\left\langle \dot{\mathsf{N}}_3\right\rangle = \left\langle \dot{\mathsf{N}}_2\right\rangle = \left\langle \dot{C}\right\rangle = 0$, in which case, the following system of equations is found

$$ig\left(\langle \mathsf{C}\rangle\left\langle a^\dagger\right\rangle - \left\langle \mathsf{C}^\dagger\right\rangle\langle a\rangle\right) = \gamma_A[\lambda_A\langle \mathsf{N}_1\rangle - (1-\lambda_A)\langle \mathsf{N}_3\rangle], \tag{5.64}$$

$$ig\left(\langle \mathsf{C}\rangle\left\langle a^\dagger\right\rangle - \left\langle \mathsf{C}^\dagger\right\rangle\langle a\rangle\right) = -\gamma_B[\lambda_B\langle \mathsf{N}_1\rangle - (1-\lambda_B)\langle \mathsf{N}_2\rangle], \tag{5.65}$$

$$\langle \mathsf{C}\rangle = \frac{2ig}{\Gamma}\langle a\rangle\langle \mathsf{N}_3 - \mathsf{N}_2\rangle\,, \tag{5.66}$$

where I defined $\Gamma \equiv \gamma_A(1-\lambda_A) + \gamma_B(1-\lambda_B)$ and $\langle \mathsf{N}_1\rangle$ can be eliminated by noting that $\mathsf{N}_1 = \mathbb{1} - \mathsf{N}_2 - \mathsf{N}_3$. Eliminating also $\langle \mathsf{C}\rangle$ and defining $\mathscr{E} = \langle a\rangle$

$$-\frac{4g^2|\mathscr{E}|^2}{\Gamma}\langle \mathsf{N}_3 - \mathsf{N}_1\rangle = \gamma_A[\lambda_A\langle \mathsf{N}_1\rangle - (1-\lambda_A)\langle \mathsf{N}_3\rangle], \tag{5.67}$$

$$-\frac{4g^2|\mathscr{E}|^2}{\Gamma}\langle \mathsf{N}_3 - \mathsf{N}_1\rangle = -\gamma_B[\lambda_B\langle \mathsf{N}_1\rangle - (1-\lambda_B)\langle \mathsf{N}_2\rangle]. \tag{5.68}$$

The above equations can be solved for $\langle N_2\rangle$ and $\langle N_3\rangle$. With these in hands, we can compute the quantifier of population inversion $\Delta N \equiv \langle \mathsf{N}_3 - \mathsf{N}_2\rangle$.

$$\Delta N(\mathscr{E}) = \frac{\lambda_A - \lambda_B}{\Phi + \dfrac{4g^2|\mathscr{E}|^2}{\Gamma}\Psi}, \tag{5.69}$$

with

$$\Phi \equiv 1 - \lambda_A \lambda_B, \tag{5.70}$$

$$\Psi \equiv \frac{1}{\gamma_A \gamma_B} \left[(1 + \lambda_A)\gamma_A + (1 + \lambda_B)\gamma_B \right]. \tag{5.71}$$

With that, we can study the dynamics of the laser coherence through the lasing equation

$$\dot{\mathscr{E}} = \frac{\mathscr{E}}{2} \left[\frac{4g^2}{\Gamma} \Delta N(\mathscr{E}) - \kappa \right] = \frac{\mathscr{E}}{2} \left[\frac{4g^2}{\Gamma} \Delta N(\mathscr{E}) - \kappa \right] = \frac{\mathscr{E}}{2} \left[\frac{4g^2(\lambda_A - \lambda_B)}{\Phi\Gamma + 4g^2\Psi|\mathscr{E}|^2} - \kappa \right], \tag{5.72}$$

which is obtained by substituting Eq. (5.66) in Eq. (5.63). We do not need to solve this equation to understand the lasing behaviour; remember that the cavity is still undergoing a transient and then it suffices to understand whether coherence is increasing or decreasing to assert lasing [2]. To analyze Eq. (5.72), I will parametrize it as

$$\dot{\mathscr{E}} = \frac{\mathscr{E}}{2} \left[\frac{\mathscr{G}}{1 + \mathscr{B}|\mathscr{E}|^2} - \kappa \right]. \tag{5.73}$$

with this parametrization, we have that

$$\mathscr{G} = \frac{4g^2(\lambda_A - \lambda_B)}{\Gamma\Phi}, \tag{5.74}$$

$$\mathscr{B} = \frac{4g^2\Psi}{\Gamma\Phi}, \tag{5.75}$$

which are called laser gain and saturation, respectively. First, note what happens if $g = 0$: both $\mathscr{G}$ and $\mathscr{B}$ are zero. Hence

$$\frac{\dot{\mathscr{E}}}{\mathscr{E}} = -\frac{\kappa}{2}, \tag{5.76}$$

that is, the coherences are exponentially suppressed, according to the dissipation rate of the cavity, κ. Moreover, when $\mathscr{B}$ is big compared to the gain $\mathscr{G}$, the approximation $\dot{\mathscr{E}}/\mathscr{E} \approx -\kappa/2$ is reasonable. Finally, the lasing regime is established whenever dissipation is smaller than the gain, that is $\mathscr{G}/\kappa \geq 1$. Let me then write the gain explicitly, in terms of the original parameters

$$\mathscr{G} = \frac{4g^2(\lambda_A - \lambda_B)}{(1 - \lambda_a\lambda_B)(\gamma_A(1 - \lambda_A) + \gamma_B(1 - \lambda_B))}. \tag{5.77}$$

[2] The quantity $\langle a \rangle$ is not a coherence quantifier in the sense of the resource theory framework discussed in Chapter 3. It is is yet related to the creation of certain off-diagonal elements and thus used in quantum optics.

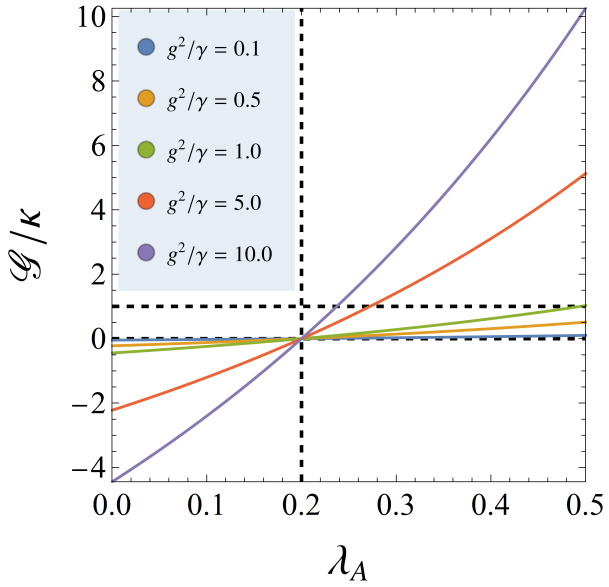

Figure 5.8: Gain relative to dissipation rate. I set $\lambda_B = 0.2$, which is identified as the vertical dashed line. The horizontal dashed lines indicate 0 and 1 relative gains. For every choice of g^2/γ, the gain is positive only above when the bath A is more populated than B; the lasing threshold is crossed for $g^2/\gamma \geq 1.0$.

For simplicity, I now set both thermal bath couplings to be equal $\gamma_A = \gamma_B = \kappa\gamma$ and $g \to \kappa g$

$$\frac{\mathscr{G}}{\kappa} = \frac{g^2}{\gamma}\frac{4(\lambda_A - \lambda_B)}{(1-\lambda_A\lambda_B)(2-\lambda_A-\lambda_B))}, \tag{5.78}$$

which highlights that the ratio between the squared coupling and the heat baths dissipation is central in achieving lasing. I now fix $\lambda_B = 0.2$ and, for different ratios g^2/γ, plot the relative gain versus the hot bath population λ_A.

In Fig. 5.8 we witness the parameter region in which lasing is achieved. For that, note that the ratio $g^2/\gamma \geq 1.0$ and the population of A must be greater than that of B.

In the collisional model framework, the analogous analysis is the change of the state of the cavity ancilla. I focused on its steady-state, but I could, equivalently, have let the cavity outside until the atom is in its steady-state and then — as it was done in the present discussion — analyze the transient variation of its coherence term, $\langle a \rangle$. The main advantages of the CM framework will be discussed in the next Chapter, but for now we have seen that allowing for non-conservative interactions enables a simple and equivalently valid description of the SSDB engine acting as a maser: a device which creates coherent photons powered by noisy environments.

Chapter 6

Fluctuations theorems

Non-equilibrium systems are marked by the presence of currents in their steady-state; either in the form of energy flux (heat and work) or fluxes of other physical quantities, such as particles or charges. For macroscopic systems, the behaviour of these currents is well described by experimental observations which only fluctuate due to imperfections in the measurement apparatus. Once smaller systems are considered, the measured quantities begin to deviate beyond experimental error, since their underlying probabilistic nature is no longer wiped by the law of large numbers. The origins of these deviations are either many-body chaotic regimes in classical systems or inherent fluctuations of quantum systems — the latter, even in the few body case. In equilibrium situations, the Gibbs ensemble completely characterizes the distribution associated to the system of interest, but the situation is radically different far from equilibrium. In this case, dynamics must be considered and the prescriptions become much more involved due to the emergence of fluctuating currents.

To account for charge current fluctuations in electric circuits the field of full counting statistics (FCS, or simply counting statistics) was developed [95–99]. It provided analytical tools to construct current probability distributions, usually through path integral techniques or non-equilibrium Green's functions [31, 100–103]. Naturally, the formalism was extended to heat and work[1], constituting an important tool to study thermodynamics beyond averages [31, 82, 104–109].

In parallel to the development of FCS techniques, the abstract idea that thermodynamic quantities should be considered as random variables hinted that the laws of thermodynamics were expected to hold for averages, but not necessarily for individual realizations of physical

[1] In the grand-canonical ensemble, work is often associated to counting charge carriers.

processes [38, 39]. This paradigm shift lead to the development of new laws of thermodynamics, which the probability distributions of heat, work and entropy production should satisfy. The so called fluctuation theorems (FTs)[2] [40, 41, 112–116] are considered cornerstones of stochastic thermodynamics and, since at the time of their development quantum mechanics was already mature, they were simultaneously considered at the quantum realm.

In this Chapter, I discuss some FTs, with special interest in their quantum formulations, since they constitute an active research topic [43, 81, 116–122] related to the main developments of this dissertation. In Chapter 7, I discuss the FCS technique within the context of CMs.

6.1 Entropy production

The first fluctuation theorem I will introduce is a simple extension of the discussion in Section 4.2. I proceed from the expression of the stochastic entropy production which led to the generalized second law in Eq. (4.15);

$$\sigma[\gamma] = \ln \frac{P[\gamma]}{\tilde{P}[\gamma]}, \tag{6.1}$$

in which I still did not assume anything about how to reverse the trajectory. By taking the exponential of both sides we find

$$\frac{P[\gamma]}{\tilde{P}[\gamma]} = e^{\sigma[\gamma]}, \tag{6.2}$$

and, averaging over $P[\gamma]$,

$$\mathbb{E}[e^{-\sigma}] = 1. \tag{6.3}$$

If we consider that for any convex function $f(x)$, $f(\mathbb{E}[x]) \leq \mathbb{E}[f(x)]$, the so-called *Jensen's inequality*, in Eq. (6.3) we then have that

$$e^{-\mathbb{E}[\sigma]} \leq 1, \tag{6.4}$$

[2]For reviews, see [31, 110] and for an introductory text on work fluctuations see [111].

and therefore

$$\mathbb{E}[\sigma] = \Sigma \geq 0. \tag{6.5}$$

Equation (6.2) is called a *detailed* fluctuation theorem and Eq. (6.3) an *integral* fluctuation theorem. They compose very general statements about irreversibility; should we assume the same measurement protocol of Section 4.2, we would have found that Eq. (6.5) reproduces the same generalized second law of Eq. (4.15). Yet, Eqs. (6.3) and (6.2) are more general in two senses: (i) they do not assume anything about the measurement protocol (ii) they are statements about the probabilistic behaviour of σ, and not just about the average. They update the second law, which states that entropy production is positive, to an equality which allows realizations of entropy production to be negative, but with exponentially smaller probabilities than their positive counterparts.

The procedure here discussed [81] is a modern and abstract one, in which we *define* stochastic entropy production so as to behave in that way. However, it was preceded by several investigations, *e.g.*, [41, 114], in which the actual dynamics and particular forms of Σ were studied and verified to attain the same structure. The definition of $\sigma[\gamma]$ can, in fact, be motivated through classical information theory; it resembles a stochastic version of the relative entropy between distributions $P[\gamma]$ and $\tilde{P}[\gamma]$.

6.2 Heat

Let me now discuss some FTs in more concrete settings. I begin by considering two quantum systems A and B, both prepared in thermal states $\rho_X^{\text{th}} = e^{-\beta_X \mathsf{H}_X}/Z_X, X = A, B$, and $\rho = \rho_A^{\text{th}} \otimes \rho_B^{\text{th}}$. They interact unitarily through $\mathsf{U} = e^{-i\tau\mathsf{H}}$, with $\mathsf{H} = \mathsf{H}_A + \mathsf{H}_B + \mathsf{V}$. For simplicity, I also assume that H is time-reversal invariant, *e.g.*, if it contains momenta they should appear in even powers.

Performing the TPM protocol in the energy eigenbasis, the probability distribution associated to the process is

$$P[\gamma] = \text{Tr}\Big(\mathsf{U}^\dagger \Pi_{a'b'} \mathsf{U} \Pi_{ab} \rho\Big) = p_a p_b |\langle a'b'| \mathsf{U} |ab\rangle|^2, \tag{6.6}$$

where $\gamma = (a, b, a', b')$ are energy outcomes and $p_a = e^{-\beta_A a}/Z_A$, $p_b = e^{-\beta_B b}/Z_B$. To reverse the

process, note again that U is reversed by daggering[3] and since all measurements were performed in the energy eigenbasis, the reversed initial state is ρ itself. Hence,

$$\tilde{P}[\gamma] = \mathrm{Tr}\Big(\mathsf{U}\Pi_{ab}\mathsf{U}^{\dagger}\Pi_{a'b'}\rho\Big) = p_{a'}p_{b'}|\langle a'b'|\,\mathsf{U}\,|ab\rangle|^2, \tag{6.7}$$

and, therefore

$$\frac{P[\gamma]}{\tilde{P}[\gamma]} = \exp[\beta_A(a'-a)+\beta_B(b'-b)], \tag{6.8}$$

which is already in the form of Eq. (6.2). Further, the terms $(a'-a)$ and $(b'-b)$ encompass the stochastic energy variation in thermal states; they are thus called stochastic heats, $q_A[\gamma]$ and $q_B[\gamma]$, respectively. Furthermore, applying $\ln(\bullet)$ to Eq. (6.8) and averaging we find

$$\mathbb{E}\left[\ln\frac{P[\gamma]}{\tilde{P}[\gamma]}\right] = \beta_A\,\mathrm{Tr}(\mathsf{H}_A(\rho'-\rho)) + \beta_B\,\mathrm{Tr}(\mathsf{H}_B(\rho'-\rho)) \tag{6.9}$$

$$= \beta_A Q_A + \beta_B Q_B = \Sigma, \tag{6.10}$$

where $\rho' = \mathsf{U}\rho\mathsf{U}^{\dagger}$. That is, we recover the entropy production for the heat exchange between two thermal states. This further motivates the definition of $\sigma[\gamma]$. Equation (6.8) can be also averaged to obtain the integral form (6.3).

The trajectory $P[\gamma]$ can now be used to establish the joint probability density of heats

$$P(q_A,q_B) = \mathbb{E}[\delta(q_A-q_A[\gamma])\delta(q_B-q_B[\gamma])] = \sum_{\gamma}\delta(q_A-q_A[\gamma])\delta(q_B-q_B[\gamma])P[\gamma], \tag{6.11}$$

where I denote q_X as the continuous embedding of the discrete variable $q_X[\gamma] = x'-x$, for $X = A, B$. I shall now use it to discuss FTs for $P(q_A,q_B)$. It is yet cumbersome to work with the δ[4] and I so perform the Fourier transform of Eq. (6.11)

$$\Phi(x,y) = \int_{-\infty}^{\infty} dq_A dq_B P(q_A,q_B)e^{ixq_A+iyq_B}, \tag{6.12}$$

which is the characteristic function of $P(q_A,q_B)$. However, I convey henceforth the usage of its

[3]Consider the anti-unitary time-reversal operator Θ, $\Theta^{\dagger}\mathsf{U}\Theta = \Theta^{\dagger}e^{-i\tau\mathsf{H}}\Theta = e^{+i\tau\mathsf{H}} = \mathsf{U}^{\dagger}$.

[4]Depending on the precise system of interest and measurements involved it can be either a Dirac's or a Kronecker's delta. For generality, we can use Dirac's delta.

Wick rotated version, the so-called generating function (GF)

$$G(x,y) = \int_{-\infty}^{\infty} dq_A dq_B P(q_A, q_B) e^{xq_A + yq_B}, \tag{6.13}$$

which can be equivalently expressed as the discrete average

$$G(x,y) = \sum_{\gamma} e^{xq_A[\gamma] + yq_B[\gamma]} P[\gamma]. \tag{6.14}$$

Let me now manipulate this expression, so to write it as a quantum average. According to Eq. (6.6), we can write $P[\gamma]$ through the Born rule. Hence,

$$G(x,y) = \sum_{\gamma} \mathrm{Tr}\Big(\mathsf{U}^{\dagger} e^{xa' + yb'} \Pi_{a'b'} \mathsf{U} e^{-xa - yb} \Pi_{ab} \rho\Big). \tag{6.15}$$

We can then perform the sum $\sum_{ab} e^{-xa-yb}\Pi_{a,b} = e^{-x\mathsf{H}_A - y\mathsf{H}_B}$, and similarly for its primed counterpart. In this manner, the sum in Eq. (6.15) gives

$$G(x,y) = \mathrm{Tr}\Big(\mathsf{U}^{\dagger} e^{x\mathsf{H}_A + y\mathsf{H}_B} \mathsf{U} e^{-x\mathsf{H}_A - y\mathsf{H}_B} \rho\Big). \tag{6.16}$$

Following [31], the structure of Eq. (6.16) will be considered the defining relation for the full counting statistics of a quantum current.

I now analyze a symmetry property of this function. For this sake, I explicitly write the thermal states

$$G(x,y) = \frac{1}{Z_A Z_B} \mathrm{Tr}\Big(\mathsf{U}^{\dagger} e^{x\mathsf{H}_A + y\mathsf{H}_B} \mathsf{U} e^{-(x+\beta_A)\mathsf{H}_A - (y+\beta_B)\mathsf{H}_B}\Big). \tag{6.17}$$

and introduce the GF associated to the time-reversed process

$$\tilde{G}(x,y) = \frac{1}{Z_A Z_B} \mathrm{Tr}\Big(\mathsf{U} e^{x\mathsf{H}_A + y\mathsf{H}_B} \mathsf{U}^{\dagger} e^{-(x+\beta_A)\mathsf{H}_A - (y+\beta_B)\mathsf{H}_B}\Big). \tag{6.18}$$

Comparing both GFs, we then conclude that

$$G(x,y) = \tilde{G}(-x-\beta_A, -y-\beta_B), \tag{6.19}$$

which is so-called *Gallavotti-Cohen weak symmetry*[5]. By transforming back to probability densities, we find a FT for heat exchange

$$\frac{P(q_A, q_B)}{\tilde{P}(-q_A, -q_B)} = e^{\beta_A q_A + \beta_B q_B}, \tag{6.20}$$

As a particular case, we can also consider interactions s.t. $[\mathsf{U}, \mathsf{H}_A + \mathsf{H}_B] = 0$, which, for non-degenerate $\mathsf{H}_A + \mathsf{H}_B$, guarantee that $q_A = -q_B$. In this case, the joint distribution can be reduced to a single variable

$$\frac{P(q_A)}{\tilde{P}(-q_A)} = e^{\Delta\beta q_A}, \tag{6.21}$$

where $\Delta\beta = \beta_A - \beta_B$. The above is known as *Jarzynski-Wójcik Fluctuation Theorem* [113]. This result was also generalized for multiple baths and particle flows [31, 115, 123]. Recently, it was also extended to sequential heat exchanges [120] and initially coherent systems [28, 122].

6.3 Work

I now move to a different setup, in which I discuss a fluctuation theorem for work. Consider a single quantum system subjected to an external driving protocol, *i.e.*, $\mathsf{H} = \mathsf{H}(t)$. For $t = 0$, I set $\mathsf{H}(0)\,|n\rangle = n\,|n\rangle$ and, for $t = \tau$, I set $\mathsf{H}(\tau)\,|n\rangle = n'\,|n'\rangle$. Then, I initialize the system in a thermal state $\rho = e^{-\beta\mathsf{H}(0)}/Z(0)$, which does not exchange heat with the environment but whose internal energy varies due to the time dependence. In this manner, $w[n', n] \equiv n' - n$ is the stochastic work and its generating function is again obtained through the TPM protocol, performed at $t = 0$ and $t = \tau$;

$$G(\lambda) = \sum_{n'n} e^{\lambda(n'-n)} p_n |\langle n'|\, U\, |n\rangle|^2. \tag{6.22}$$

Further, it assumes the same structure of Eq. (6.16) upon summation

$$G(\lambda) = \mathrm{Tr}\Big(\mathsf{U}^\dagger e^{\lambda\mathsf{H}(\tau)}\mathsf{U}e^{-\lambda\mathsf{H}(0)}\rho\Big), \tag{6.23}$$

[5] Whenever the tilde can be removed, the name strong is used instead.

explicitly writing $\rho = e^{-\beta \mathsf{H}(0) - \ln Z(0)}$ and setting $\lambda = \beta$ we then find

$$G(-\beta) = \mathrm{Tr}\Big(\mathsf{U}^\dagger e^{-\lambda \mathsf{H}(\tau)} \mathsf{U}\Big) e^{-\ln Z(0)}, \tag{6.24}$$

where we can recognize that $\mathrm{Tr}\Big(\mathsf{U}^\dagger e^{\beta \mathsf{H}(\tau)} \mathsf{U}\Big) = \mathrm{Tr}\Big(\mathsf{U}^\dagger e^{-\beta \mathsf{H}(\tau)} \mathsf{U}\Big) = Z(\tau)$ is an equilibrium partition function at the end of the protocol. Then, we find *Jarzynski's equality* [40]

$$\mathbb{E}[e^{-\beta w}] = e^{-\beta \Delta F}, \tag{6.25}$$

where $\Delta F = -\beta^{-1}(\ln Z(\tau) - \ln Z(0))$ is the *equilibrium* free energy difference between the initial thermal state and a reference equilibrium state $e^{-\beta \mathsf{U}^\dagger \mathsf{H}(\tau) \mathsf{U}}/Z(\tau)$. Yet, one should note that the state at the end of the process is not generally in equilibrium; it is remarkable to attain a statement about a non-equilibrium processes which is associated to equilibrium properties. Intuitively, Jarzynski's equality relates the actual process to an idealized protocol performed quasi-statically. Equation (6.25) further recovers a statement of the second law in the absence of heat; by applying Jensen's inequality to (6.25)

$$\mathcal{W} \geq \Delta F. \tag{6.26}$$

Jarzynski's equality also holds in classical scenarios and, in this case, has been verified experimentally in [124]. More recently, the quantum Jarzynski equality, Eq. (6.25), has been also verified in a trapped ion setup [16] and in nuclear magnetic resonance setups [125].

We can now discuss a fluctuation theorem associated to work. For this sake we again write the GF associated to the reversed process

$$\tilde{G}(\lambda) = \frac{1}{Z(\tau)} \mathrm{Tr}\Big\{\mathsf{U} e^{\lambda \mathsf{H}(0)} \mathsf{U}^\dagger e^{-\lambda \mathsf{H}(\tau) - \beta \mathsf{H}(\tau)}\Big\}, \tag{6.27}$$

where, since the Hamiltonian is time dependent, the reversed path sets $t \to \tau - t$. Comparing it with the forward GF written as

$$G(\lambda) = \frac{1}{Z(0)} \mathrm{Tr}\Big\{\mathsf{U}^\dagger e^{\lambda \mathsf{H}(0)} \mathsf{U} e^{-\lambda \mathsf{H}(\tau) - \beta \mathsf{H}(\tau)}\Big\}, \tag{6.28}$$

we recognize that they are related by

$$G(\lambda) = \frac{Z(\tau)}{Z(0)}\tilde{G}(-\lambda-\beta) = e^{-\beta\Delta F}\tilde{G}(-\lambda-\beta). \tag{6.29}$$

Transforming to the associated probability distributions, we then find

$$\frac{P(w)}{\tilde{P}(-w)} = e^{\beta(w-\Delta F)}, \tag{6.30}$$

the so-called *Crooks Fluctuation Theorem* [41], experimentally verified in [126].

Even though FT's associated to σ, such as Eq. (6.2), are amenable to generalizations and assume very little about the system, FT's associated to heat and work distributions have assumed very particular settings for their derivations. For example, in either of the setups here discussed, closed system dynamics was assumed and in either case the systems departed from thermal states or locally thermal states (products of thermal states). Hence, despite they provide an improvement about our knowledge in some out-of-equilibrium scenarios, they by no means comprehend all kinds of non-equilibrium situations. In particular, the simple setup of a system which interacts with two thermal baths at different temperatures does not have a heat or work FT for an arbitrary initial state; under certain circumstances these results emerge for integrated currents in the infinite-time limit [31, 110]. Consequently, we should not expect, in principle, that these kinds of FTs hold in general steady-states; for instance, a single collision in the steady-state of the SSDB engine does not necessarily satisfy these relations.

Chapter 7

Counting statistics in collisional models

In this Chapter, I combine the counting statistics technique, developed based on the two-point measurement protocol (see Subsection 4.2), with the the CM (see Chapter 3). In [31], the authors consider a generic unitary dynamics and, from there, derive master equations and Green's function techniques. The CM framework is capable of providing the local master equation limit of the formalism too, yet, regardless of this particular limit, it renders a tractable — either numerically or analytically — unitary interaction within each collision without resorting to approximations.

Initially, I concentrate in the formulation of full counting statistics of heats. Subsequently, it is a natural to push the formalism to account for the statistics of work. As early noted in [98] in the context of charge transport and lately in broader thermodynamic context [82, 104–107], the FCS of a general current may lead to negative probabilities. In terms of quantum work, this peculiarity can be traced back to the presence of coherence and was consolidated in a no-go theorem for quantum work [42]. This issue will be addressed in Chapter 8; in the present one, I will limit the discussion to work fluctuations in incoherent systems.

7.1 Heat counting statistics in a single collision

In this section, I lay the foundations for the acquisition of heat statistics in a single collision of the CM framework. For the sake of generality, I work for now with a *locally thermal state*,

accounting for multiple the ancillae, $\rho_E = \rho_E^{\text{lth}}$, with

$$\rho_E^{\text{lth}} \equiv \bigotimes_{i=1}^{N} \rho_{E_i}^{\text{th}}, \tag{7.1}$$

where each $\rho_{E_i}^{\text{th}}$ has, in principle, a different temperature and self-Hamiltonian H_{E_i}. I also define a collective projector in their energy eigenstates $\mathsf{H}_{E_i}|\mu_i\rangle = \mu_i|\mu_i\rangle$ by

$$\Pi_{\boldsymbol{\mu}} = |\boldsymbol{\mu}\rangle\langle\boldsymbol{\mu}| \otimes \mathbb{1}_S, \tag{7.2}$$

and $\boldsymbol{\mu} \equiv (\mu_1, \mu_2, ..., \mu_N)$ is a vector-valued index. This notation allow us to compactly write the framework for an arbitrary number of environments interacting with S. Whenever I need to present particular examples I will switch to a simpler notation; for instance, lest we study two-environment statistics, say A, B, I set $\boldsymbol{\mu} = (a, b)$.

I consider the system in an arbitrary state ρ_S and the global state is then initialized as $\rho = \rho_E^{\text{lth}} \otimes \rho_S$. In a single collision, the joint system evolves unitarily according to

$$\rho' = \mathsf{U}\rho\mathsf{U}^\dagger, \tag{7.3}$$

with $\mathsf{U} = \mathcal{T}_{>} e^{-i\int_0^\tau \mathsf{H}(t)}$ and

$$\mathsf{H}(t) = \underbrace{\sum_i \mathsf{H}_{E_i}}_{\mathsf{H}_E} + \mathsf{H}_S(t) + \underbrace{\sum_i \mathsf{V}_i}_{\mathsf{V}}. \tag{7.4}$$

For generality, I have included a time-dependence on H.

To achieve heat FCS, I then perform the TPM protocol on the baths only, producing a probability distribution

$$P[\gamma] = \text{Tr}\Big(\mathsf{U}^\dagger \Pi_{\mu'} \mathsf{U} \Pi_{\mu} \rho\Big) = p_{\mu} p(\mu'|\mu), \tag{7.5}$$

where $\gamma = (\boldsymbol{\mu}, \boldsymbol{\mu}')$, $p_{\boldsymbol{\mu}} = \prod_i e^{-\beta_i \mu_i}/Z_{E_i}$ and, since the system remains unmeasured, the conditional probability now involves a partial trace w.r.t. the system's degrees of freedom

$$p(\boldsymbol{\mu}'|\boldsymbol{\mu}) = \langle\boldsymbol{\mu}'| \,\text{Tr}_S\left(\mathsf{U}\,|\boldsymbol{\mu}\rangle\langle\boldsymbol{\mu}| \otimes \rho_S \mathsf{U}^\dagger\right) |\boldsymbol{\mu}'\rangle\,. \tag{7.6}$$

Notably, since $\rho_E^{\text{lth}} = \sum_{\boldsymbol{\mu}} p_{\boldsymbol{\mu}} |\boldsymbol{\mu}\rangle\langle\boldsymbol{\mu}|$, the measurement $\Pi_{\boldsymbol{\mu}}$ is *non-invasive*[1]. Further, nothing prohibits $\rho'_E = \text{Tr}_S \, \mathsf{U}\rho\mathsf{U}^\dagger$ to be coherent, and thus the second measurement $\Pi_{\boldsymbol{\mu}'}$ is generally invasive. This measurement has yet a different status compared to the first one; since after the collision the ancilla never interacts again with the system, the absent coherence does not influence any forthcoming processes. This is an advantage of formulating the dynamics using (Markovian) collisional models.

I now introduce the stochastic heat exchanged with each thermal state $q_i[\gamma] = \mu'_i - \mu_i$ and the collective notation $\boldsymbol{q}[\gamma] = (q_1[\gamma], ..., q_N[\gamma])$. With it, we can verify that, for any $n \in \{1, .., N\}$,

$$\mathbb{E}[q_n] = \sum_{\gamma} q_n[\gamma] P[\gamma] = \text{Tr}\{\mathsf{H}_{E_n}(\rho' - \rho)\} = Q_n, \tag{7.7}$$

where the spectral resolution of H_{E_n} and the cyclic property of the trace were used. We can now compute heat fluctuations, such as the second moment

$$\begin{aligned}
\mathbb{E}[q_n^2] &= \sum_{\gamma} q_n[\gamma]^2 P[\gamma] && (7.8)\\
&= \sum_{\gamma} [(\mu'_n)^2 + \mu_n^2 + 2\mu'_n\mu_n] \, \text{Tr}\Big(\mathsf{U}^\dagger \Pi_{\mu'} \mathsf{U} \Pi_{\boldsymbol{\mu}} \rho_E \otimes \rho_S \mathsf{U}\Big) && (7.9)\\
&= \sum_{\mu_n \, \mu'_n} [(\mu'_n)^2 + \mu_n^2 + 2\mu'_n\mu_n] \, \text{Tr}\Big(\mathsf{U}^\dagger \Pi_{\mu'_n} \mathsf{U} \Pi_{\mu_n} \rho_E \otimes \rho_S \mathsf{U}\Big) && (7.10)\\
&= \text{Tr}\Big(\mathsf{U}^\dagger \mathsf{H}_{E_n}^2 \mathsf{U} \rho_E \otimes \rho_S\Big) + \text{Tr}\Big(\mathsf{H}_{E_n}^2 \rho_E \otimes \rho_S\Big) + 2\,\text{Tr}\Big(\mathsf{U}^\dagger \mathsf{H}_{E_n} \mathsf{U} \mathsf{H}_{E_n} \rho_E \otimes \rho_S\Big), && (7.11)
\end{aligned}$$

where I have considered the spectral resolutions $\mathsf{H}_{E_n} = \sum_{\mu_n^{(\prime)}} \mu_n^{(\prime)} \left|\mu_n^{(\prime)}\right\rangle\!\left\langle\mu_n^{(\prime)}\right|$. To simplify the notation, we can also write the result in Heisenberg's picture $\mathsf{H}'_{E_n} = \mathsf{U}^\dagger \mathsf{H}_{E_n} \mathsf{U}$;

$$\mathbb{E}[q_n^2] = \left\langle (\mathsf{H}'_{E_n})^2 + \mathsf{H}_{E_n}^2 - 2\mathsf{H}'_{E_n}\mathsf{H}_{E_n} \right\rangle, \tag{7.12}$$

where I set $\langle \bullet \rangle \equiv \text{Tr}(\bullet\rho)$. Note that the above is generally different from

$$\text{Tr}\Big((\mathsf{H}'_{E_n} - \mathsf{H}_{E_n})^2 \rho\Big) = \left\langle (\mathsf{H}'_{E_n})^2 \right\rangle + \left\langle (\mathsf{H}_{E_n})^2 \right\rangle + \left\langle \{\mathsf{H}'_{E_n}, \mathsf{H}_{E_n}\} \right\rangle. \tag{7.13}$$

[1] In this dissertation, this term is used whenever a measurement does not destroy *local* coherences.

It is instinctive to promote the above procedure to higher moments, as follows;

$$\mathbb{E}[q_n^p] = \sum_\gamma (\mu_n' - \mu_n)^j P[\gamma] = \sum_\gamma \sum_{j=0}^{p} \binom{p}{j} (\mu_n')^p (-\mu_n)^{p-j} P[\gamma], \tag{7.14}$$

where I have used the binomial theorem and

$$\binom{p}{j} = \frac{p!}{(p-j)!j!}. \tag{7.15}$$

Performing the sum in γ separately, we find

$$\sum_\gamma (\mu_n')^j (-\mu_n)^{p-j} P[\gamma] = \mathrm{Tr}\Big(\mathsf{U}^\dagger \mathsf{H}_{E_n}^j \mathsf{U} (-\mathsf{H}_{E_n})^{p-j} \mathsf{H} \rho\Big), \tag{7.16}$$

using the spectral resolution of H_{E_n}. In this manner, substituting Eq. (7.16) in Eq. (7.14), we have

$$\mathbb{E}[q_n^p] = \sum_{j=0}^{p} \binom{p}{j} \left\langle (\mathsf{H}_{E_n}')^j (-\mathsf{H}_{E_n})^{p-j} \right\rangle. \tag{7.17}$$

It is tempting to push the sum inside the average and perform it through the binomial theorem, but this is not licit. The binomial theorem is only valid for commutative objects; then, if $[\mathsf{H}_{E_n}', \mathsf{H}_{E_n}] = 0$ the sum is trivially performed

$$\mathbb{E}[q_n^p] = \left\langle (\mathsf{H}_{E_n}' - \mathsf{H}_{E_n})^p \right\rangle. \tag{7.18}$$

To gain insight on the non-commutative case, let us observe the explicit sum

$$\begin{aligned} \mathbb{E}[q_n^p] = &\left\langle (-\mathsf{H}_{E_n})^p + \frac{p!}{(p-1)!1!} (\mathsf{H}_{E_n}')^1 (-\mathsf{H}_{E_n})^{p-1} + \frac{p!}{(p-2)!2!} (\mathsf{H}_{E_n}')^2 (-\mathsf{H}_{E_n})^{p-2} \dots \right\rangle \\ &+ \left\langle \dots + \frac{p!}{(p-2)!} (\mathsf{H}_{E_n}')^{p-2} (-\mathsf{H}_{E_n})^2 + \frac{p!}{(p-1)!1!} (\mathsf{H}_{E_n}')^{p-1} (-\mathsf{H}_{E_n})^1 + (\mathsf{H}_{E_n}')^p \right\rangle, \end{aligned} \tag{7.19}$$

and compare it to what we would obtain by computing powers of the operator difference

$$(\mathsf{H}_{E_n}' - \mathsf{H}_{E_n})^2 = (\mathsf{H}_{E_n}')^2 + \{\mathsf{H}_{E_n}', \mathsf{H}_{E_n}\} + (\mathsf{H}_{E_n})^2, \tag{7.20}$$

$$(\mathsf{H}_{E_n}' - \mathsf{H}_{E_n})^3 = (\mathsf{H}_{E_n}')^3 + \{\mathsf{H}_{E_n}', \{\mathsf{H}_{E_n}', \mathsf{H}_{E_n}\}\} - \{\mathsf{H}_{E_n}, \{\mathsf{H}_{E_n}', \mathsf{H}_{E_n}\}\} + (-\mathsf{H}_{E_n})^3, \tag{7.21}$$

$$\vdots \tag{7.22}$$

From them, we learn that, in general, the powers of non-commutative objects must consider every possible combination of operators, since ordering matters. In powering the difference of *commuting* operators, the binomial coefficients collect combinations that reduce to the same result. But only time ordered operators appear in Eq. (7.19) *with* binomial coefficients. So, the recipe to assess $\mathbb{E}[q_n^p]$ is summarized in computing $(\mathsf{H}'_{E_n} - \mathsf{H}_{E_n})^p$ and piecing the result in the correct time-order

$$\mathbb{E}[q_n^p] = \left\langle \mathcal{T}_>(\mathsf{H}'_{E_n} - \mathsf{H}_{E_n})^p \right\rangle . \tag{7.23}$$

The occurrence of the time-ordering symbol here is not related to the time dependence in $\mathsf{H}(t)$, and appears even when H is time-independent. In fact, it comes directly from the Born rule whence $P[\gamma]$ originates, Eq. (7.5). That is, $\mathcal{T}$ enforces the time ordering established by a definite causal structure in which measurements are performed in the TPM protocol.

The above results also generalize for correlations between heats from multiple baths, *e.g.,*

$$\mathbb{E}[q_n^p q_m^r] = \left\langle \mathcal{T}_>(\mathsf{H}'_{E_n} - \mathsf{H}_{E_n})^p (\mathsf{H}'_{E_m} - \mathsf{H}_{E_m})^r \right\rangle . \tag{7.24}$$

The time-ordered structure of heat moments has a vital implication. The formalism here presented is a generalization of the procedure used to construct heat distributions in the previous Chapter, which led to quantum fluctuation theorems. All these results agree both with experimental observations and with their classical counterparts. A natural way to extend heat to the quantum realm is to associate the operator [104, 127, 128] $\mathsf{H}'_{E_n} - \mathsf{H}_{E_n}$ to it, and then try to compute heat statistics through such heat operator. As we have seen, the moments of this object do *not* coincide with those of TPM distributions and, therefore, a statistical description of heat in quantum mechanics which is consistent with fluctuation theorems cannot be obtained through *the* operator $\mathsf{H}'_{E_n} - \mathsf{H}_{E_n}$. In fact, the issue is similar for work in incoherent systems and was addressed in [82]. Indeed, there is nothing formally wrong in prescribing an observable $\mathsf{H}'_{E_n} - \mathsf{H}_{E_n}$ when it comes to the rules of quantum theory, it is a licit Hermitian operator. Its weakness is that it is incompatible with fluctuation theorems. Another case against the observable of heat is that, classically, heat is not an observable; classical observables are functions of phase-space variables, and heat is an average over a distribution supported in the phase-space. Thus, it is independent of phase-space variables. This consideration will be central once I discuss statistics of coherent work in the next Chapter.

Now, let me finish the formal development of the theory by introducing the generating function of heats. For that sake, I define another vector-valued index $\boldsymbol{x} = (x_1, x_2, ..., x_N)$ and set

$$G(\boldsymbol{x}) = \sum_{\gamma} e^{\boldsymbol{x}^T \boldsymbol{q}[\gamma]} P[\gamma], \tag{7.25}$$

where $\boldsymbol{x}^T \boldsymbol{q}[\gamma] = x_1 q_1[\gamma] + x_2 q_2[\gamma] + ... + x_N q_N[\gamma]$ and T indicates transposition. By explicitly writing the TPM distribution and summing we find the

Heat Generating Function

$$G(\boldsymbol{x}) = \mathrm{Tr}\Big(\mathsf{U}^\dagger e^{\sum_i x_i \mathsf{H}_{E_i}} \mathsf{U} e^{-\sum_i x_i \mathsf{H}_{E_i}} \rho\Big), \tag{7.26}$$

or, in Heisenberg's picture

$$G(\boldsymbol{x}) = \left\langle e^{\sum_i x_i \mathsf{H}'_{E_i}} e^{-\sum_i x_i \mathsf{H}_{E_i}} \right\rangle. \tag{7.27}$$

Moreover, I can define the

Heat Cumulant Generating Function

$$K(\boldsymbol{x}) = \ln \mathrm{Tr}\Big(\mathsf{U}^\dagger e^{\sum_i x_i \mathsf{H}_{E_i}} \mathsf{U} e^{-\sum_i x_i \mathsf{H}_{E_i}} \rho\Big). \tag{7.28}$$

Any heat moment can be now computed through $(d/dx_n)^r G(\boldsymbol{x})|_{\boldsymbol{x}=0} = \mathbb{E}[q_n^r]$. Similarly, the cumulants of heats are given by $(d/dx_i)^r K(\boldsymbol{x})_{\boldsymbol{x}=0} = k_n^{(r)}$.

Equation (7.26) is indeed very similar to the ones previously discussed, such as Eq. (6.16). But there is one fundamental difference: $\rho = \rho_E^{\mathrm{lth}} \otimes \rho_S$, that is, there is an arbitrary state (ρ_S) among the thermal states which makes symmetries of the GF much more complicated to spot. Equation (7.26) can also be rewritten in another form. Exploiting the fact that $[\mathsf{H}_{E_i}, \rho] = 0 \quad \forall i$ we can cast it as

$$G(\boldsymbol{x}) = \mathrm{Tr}\Big\{\tilde{\mathsf{U}}(\boldsymbol{x}) \rho \tilde{\mathsf{U}}^\dagger(\boldsymbol{x})\Big\}, \tag{7.29}$$

with $\tilde{\mathsf{U}}(\boldsymbol{x}) = e^{\sum_i (x_i/2) \mathsf{H}_{E_i}} \mathsf{U} e^{-\sum_i (x_i/2) \mathsf{H}_{E_i}}$. Equation (7.29) is known as *counting-field dressed partition function*; it can be regarded as the trace of an unnormalized state, which evolves with an unitary operator dressed by a counting field. Note that the dressed evolution $\tilde{\mathsf{U}}$ is not generally

unitary, otherwise $\boldsymbol{q}$ would not fluctuate. This is indeed the kind of interpretation that associates this object to the name full counting statistics and is closely connected to von Neumann's measurement scheme, which implements the measurement apparatus as a bosonic counting field [6] (pointer). In fact, the usage of pointer systems has been proposed more recently to probe heat/work distributions [13, 129–131].

7.2 Full counting in the LME limit

I now consider the LME limit (see Section 3.40), in which case $\mathsf{V} \to \sqrt{\tau}^{-1}\mathsf{V}$. For simplicity, I also take H_S to be time independent. In this case the unitary operator can be expanded as

$$\mathsf{U} \approx \mathbb{1} - i\sqrt{\tau}\mathsf{V} - i\tau\mathsf{H}_0 - \frac{\tau}{2}\mathsf{V}, \tag{7.30}$$

with which Eq. (7.26) gives, up to order τ,

$$G(\boldsymbol{x}) = \mathbb{1} - i\sqrt{\tau}\mathrm{Tr}\Big(\big[\mathsf{V}, e^{\sum_i x_i \mathsf{H}_{E_i}}\big]e^{-\sum_i x_i \mathsf{H}_{E_i}}\rho\Big) - i\tau\,\mathrm{Tr}\Big(\big[\mathsf{H}_0, e^{\sum_i x_i \mathsf{H}_{E_i}}\big]e^{\sum_i x_i \mathsf{H}_{E_i}}\rho\Big) \tag{7.31}$$

$$+ \tau\,\mathrm{Tr}\Big(\Big(\mathsf{V}e^{\sum_i x_i \mathsf{H}_{E_i}}\mathsf{V} - \frac{1}{2}\{\mathsf{V}^2, e^{\sum_i x_i \mathsf{H}_{E_i}}\}\Big)e^{-\sum_i x_i \mathsf{H}_{E_i}}\rho\Big), \tag{7.32}$$

where the first trace evaluates to zero, due to thermal states commuting with the exponentials and the commutator in the second trace is zero. We then have that

$$G(\boldsymbol{x}) = \mathbb{1} + \tau\,\mathrm{Tr}\Big(\mathfrak{D}\left(e^{\sum_i x_i \mathsf{H}_{E_i}}\right)e^{-\sum_i x_i \mathsf{H}_{E_i}}\rho\Big), \tag{7.33}$$

with $\mathfrak{D}(\bullet) \equiv \mathsf{V}\bullet\mathsf{V} - (1/2)\{\mathsf{V}^2, \bullet\}$. Considering that $\ln(1+ax) \approx xa$ for $x << 1$ we then have that the CGF is

$$K(\boldsymbol{x}) = \tau\,\mathrm{Tr}\Big(\mathfrak{D}\left(e^{\sum_i x_i \mathsf{H}_{E_i}}\right)e^{-\sum_i x_i \mathsf{H}_{E_i}}\rho\Big). \tag{7.34}$$

The above can now be attributed a rate version, $\dot{K} \equiv \lim_{\tau\to 0} K/\tau$,

$$\dot{K}(\boldsymbol{x}) = \mathrm{Tr}\Big(\mathfrak{D}\left(e^{\sum_i x_i \mathsf{H}_{E_i}}\right)e^{-\sum_i x_i \mathsf{H}_{E_i}}\rho\Big),. \tag{7.35}$$

One could also write the above expressions in terms of the Lindblad dissipators of the ancilla. Writing it in terms of the system's quantities is also possible, whenever non-conservative terms are due to the system and can be properly singled out[2].

I now analyze an important particularity of the LME limit: the supression of spatial correlations. To be minimal and concrete, suppose there are only two environments $E_1 \equiv A$ and $E_2 \equiv B$ and that the system is bipartite $\mathsf{H}_S = \mathsf{H}_{S_1} + \mathsf{H}_{S_2} + \mathsf{H}_{12}$, with A coupled to S_1 and B coupled to S_2. Note that, since $\mathsf{V} = \mathsf{V}_A + \mathsf{V}_B$ this assumption leads to $[\mathsf{V}_A, \mathsf{V}_B] = 0$ and, in the LME limit the dissipative terms are thus independent $\mathfrak{D}(\bullet) = [\mathsf{V}, [\mathsf{V}, \bullet]] = \mathfrak{D}_A(\bullet) + \mathfrak{D}_B(\bullet)$, with

$$\mathfrak{D}_X(\bullet) = \mathsf{V}_X \bullet \mathsf{V}_X - \frac{1}{2}\left\{\mathsf{V}_X^2, \bullet\right\} \quad X = A, B, \tag{7.36}$$

by this virtue, the dissipative term of A does not act on operators in B and vice-versa. Considering this fact, the GF in Eq. (7.33) writes

$$G(x, y) = \mathbb{1} + \tau \operatorname{Tr}\Big(\mathfrak{D}_A(e^{x\mathsf{H}_A})e^{-x\mathsf{H}_A}\rho\Big) + \tau \operatorname{Tr}\Big(\mathfrak{D}_B(e^{y\mathsf{H}_B})e^{-y\mathsf{H}_B}\rho\Big), \tag{7.37}$$

which results in a CGF

$$K(x, y) = \tau \operatorname{Tr}\Big(\mathfrak{D}_A(e^{x\mathsf{H}_A})e^{-x\mathsf{H}_A}\rho\Big) + \tau \operatorname{Tr}\Big(\mathfrak{D}_B(e^{y\mathsf{H}_B})e^{-y\mathsf{H}_B}\rho\Big) = K(x) + K(y). \tag{7.38}$$

We have just concluded that q_A and q_B are statistically independent, since the CGF is additive. The essence of the LME limit is precisely that the interactions happen so fast that spatial[3] correlations cannot develop. There are still relevant fluctuations in the LME limit and correlations between system and ancillae still arise but the LME regime is, for a vast number of applications, meager when it comes to heat-heat correlations. This is one reason why in this dissertation I emphasize the study of interactions at finite time. In the literature, there has been a lot of debate between local and global master equations [132]; one of their differences is the fact that LMEs suppress the spread of operators associated to dissipation across local partitions of the Hilbert space. The dicotomy between finite time and instantaneous (LME) collisional models thus seems in fair parallel, since global master equations couple non-locally to the system of interest.

[2] See Section 4.4 and, for details on the conditions, Sec. IV. D. of [2]

[3] Here, I use the term spatial with regards to locallity in Hilbert space. One should not confuse it with actual position degrees of freedom in first quantization.

What does it mean, at the stochastic level, the heat exchanged with a thermal bath? How big are fluctuations compared with the heat averages? What is the role of strict energy conservation in the heat exchange? These are all questions that are better tackled through an illustrative example.

7.3 Heat and work in incoherent systems: insights from a minimal example

Consider an incoherent qubit model, the same from Example 3.3 whose thermodynamics at the level of averages has been studied at Fig 4.2. I now depict in Fig 7.1 the energy levels of each party during a single collision.

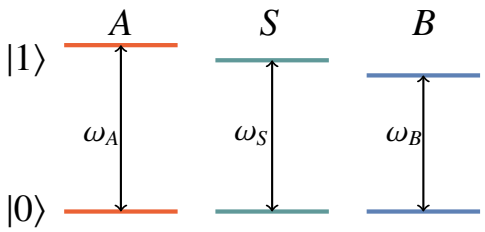

Figure 7.1: Single collision for an incoherent engine constituted of two qubit baths (A and B) and a qubit system (S). In general, each qubit (system and ancillae) has a different gap which causes work to be non-vanishing. Yet, exploiting spin-z conservation we can fully determine work by measuring heats.

For simplicity, I assume that S is already in its (incoherent) steady-state. Suppose now that we acquire the statistics of heats; that is, the TPM is performed in each ancilla. Indeed, to witness every possible process one has to let the system arrive at the steady-state many times, each time corresponding to a trial, since if we keep measuring the ancillae across multiple collisions the dynamics will be conditioned to the outcomes and, thus, the system will deviate from the steady-state with each consecutive measurement. This particular situation will be explored in Section 7.6.

Since each qubit has only two levels, the possible energy outcomes of each bath are given by $x \in \{\omega_X/2, -\omega_X/2\}$, $X = A, B$, $x = a, b$. Hence, the heat outcomes of each ancilla are $q_X[\gamma] \in \{\omega_X, 0, -\omega_X\}$. Then, in the case that $\omega_A = \omega_B = \omega_S = \omega$ we have strict energy conservation (Eq. 3.2.4) and, thus, $(a' - a) + (b' - b) + (n' - n) = 0$, where n', n are the system's energy eigenvalues. This expression can be written in terms of the stochastic heats and internal

energy as

$$q_A[\Gamma] + q_B[\Gamma] + \delta u[\Gamma] = 0 = w[\Gamma], \tag{7.39}$$

where $\Gamma = \{a, b, n, a', b', n'\}$. This resembles the first law, but at the stochastic level and also indicates that work is not zero just on average but stochastically too. Moreover, the joint distribution of heats

$$P(q_A, q_B) = \sum_{\gamma} P[\gamma]\delta(q_A - q_A[\gamma])\delta(q_B - q_B[\gamma]), \tag{7.40}$$

fully determines the internal energy fluctuations, without the need to measure the system; from Eq. (7.39) we have that

$$P(\delta u) = \int dq_A dq_B \delta(\delta u - q_A - q_B) P(q_A, q_B). \tag{7.41}$$

This holds whenever strict energy conservation holds, not just for this simple example.

Now, for this particular system, we have discussed in Chapter 3 that the the total spin-z is conserved. This fact can be exploited to acquire knowledge about work through heats when strict energy conservation breaks down. To do that, we just need to note that each energy outcome is just a constant times the spin-z component $y = s_Y \omega_Y, \quad Y = A, B, S \quad y = a, b, n$, where s_Y is an eigenvalue of σ_Y^z. Then, we can write

$$w[\Gamma] = \omega_A(s'_A - s_A) + \omega_B(s'_B - s_B) + \omega_S(s'_S - s_S), \tag{7.42}$$

in which we can eliminate the system variables by using spin-z conservation $(s'_S - s_S) = -(s'_A - s_A) - (s'_B - s_B)$. Finally we can rewrite in terms of energy outcomes

$$w[\Gamma] = w[\gamma] = \left(1 - \frac{\omega_S}{\omega_A}\right) q_A[\gamma] + \left(1 - \frac{\omega_S}{\omega_B}\right) q_B[\gamma]. \tag{7.43}$$

Thereby, a distribution of work can be constructed

$$P(w) = \int dq_A dq_B \delta(w - w[\gamma]) P(q_A, q_B). \tag{7.44}$$

Note that, when $\omega_S = \omega_A = \omega_B = 1$, Eq. (7.43) recovers Eq. (7.39) and $P(w) = \delta(0)$. It is

remarkable that we can access full statistics of work by only measuring the baths. Note that, according to Eq. (7.43), work could attain $3\times3\times3$ realizations, due to each qubit allowing three heat/internal energy outcomes. Yet, as it is commonplace in quantum mechanics, symmetries constrain the possible processes through selection rules. In practice, spin-z conservation renders vanishing every matrix element $\langle a'b'n'|\,\mathsf{U}\,|abn\rangle$ which violates this symmetry, and the support of the TPM distribution associated to Γ is directly impaired, since $P[\Gamma] = p_a p_b p_n |\langle a'b'n'|\,\mathsf{U}\,|abn\rangle|^2$ for an *incoherent* initial state.

Of course, one could in principle access work by measuring the system in the energy eigenbasis, since $\rho_S \in \mathscr{I}$. However, there are good reasons to avoid disturbing the system. First, for coherent systems this would be invasive; second, in practice, one always wants the less redundant measurement scheme. Within the paradigm of FCS, I then emphasize *the most information one can extract by solely measuring heats*.

Under all these considerations, we have established a complete picture of fluctuating heat and work in this simple system. I now explore simulations of this. I set $\omega_A = \omega_S = g = 1$ and vary ω_B; in this case we have

$$w[b', b] = \left(1 - \frac{1}{\omega_B}\right)(b' - b), \tag{7.45}$$

and then

$$P(w) = \int dq_B \delta(w - w[b', b]) P(q_b), \tag{7.46}$$

where $P(q_B) = \int dq_A P(q_A, q_B)$. From this we conclude that, although q_A and q_B are generally correlated, w depends only on knowledge of q_B — which makes sense, since this work comes precisely from the mismatch between the gap sizes of S and B. According to Fig. 4.2(a), there are three regimes of average work of this system; $\omega_B < 1$ and $\mathcal{W} < 0$, $\omega_B = 1$ and $\mathcal{W} = 0$, $\omega_B > 1$ and $\mathcal{W} > 0$. I discuss now two illustrative choices $\omega_B = 0.1, 1.0$ and produce tables for the stochastic process of single collisions (Figs. 7.2 and 7.3).

$$\omega_B = 1.0, Q_A = -0.25, Q_B = 0.25, \mathcal{W} = 0.$$

$(a,b) \to (a',b')$	$P[\gamma]$	$q_A[\gamma]$	$q_B[\gamma]$	$w[\gamma]$
(-1.,-1.)→(-1.,-1.)	0.41	0.	0.	0.
(-1.,-1.)→(-1.,1.)	0.066	0.	2.	0.
(-1.,-1.)→(1.,-1.)	0.066	2.	0.	0.
(-1.,-1.)→(1.,1.)	0	2.	2.	0.
(-1.,1.)→(-1.,-1.)	0.022	0.	-2.	0.
(-1.,1.)→(-1.,1.)	0.02	0.	0.	0.
(-1.,1.)→(1.,-1.)	0.011	2.	-2.	0.
(-1.,1.)→(1.,1.)	0.0073	2.	0.	0.
(1.,-1.)→(-1.,-1.)	0.13	-2.	0.	0.
(1.,-1.)→(-1.,1.)	0.064	-2.	2.	0.
(1.,-1.)→(1.,-1.)	0.12	0.	0.	0.
(1.,-1.)→(1.,1.)	0.044	0.	2.	0.
(1.,1.)→(-1.,-1.)	0	-2.	-2.	0.
(1.,1.)→(-1.,1.)	0.015	-2.	0.	0.
(1.,1.)→(1.,-1.)	0.015	0.	-2.	0.
(1.,1.)→(1.,1.)	0.011	0.	0.	0.

Figure 7.2: In this collision, I set $g = \tau = \omega_A = \omega_B = \omega_S = 1, \lambda_A = 0.4, \lambda_B = 0.1$. The first column indicates the concerned process, the second its associated probability. The third and forth the stochastic heats of A and B, respectively. The last column corresponds to stochastic work. The probabilities are colored according to their values; red is close to 0.5, blue close to 0.0 .

In Fig. 7.2, from left to right, the first column provides each trajectory (process). For $\omega_B = 1.0$, we have strict energy conservation and, as expected, the last column yields zero stochastic work. There are two trajectories which are forbidden, that is, their probabilities are exactly zero. Before proceeding, note that I did not include a column for internal energy; the reason is that, in general $\delta u[\gamma]$ can be assessed through Eq. (7.39). But, one should bear in mind that the original statement of strict energy conservation, Eq. (3.2.4), is a constraint in the possible transitions, *i.e.*, Eq. (7.39) holds whenever $P[\gamma] \neq 0$ and thus it does not hold for two lines in the table. The values of heats are, as expected, $q_X[\gamma] = 0, \pm 2$.

The case of Fig. 7.2 is in some sense trivial, due to strict-energy conservation, but highlights an ubiquitous feature in the stochastic behaviour of small systems: *most of the time nothing happens*. Or, equivalently, *in small systems fluctuations are prominent*. Let me explain through the table. At the first line we see that the process $(-1,-1) \to (-1,-1)$ corresponds to the event in which both ancillae are found at the state $|0\rangle$ at the beginning and at the end of the collision. That they are very likely to be found initially in such state is a direct consequence of the Gibbs structure of the baths; accordingly, note that this process amounts to $P[\gamma] = 0.41$, *i.e.*, in a

relevant number of collisions no energy is transferred. Further, there are other three processes, $(\pm 1, \mp 1) \to (\pm 1, \mp 1), (+1, +1) \to (+1, +1)$, which equally lead to no heat transferred. Now, if you compare the values of the stochastic heats with the average heat for $\omega_B = 1.0$ (at the top of the table in Fig. 7.2) you will see that those are one order of magnitude lower than what each realization yields, $q_B[\gamma]$. Combined with the fact that most of the times nothing happens, the picture drawn of stochastic quantum systems is that the thermodynamics of averages starkly deviates from the actual realizations. The average heat is leveraged precisely by those very unlikely events, in which quanta is exchanged in bigger chunks. For instance, we expect heat to flow from hot to cold and then $\mathcal{Q}_B > 0$, yet, only three process with non-zero probabilities are such that $q_B > 0$ and the most probable of them has merely $P[\gamma] = 0.066$. As we lower the scales, the quantized nature of energy inevitably leads to this sort of phenomena.

$$\omega_B = 0.1, \mathcal{Q}_A = -0.021, \mathcal{Q}_B = 0.021, \mathcal{W} = -0.94$$

$(a,b) \to (a',b')$	$P[\gamma]$	$q_A[\gamma]$	$q_B[\gamma]$	$w[\gamma]$
(0,-1)→(0,-1)	0.44	0.	0.	0.
(0,-1)→(0,1)	0.062	0.	2.	-9.
(0,-1)→(0,-1)	0.041	0.2	0.	0.
(0,-1)→(0,1)	0	0.2	2.	-9.
(0,1)→(0,-1)	0.025	0.	-2.	9.
(0,1)→(0,1)	0.022	0.	0.	0.
(0,1)→(0,-1)	0.0085	0.2	-2.	9.
(0,1)→(0,1)	0.0045	0.2	0.	0.
(0,-1)→(0,-1)	0.097	-0.2	0.	0.
(0,-1)→(0,1)	0.051	-0.2	2.	-9.
(0,-1)→(0,-1)	0.17	0.	0.	0.
(0,-1)→(0,1)	0.042	0.	2.	-9.
(0,1)→(0,-1)	0	-0.2	-2.	9.
(0,1)→(0,1)	0.011	-0.2	0.	0.
(0,1)→(0,-1)	0.017	0.	-2.	9.
(0,1)→(0,1)	0.013	0.	0.	0.

Figure 7.3: In this collision, I set $g = \tau = \omega_A = \omega_S = 1, \omega_B = 0.1, \lambda_A = 0.4, \lambda_B = 0.1$. The first column indicates the concerned process, the second its associated probability. The third and forth the stochastic heats of A and B, respectively. The last column corresponds to stochastic work. The probabilities are colored according to their values; red is close to 0.5, blue close to 0.0.

The table in Fig. 7.3 represents the same parameter region but with $\omega_B = 0.1$ and then $\mathcal{W} < 0$. Now, we witness non-vanishing stochastic work, with values ± 9, which is one order of magnitude bigger than the average $\mathcal{W} = -0.94$. Overall, the probability that $w < 0$ is only ≈ 0.15, but still higher than that of $w > 0$, which is ≈ 0.05. The possibilities with zero probability now represent the violation of (total) energy, since for them we cannot infer $\delta[\gamma]$

from $q_A[\gamma] + q_B[\gamma] - w[\gamma]$.

7.4 Cumulants and derived quantities

The discussion through the tables in the last section is instructive to build intuition in the microscopic processes, but rapidly becomes impractical. Thus, for a lot of situations it is easier to characterize fluctuations through cumulants and associated quantities. On this wise, I reserve this brief section to book-keep these quantities and provide their quantum mechanical expressions.

First, I begin with the variance of a heat current

$$\mathrm{var}q_n = \mathbb{E}[(q_n - Q_n)^2] = \mathbb{E}[q_n]^n - Q_n^2, \tag{7.47}$$

which, in accordance with the structure of the CGF (7.28), can be written as

$$\mathrm{var}q_n = \left\langle \mathsf{H}_n(\tau)^2 + \mathsf{H}_n^2 - 2\mathsf{H}_n(\tau)\mathsf{H}_n \right\rangle - Q_n^2. \tag{7.48}$$

Associated to the variance, I can define a figure of merit for the fluctuations of a given heat relative to its average,

$$\mathrm{snr}q_n \equiv \frac{\mathrm{var}q_n}{Q_n^2}, \tag{7.49}$$

the so-called *signal-to-noise ratio* (SNR)[4]. Whenever the SNR is bigger than one the fluctuations are dominant.

Consider now the covariance between two heat currents

$$\mathrm{cov}q_n q_m = \mathbb{E}[(q_n - Q_n)(q_m - Q_m)] = \mathbb{E}[q_n q_m] - Q_n Q_m, \tag{7.50}$$

whose quantum mechanical form is given by

$$\mathrm{cov}q_n q_m = \langle \mathsf{H}_n(\tau)\mathsf{H}_m(\tau) + \mathsf{H}_n\mathsf{H}_m - \mathsf{H}_n(\tau)\mathsf{H}_m - \mathsf{H}_m(\tau)\mathsf{H}_n \rangle - Q_n Q_m. \tag{7.51}$$

Associated to the covariance, I also introduce the relative contribution of covariances w.r.t. the

[4] Some authors define the SNR as the inverse of this quantity.

variance

$$\mathrm{corr} q_n q_m = \frac{\mathrm{cov} q_n q_m}{\sqrt{\mathrm{var} q_n \mathrm{var} q_m}} \in [-1, 1], \tag{7.52}$$

the so-called *correlations*.

All these quantities generalize in a straightforward manner to work in incoherent systems. With those in hands, we will now be able to investigate the role of fluctuations of heat in the SSDB model.

7.5 Steady-state fluctuations in the SSDB refrigerator

In the case of the SSDB model operating as a refrigerator, coherence is not a necessary ingredient and the desired task which one aims to achieve with such device does not rely on the concept of work to be quantified. Intuitively, the efficiency of such device is measured by the amount of heat one has to inject through the cavity in exchange of heat flowing out of the cold bath. The stochastic behaviour of these quantities can be fully described by the formalism developed hitherto.

Different from the refrigerator discussed in Section 5.3, here I work in the finite τ regime; the only relevant difference at the level of averages is that the transition to the refrigeration regime is slightly displaced. Yet, in this regime, correlations are prone to emerge, in accordance with the discussion in Section 7.2. Here, I denote the stochastic heats associated to baths A, B, C as q_A, q_B, q_C, in which I remind that C is the cavity photonic ensemble.

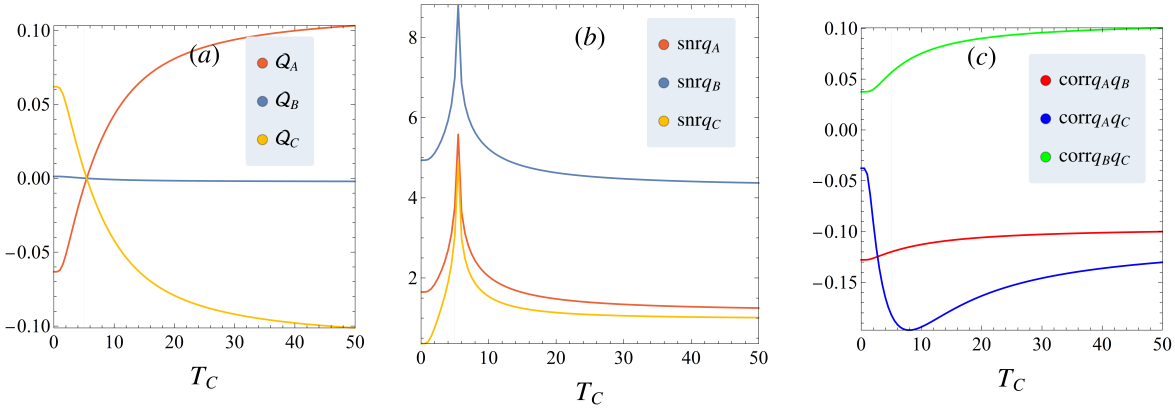

Figure 7.4: Steady-state operation of the SSDB engine for $\gamma_B = 0.1, \gamma_A = \gamma_C = 1.0, T_A = 5, T_B = 1, \omega_3 = 5, \omega_2 = 0.1, \tau = 1.0$. (a) Operation at the level of averages, analogous to Fig. 5.5. (b) SNR of each of the heat currents ($\log_{10}$ scale); all them diverge when the currents are zero, but are represented as finite due to numerical truncation. (c) correlations between each of the currents.

Figure 7.4 represents the SSDB engine operating with $g_B = \sqrt{0.1}, g_A = g_C = 1.0, T_A = 5, T_B = 1, \omega_3 = 5, \omega_2 = 0.1, \tau = 1.0$. In (a) we see that slightly above $T_C = 5$ all heat currents change sign and the system operates as a refrigerator. In (b) we see that fluctuations are dominant, for all heat currents (except for C when T_C is very small). Notably, q_B is the most sensible to fluctuations and, excluding the vicinity of the divergent region, q_A and q_B fluctuate less in the refrigeration regime than before the transition. Of course, this is not true for q_C, since in the refrigeration regime its temperature is high. Figure 7.4(c) the correlations between these currents are remarkably sensible to the transition; of particular interest is the correlation between q_A and q_C and between q_B and q_C. The first is very small for T_C bellow the transition, but dramatically increases through it. Its sign entails the fact that when q_C deviates towards bigger positive values, q_A deviates in the opposite direction; it displays a minimum precisely in the transition. It can also be compared with the SWAP engine studied in [133]; there, a two-stroke engine is studied and, instead of a third bath, there is work introduced by a SWAP between qubits, as in the present case the machine displays a negative correlation between the hot bath's heat and work (analogous to q_C).The second correlation is a positive, encoding the fact that the fluctuations in the photonic and cold bath agree in sign; in the refrigeration region, when the photonic bath tends to lose quanta to the system, the cold bath tends to do so simultaneously. The coincidences are yet less frequent between q_A and q_B, which tend to stay with smaller (yet, always negative) correlations and much smoother in the region in which the transition occurs; this entails the fact that the transport between A and B is mediated by C.

7.6 Many collisions and the quantum Bayesian networks formalism

As a natural generalization of the framework presented hitherto, I now discuss the case that we monitor the ancillae through many collisions. Although this scenario is not the focus of this dissertation, I take the opportunity to introduce quantum Bayesian networks [43], which provide a graphical representation of the stochastic evolution and make the manipulation of many-collision expressions more pictorial. Notably, the quantum Bayesian network framework will play a central role in addressing coherent systems in the next Chapter.

7.6.1 Bayesian networks

Consider a set of random variables $x_1, ..., x_N$. In general, their joint distribution is of the form $P(x_1, x_2.., x_N)$ and it would factor out as $P(x_1)...P(x_N)$ only in the case that they are all independent. Of course, there could be many things in the middle.

In practice, we can formulate our model in terms of a graph, depicting the direct dependence between each random variable. As an example consider Fig. 7.5.

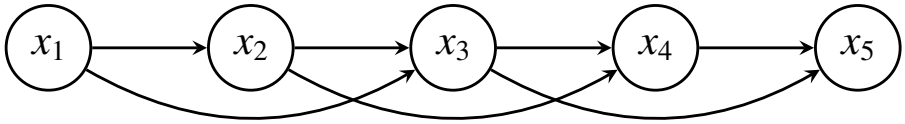

Figure 7.5: A simple example of a Directed Acyclic Graph. A arrow point to a node indicates that pointed node is a child (cause) of the pointer, the parent node and thereby allow the prescription of transition probabilities between childs and parents. The graph as a whole is dual to a probability distribution which can be read from it.

This is a so-called directed acyclic graph (DAG) [134], each node represents a random variable and, whenever an arrow is entering a node, it means such node is directly dependent on the one from which the arrow originates; the latter are so-called *parents*. Conversely, the node receiving the arrow is so-called *child* (w.r.t. that parent). In general, we can read from the DAG the probability distribution

$$P(x_1, ..., x_N) = \prod_{i=1}^{N} p(x_i| \text{ all parents of } x_i). \tag{7.53}$$

In particular, Fig. 7.5 gives

$$P(x_1, ..., x_5) = p(x_1)p(x_2|x_1)p(x_3|x_2x_1)p(x_4|x_3x_2)p(x_5|x_4x_3). \tag{7.54}$$

Bayesian networks can be written whenever a causal relation between random variables can be established and does not form a cycle. For this reason its arrows are directional and the transition probabilities are conditionals $p(a|b)$, which is asymmetric in $a \leftrightarrow b$.

Hidden Markov Models

In a series of applications it is useful to introduce a hidden layer within a DAG, so that a hidden model relates random variables which one is interested through other random variables. We can have an event which we cannot directly probe, described by hidden random variables $h_1, ..., h_5$. Yet, we can probe a property of each h_i so-called a_1. In this case, we can represent it as in Fig. 7.6.

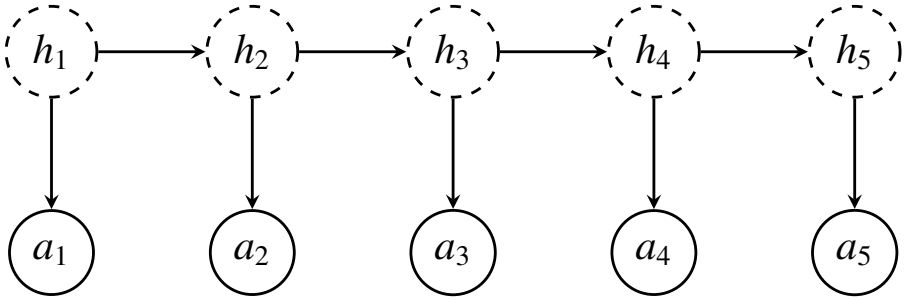

Figure 7.6: A simple example of a Hidden Markov Model, which prescribes $P(a_1, .., a_5)$. The dashed layers are so-called hidden layers (h_i) and ought to be marginalized in the probability distribution read from the graph.

In this case we can write

$$P(h_1, ..., h_5, a_1, ..., a_5) = p(h_1)p(a_1|h_1)\prod_{i=2}^{5} p(h_i|h_{i-1})p(a_i|h_i), \tag{7.55}$$

which, by marginalizing over the hidden variables, gives

$$P(a_1, ..., a_5) = \sum_{h_1,...,h_5} p(h_1)p(a_1|h_1)\prod_{i=2}^{5} p(h_i|h_{i-1})p(a_i|h_i). \tag{7.56}$$

Equation (7.56) is the probability distribution associated with Fig 7.6, so that dashed lines represent the hidden layer and, formally, the associated nodes are ought to be marginalized.

7.6.2 Quantum Bayesian network for a single collision

Consider now a single collision, as assumed throughout this Chapter. The reasoning established here is valid for an arbitrary number of baths interacting with the system, but, for concreteness, I assume that there are only two, *i.e.*, $\rho_E = \rho_A^{\rm th} \otimes \rho_B^{\rm th}$. Then, the stroboscopic map writes

$$\mathcal{E}(\rho_S) = \mathrm{Tr}_{AB}\{\mathsf{U}(\rho_A^{\rm th} \otimes \rho_B^{\rm th} \otimes \rho_S)\mathsf{U}^\dagger\} = \sum_\gamma \mathsf{M}_\gamma \rho_S \mathsf{M}_\gamma, \tag{7.57}$$

where $\gamma = (a, b, a', b') \equiv (\boldsymbol{\mu}, \boldsymbol{\mu}')$ and I have introduced the Kraus representation of the map

$$\mathsf{M}_\gamma = \sqrt{p_a p_b}\, \langle a'b' |\, \mathsf{U}\, | ab \rangle \equiv \sqrt{p_{\boldsymbol{\mu}}}\, \langle \boldsymbol{\mu}' |\, \mathsf{U}\, | \boldsymbol{\mu} \rangle\,. \tag{7.58}$$

Note that each Kraus component provides the stochastic realizations of the dynamics under the TPM. The objective of this Section is to introduce a graph representation of the stochastic evolution, namely a quantum Bayesian network, $P_{\rm QBN}[\gamma]$, which reproduces the TPM distribution

$$P_{\rm TPM}[\gamma] = p_{\boldsymbol{\mu}}\, \langle \boldsymbol{\mu}' |\, \mathrm{Tr}_S\{\mathsf{U}(|\boldsymbol{\mu}\rangle\langle\boldsymbol{\mu}| \otimes \rho_S)\mathsf{U}^\dagger\}\, | \boldsymbol{\mu}' \rangle\,. \tag{7.59}$$

For this sake, I first introduce the spectral decomposition of the system's initial state

$$\rho_S = \sum_{\alpha_0} p_{\alpha_0}\, |\alpha_0\rangle\langle\alpha_0|\,, \tag{7.60}$$

where $|\alpha_0\rangle$ are generic eigenvectors, accounting for cases in which the system is coherent. I now look at the stochastic evolution of a single choice of α_0

$$|\alpha_0\rangle \to \mathsf{M}_\gamma\, |\alpha_0\rangle\,. \tag{7.61}$$

To define a proper evolved state, we then need to normalize the above, yielding

$$\left|\psi^\gamma_{\alpha_1}\right\rangle \equiv \frac{\mathsf{M}_\gamma}{\sqrt{\langle\alpha_0|\, \mathsf{M}_\gamma^\dagger \mathsf{M}_\gamma\, |\alpha_0\rangle}}\, |\alpha_0\rangle\,, \tag{7.62}$$

which can also be written, by substituting Eq. (7.58), as

$$\left|\psi^\gamma_{\alpha_1}\right\rangle = \frac{\mathsf{M}_\gamma}{\sqrt{p(\gamma|\alpha_0)}}\, |\alpha_0\rangle\,, \tag{7.63}$$

where $p(\gamma|\alpha_0) = p_\mu \langle \boldsymbol{\mu}\alpha_0| \mathsf{U}^\dagger |\boldsymbol{\mu}'\rangle\langle\boldsymbol{\mu}'| \otimes \mathbb{1}_S \mathsf{U} |\boldsymbol{\mu}\alpha_0\rangle$. Note that we can regard this term as a marginal over an arbitrary basis through the resolution $\mathbb{1}_S = \sum_\phi |\phi\rangle\langle\phi|$, *i.e.*,

$$p_\mu \langle \boldsymbol{\mu}\alpha_0| \mathsf{U}^\dagger(|\boldsymbol{\mu}'\rangle\langle\boldsymbol{\mu}'| \otimes \mathbb{1}_S)\mathsf{U} |\boldsymbol{\mu}\alpha_0\rangle = p_\mu \sum_\phi |\langle \boldsymbol{\mu}'\phi| \mathsf{U} |\boldsymbol{\mu}\alpha_0\rangle|^2 = \sum_\phi p(\gamma\phi|\alpha_0). \tag{7.64}$$

Further, observe that I use the notation $|\psi^\gamma_{\alpha_1}\rangle$ to emphasize that, in general, $\langle\alpha_0|\psi^\gamma_{\alpha_1}\rangle \neq \delta_{\alpha_0,\alpha_1}$. Importantly, whenever we fix α_0 and γ, the state $|\psi^\gamma_{\alpha_1}\rangle$ is *given* and will be associated to conditionals of the form $p(...|\alpha_1)$.

Below, I now show that this state provides a diagonal decomposition of the final conditioned state of the system

$$\rho'_{S|\gamma} = \sum_{\alpha_0} \frac{1}{P[\gamma]} \mathsf{M}_\gamma \rho_S \mathsf{M}_\gamma^\dagger \tag{7.65}$$

$$= \sum_{\alpha_0} \frac{p_{\alpha_0}}{P[\gamma]} \mathsf{M}_\gamma |\alpha_0\rangle\langle\alpha_0| \mathsf{M}_\gamma^\dagger \tag{7.66}$$

$$= \sum_{\alpha_0} \frac{p_{\alpha_0} p(\gamma|\alpha_0)}{P[\gamma]} |\psi^\gamma_{\alpha_1}\rangle\langle\psi^\gamma_{\alpha_1}| \tag{7.67}$$

$$= \sum_{\alpha_0} p(\alpha_0|\gamma) |\psi^\gamma_{\alpha_1}(\alpha_0)\rangle\langle\psi^\gamma_{\alpha_1}(\alpha_0)|, \tag{7.68}$$

where I have used Eq. (7.63) and Bayes' rule and emphasized that the evolved state $|\psi^\gamma_{\alpha_1}\rangle$ depends on α_0. Moreover, we have $\sum_\gamma \rho_{S|\gamma} P[\gamma] = \mathcal{E}(\rho_S) = \rho'_S$.

With that, we have all the elements to write the graph-like representation for a single collision, which I depict in Fig. 7.7. Before writing the QBN distribution, note that in the picture in Fig. 7.7(b) there are non-directional arrows connecting a', b' and α_1; these arrows are causally neutral, because they are associated to the measurement intervention and the only causality we can establish is due to the unitary evolution. Formally, we no longer have a DAG, but we can still consider the same ideas by regarding (a', b', α_1) as a (vector-valued) random variable[5]. We shall refer to this structure as a quantum Bayesian network (QBN) henceforth, since it combines the two fundamental state transformations of quantum theory in a graph-like representation[6].

[5] In this case, the parental nodes can be connected to any of the child nodes (a', b', α_1), meaning they all share the same parents due to the lack of causality between the childs.

[6] Undirected graphs (UGs) are referred as Markov networks. QBNs combine directed connections, associated to time evolution and undirected connections, usually associated to simultaneous measurements. Formally, they are so-called acylic mixed graphs.

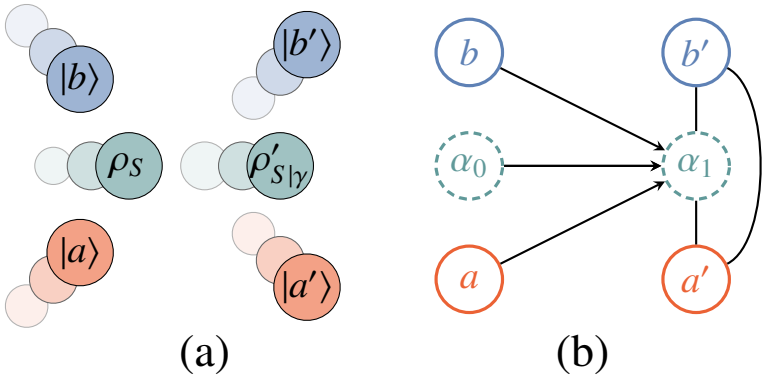

Figure 7.7: (a) Single collision under the TPM protocol. The baths are measured before and after the interaction with S. The final state of S is thus conditioned to γ. (b) Graphical model describing the single collision. Dashed lines are marginalized variables; the sum over the hidden layers restores the system's states depicted in (a). The line without arrows is an undirected connection.

The distribution associated to the graph is given by

$$P_{\text{QBN}}[\Gamma] = \sum_{\alpha_0,\alpha_1} p_{\alpha_0} p_a p_b p(a'b'\alpha_1|ab\alpha_0), \tag{7.69}$$

where

$$p_a p_b p(a'b'\alpha_1|ab\alpha_0) = p(\gamma\alpha_1|\alpha_0) = |\langle\alpha_1|\,\mathsf{M}_\gamma\,|\alpha_0\rangle|^2 = p_a p_b |\langle a'b'\alpha_1|\,\mathsf{U}\,|ab\alpha_0\rangle|^2. \tag{7.70}$$

summing over $|\alpha_1\rangle$, we then have

$$P_{\text{QBN}}[\Gamma] = \sum_{\alpha_0} p_{\alpha_0} p_a p_b \langle a'b'|\,\text{Tr}_S\{\mathsf{U}\,|ab\alpha_0\rangle\langle ab\alpha_0|\,\mathsf{U}^\dagger\}\,|a'b'\rangle \tag{7.71}$$

and, finally, summing over α_0

$$P_{\text{TPM}}[\gamma] = \text{Tr}\left(\mathsf{M}_\gamma \rho_S \mathsf{M}_\gamma^\dagger\right) = p_a p_b \sum_{\alpha_0} p_\alpha p(a'b'|ab\alpha_0). \tag{7.72}$$

7.6.3 Statistics of many collisions

Bearing the discussion of the last subsection, we are ready to consider multiple sequential collisions. I shall go to the most general scenario now, in which I consider an arbitrary number of collisions *and* reservoirs. As before, I denote the trajectory of the first collision as $\gamma_0 \equiv (\boldsymbol{\mu}_0, \boldsymbol{\mu}'_0)$, where $\boldsymbol{\mu}_0 \equiv (\mu_1^0, \mu_2^0, ...)$. I now pack all environments in the (vector-valued) nodes in the Bayesian

network in Fig. 7.8. The statistical dependence between environments in the same collision will not be manifest in the graph, but this notation will keep the graphs simpler.

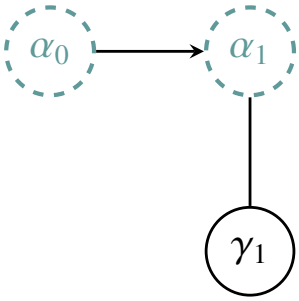

Figure 7.8: The quantum Bayesian network of a single stroke of our collisional model with multiple baths. The nodes $\boldsymbol{\mu}_0$ and $\boldsymbol{\mu}_0'$ encompass the TPM outcomes in all environments and are summarized in a single node labeled γ.

In the QBN scheme, the many collision case is just a concatenation of multiple graphs of the form of Fig. 7.8. The outcome is depicted in Fig. 7.9

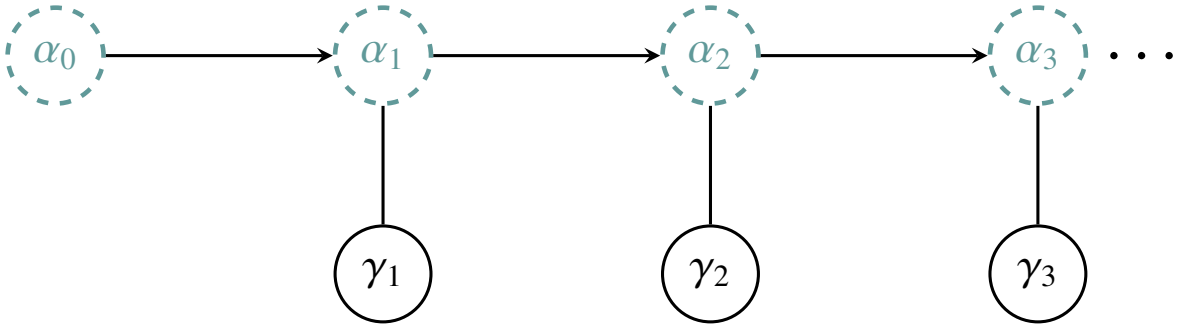

Figure 7.9: The quantum Bayesian Network of multiple collisions of the CM framework. For multiple collisions one has to concatenate multiple single-collision graphs.

For N collisions, the associated probability distribution is then[120, 135]

$$P[\gamma] = \sum_{\{\alpha\}} p_{\alpha_0} \prod_{i=1}^{N} p(\alpha_i \gamma_i | \alpha_{i-1}), \tag{7.73}$$

where I denoted $\{\alpha\} = \alpha_0, ..., \alpha_N$. The underlying quantum evolution after N collisions is described by multiple applications of $\mathcal{E}$

$$\rho_S^N = \mathcal{E}^N(\rho_S^0) = \sum_{\{\gamma\}} \mathsf{M}_{\gamma_N} ... \mathsf{M}_{\gamma_2} \mathsf{M}_{\gamma_1} \rho_S^0 \mathsf{M}_{\gamma_1}^\dagger \mathsf{M}_{\gamma_2}^\dagger ... \mathsf{M}_{\gamma_N}^\dagger \tag{7.74}$$

$$= \sum_{\alpha} p_{\alpha_0} \sum_{\{\gamma_0\}} ... \mathsf{M}_{\gamma_2} \mathsf{M}_{\gamma_1} |\alpha_0\rangle\langle\alpha_0| \mathsf{M}_{\gamma_1}^\dagger \mathsf{M}_{\gamma_2}^\dagger ... \mathsf{M}_{\gamma_N}^\dagger, \tag{7.75}$$

where I denoted $\{\gamma\} = \gamma_0, \gamma_1, \dots, \gamma_N$. As before, at any collision we can define a normalized state

$$\left|\psi_{\alpha_j}\right\rangle \equiv \frac{\mathsf{M}_{\gamma_j}}{\sqrt{p(\gamma_j|\alpha_{j-1})}}\left|\psi_{\alpha_{j-1}}\right\rangle = \frac{\prod_i^j \mathsf{M}_{\gamma_j}}{\prod_i^j \sqrt{p(\gamma_i|\alpha_{i-1})}}\left|\alpha_0\right\rangle. \tag{7.76}$$

For simplicity, consider $N = 2$. We then have

$$P_{\mathrm{QBN}}[\gamma] = \sum_{\alpha_0,\alpha_1,\alpha_2} p_{\alpha_0} p(\gamma_1\alpha_1|\alpha_0) p(\gamma_2\alpha_2|\alpha_1), \tag{7.77}$$

with

$$p(\gamma_1\alpha_1|\alpha_0) = p_{\mu_1}|\left\langle \boldsymbol{\mu}_1'\alpha_1\right|\mathsf{U}\left|\boldsymbol{\mu}_1\alpha_0\right\rangle|^2 \tag{7.78}$$

$$p(\gamma_2\alpha_2|\alpha_1) = p_{\mu_2}|\left\langle \boldsymbol{\mu}_2'\alpha_2\right|\mathsf{U}\left|\boldsymbol{\mu}_2\psi_{\alpha_1}\right\rangle|^2 \tag{7.79}$$

$$= p_{\mu_2}\left|\left\langle \boldsymbol{\mu}_2'\alpha_2\right|\mathsf{U}\left|\boldsymbol{\mu}_2\right\rangle \otimes \left(\frac{\sqrt{p_{\mu_1}}\left\langle \boldsymbol{\mu}_1'\right|\mathsf{U}\left|\boldsymbol{\mu}_1\right\rangle}{\sqrt{p(\gamma_1|\alpha_0)}}\right)\left|\alpha_0\right\rangle\right|^2 \tag{7.80}$$

$$= \frac{p_{\mu_1}p_{\mu_2}}{p(\gamma_1|\alpha_0)}\left|\left\langle \boldsymbol{\mu}_2'\alpha_2\right|\mathsf{U}\left|\boldsymbol{\mu}_2\right\rangle \otimes \left(\left\langle \boldsymbol{\mu}_1'\right|\mathsf{U}\left|\boldsymbol{\mu}_1\right\rangle\right)\left|\alpha_0\right\rangle\right|^2. \tag{7.81}$$

By explicitly including the stochastic evolution, we eliminate the dependence in α_1 of the second term. In this manner, we find that the term conditioned in α_1 only depends on α_0 and we can perform the sum over α_1 in Eq. (7.77)

$$P_{\mathrm{QBN}}[\gamma] = \sum_{\alpha_0\alpha_2} p_{\alpha_0}p_{\mu_1}p_{\mu_2}\frac{\sum_{\alpha_1} p(\gamma_1\alpha_1|\alpha_0)}{p(\gamma_1|\alpha_0)}\left|\left\langle \boldsymbol{\mu}_2'\alpha_2\right|\mathsf{U}\left|\boldsymbol{\mu}_2\right\rangle \otimes \left(\left\langle \boldsymbol{\mu}_1'\right|\mathsf{U}\left|\boldsymbol{\mu}_1\right\rangle\right)\left|\alpha_0\right\rangle\right|^2, \tag{7.82}$$

and over α_2, α_0

$$P_{\mathrm{QBN}}[\gamma] = \sum_{\alpha_0} p_{\alpha_0}p_{\mu_1}p_{\mu_2}\,\mathrm{Tr}\left\{\left\langle \boldsymbol{\mu}_2'\right|\mathsf{U}\left|\boldsymbol{\mu}_2\right\rangle\left\langle \boldsymbol{\mu}_1'\right|\mathsf{U}\left|\boldsymbol{\mu}_1\right\rangle|\alpha_0\rangle\langle\alpha_0|\left\langle \boldsymbol{\mu}_1\right|\mathsf{U}^\dagger\left|\boldsymbol{\mu}_1\right\rangle\left\langle \boldsymbol{\mu}_2\right|\mathsf{U}^\dagger\left|\boldsymbol{\mu}_2'\right\rangle\right\} \tag{7.83}$$

$$= \sum_{\alpha_0} p_{\alpha_0}\,\mathrm{Tr}\left\{\mathsf{M}_{\gamma_2}\mathsf{M}_{\gamma_1}|\alpha_0\rangle\langle\alpha_0|\mathsf{M}_{\gamma_1}^\dagger\mathsf{M}_{\gamma_2}^\dagger\right\} \tag{7.84}$$

$$= \mathrm{Tr}\left\{\mathsf{M}_{\gamma_2}\mathsf{M}_{\gamma_1}\rho_S\mathsf{M}_{\gamma_1}^\dagger\mathsf{M}_{\gamma_2}^\dagger\right\} = P_{\mathrm{TPM}}[\gamma]. \tag{7.85}$$

The argument goes the same way for an arbitrarily large chain of collisions; the last term in the chain will always carry information about the whole process and cancel out the earlier terms. The physical reasoning behind conditionals such as Eq. (7.82) is that we can only condition on

the actual physical process, entailed by the state $\left|\psi_{\alpha_1}^{\gamma_1}\right\rangle$ — which is determined once we fix the initial outcome α_0 and measure γ_1 — while we can conjecture about its projections on $|\alpha_2\rangle$ after it has stochastically evolved through M_{γ_1}. In other words, when we condition on a node α_n, we exploit the fact that the state of the system is determined by the data in the past $(\alpha_0, \gamma_1, ..., \gamma_n)$ and is not generally in a state in the base $\{|\alpha_0\rangle\}_{\alpha_0}$, but when we are interested in the probability of α_n we conjecture about the projection of the system's state on that base. Notably, such conjecturing process is *not* an actual measurement and is not considered to have back-acted in the further steps of the physical evolution. This peculiarity of QBNs will be discussed in Chapter 8.

In summary, the above description provides a recipe to write a multi-collision TPM description inspired by directed acyclic graphs. Rigorously, quantum Bayesian networks are not DAGs, but can be turned into DAGs if the non-causally connected nodes are regarded as a vector-valued variable. Moreover, to write the correct distribution one has to account for the actual states evolving in the hidden layer through the stroboscopic map governing the open-quantum dynamics.

7.6.4 Minimal qubit example

Consider the CM for a qubit interacting with a single bath

$$\mathsf{H}_S = \omega_S \sigma_S^z + h\sigma_S^x, \tag{7.86}$$

$$\mathsf{H}_A = \omega_A \sigma_A^z, \tag{7.87}$$

$$\mathsf{V} = g(\sigma_A^- \sigma_S^+ + \sigma_A^+ \sigma_S^-), \tag{7.88}$$

$$\mathsf{H} = \mathsf{H}_A + \mathsf{H}_S + \mathsf{V}. \tag{7.89}$$

By setting $\mathsf{U} = e^{-i\mathsf{H}}$ we obtain the steady-state $\rho_S^* = \mathcal{E}(\rho_S^*)$ with

$$\mathcal{E}(\rho_S) \equiv \mathrm{Tr}_A\{\mathsf{U}(\rho_A^{\mathrm{th}} \otimes \rho_S)\mathsf{U}^\dagger\}, \tag{7.90}$$

where, as usual, the ancillae are identical. Here, I will explore the simplest scenario in which, in the steady-state, $\mathcal{Q} \neq 0$. For that, I set $h \neq 0$ and $\omega_S = \omega_A$ the steady-state is coherent and we again have heat and work.

Once we start monitoring collisions sequentially the system will deviate from the steady

state; the initial measurement makes the ancillae either assume a spin up or spin down state with Gibbs probabilities, and then, under sequential monitoring the ancillae are generally different. For instance, suppose we monitor 3 sequential collisions starting from $\rho_S^0 = \rho_S^*$ with outcomes $\gamma_1, \gamma_2, \gamma_3$, where $\gamma_i = (a_i, a_i')$. Then, the system will evolve as $\rho_S^0 \to \rho_{S|\gamma_1}^1 \to \rho_{S|\gamma_1,\gamma_2}^2 \to \rho_{S|\gamma_1,\gamma_2,\gamma_3}^3$. It is yet true that if we average over γ_1 we obtain

$$\sum_{\gamma_1} P[\gamma_1] = \rho_{S|\gamma_1}^1 = \sum_{\gamma_1} P[\gamma_1] \mathsf{M}_{\gamma_1} \frac{\rho_S^*}{P[\gamma_1]} \mathsf{M}_{\gamma_1}^\dagger \tag{7.91}$$

$$= \mathcal{E}(\rho_S^*) = \rho_S^*. \tag{7.92}$$

And, should we average over γ_2, γ_3 we would find out that, even though the system stochastically deviates from the steady-state, the average over all realizations recovers the steady-state.

What happens with the heat exchanged? In general, it depends on the earlier collision. Nonetheless, since on average we are at the steady-state, the average heat exchanged within each stroke is equal $Q^0 = Q^1 = Q^2 = ...$, if we start the monitoring at the steady-state. More generally, it is true that, given we started at the steady-state, the random variables q_i are identically distributed, *i.e.*, $P(q_i) = \int \left[\prod_{j\neq i} dq_j\right] P(q_1, q_2, ..) = P(q_k)\ \forall i, k$. However, they are still correlated $P(q_1, q_2, ..) \neq P(q_1)P(q_2)...$. What I want to discuss here is whether a central-limit-like behaviour emerges if we acquire the statistics of a large number of collisions and a large variety of trajectories. In particular, the random variable which I will explore is

$$\bar{q}[\gamma] \equiv \frac{1}{N} \sum_{j=1}^{N} q[\gamma_j], \tag{7.93}$$

where N is the number of collisions after the SS collision, $q[\gamma_j] = a_j' - a_j$ and the distribution of this quantity is simply

$$P(\bar{q}) = \sum_{\gamma} \delta(\bar{q} - \bar{q}[\gamma]) P[\gamma], \tag{7.94}$$

$$P[\gamma] = \sum_{\alpha} p_\alpha \prod_{i=1}^{N} p(a_i'|a_i\alpha_{i-1}) p_{a_i} \tag{7.95}$$

Note that, since the average heat in each collision is the same, we already know that

$$\mathbb{E}[\bar{q}] = Q^0 = \mathrm{Tr}\left\{\mathsf{H}_A(\rho_A' - \rho_A^{\mathrm{th}})\right\} \equiv Q. \tag{7.96}$$

I now numerically construct the distribution of $P(\bar{q})$ by sampling $P[\gamma]$. That is, I use the QBN distribution to randomly sample from $P[\gamma]$ for a large number of collisions, in each run I compute $\bar{q}[\gamma]$ and repeat the process many times to construct from the data the distribution. Figure 7.10 is a histogram for the probability density function of 2000 different trajectories each with 2000 collisions. In it, I set excited ancilla population $\lambda = 0.4$, $\omega_A = \omega_S = h = g = \tau = 1$.

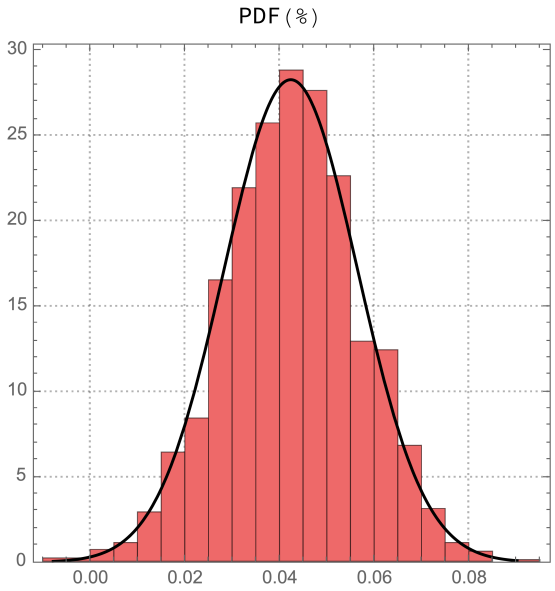

Figure 7.10: Histogram for the probability density function of 1000 trajectories, each with 1000 collisions. I set $\lambda = 0.4$, $\omega_A = \omega_S = h = g = \tau = 1.0$. A Gaussian function fit yields $P(\bar{q}) = 28.0696e^{-2475.27(\bar{q}-0.0418755)^2}$.

As we can see, the Gaussian function fits with good agreement. Where a Gaussian fit has been employed

$$P(\bar{q}) = \left(\sqrt{2\pi}\sigma\right)^{-1} \exp\left\{-\frac{(\bar{q}-Q)^2}{2\sigma^2}\right\}, \tag{7.97}$$

where the variance σ^2 and the average Q are given in Table 7.1, below. Further, in this table I compare the mean, variance, skewness and kurtosis of the fit with the data. The skewness is defined as

$$Sk\bar{q} = \mathbb{E}\left[\left(\frac{\bar{q}-Q}{\sqrt{\mathrm{var}\bar{q}}}\right)^3\right], \tag{7.98}$$

and it quantifies the asymmetry of the data w.r.t. the average, for Gaussians, its value is always

zero. The kurtosis is defined as

$$Kt\bar{q} = \mathbb{E}\left[\left(\frac{\bar{q} - Q}{\sqrt{\mathrm{var}\bar{q}}}\right)^4\right], \tag{7.99}$$

and it quatifies the "taildness" of the distribution, that is, the amount of data far from the average. For Gaussians, its value is always three.

Table 7.1: Comparison between sampled data and Gaussian fit.

	Mean	Variance	Skewness	Kurtosis
Data	0.0420395	0.000215586	0.0439892	3.13239
Fit	0.0420396	0.000215469	0	3

As we see in Table 7.1 both mean and variance of the fit are in stark agreement with the data. We can also use them to compute the SNR, which gives $\mathrm{snr}\bar{q} \approx 0.1$ (averages dominate fluctuations). Moreover, for Gaussians, every higher cumulant is the same regardless of the parameters. In particular, the Skewness and Kurtosis further emphasize that the data is approaching a Gaussian; their mismatch is still manifest but likely to disappear by considering a larger numbers of trajectories. From this analysis we see that, at the level of averages, the many collision scenario inherits the behaviour of the steady-state. Since every univariate marginal is equal, the variances and higher univariate cumulants are the same as the steady-state ones. What is non-trivial is that the variance attained by the Gaussian is not manifestly related to the fluctuations of a single steady-state collision. We can see this by computing

$$\mathrm{var}\bar{q} = \sum_{\gamma} P[\gamma]\left(\sum_i \frac{q[\gamma_i] - Q^i}{N}\right)^2, \tag{7.100}$$

where

$$\sum_{\gamma}\left(\sum_i \frac{q[\gamma_i] - Q^i}{N}\right)^2 = \frac{1}{N^2}\left(\sum_{i=1}^{N}(q[\gamma_i] - Q^i)^2 + 2\sum_{i=1}^{N}\sum_{j=1}^{i-1}(q[\gamma_i]q[\gamma_j] - Q^iQ^j)\right), \tag{7.101}$$

and then

$$\mathrm{var}\bar{q} = \frac{1}{N^2}\left(\sum_{i=1}^{N}\mathrm{var}q^i + 2\sum_{i=1}^{N}\sum_{j=1}^{i-1}\mathrm{cov}q^iq^j\right). \tag{7.102}$$

Now, since all variables are identically distributed, we have

$$\frac{1}{N^2}\sum_{i=0}^{N}\mathrm{var}q^i = \frac{1}{N}\mathrm{var}q^0, \tag{7.103}$$

which vanishes in the limit of large N. The point which sets the statistics of $\bar{q}$ apart from the the statistics of q^0 is precisely the remaining term; the covariances are in general distinct and the number of covariances scales similarly to N^{-2}. More concretely, consider upper(lower) bounds for the covariances $c_{+(-)} \equiv \max(\min)\{\mathrm{cov}q^i q^j\}_{i,j}$ and then we have in the limit $N \to \infty$

$$c_- \leq \mathrm{var}\bar{q} \leq c_+, \tag{7.104}$$

where I considered that $2\sum_{i=1}^{N}\sum_{j=1}^{i-1} 1 = (N-1)N$ and that all variances and covariances are finite. Thus, in general, this term contributes and its precise value depends on all covariances. As we could see from the histogram, is still relevant. One could estimate it by considering that such correlations are zero above certain threshold length. It is unclear in what circumstances this can be done and it is an interesting line of investigation to understand the role of genuine quantum effects in the correlation length. Note that, since we started the monitoring in the steady-state, $\mathrm{cov}(q_i, q_j)$ depends only on the distance $|j-i|$. The regime of multiple collisions is particularly relevant since it is the same in which some steady-state fluctuation theorems have been established [31, 110].

Chapter 8

Quantum Bayesian networks for coherent systems

Throughout a century of quantum mechanics, we have witnessed a plethora of experiments and formal developments which, on the one hand, confirmed its marked distinction from classical physics and, on the other hand, raised more and more questions regarding the classification and quantification of genuine quantum features. Roughly, quantum mechanics can be regarded as a non-commutative generalization of classical probability theory [136] and, whenever one is interested in a single observable, A, it reduces to usual probabilities, $p(a)$, in its spectral representation. The moment one looks at multiple observables the situation is starkly different: whenever $[\mathsf{A},\mathsf{B}] \neq 0$ one cannot unambiguously prescribe a *joint* distribution, $p(a,b)$, to the spectra of A and B associated to a spectral decomposition.

When it comes to thermodynamics, the energy eigenbasis is particularly important. Off-diagonal elements with respect to such basis give rise to superposition and coherence, which impair thermodynamic processes. Quantum mechanics, in its standard textbook state, is not a theory of processes. Rather, it is a theory of unitaries and measurements. These transformations are the cornerstones of thermodynamic processes, as it is the case of the TPM protocol. The success of the TPM protocol in bridging the gap between classical, well established, fluctuation theorems and their quantum formulations is simultaneously relieving and painful. The reason is that, while it sets a commonplace for the two theories, it also leaves coherence uncovered. Thus, a statistical description of genuine quantum-thermodynamic processes is still lacking.

This Chapter is devoted to the extension of probabilistic descriptions to the phenomena of coherence. In particular, this issue arises naturally when trying to describe quantum work in

initially coherent systems. We start by discussing fundamental limitations encoded in a no-go theorem for quantum work [42], some of the proposals available in the literature and, finally, the usage of quantum Bayesian networks to account for coherent work [43].

8.1 No-go theorem for quantum work

In this Section, I discuss the content of [42] and, as a more comprehensive reference, I also point to Part II, Chapter 11 of [13].

For simplicity, consider the simple scenario of an isolated quantum system subjected to an external drive for a time τ. All considerations are directly extensible to the general context we have been discussing throughout this dissertation, *i.e.*, open quantum systems involving heat and whose work can originate from external drives or non-conservative interaction (see Section 4.3).

Let me discuss the main ingredients which one should require from a distribution of work, $P(w)$. First, whatever probabilistic description of work we choose must *always* recover the correct average work, that is

$$\mathbb{E}[w] = \int_0^\tau dw P(w) w = \mathrm{Tr}\{\mathsf{H}(\tau)\rho(\tau) - \mathsf{H}(0)\rho(0)\}. \tag{8.1}$$

Second, whatever $P(w)$ must recover the quantum counterparts of classical FTs, those discussed in Chapter 6. That is, *for incoherent systems* we must recover the results of the TPM protocol

$$P_{\mathrm{TPM}}(w) = \sum_{n',n} \delta[w - (n' - n)] P_{\mathrm{TPM}}[n', n], \tag{8.2}$$

with

$$P_{\mathrm{TPM}}[n', n] = \mathrm{Tr}\Big(\mathsf{U}^\dagger \Pi_{n'} \mathsf{U} \Pi_n \rho(0)\Big), \tag{8.3}$$

where $\mathsf{H}(\tau)\,|n'\rangle = n'\,|n'\rangle$ and $\mathsf{H}(0)\,|n\rangle = n\,|n\rangle$.

Before giving the formulation of the no-go theorem, let me motivate it discussing some candidates and their shortcomings. When discussing heat in Section 7.1, we have already discarded a prominent candidate, the operator of work (OW), $\mathsf{W} = \mathsf{H}(\tau) - \mathsf{H}$. Similarly to heat, the TPM

for incoherent systems provides a time-ordered structure for the generating function

$$G_{\mathrm{TPM}}(\lambda) = \mathrm{Tr}\Big(e^{\lambda \mathsf{U}^\dagger \mathsf{H}(\tau)\mathsf{U}} e^{-\lambda \mathsf{H}(0)} \rho(0)\Big), \tag{8.4}$$

while the operator of work has a GF of the form

$$G_{\mathrm{OW}}(\lambda) = \mathrm{Tr}\Big(e^{\lambda \mathsf{U}^\dagger \mathsf{H}(\tau)\mathsf{U} - \lambda \mathsf{H}(0)} \rho(0)\Big), \tag{8.5}$$

so that they can only agree if $[\mathsf{H}(\tau), \mathsf{H}(0)] = 0$, which is not generally true even for incoherent states, $\rho(0) \in \mathscr{I}$. Thus, the statistics of W disagrees with classical fluctuation theorems [82].

Now, let me discuss the limitations of the TPM protocol. Consider $\rho(0) \in \mathscr{I}$, say $\rho(0) = \sum_{nm} \varrho_{nm} |n\rangle\langle m|$ and apply the TPM to obtain

$$P_{\mathrm{TPM}}[n', n] = \mathrm{Tr}\Big(\mathsf{U}^\dagger \Pi_{n'} \mathsf{U} \Pi_n \rho(0)\Big) = \varrho_{nn} |\langle n'| \mathsf{U} |n\rangle|^2, \tag{8.6}$$

Computing the average, we then find

$$\mathbb{E}[w] = \mathrm{Tr}(\mathsf{H}(\tau)\Delta\rho(\tau) - \mathsf{H}(0)\Delta\rho(0)), \tag{8.7}$$

where $\Delta\rho(0) = \sum_n \varrho_{nn} |n\rangle\langle n|$, $\Delta\rho(\tau) = \mathsf{U}\Delta\rho(0)\mathsf{U}^\dagger$. That is, we do not attain the correct average. Further, the whole statistics of coherent systems under the TPM protocol is devoid of initial coherence

$$G_{\mathrm{TPM}}(\lambda) = \mathrm{Tr}\Big(e^{\lambda \mathsf{U}^\dagger \mathsf{H}(\tau)\mathsf{U}} e^{-\lambda \mathsf{H}(0)} \Delta\rho(0)\Big). \tag{8.8}$$

A natural solution to this problem is to disregard the TPM protocol and simply define the GF for the coherent case as [122]

$$G(\lambda) = \mathrm{Tr}\Big(e^{\lambda \mathsf{U}^\dagger \mathsf{H}(\tau)\mathsf{U}} e^{-\lambda \mathsf{H}(0)} \rho(0)\Big). \tag{8.9}$$

This solution works well to certain extent; it attains the correct average and recovers the TPM for incoherent system. However, it has two drawbacks: it does not have a straightforward measurement protocol associated to it and $G(\lambda)$ does not generally lead to positive probabilities.

The negativeness can be spotted by rewriting Eq. (8.9) as

$$G(\lambda) = \sum_{n'nm} e^{\lambda(n'-n)} \varrho_{nm} \langle n' | \mathsf{U} | n \rangle\langle m | \mathsf{U}^\dagger | n' \rangle . \tag{8.10}$$

In this way, we see that we have a quasi-probability weight $\tilde{P}[n', n, m] \equiv \varrho_{nm} \langle n' | \mathsf{U} | n \rangle\langle m | \mathsf{U}^\dagger | n' \rangle$, which can be negative and is generally complex. Then, its associated transform is a quasi-probability distribution (QPD)[97, 98, 104–107, 122, 137–140]

$$\tilde{P}(w) = \sum_{n',n,m} \delta[w - (n' - n)] \tilde{P}[n', n, m]. \tag{8.11}$$

In fact, there is a whole zoo of QPDs which attain the correct average and agree with the TPM distribution in incoherent systems. Below, I summarize a large class parametrized by ζ in the GF

$$G_{\mathrm{QPD}}(\lambda, \zeta) = \sum_{n',n,m} \exp\left\{ n' - \left(\frac{n}{\zeta} + \frac{m(\zeta - 1)}{\zeta} \right) \right\} \tilde{P}[n', n, m]. \tag{8.12}$$

Of particular relevance, is the case $\zeta = 2$

$$G_{\mathrm{QPD}}(\lambda, 2) = \sum_{n',n,m} \exp\left\{ n' - \left(\frac{n}{2} + \frac{m}{2} \right) \right\} \tilde{P}[n', n, m], \tag{8.13}$$

which leads to the only real QPD among this class

$$\tilde{P}(w, 2) = \sum_{n',n,m} \delta \left[n' - \frac{(n + m)}{2} \right] \tilde{P}[n', n, m], \tag{8.14}$$

the above is referred to as smeared QPD, due to the symmetry $n \leftrightarrow m$, and it is also by this virtue that it can be shown to be real. To see this, we just have to symmetrize the sum $\sum_{nm} M_{nm} \to 1/2 \sum_{nm} (M_{nm} + M_{mn})$;

$$\tilde{P}(w, 2) = \sum_{n',n,m} \delta \left[n' - \frac{(n + m)}{2} \right] \mathrm{Re}\left\{ \varrho_{nm} \langle n' | \mathsf{U} | n \rangle\langle m | \mathsf{U}^\dagger | n' \rangle \right\}. \tag{8.15}$$

Equation 8.15 originated in studies of FCS in coherent electron transport [97, 98]. It was later used in thermodynamics to describe general work distributions [104–107, 138, 139]. In fact, the quasi-probability $\mathrm{Re}\left\{ \varrho_{nm} \langle n' | \mathsf{U} | n \rangle\langle m | \mathsf{U}^\dagger | n' \rangle \right\}$ far precedes all these applications and is called

Terletsky-Margenau-Hill (quasi)-distribution [137].

Quasi-probabilities are associated with weak-measurement protocols [141], which also makes them strong candidates to account for coherent work and, although their interpretation is still puzzling, a lot of progress has been made in understanding them, both theoretically and experimentally [142–144]. The negativity of QPDs has also been shown to witness contextuality of work distributions [140] and later used to discuss generalizations of quantum fluctuation theorems [122].

There seems to be no way to conciliate a (positive) distribution, the TPM protocol and a correct average. This is the spirit of the no-go theorem for work [42], which states that this is not just due to lack of effort, but a fundamental impossibility once another technical requirement is included. Below, I reproduce the theorem in the form presented in [13], rather than in the original paper.

No-go theorem for work — Let $P_{\mathcal{P}}(w)$ be a candidate of work distribution. There is no prescription $\mathcal{P}$ which, for all $\rho(0)$, $\mathsf{H}(\tau)$, $\mathsf{H}(0)$, U, simultaneously satisfies

(I) The first requirement can be cast in two equivalent ways:

(i) $P_{\mathcal{P}}(w)$ *is a linear probability distribution*. This corresponds to the assumption that $P_{\mathcal{P}}(w)$ is $P_{\mathcal{P}}(w) > 0$, $\sum_w P_{\mathcal{P}}(w) = 1$ and linear under mixtures of ρ. Linearity is defined as: let $\mathcal{P}^i$, $i = 0, 1, 2$ be prescriptions differing only by the initial state ρ_i. Then, if $\rho_0 = \lambda\rho_1 + (1-\lambda)\rho_2$ with $\lambda \in [0, 1]$, we demand that $P_{\mathcal{P}^0} = \lambda P_{\mathcal{P}^1} + (1-\lambda)P_{\mathcal{P}^2}$. This corresponds to the natural requirement that, if we condition the choice of the protocol on a coin toss, the measured fluctuations are simply the convex combination of those observed in the individual protocols.

(ii) There exists a Positive-Operator-Valued Measure (POVM), *i.e.*, a set of positive operators $\{M_w\}$, dependent on $\mathsf{H}(\tau)$, $\mathsf{H}(0)$ and U but *not* $\rho(0)$ that satisfy $P_{\mathcal{P}}(w) = \mathrm{Tr}(M_w\rho(0))$, with $\sum_w M_w = \mathbb{1}$.

(II) *Agreement with the TPM scheme for non-coherent initial states.* The second requirement is based on the assumption that the TPM scheme yields the correct statistics for diagonal states, *i.e.*,

$$P_{\mathcal{P}}(w) = P_{\mathrm{TPM}}(w) \quad \forall\rho(0) \quad \text{such that} \quad [\rho(0), \mathsf{H}(0)] = 0. \tag{8.16}$$

(III) *Average energy changes are respected by the measurement process*. Finally, we demand that the average energy change predicted by $\mathcal{P}$ equals the average energy change induced by U on $\rho(0)$

$$\sum_w w P_{\mathcal{P}}(w) = \mathrm{Tr}\Big(\mathsf{H}(\tau)\mathsf{U}\rho(0)\mathsf{U}^\dagger - \mathsf{H}(0)\rho(0)\Big), \quad \forall\rho(0). \tag{8.17}$$

Requirements (II) and (III) are just the ones we have already discussed, and we shall take them as lines we by no means want to cross. Requirement (I) is more subtle; in the form of (i) it demands some reasonability and universality criteria that a distribution should satisfy; in [42] this criteria is then shown to be equivalent to requiring that the protocol can be implemented through a state-independent POVM. By violating (I), QPDs have been shown good prospects, but they may cause discomfort by assuming negative probabilities. Here, we explore another way of violating (I), which by its turn leads to positive probabilities.

8.2 Full statistics of work through Bayesian networks

The technique here discussed is not an original contribution of my work. It was envisioned by Micadei *et al.* [43] to treat a mathematically similar problem, the prescription of a joint heat distribution for two locally thermal states with initial global coherence. Using this technique, they have extended the Jarzynsky-Wójcik FT to that scenario. It was later verified experimentally in [145] and its relation with the no-go theorem has been recently discussed in [146]. This Section also builds on the quantum Bayesian network formalism introduced in Section 7.6. I start by generalizing it to work in incoherent systems and then extending it to coherent systems.

8.2.1 Incoherent work

Consider a single collision with an arbitrary number of baths of different temperatures $\rho_E = \rho^{\mathrm{lth}}$, with $\langle\boldsymbol{\mu}|\rho^{\mathrm{lth}}|\boldsymbol{\mu}\rangle = p_{\boldsymbol{\mu}}$, $\boldsymbol{\mu} = (\mu_1, \mu_2, ...)$ and the heat TPM outcomes entailed by $\gamma \equiv (\boldsymbol{\mu}, \boldsymbol{\mu}')$. Let the system state be denoted by $\rho_S \in \mathscr{I}$, and I denote its spectral decomposition $\rho_S = \sum_n p_n |n\rangle\langle n|$ in the energy eigenbasis $\mathsf{H}(0)|n\rangle = n|n\rangle$. The system's Hamiltonian is generally time-dependent and, at the end of the collision, we have $\rho'_S = \sum_{n'} p_{n'} |n'\rangle\langle n'|$ with $\mathsf{H}(\tau)|n'\rangle = n'|n'\rangle$; this also means that the stroboscopic map $\mathcal{E}$ is at least a maximally incoherent operation (see Section 3.2.5).

Note that, here, the bases $\{|n\rangle\}_n, \{|n'\rangle\}_{n'}$ correspond to the hidden layers in Subsection 7.6.2. Yet, we are now interested in the augmented trajectory $\Gamma \equiv (\gamma, n, n')$. That is, we are interested in the graph in Fig. 8.1

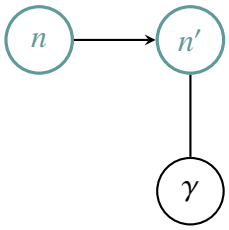

Figure 8.1: Quantum Bayesian network for an incoherent work distribution. It amount to re-introducing the once hidden layer, and considering that the system is diagonal in the energy eigenbasis.

whose associated distribution is simply

$$P_{\text{QBN}}[\Gamma] = p_n p_\mu p(\boldsymbol{\mu} n' | \boldsymbol{\mu} n), \tag{8.18}$$

that is, the once hidden layers are no longer marginalized. Similar to the discussion in Subsection 7.6.2, we then have that it coincides with a Γ-TPM distribution

$$P_{\text{TPM}}[\Gamma] = p_n p_\mu |\langle \boldsymbol{\mu} n' | \cup | \boldsymbol{\mu} n \rangle|^2. \tag{8.19}$$

8.2.2 Coherent work

The situation with coherent work is technically simple, but its meaning is tricky. In this Subsection I focus on the technical aspects and in the consistency of the framework.

Consider now a generic initial state $\rho_S = \sum_{\alpha_0} p_{\alpha_0} |\alpha_0\rangle\langle\alpha_0|$. The idea here is to consider the *trajectory* $\Omega = (\gamma, \alpha_0, \alpha_1)$, augment it to the *random variable* $\Xi = (\Omega, n', n)$ in order to make inferences about the *random variable* $\Gamma = (\gamma, n', n)$. This is encoded in the following graph.

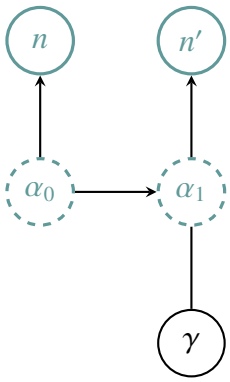

Figure 8.2: Quantum Bayesian network for a coherent work distribution. In this case, the system remains evolving in its diagonal eigenbasis, in general not the energy eigenbasis. We then conjecture about its projections on energy eigenstates without collapsing the the state which is actually evolving for each initial possible α_0.

Figure 8.2 depicts the QBN associated to coherent work. The associated distribution is then given by

$$P_{\text{QBN}}[\Gamma] = \sum_{\alpha_0,\alpha_1} p_{\alpha_0} p_{\mu} p(\boldsymbol{\mu}'\alpha_1|\boldsymbol{\mu}\alpha_0) p(n|\alpha_0) p(n'|\alpha_1). \tag{8.20}$$

In Section 7.6 we already discussed the quantum mechanical structure of the first transition probability in the above. Let us discuss the last two now. First, $p(n|\alpha_0) = |\langle n|\alpha_0\rangle|^2$; second,

$$p(n'|\alpha_1) = \left|\langle n'|\psi_{\alpha_1}\rangle\right|^2 \tag{8.21}$$

$$= \frac{|\langle n'|M_{\gamma}|\alpha_0\rangle|^2}{p(\gamma|\alpha_0)} \tag{8.22}$$

$$= \frac{|\langle \boldsymbol{\mu}' n'|\mathsf{U}|\boldsymbol{\mu}\alpha_0\rangle|^2}{p(\boldsymbol{\mu}'|\boldsymbol{\mu}\alpha_0)}. \tag{8.23}$$

Substituting in Eq. (8.20) and summing over α_1 we obtain the coherent QBN

$$P_{\text{QBN}}[\Gamma] = \sum_{\alpha_0} p_{\alpha_0} p_{\mu} |\langle n|\alpha_0\rangle|^2 |\langle n'\boldsymbol{\mu}'|\mathsf{U}|\boldsymbol{\mu}\alpha_0\rangle|^2, \tag{8.24}$$

The transition from Eq. (8.20) to Eq. (8.24) is non-trivial, mainly due to the rules associating conditionals to their quantum counterparts. Yet, this transition is no longer necessary once we understand Eq. (8.24). Basically, if we had actually measured the system we would have back-action, *i.e.*, the (invasive) TPM structure would emerge by simply substituting $|\alpha_0\rangle \to |n\rangle$ in the

last factor of Eq. (8.24),

$$\sum_{\alpha_0} p_{\alpha_0} p_\mu |\langle n|\alpha_0\rangle|^2 |\langle \boldsymbol{\mu}' n'|\,\mathsf{U}\,|\boldsymbol{\mu} n\rangle|^2 = p_\mu \langle n|\,\rho_S\,|n\rangle\,|\langle \boldsymbol{\mu}' n'|\,\mathsf{U}\,|\boldsymbol{\mu} n\rangle|^2 \tag{8.25}$$

$$= \mathrm{Tr}\Big(\Pi_{\mu'}\Pi_{n'}\mathsf{U}\Pi_\mu\Pi_n\rho_E\otimes\rho_S\Pi_\mu\Pi_n\mathsf{U}^\dagger\Pi_{\mu'}\Pi_{n'}\Big) \tag{8.26}$$

$$= P_{\mathrm{TPM}}[\Gamma]. \tag{8.27}$$

Conversely, the QBN can be regarded as the back-action free version of a Γ-TPM. The rationale behind it will be discussed in the next Section, but for now the rule is basically forcing back-action to not take place in the formal expression of the distribution.

Let me now perform some sanity checks. First, note that whenever ρ_S is incoherent we have $|\langle n|\alpha_0\rangle|^2 = \delta_{n\alpha_0}$ and we obtain the TPM expression in Eq. (8.19). Moreover, should we marginalize on n, n' we would always recover

$$\sum_{n,n'} P_{\mathrm{QBN}}[\Gamma] = \sum_{\alpha_0} p_{\alpha_0} p_\mu \cancelto{1}{\mathrm{Tr}(|\alpha_0\rangle\langle\alpha_0|)} \langle \boldsymbol{\mu}'|\,\mathrm{Tr}_S\{\mathsf{U}\,|\boldsymbol{\mu}\alpha_0\rangle\langle\boldsymbol{\mu}\alpha_0|\,\mathsf{U}^\dagger\}\,|\boldsymbol{\mu}'\rangle \tag{8.28}$$

$$= p_\mu \langle \boldsymbol{\mu}'|\,\mathrm{Tr}_S\{\mathsf{U}\,|\boldsymbol{\mu}\rangle\langle\boldsymbol{\mu}|\otimes\rho_S\,\mathsf{U}^\dagger\}\,|\boldsymbol{\mu}'\rangle \tag{8.29}$$

$$= P_{\mathrm{TPM}}[\gamma], \tag{8.30}$$

the γ-TPM associated to heat exchange. Finally, let me show that the average work is correct; consider $w[\Gamma] \equiv \boldsymbol{q}[\gamma] + n' - n$, thus

$$\mathbb{E}[w] = \sum_\Gamma w[\Gamma] P_{\mathrm{QBN}}[\Gamma] \tag{8.31}$$

$$= \sum_\gamma \overbrace{\sum_{\alpha_0,n',n} p_{\alpha_0} p_\mu |\langle n|\alpha_0\rangle|^2 |\langle n'\boldsymbol{\mu}'|\,\mathsf{U}\,|\boldsymbol{\mu}\alpha_0\rangle|^2}^{P[\gamma]} \boldsymbol{q}[\gamma] + \sum_\Gamma (n'-n) P_{\mathrm{QBN}}[\Gamma] \tag{8.32}$$

$$= Q_{\mathrm{tot}} + \sum_\Gamma (n'-n) P_{\mathrm{QBN}}[\Gamma], \tag{8.33}$$

where $Q_{\text{tot}} = \sum_i Q_i = \sum_i \text{Tr}\{\mathsf{H}_{E_i}(\rho' - \rho)\}$. Considering now the remaining term, we have

$$\sum_{\Gamma}(n' - n)P_{\text{QBN}}[\Gamma] = \sum_{\boldsymbol{\mu}\boldsymbol{\mu}'\alpha_0} p_{\alpha_0} p_{\boldsymbol{\mu}} \text{Tr}(|\alpha_0\rangle\langle\alpha_0|) \overbrace{\langle\boldsymbol{\mu}'|\,\text{Tr}_S\{\mathsf{H}_S(\tau)\mathsf{U}\,|\boldsymbol{\mu}\alpha_0\rangle\langle\boldsymbol{\mu}\alpha_0|\,\mathsf{U}^\dagger\}\,|\boldsymbol{\mu}'\rangle}^{1} \tag{8.34}$$

$$- \sum_{\boldsymbol{\mu}\boldsymbol{\mu}'\alpha_0} p_{\alpha_0} p_{\boldsymbol{\mu}}\,\text{Tr}(\mathsf{H}_S(0)\,|\alpha_0\rangle\langle\alpha_0|)\,\langle\boldsymbol{\mu}'|\,\text{Tr}_S\{\mathsf{U}\,|\boldsymbol{\mu}\alpha_0\rangle\langle\boldsymbol{\mu}\alpha_0|\,\mathsf{U}^\dagger\}\,|\boldsymbol{\mu}'\rangle \tag{8.35}$$

$$= \text{Tr}\Big(\mathsf{H}_S(\tau)\mathsf{U}\rho_S\,\mathsf{U}^\dagger\Big) - \sum_{\alpha_0} p_{\alpha_0}\,\text{Tr}(\mathsf{H}_S(0)\,|\alpha_0\rangle\langle\alpha_0|)\overbrace{\text{Tr}\Big(\mathsf{U}\rho_E\otimes|\alpha_0\rangle\langle\alpha_0|\,\mathsf{U}^\dagger\Big)}^{1} \tag{8.36}$$

$$= \text{Tr}\Big(\mathsf{H}_S(\tau)\mathsf{U}\rho_E\otimes\rho_S\,\mathsf{U}^\dagger\Big) - \text{Tr}(\mathsf{H}_S(0)\rho_S) = \Delta U. \tag{8.37}$$

Therefore,

$$\mathbb{E}[w] = Q_{\text{tot}} + \Delta U = \mathcal{W}. \tag{8.38}$$

We have achieved a distribution of work which recovers the TPM distribution for incoherent states, attains the correct average and is consistent with the γ-TPM discussed in the previous chapters.

To conclude the formal developments, I now provide the GF associated to $w[\Gamma] = \boldsymbol{q}[\gamma] + n' - n$,

$$G_{\text{QBN}}(\lambda) = \sum_{\Gamma\alpha} e^{\lambda w[\Gamma]} p_{\alpha_0} p_{\boldsymbol{\mu}} |\langle n|\alpha\rangle|^2 |\langle\boldsymbol{\mu}' n'|\,\mathsf{U}\,|\boldsymbol{\mu}\alpha_0\rangle|^2 \tag{8.39}$$

$$= \sum_{\gamma\alpha} p_{\alpha_0} p_{\boldsymbol{\mu}}\,\text{Tr}\Big(e^{-\lambda\mathsf{H}_S(0)}\,|\alpha_0\rangle\langle\alpha_0|\Big)\,\langle\boldsymbol{\mu}'|\,\text{Tr}_S\left\{e^{\lambda\mathsf{H}_E+\lambda\mathsf{H}_S(\tau)}\mathsf{U}(e^{-\lambda\mathsf{H}_E}\,|\boldsymbol{\mu}\alpha_0\rangle\langle\boldsymbol{\mu}\alpha_0|)\mathsf{U}^\dagger\right\}|\boldsymbol{\mu}'\rangle \tag{8.40}$$

$$= \sum_{\alpha_0} p_{\alpha_0}\,\langle\alpha_0|\,e^{-\lambda\mathsf{H}_S(0)}\,|\alpha_0\rangle\,\text{Tr}\left\{\mathsf{U}^\dagger e^{\lambda(\mathsf{H}_E+\mathsf{H}_S(\tau))}\mathsf{U}e^{-\lambda\mathsf{H}_E}(\rho_E\otimes|\alpha_0\rangle\langle\alpha_0|)\right\}. \tag{8.41}$$

Lest we perform the remaining sum, we just need to note that $\langle\alpha_0|\,e^{-\lambda\mathsf{H}_S(0)}\,|\alpha_0\rangle = \left(e^{-\lambda\mathsf{H}_S(0)}\right)_{\alpha_0,\alpha_0}$ is a matrix element (c-number), and can be then pushed inside the trace

$$G_{\text{QBN}}(\lambda) = \text{Tr}\Big(\mathsf{U}^\dagger e^{\lambda\mathsf{H}_E} e^{\lambda\mathsf{H}_S(\tau)}\mathsf{U}e^{-\lambda\mathsf{H}_E}\mathbb{D}\left[e^{-\lambda\mathsf{H}_S(0)}\right]\rho_E\otimes\rho_S\Big), \tag{8.42}$$

where I use the special notation $\mathbb{D}[\bullet] = \sum_{\alpha_0}\langle\alpha_0|\bullet|\alpha_0\rangle\,|\alpha_0\rangle\langle\alpha_0|$ to indicate the dephasing operator with respect to the basis *in which the initial state*, ρ_S, *is diagonal* [1]. Note that whenever such

[1] It should not be confused with the an arbitrary or energy dephasing, which I denote $\Delta(\bullet)$.

state is incoherent $\mathbb{D}$ does nothing to the exponential and we recover the GF associated to the TPM prescription.

One should also note that this formalism can be generalized for many collisions by concatenating multiple graphs, in the same fashion of Section 7.6.

Finally, considering $w \equiv \boldsymbol{q} + \delta u$ we have

$$P(w) = \int d\delta u \, d\boldsymbol{q} \, \delta(w - \delta u - \boldsymbol{q}) P(\boldsymbol{q}, \delta u), \tag{8.43}$$

$$P(\boldsymbol{q}, \delta u) = \sum_{\Gamma} \delta(\boldsymbol{q} - \boldsymbol{q}[\gamma]) \delta(\delta u - \delta u[n', n]) P_{\mathrm{QBN}}[\Gamma], \tag{8.44}$$

where $\delta u[n', n] = n' - n$. Combining the above

$$P(w) = \sum_{\Gamma} \delta(w - w[\Gamma]) P_{\mathrm{QBN}}[\Gamma], \tag{8.45}$$

where $w[\Gamma] = \boldsymbol{q}[\gamma] + \delta u[n', n]$.

8.2.3 Interpretation and connection with the no-go theorem

In the last Subsection, I have intentionally distinguished trajectories from random variables. The reason is that, while the outcomes γ can be interpreted as measurement outcomes of a single shot experiment, n and n' do not need to take part in it. To be more precise, the data from n and n' could be obtained from a different experiment, designed only for the purpose of tomographying ρ_S and, once its matrix elements were determined, a table of transition probabilities $p(n|\alpha_0)$ could be constructed. Once we come to measure γ, these provide an extra piece of information to determine $P[\Gamma]$, without ever knowing which trajectory Γ the system undertook. Indeed, giving up access to a trajectory is the toll we pay to thwart back-action in the QBN description; faced with the impossibility of (non-invasibly) accessing *what happened* we comply with describing *what could have happened* — the first is endowed with a notion of a probability distribution constructed from repetitions of equal preparations of a single-shot experiment, while the second subjectively establishes possibilities by considering data which are fundamentally generated by quantum theory, but not necessarily in a single-shot. To further

this reasoning, consider

$$P_{\mathrm{QBN}}[\Gamma] = \sum_{\alpha_0} p_{\alpha_0} p_{\boldsymbol{\mu}} |\langle \alpha_0 | n \rangle|^2 |\langle \boldsymbol{\mu}' n' | \mathsf{U} | \boldsymbol{\mu} \alpha_0 \rangle|^2; \tag{8.46}$$

this prescription depends on the system's state since we have to know the basis in which the system is diagonal to measure it, that is, we violate (I) of the no-go theorem. Yet, this particular violation does not make the QBN distribution negative. Let me rewrite the above in terms of traces

$$P_{\mathrm{QBN}}[\Gamma] = \sum_{\alpha_0} \mathrm{Tr}(\Pi_n \Pi_{\alpha_0}) \, \mathrm{Tr}\Big(\mathsf{U}^\dagger \Pi_{\boldsymbol{\mu}'} \otimes \Pi_{n'} \mathsf{U} \Pi_{\boldsymbol{\mu}} \otimes \Pi_{\alpha_0} \rho_E \otimes \rho_S \Big). \tag{8.47}$$

Rather than a single trace, we have the product of two, which can be interpreted as two separate protocols (or experiments), in each experiment the protocol applied to $|\alpha_0\rangle$ is distinct, *i.e.*, in practice one needs two copies of $|\alpha_0\rangle$. Matching outcomes α_0 are then interpolated through Bayesian inference. Apparently, there seems to be no way to write the above as $P[\Gamma] = \mathrm{Tr}(\mathsf{K}_\Gamma \rho)$. But, should it not be possible, would this make Eq. (8.47) not plausible? Consider a hypothetical situation in which we want to measure a quantum system with an usual mercury thermometer [experiment (1)]. At some point in history there were experiments establishing a correspondence table between the height of the mercury column and the Celsius scale [experiment (2)]. This correspondence table is given in the context of experiment (1), which is concerned with the unitary interaction between the mercury and the system of interest. By the time of experiment (1), nobody cares about providing a POVM which describes experiments (1) and (2) altogether. Nevertheless, one uses a subjective belief — the prior validation of experiment (2) — encoded in the thermometer marks. The crucial point is that it does not necessarily make sense to provide a POVM to an inference-based method and this does not hurt our everyday scientific practice. By the contrary, Science is filled with Bayesian reasoning and it does not need to be embedded in quantum theory. To better qualify Bayesian reasoning, I refer to the following quote.

"*The abandonment of superstitious beliefs about the existence of Phlogiston, the Cosmic Ether, Absolute Space and Time, . . . , or Fairies and Witches, was an essential step along the road to scientific thinking. Probability, too, if regarded as something endowed with some kind of objective existence, is no less a misleading misconception, an illusory attempt to exteriorize or materialize our true probabilistic beliefs.(...)*

Probabilistic reasoning—always to be understood as subjective—merely stems from our

being uncertain about something. It makes no difference whether the uncertainty relates to an unforseeable future, or to an unnoticed past, or to a past doubtfully reported or forgotten; it may even relate to something more or less knowable (by means of a computation, a logical deduction, etc.) but for which we are not willing or able to make the effort; and so on." (de Finetti [147])

Although de Finetti takes a rather liberal stance regarding the meaning of probabilities, it would still be discomforting to conclude that no quantum experiment could sample the QBNs discussed thus far. Fortunately, this is not the case [146]. To do that, we need to realize that the traces in Eq. (8.47) can be thought as being performed over different copies of the system's Hilbert space, $\mathscr{H}_S \to \mathscr{H}_{S_1} \otimes \mathscr{H}_{S_2}$. Doing so, we can write a single trace

$$P_{\text{QBN}}[\Gamma] = \sum_{\alpha_0} p_{\alpha_0} \operatorname{Tr}\left\{\left([\mathsf{U}^\dagger \otimes \mathbb{1}_{S_2}]\Pi_{\mu'} \otimes \Pi_{n'} \otimes \mathbb{1}_{S_2}[\mathsf{U} \otimes \mathbb{1}_{S_2}]\Pi_{\mu} \otimes \mathbb{1}_{S_1} \otimes \Pi_n\right)\rho_E \otimes |\alpha_0\alpha_0\rangle\langle\alpha_0\alpha_0|\right\}. \tag{8.48}$$

Then, define the broadcast state $\rho_{\text{bro}} \equiv \sum_{\alpha_0} p_{\alpha_0} |\alpha_0\alpha_0\rangle\langle\alpha_0\alpha_0| \in \mathcal{L}(\mathscr{H}_{S_1} \otimes \mathscr{H}_{S_2})$ and the operator $\mathsf{K}_\Gamma \equiv [\mathsf{U}^\dagger \otimes \mathbb{1}_{S_2}]\Pi_{\mu'} \otimes \Pi_{n'} \otimes \mathbb{1}_{S_2}[\mathsf{U} \otimes \mathbb{1}_{S_2}]\Pi_{\mu} \otimes \mathbb{1}_{S_1} \otimes \Pi_n \in \mathcal{L}(\mathscr{H}_E \otimes \mathscr{H}_{S_1} \otimes \mathscr{H}_{S_2})$ and we have

$$P_{\text{QBN}}[\Gamma] = \operatorname{Tr}(\mathsf{K}_\Gamma \rho_E \otimes \rho_{\text{bro}}). \tag{8.49}$$

In the original no-go paper [42] the authors have suggested a state-dependent protocol to measure coherent work based on using multiple copies of the quantum system. In [146] the connection between QBNs and the broadcast state suggests that entanglement between copies allows going beyond the original proposal. The shortcoming of this method is that you cannot sample the QBN distribution from the original system of interest. Note that we do not achieve the form suggested in (ii) of the no-go theorem (pg. 114), $P_{\text{QBN}}[\Gamma] = \operatorname{Tr}(\mathsf{K}_\Gamma \rho_E \otimes \rho)$; instead, we resorted to the preparation of a particular entangled state to book-keep copies of a projected state, so that an extra measurement could be performed on the copy while the original state keeps evolving without suffering the back-action from this extra measurement. Another way to achieve this procedure is to perform post-selection; instead of considering a special initial preparation ρ_{bro}, we consider a "measurement" $\Pi_{\alpha_0} \otimes \Pi_{\alpha_0}$ [146]. Indeed, we consider $\Pi_{\alpha_0} \otimes \Pi_{\alpha_0'}$ and discard whatever data with $\alpha_0' \neq \alpha_0$. The QBN we have considered here is subtle because it combines actual measurements (γ-TPM) with inferred possibilities (which stem either from prior characterization/different experiments or broadcast states/post-selection).

As a take-home message, we have discussed that the initial reasoning behind $P_{\mathrm{QBN}}[\Gamma]$, arguably, does not need to be embedded in a single quantum experiment to make sense. However, it is not inconsistent with such program since one can provide a POVM to extract quantum Bayesian networks. I also emphasize that the no-go result is not contradicted by the QBN formalism, since it depends on the system's initial state and $\rho_S = \alpha\rho'_S + (1-\alpha)\rho''_S$ does *not* imply that $P_{\mathrm{QBN}}(\rho_S) = \alpha P_{\mathrm{QBN}}(\rho'_S) + (1-\alpha)P_{\mathrm{QBN}}(\rho''_S)$, again violating one of the formulations of (I) in pg. 114.

8.3 Application to the SSDB amplifier

Consider the SSDB amplifier introduced in Section 5.3, which generally operates in a coherent steady-state. Here, I use this system as an illustrative example to compare four approaches to the work distribution: quasi-probabilities (QPDs), quantum Bayesian network (QBNs), the (invasive) two-point measurement (TPM) and the operator of work (OW). For that sake, I study the statistics according to each prescription, $P_{\mathcal{P}}$, of the parameter h, which controls the amount of coherence in the model (as reference for $C_{\mathrm{rel}}(\rho_S)$ see Fig. 5.6(c)). In the QPD case, I concentrate in the real QPD corresponding to Eq. (8.14).

We already know that, except by the TPM, all approaches coincide at the level of averages. For this reason, in Fig. 8.3, I plot the work variance and third moment varying h and the generating functions for $h = 2.0$

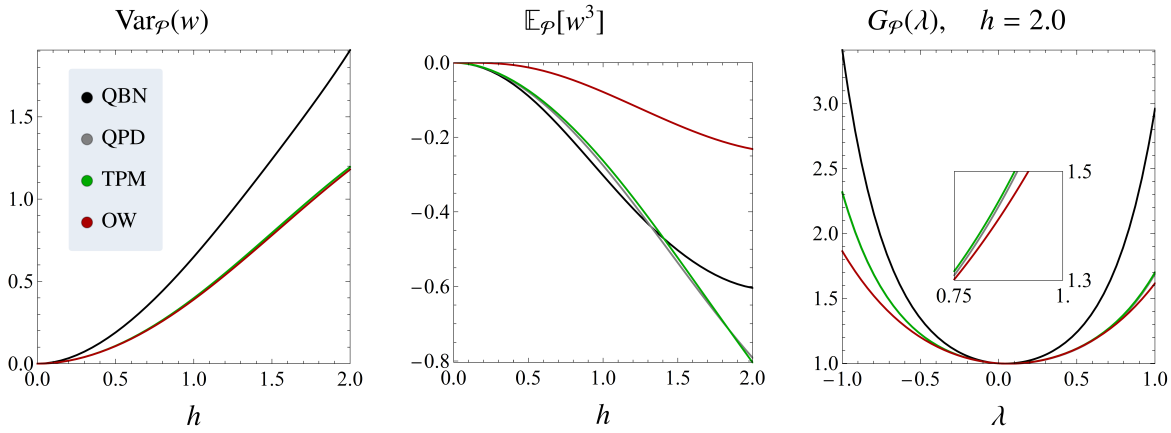

Figure 8.3: In all plots, I set $\lambda_A = 0.4$, $\lambda_B = 0.1$, $\omega_3 = 2.0, \omega_2 = 1.0 = g = \tau$. (a) Variance for four approaches. (b) Third moment for four approaches. (c) Generating functions, where I fixed $h = 2.0$. In the inset, I enlarge the region $\lambda \in [0.75, 1.0]$ to highlight the distinction between the plots.

Figure 8.3 highlights the differences between all the descriptions. For the variance ,Fig. 8.3

(a), they all coincide for $h = 0$, since at this point strict energy conservation is established. We observe that the QBN has the biggest variance in all regions. Further, all the remaining curves are very close to each other. In particular, OW and QPD overlap and are always lower than the TPM variance. Indeed, QPD and OW variances coincide analytically, since I worked with the QPD which has $\zeta = 2$ (see Eq. (8.12)), yet coincidences do not survive in higher moments. Figure 8.3 (b) displays the third moments, we see that this time OW is starkly different from the rest. Bayesian networks, QPD and TPM remain close until $h \approx 1.5$, where QBN start to differ from the others more significantly. The TPM and the QPD approaches neither coincide nor bound each other. Finally, Fig. 8.3 (c) fixes $h = 2.0$ and depicts more generally the differences at the level of all moments. At this parameter choice the QBN approach is always steeper, and the rest of the prescriptions are close to each other. In the inset we can distinguish between them, with the TPM very close and higher than QPD and OW smaller than both.

Even in concrete cases, it is hard to spot the physical difference from QPDs and QBNs, which are the approaches which attain correct averages and agreement with classical FTs. In general, the best we can say is that they provide different results and are associated to distinct measurement protocols. Moreover, the QPD's moments are difficult to interpret in the usual statistical sense due to the negativeness of quasi-probabilities.

Chapter 9

The quantum mean-square predictor of work

This Chapter is the main original contribution of this dissertation [45]. It is devoted to formulate and solve the following problem: *given one can measure the heats, what is the best she can guess about work?*

Before further discussing the problem, I shall mention that the techniques considered in the last Chapter were not the only directions of investigation to avoid the enigma of quantum work. Other approaches take a more pragmatic path and, instead of extracting all information about the work distribution, they avoid some of the measurements in order to leave coherence untouched. This track is also interesting for experimental reasons, since the TPM scheme is not always easily implemented in the lab. For example, in [148], the authors provide a Jarzynski-like equality for a driven closed system, in which the first measurement of the TPM protocol is neglected. Later, this work was generalized to open quantum systems in [121]. In these cases the equality has a correction term accounting for the neglected measurement, but it does not destroy initial coherences.

In [121], they rely on guessing a distribution and then finding the best possible guess in the sense of maximizing the von Neumann entropy. The spirit of such optimization task is to find the most unbiased guess for an unknown distribution, while fixing some average quantities. We have taken some inspiration from these works, but here we instead want to find the distribution that better approximates the Bayesian network distribution without system measurements. Indeed, we combine this class of methods with the QBN formalism discussed in the last Chapter. As I have discussed in the previous Chapter, the shortcoming of the QBN approach is the real-

izing the system measurements, although it provides a formally consistent probabilistic model. The QBN model embeds a causal structure grounded in the underlying quantum channels, reproduces the correct average and TPM for incoherent system; these therefore qualify it as a robust model for work distributions, although it is manifestly hard to access in practice. This leads us to the concept of *statistical prediction*, which will provide a systematic way of estimating a distribution given limited information about it. As the main reference for statistical prediction I follow Bickel and Doksum's book [44]. After discussing its basic features, I formulate the problem in the thermodynamics context and develop its quantum version, which relies on the QBN model and the Kraus operators generating the open system evolution. Finally, the framework is applied to a qubit model and to the SSDB amplifier.

9.1 Statistical prediction

Suppose you are a Physics professor and you want to forecast the grades of the students in their Physics (I) exam, which I name by a random variable Y. There is no way to obtain this data, since the exam has not been applied yet. So, you consider another set of data, the grades the same students had in their Physics test for the college admission, which I call a random variable X. These two sets of data are arguably correlated, and jointly described by a distribution $P(X,Y) \neq P(X)P(Y)$. Statistical prediction [44] consists in exploiting such correlations to guess Y based on X. Formally, we need a function $g(X)$ which predicts Y; further, we also need a figure to quantify "best". Note that, prior to the solution of the problem, we also assumed the existence of some model $P(X,Y)$ which relates X and Y, although we do not have access to the data Y. The model expresses our beliefs about the distribution based on general principles or other subjective beliefs.

The concept of best, or optimal, that I assume here is based on the mean-square error (MSE)[1]:

$$\epsilon^2_{\text{MSE}}(Y, g(X)) \equiv \mathbb{E}[(Y - g(X))^2], \tag{9.1}$$

[1]The MSE is the Euclidean squared-distance equivalent for random variables. The method presented here generalizes to other notions of distance, but the MSE is the traditional measure in mathematical theory of prediction, whose deepest results build upon [44].

with $\mathbb{E}[\bullet] = \int dXdY \bullet P(X,Y)$. That is, we want the function $f_{\text{opt}}(X)$ such that

$$\mathbb{E}[(Y - g(X))^2] \geq \mathbb{E}[(Y - f_{\text{opt}}(X))^2], \quad \forall g. \tag{9.2}$$

Note that, since $P(X,Y) \geq 0$ the RHS of the inequality is always non-negative. This is a trivial remark in the realm of statistics, but once we put it in the perspective of QPDs it will come relevant. Starting from a simplified case, suppose $g(X) = c$, that is, a constant and define $\mathcal{Y} = \mathbb{E}[Y]$. Then, writing $Y - c = Y - \mathcal{Y} + \mathcal{Y} - c$ we have

$$\mathbb{E}[(Y-c)^2] = \mathbb{E}[(Y-\mathcal{Y})^2] + (\mathcal{Y}-c)^2 + 2(\mathcal{Y}-c)\cancelto{0}{\mathbb{E}[Y-\mathcal{Y}]} \tag{9.3}$$

$$= \mathbb{E}[(Y-\mathcal{Y})^2] + (\mathcal{Y}-c)^2 \geq \mathbb{E}[(Y-\mathcal{Y})^2], \tag{9.4}$$

with equality *iff* $c = \mathcal{Y}$. Then, the constant which better approximates Y is its average $\mathcal{Y}$.

Now, consider the *univariate* distribution $P(Y|X)$, with an associated averaging operation $\mathbb{E}[\bullet|X]$. The above reasoning for constants apply also to this case since X is given, by considering the (conditioned) average $\mathcal{Y}(X) \equiv \mathbb{E}[Y|X]$. Thus,

$$\mathbb{E}[(Y-g(X))^2|X] = \mathbb{E}[(Y-\mathcal{Y}(X))^2|X] + (g(X)-\mathcal{Y}(X))^2 \tag{9.5}$$

$$= \int dY P(Y|X)(Y-g(X))^2 + (g(X)-\mathcal{Y}(X))^2. \tag{9.6}$$

Now, multiply both sides by $P(X)$ and integrate over dX to obtain

$$\mathbb{E}[(Y-g(X))^2] = \int dXdY P(Y|X)P(X)(Y-g(X))^2 + \int dX P(X)(g(X)-\mathcal{Y}(X))^2 \tag{9.7}$$

$$= \mathbb{E}[(Y-\mathcal{Y}(X))^2] + \mathbb{E}[(g(X)-\mathcal{Y}(X))^2], \tag{9.8}$$

where Bayes' rule, $P(X,Y) = P(Y|X)P(X)$, is regarded. Thereof, we have the inequality

$$\mathbb{E}[(Y-g(X))^2] \geq \mathbb{E}[(Y-\mathcal{Y}(X))^2], \quad \forall g, \tag{9.9}$$

which guarantees that $f_{\text{opt}}(X) = \mathcal{Y}(X)$; *i.e.*, the conditioned average is the optimal mean-square predictor (MSP).

Let me consider a limiting situation in which we can find a function $f(X) = Y$, we then have that the optimal prediction is *exact*: $\epsilon^2_{\text{MSP}} = \mathbb{E}[(f_{\text{opt}}(X) - \mathcal{Y}(X))^2] = 0$. All the mathematical

results from this section can be derived in a more rigorous way in [44]. In physical situations, this can be traced back to exploiting some kind of symmetry (see Subsection 7.3).

9.2 The quantum mean-square predictor of work

We are now ready to formulate and answer the main question of this Chapter. Suppose we have a quantum systems coupled to an arbitrary number of environments, exchanging heat q_i with each of them, and let again $\boldsymbol{q} = (q_1, q_2, ..)$. Suppose now that one cannot measure the system energy changes together with heat, but still needs to estimate work. That is, we want the function $\mathcal{W}(\boldsymbol{q})$ which minimizes the mean-square error

$$\epsilon^2 = \int dw \, [w - \mathcal{W}(\boldsymbol{q})]^2 \, P(w, \boldsymbol{q}), \tag{9.10}$$

or, equivalently[2],

$$\epsilon^2 = \int d\boldsymbol{q} \, d\delta u \;\; [\boldsymbol{q} + \delta u - \mathcal{W}(\boldsymbol{q})]^2 \, P(\boldsymbol{q}, \delta u). \tag{9.11}$$

According to the last section, the mean-square predictor must be the conditioned average of w. With respect to the distribution $P(\boldsymbol{q}, \delta u)$ this is

$$\mathcal{W}_{\rm opt}(\boldsymbol{q}) = \int d\delta u \; (\boldsymbol{q} + \delta u) P(\boldsymbol{q}, \delta u | \boldsymbol{q}), \tag{9.12}$$

where I have used Eq. (8.43). We then have that

$$\mathcal{W}_{\rm opt}(\boldsymbol{q}) = \boldsymbol{q} + \int d\delta u \; \delta u \frac{P(\boldsymbol{q}, \delta u)}{P(\boldsymbol{q})}. \tag{9.13}$$

[2] $$P(w, \boldsymbol{q}) = \int d\boldsymbol{q}' \; d\delta u \; \delta(\boldsymbol{q} - \boldsymbol{q}') \delta(w - \delta u - \boldsymbol{q}') P(\boldsymbol{q}', \delta u) = \int d\delta u \; \delta(w - \delta u - \boldsymbol{q}) P(\boldsymbol{q}, \delta u),$$
then
$$\epsilon^2 = \int dw [w - \mathcal{W}(\boldsymbol{q})]^2 P(w, \boldsymbol{q}) = \int d\delta u \;\; \int dw \; [w - \mathcal{W}(\boldsymbol{q})]^2 \delta(w - \delta u - \boldsymbol{q}) P(\boldsymbol{q}, \delta u).$$
Integrating over dw then leads to Eq. (9.11).

where $P(\boldsymbol{q}, \delta u)$ is given by the QBN distribution

$$P(\boldsymbol{q}, \delta u) = \sum_{\Gamma} \underbrace{\left[\prod_i \delta[q_i - (\mu_i' - \mu_i)]\right]}_{\equiv \delta(\boldsymbol{q} - \boldsymbol{q}[\gamma])} \delta[\delta u - (n' - n)] P_{\mathrm{QBN}}[\Gamma]. \tag{9.14}$$

Then, combining Eqs. (9.13) and (9.14) and integrating in δu we have

$$\mathcal{W}_{\mathrm{opt}}(\boldsymbol{q}) = \boldsymbol{q} + \frac{1}{P(\boldsymbol{q})} \sum_{\gamma} \delta(\boldsymbol{q} - \boldsymbol{q}[\gamma]) \sum_{n',n} (n' - n) P_{\mathrm{QBN}}[\Gamma], \tag{9.15}$$

where I have again denoted $\gamma = (\boldsymbol{\mu}, \boldsymbol{\mu}') = (\mu_1, \mu_2, ..., \mu_1', \mu_2', ...)$ and $\Gamma = (\gamma, n, n')$. I now derive its quantum-mechanical expression, by working the last term in Eq. (9.15)

$$\sum_{nn'} (n' - n) P_{\mathrm{QBN}}[\Gamma] = \sum_{nn'\alpha} (n' - n) p_\alpha p_\mu |\langle n|\alpha_0\rangle|^2 |\langle \boldsymbol{\mu}' n'| \mathsf{U} |\boldsymbol{\mu}\alpha_0\rangle|^2 \tag{9.16}$$

$$= \Bigg(\sum_{\alpha} p_\alpha p_\mu \langle \boldsymbol{\mu}'| \mathrm{Tr}_S \left(\mathsf{H}_S(\tau) \mathsf{U} |\boldsymbol{\mu}\alpha_0\rangle\langle\boldsymbol{\mu}\alpha_0| \mathsf{U}^\dagger \right) |\boldsymbol{\mu}'\rangle \tag{9.17}$$

$$- \sum_{\alpha} p_\alpha p_\mu \langle \alpha_0| \mathsf{H}_S(0) |\alpha_0\rangle \langle \boldsymbol{\mu}'| \mathrm{Tr}_S \left(\mathsf{U} |\boldsymbol{\mu}\alpha_0\rangle\langle\boldsymbol{\mu}\alpha_0| \mathsf{U}^\dagger \right) |\boldsymbol{\mu}'\rangle \Bigg) \tag{9.18}$$

$$= p_\mu \mathrm{Tr}\Big(\mathsf{H}_S(\tau) \langle \boldsymbol{\mu}'| \mathsf{U} |\boldsymbol{\mu}\rangle \rho_S \langle \boldsymbol{\mu}| \mathsf{U}^\dagger |\boldsymbol{\mu}'\rangle - \mathbb{D}\left[\mathsf{H}_S(0)\right] \langle \boldsymbol{\mu}| \mathsf{U}^\dagger |\boldsymbol{\mu}'\rangle \langle \boldsymbol{\mu}'| \mathsf{U} |\boldsymbol{\mu}\rangle \rho_S \Big), \tag{9.19}$$

where $\mathbb{D}(\bullet) \equiv \sum_\alpha \langle\alpha_0| \bullet |\alpha_0\rangle |\alpha_0\rangle\langle\alpha_0|$. By defining $\mathsf{M}_\gamma \equiv \sqrt{p_\mu} \langle \boldsymbol{\mu}'| \mathsf{U} |\boldsymbol{\mu}\rangle$ and substituting back in Eq. (9.15) we find

$$\mathcal{W}_{\mathrm{opt}} = \boldsymbol{q} + \frac{1}{P(\boldsymbol{q})} \sum_{\gamma} \delta(\boldsymbol{q} - \boldsymbol{q}[\gamma]) \mathrm{Tr}\Big(\mathsf{H}_S(\tau) \mathsf{M}_\gamma \rho_S \mathsf{M}_\gamma^\dagger - \mathbb{D}[\mathsf{H}_S(0)] \mathsf{M}_\gamma^\dagger \mathsf{M}_\gamma \rho_S \Big) \tag{9.20}$$

$$= \boldsymbol{q} + \frac{1}{P(\boldsymbol{q})} \sum_{\gamma} \delta(\boldsymbol{q} - \boldsymbol{q}[\gamma]) \left\langle \mathsf{M}_\gamma^\dagger \mathsf{H}_S(\tau) \mathsf{M}_\gamma - \frac{1}{2} \left\{ \mathbb{D}[\mathsf{H}_S(0)], \mathsf{M}_\gamma^\dagger \mathsf{M}_\gamma \right\} \right\rangle_{\rho_S}. \tag{9.21}$$

Our main result can now be summarized as follows

Quantum mean-square predictor of work — The predictor of work $\mathcal{W}_{\text{opt}}(\boldsymbol{q})$ which minimizes the mean-square error, Eq. (9.11), is

$$\mathcal{W}_{\text{opt}}(\boldsymbol{q}) = \boldsymbol{q} + \frac{1}{P(\boldsymbol{q})}\sum_{\gamma}\delta(\boldsymbol{q}-\boldsymbol{q}[\gamma])\left\langle \mathsf{M}_{\gamma}^{\dagger}\mathsf{H}_{S}(\tau)\mathsf{M}_{\gamma} - \frac{1}{2}\left\{\mathbb{D}[\mathsf{H}_{S}(0)], \mathsf{M}_{\gamma}^{\dagger}\mathsf{M}_{\gamma}\right\}\right\rangle_{\rho_{S}} . \tag{9.22}$$

Equivalently [45], the predictor of work $\mathcal{W}_{\text{opt}}[\gamma]$ which minimizes the mean-square error ϵ_{QBN}

$$\epsilon_{\text{QBN}}^{2} = \sum_{\Gamma}(w[\Gamma]-\mathcal{W}[\gamma])^{2}P_{\text{QBN}}[\Gamma]. \tag{9.23}$$

is

$$\mathcal{W}_{\text{opt}}[\gamma] = \boldsymbol{q}[\gamma] + \frac{1}{P[\gamma]}\left\langle \mathsf{M}_{\gamma}^{\dagger}\mathsf{H}_{S}(\tau)\mathsf{M}_{\gamma} - \frac{1}{2}\left\{\mathbb{D}[\mathsf{H}_{S}(0)], \mathsf{M}_{\gamma}^{\dagger}\mathsf{M}_{\gamma}\right\}\right\rangle_{\rho_{S}} . \tag{9.24}$$

9.2.1 Discussion

At this point, we must note that the above results are much more general than the collisional model framework. There are various ways in which one can generate the same quantum channel M_{γ} and we could have derived a similar result based on considerations associated to other open quantum system approaches. This makes the QMSP extremely general and suited to several kinds of applications.

The first way to cast the result, Eq. (9.2), highlights that the prediction of work is based primarily on the heat measurements, and not on the TPM scheme. As we will further discuss in the following applications, one does not necessarily measure or cast heat exchanges in terms of TPMs. On this wise, I would like to emphasize the following picture:

$$\overbrace{\mathcal{W}_{\text{opt}}(\boldsymbol{q})}^{\text{prediction}} = \underbrace{\boldsymbol{q} + \frac{1}{P(\boldsymbol{q})}}_{\text{experiment}} \overbrace{\sum_{\gamma}\delta(\boldsymbol{q}-\boldsymbol{q}[\gamma])\left\langle \mathsf{M}_{\gamma}^{\dagger}\mathsf{H}_{S}(\tau)\mathsf{M}_{\gamma} - \frac{1}{2}\left\{\mathbb{D}[\mathsf{H}_{S}(0)], \mathsf{M}_{\gamma}^{\dagger}\mathsf{M}_{\gamma}\right\}\right\rangle_{\rho_{S}}}^{\text{model}} . \tag{9.25}$$

Our model is constituted by some prior characterization involving ρ_S, H_S and eventually the γ-TPM protocol. Once the model is settled, we can collect data in the lab to establish $P(\boldsymbol{q})$.

Whether the precise experiment we perform is the γ-TPM or not is unimportant, as long as we are able to measure $\boldsymbol{q}$, construct an histogram for $P(\boldsymbol{q})$ and check if it agrees with the theoretical predictions of the γ-TPM. In general, the TPM has more information than we need if we are interested in heat and work. If the Bohr frequencies $\mu_i' - \mu_i$ are degenerate[3], there are several pairs (μ_i, μ_i') associated to each $q_i[\gamma]$ and we do not need to distinguish them to attain the desired prediction of work.

However, the TPM is still appealing since it connects heats with observables and I now resort to the formulation in Eq. (9.24) to discuss the intuition behind the result. For this sake, I review some central ideas discussed throughout this dissertation. For simplicity, let me consider the CM framework and suppose that ρ_S is the steady-state, ρ_S^*. I also consider H_S time-independent. At the level of averages, we have the first law

$$Q_{\text{tot}} = \mathcal{W}, \tag{9.26}$$

which means that we can infer work exactly by measuring heats. When it comes to fluctuations, the situation gets more involved; although $\Delta U = 0$, internal energy changes still fluctuate and pose a problem to infer work from the first law. But, exploiting certain properties of the evolution map (see Subsection 3.2.5), we can still infer work under certain conditions. For instance, when we have $[\mathsf{H}_E + \mathsf{H}_S, \mathsf{U}] = 0$,

$$\boldsymbol{q}[\gamma] + \delta u[n, n'] = 0 = w[\Gamma], \quad \forall \Gamma \quad \text{s.t.} \quad P[\Gamma] \neq 0. \tag{9.27}$$

This assures that work is not only zero but does not fluctuate too and we can exactly determine it. This is the case in which the stroboscopic map is an incoherent operation (see Chapter 3).

In some cases, we can still infer work exactly with $[\mathsf{H}_E + \mathsf{H}_S, \mathsf{U}] \neq 0$. This can be done if a conserved quantity that allows the elimination of system's degrees of freedom from $w[\Gamma]$ can be constructed. In practice, this allows the assignment $f[\gamma] = \Gamma$. This situation fits some incoherent steady-states, as discussed in Subsection 7.3, a case interesting by itself, since it can reduce the amount of measurements needed to obtain a work distribution.

Suppose now we cannot measure the system and we cannot in general eliminate the system variables. For example, if the system of interest is too complicated to find suitable conserved quantities and we cannot measure it for some experimental limitation. Or, if quantum mechan-

[3]Note that this can happen regardless of the environment Hamiltonians being degenerate.

ics flaunts the impasse of energetic coherences. We have to deal with the fact that we will not dispose of the complete information and start to make guesses. First, we can just roughly set internal energy fluctuations to zero, and estimate work fluctuations directly from $w[\gamma] \approx \boldsymbol{q}[\gamma]$. Or, in the case we are not in the steady-state we would estimate $w[\gamma] \approx \boldsymbol{q}[\gamma] + \Delta U$, using the knowledge of the average. But, even in the steady state, we can update our knowledge about the internal energy fluctuations beyond averages, based only on the information acquired about heats; this leads to the refinement $\mathcal{W}[\gamma] = \boldsymbol{q}[\gamma] + \Delta U[\gamma]$. The QMSP of work is the formalization of this idea, it shows that the optimal way to update information about the system's energy based on heat outcomes is the conditioned average and accompanies a systematic way to track the precision of such guess. The MSE is an important technical piece, since it provides the necessary frame of optimization to derive the QMSP but, from the physical standpoint, the QMSP is itself meaningful: it sits in a middle step between the average first law and a "complete" stochastic formulation of it. Since a "complete" stochastic first law misses out the role of coherence, the QMSP can be regarded as a stochastic first law which accounts for coherence in an optimal way.

Another central aspect of the method presented here is the probabilistic model we have used as the background. In classical scenarios, the background model could be better or worse depending on how we use it to encode our beliefs about the object of description. But a classical mindset allows one to blame herself for not being able to provide the greatest probabilistic model, maybe due to the lack of technology or team to collect data. As we have seen in the previous Chapter, there are a couple different ways in which one can ascribe (quasi) probabilities to work, but neither of them is perfect due to fundamental limitations. In fact, there are roughly[4] two possibilities if we want to produce correct averages and agree with classical FTs: QBNs and QPDs. One now may then wonder whether we could have developed a QMSP based on a QPD. We can indeed always produce a legit conditioned average. For instance, according to the QPD of the form in Eq. (8.14) we would have

$$\mathcal{W}[\gamma] = \boldsymbol{q}[\gamma] + \frac{1}{P[\gamma]} \left\langle \mathsf{M}_\gamma^\dagger \mathsf{H}_S(\tau) \mathsf{M}_\gamma - \frac{1}{2} \left\{ \mathsf{H}_S(0), \mathsf{M}_\gamma^\dagger \mathsf{M}_\gamma \right\} \right\rangle_{\rho_S} , \tag{9.28}$$

which is the same result of the incoherent case of the QBN formalism. Yet, the anti-commutator

[4] As pointed in [122], QBNs can be classified, together with other techniques not discussed here, as methods lacking σ-additivy. In the same way, there are different types of QPDs and measurements schemes not considered here [13]. These sets of methods represent different ways of violating (I) of the no-go theorem. For simplicity, I contrast only QBNs and QPDs as representatives.

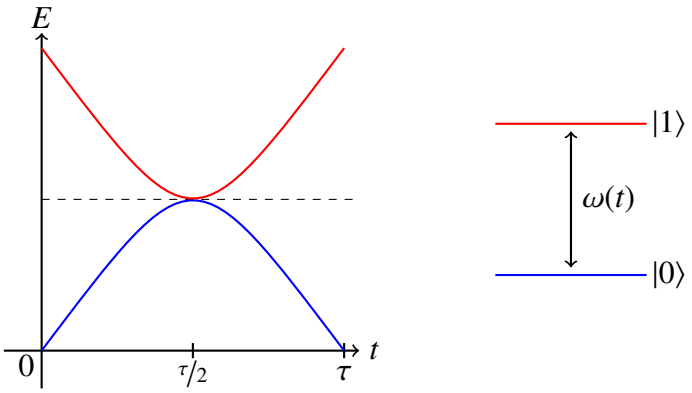

Figure 9.1: Avoided crossing scenario for a single qubit.The energy gap between the qubits, $\omega(t)$, is varied through a time interval $[0, \tau]$, so that at $t = \tau/2$ the jump probability is arbitrarily large.

here enforces the fact the $[\rho_S, \mathsf{H}_S(0)] = 0$, while in the general QBN case $[\rho_S, \mathbb{D}[\mathsf{H}_S(0)]] = 0$. The structure of such QPD's conditioned average was discussed in [149], where instead of heat baths the Kraus components encode a generic measuring apparatus, associated to weak-measurement schemes. However, the usage of QPDs has a shortcoming in the viewpoint of statistical prediction: we cannot assure that the conditioned average is the optimal predictor. This subtlety comes from inequality (9.2), whose RHS is only guaranteed to be positive because the probabilities are positive. Thus, the lower bound provided by the QPD's conditioned average may have an *absolute value* greater than some other candidate, thereby making a non-optimal prediction. Therefore, it is unclear in what circumstances the technique here presented is applicable to QPDs and Bayesian networks stand as the natural language to safely work with traditional inference methods.

9.3 Minimal qubit example: two-step processes

Before applying the QMSP to a more complicated system, we need to develop some intuition on how it works. This application also connects our framework with certain experimental implementations [26], and allows looking beyond the CM framework.

Consider a system and a bath, namely S and E with ρ_S an arbitrary state and $\rho_E = \rho_E^{\text{th}}$. They interact through an unitary map which we can be split in two parts, $\mathsf{U} = \mathsf{U}_h(\mathbb{1}_E \otimes \mathsf{U}_w)$.

The first part, $\mathsf{U}_w \in \mathcal{L}(\mathscr{H}_S)$, encompasses a pure work protocol in S which *always* leads to energy jumps in the system. It can be implemented through $\mathsf{U}_w = \mathcal{T} e^{-i\int_0^\tau dt \mathsf{H}_S(t)}$, but what matters is that, given initial system energy eigenstuff $\mathsf{H}_S(0)\,|n_i\rangle = n_i\,|n\rangle$, they are modified to

$\mathsf{H}_S(\tau)\,|m'\rangle = m'\,|m'\rangle$. This is the case of an avoided crossing protocol in a qubit [26], as depicted in Fig. 9.1; during the interval $[0, \tau/2]$, the gap is decreased and by $t = \tau/2$ the probability of a jump (either from the excited to the ground or vice-versa) reaches 1 and, because a jump has certainly occurred (either if we start with an excited or a ground state), and the levels split again during the remaining interval $[\tau/2, \tau]$ instead of crossing each other. For qubits, the simplest way to summarize this process is $\mathsf{U}_w = \sigma_S^x$.

The second part, U_h entails only heat exchange between E and S, *i.e.*, it satisfies $[\mathsf{H}_A + \mathsf{H}_S(\tau), \mathsf{U}_h] = 0$. In the case of a qubit, we can also use a simple unitary to implement this, a swap

$$\mathsf{U}_{\text{swap}} = \begin{pmatrix} 1 & 0 & 0 & 0 \\ 0 & 0 & 1 & 0 \\ 0 & 1 & 0 & 0 \\ 0 & 0 & 0 & 1 \end{pmatrix}. \tag{9.29}$$

The swap can be viewed as a limiting case of the same kind of interaction we have been studying in most examples, we can see this by writing

$$e^{ig(\sigma_S^-\sigma_E^+ + \sigma_S^+\sigma_E^-)} = \begin{pmatrix} 1 & 0 & 0 & 0 \\ 0 & \cos g & i\sin g & 0 \\ 0 & i\sin g & \cos g & 0 \\ 0 & 0 & 0 & 1 \end{pmatrix}, \tag{9.30}$$

in which we appropriately choose g and ignore a phase factor. In practice, the physics behind the present choice of U is very close to what we have been discussing throughout this dissertation, with the roles of work and heat separated in different steps.

What will be a little bit different is that, instead of the steady-state, we study a generic initial state. For qubits, a generic state can be parametrized in the following way; we start with a diagonal state $\text{Diag}\{(1-s)/2, (1+s)/2\}$ with $s \in [0, 1]$, in the computational basis $\{|1\rangle, |0\rangle\}$ and then perform a general rotation in the Bloch sphere, producing

$$\rho_S = \frac{1}{2}\begin{pmatrix} 1 + s\cos\theta & se^{-i\phi}\sin\theta \\ se^{i\phi}\sin\theta & 1 - s\cos\theta \end{pmatrix}. \tag{9.31}$$

For simplicity, I set henceforth $\phi = 0$. In this manner, θ is responsible for tracking coherence

($\theta = 0, \pi$ give incoherent states). Moreover, $\mathsf{H}_S(\tau) = \mathsf{H}_S(0) = \omega\sigma_S^+\sigma_S^- = \omega\,|1\rangle_S\langle 1|$ and $\mathsf{H}_E = \omega\sigma_E^+\sigma_E^- = \omega\,|1\rangle_E\langle 1|$.

In this scenario, although we have $[\mathsf{H}_A + \mathsf{H}_S(\tau), \mathsf{U}_h] = 0$ and hence the map will reduce the system's coherence, we still cannot measure the system non-invasively if we want to maintain initial coherence in the process. Yet, since energy is conserved, we can still know the allowed values of stochastic work when $\theta = 0$, $w[\gamma, n, n'] = q[\gamma] + n' - n$ with $q[\gamma] = \mu' - \mu$, where n' is an energy outcome of the system in the end of the heat exchange. The predictor of work can be written through the operators $\mathsf{M}_\gamma = \mathsf{N}_\gamma\mathsf{U}_w$, with $\mathsf{N}_\gamma = \mathsf{N}_{\mu\mu'} = \sqrt{p_\mu}\,\langle\mu'|\,\mathsf{U}_h\,|\mu\rangle$. For $\mathsf{U}_h = \mathsf{U}_{sw}$ we have that

$$\mathsf{N}_{11} = \sqrt{\lambda_E}\,|1\rangle\langle 1|, \qquad \mathsf{N}_{10} = \sqrt{\lambda_E}\,|1\rangle\langle 0|, \tag{9.32}$$

$$\mathsf{N}_{01} = \sqrt{1-\lambda_E}\,|0\rangle\langle 1|, \qquad \mathsf{N}_{00} = \sqrt{1-\lambda_E}\,|0\rangle\langle 0|, \tag{9.33}$$

where $\lambda_E = p_1 = e^{-\beta_E\omega}/Z$. Then, if we diagonalize ρ_S, according to the Eq. 9.24, we have all the necessary elements to construct the predictor of work analytically. The results are compiled in Table 9.1 [45].

$\mu \to \mu'$	$n \to m' \to n'$	$P[\gamma]$	$q[\gamma]$	$\mathcal{W}_{\text{opt}}[\gamma](\theta = 0)$	$\mathcal{W}_{\text{opt}}[\gamma]$	$w[\gamma, n, n']$
$0 \to 0$	$1 \to 0 \to 0$	$(1-\lambda_E)(1-s\cos\theta)/2$	0	$-\omega\left(\frac{1+s}{1-s}\right)$	$-\frac{\omega}{4}\left(\frac{3+4s\cos\theta+\cos(2\theta)}{4(1-s\cos\theta)}\right)$	$-\omega$
$0 \to 1$	$0 \to 1 \to 0$	$(1-\lambda_E)(1+s\cos\theta)/2$	ω	ω	$\omega\left(1-\frac{\sin^2\theta}{2(1+s\cos\theta)}\right)$	ω
$1 \to 0$	$1 \to 0 \to 1$	$\lambda_E(1-s\cos\theta)/2$	$-\omega$	$-\omega$	$-\omega\left(1-\frac{\sin^2\theta}{2(1-s\cos\theta)}\right)$	$-\omega$
$1 \to 1$	$0 \to 1 \to 1$	$\lambda_E(1+s\cos\theta)/2$	0	$\omega\left(\frac{1-s}{1+s}\right)$	$\frac{\omega}{4}\left(\frac{3-4s\cos\theta+\cos(2\theta)}{4(1+s\cos\theta)}\right)$	ω

Table 9.1: Trajectories and predicted work for the minimal qubit model. The second column illustrates the only possible system trajectory in the incoherent case. Since both the work protocol and system-bath interaction involve only complete transitions, there will be only one possible path $n \to m' \to n'$ for each $\mu \to \mu'$. In general, there would be multiple such paths.

Let me start discussing the incoherent case. First, observe that whenever there is a transition in the baths (column 1, lines 2 and 3), the incoherent predictor (column 5) corresponds to the exact work (column 7, lines 2 and 3). The reason is that, since both systems are qubits and we have SEC, the only way in which $q[\gamma] = \pm\omega$ is if the work is $n' - n = \pm\omega$. That is, knowing the energy variation in the baths fully determines work. Now, consider the remaining transitions which take $q[\gamma] = 0$ (column 1, lines 1 and 4); their predicted work disagrees with the stochastic work and they should: knowing that no heat was transferred is insufficient to tell in which state

the system was without measuring it, since it could be in either or even in a mixture. That is precisely the content of the predictor (column 5, lines 1 and 4): the value is weighted by the amount of mixedness of the system's state.

At this point, the analysis of the incoherent case is paramount, because through it we realize that the trade off for not measuring the system is that we end up capturing the statistical structure of the density matrix of S in the predictor. Crucially, this intuition is inherited by the coherent case. As we see in column 6, the predictor captures quantum coherence by depending on the parameter θ. Heuristically, coherence is expected to allow something beyond what is found in column 7, since those integer multiples of ω are raw algebraic combinations of energy eigenvalues, which do not comprehend superpositions of the associated eigenvectors. Had we measured the system we would have spoiled such feature. To quantify this intuition, I plot in Fig. 9.2[45], for each heat trajectory, the mismatch $\mathcal{W}_{\text{opt}}[\gamma] - w[\gamma, n, n']$, in the relevant cross section of the Bloch sphere, *i.e.*, the axes $\left\langle \sigma_S^x \right\rangle = s \sin\theta$, $\left\langle \sigma_S^z \right\rangle = s \cos\theta$.

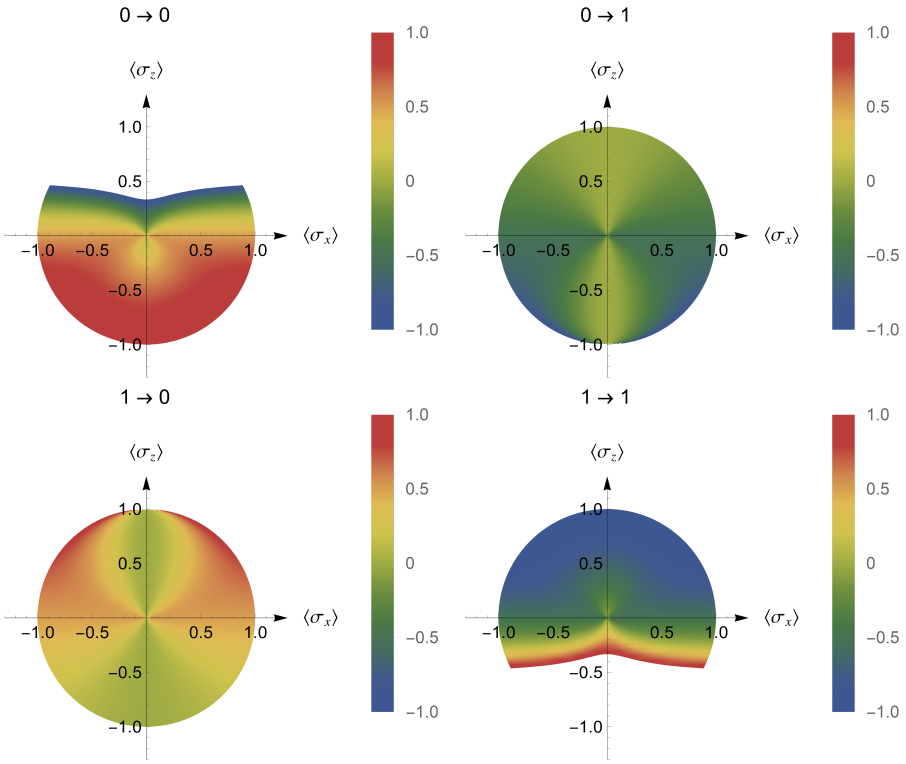

Figure 9.2: The difference $\mathcal{W}_{\text{opt}}[\gamma] - w[\gamma, n, n']$ (in units of ω) between the predicted and the actual work values for each pair $(\mu \to \mu')$, from Table 9.1, as a function of s and θ. In $(0 \to 0)$ and $(1 \to 1)$ the plots were clipped because the difference actually grows unboundedly, which would hamper the visualization.

Figure 9.2 represents the mismatch between predicted stochastic work and the predictor of work. The processes $(0 \to 1)$ and $(1 \to 0)$, at the axis $\left\langle \sigma_S^x \right\rangle = 0$ (incoherent) match the

stochastic work; whenever we deviate from this axis, we see a mismatch emerging, either due to quantum coherence or to the mixedness of the state. For $(0 \to 0)$ and $(1 \to 1)$ we see a stark mismatch in the red and blue regions, respectively. The white regions display divergences in the predictor of work, because these processes have $P[\gamma] = 0$; the predictor is normalized by a factor $(P[\gamma])^{-1}$ and such divergent processes are thus non-physical.

9.4 Application to the SSDB amplifier

Finally, I apply the QMSP predictor to a scenario in which heat and work take place concomitantly (see Chapter 5 for details on the model). At a first moment, I discuss the LME limit of the SSDB model [45], in which the QMSP has fewer non-trivial realizations, and then move to the finite time collision regime. I concentrate in the SSDB amplifier, which is our minimal autonomous engine operating in a coherent steady-state.

9.4.1 Local Master Equation limit

As in the minimal qubit case, the first step is to construct the Kraus components decomposing the evolution map in terms of bath energy outcomes. For this purpose, we begin by recalling the LME description of the model (see Section 5.3)

$$\dot{\rho}_S = -i[\mathsf{H}_S, \rho_S] + \mathcal{D}_A(\rho_S) + \mathcal{D}_B(\rho_S), \tag{9.34}$$

$$\mathsf{H}_S = \omega_3 \mathsf{N}_3 + \omega_2 \mathsf{N}_2 + h\mathsf{C}_x, \tag{9.35}$$

$$\mathcal{D}_A(\rho_S) = g^2 \left[(1-\lambda_A) \left(\mathsf{A}\rho_S \mathsf{A}^\dagger - \frac{1}{2}\left\{ \mathsf{A}^\dagger \mathsf{A}, \rho_S \right\} \right) + \lambda_A \left(\mathsf{A}^\dagger \rho_S \mathsf{A} - \frac{1}{2}\left\{ \mathsf{A}\mathsf{A}^\dagger, \rho_S \right\} \right) \right], \tag{9.36}$$

$$\mathcal{D}_B(\rho_S) = g^2 \left[(1-\lambda_B) \left(\mathsf{B}\rho_S \mathsf{B}^\dagger - \frac{1}{2}\left\{ \mathsf{B}^\dagger \mathsf{B}, \rho_S \right\} \right) + \lambda_B \left(\mathsf{B}^\dagger \rho_S \mathsf{B} - \frac{1}{2}\left\{ \mathsf{B}\mathsf{B}^\dagger, \rho_S \right\} \right) \right], \tag{9.37}$$

where A is the hot bath and B is the cold bath. In Section 4.4, we have discussed how heat and work can be cast solely in terms of system quantities. In the present case, this is possible if we identify $\mathsf{H}_S = \mathsf{H}_S^0 + \mathsf{G}$ with $\mathsf{G} = h\mathsf{C}_x$ and we then have heat rates

$$\dot{\mathcal{Q}}_A = -\operatorname{Tr}\left\{ \mathsf{H}_S^0 \mathcal{D}_A(\rho_S) \right\}, \tag{9.38}$$

$$\dot{\mathcal{Q}}_B = -\operatorname{Tr}\left\{ \mathsf{H}_S^0 \mathcal{D}_B(\rho_S) \right\}. \tag{9.39}$$

Remembering that $\mathsf{A} = |3\rangle\langle 1|\,, \mathsf{B} = |2\rangle\langle 1|$, we end up with

$$\dot{Q}_A = \omega_3 \left[(1-\lambda_A)\langle 3|\rho_S|3\rangle - \lambda_A \langle 3|\rho_S|3\rangle\right] = -\frac{d}{dt}\langle 3|\rho_S|3\rangle\,, \tag{9.40}$$

$$\dot{Q}_B = \omega_2 \left[(1-\lambda_B)\langle 2|\rho_S|2\rangle - \lambda_A \langle 2|\rho_S|2\rangle\right] = -\frac{d}{dt}\langle 2|\rho_S|2\rangle\,. \tag{9.41}$$

In this system, the heat exchanges associated to bath A can attain three different realizations: $\pm\omega_3$ and 0. This can be inferred only by considering that $\mathcal{D}_A$ couples do $3 \leftrightarrow 1$, and a similar reasoning applies to the remaining heat. Based on that, we can prescribe unravelings of the LME labelled according to the heat exchange they encompass. To see this, we go back one step in the CM derivation (see Appendix B.3), and re-introduce the first order dependence in τ

$$\delta\rho_S = \mathcal{E}(\rho_S) - \rho_S = -i\tau[\mathsf{H}_S, \rho_S] + \tau\mathcal{D}_A(\rho_S) + \tau\mathcal{D}_B(\rho_S). \tag{9.42}$$

We note that the operators associated to (non-zero) stochastic energy changes are those of the form $\mathsf{X}\rho_S\mathsf{X}^\dagger$ in Eqs. (9.36),(9.37). The remaining changes in the state ρ_S are associated to zero energy changes. In this manner, I decompose the evolution in the following operators, labeled according to the heat outcomes they provide, $\mathsf{M}(q_A, q_B)$;

$$\mathsf{M}_1 \equiv \mathsf{M}(-\omega_3, 0) = g\sqrt{\lambda_A\tau}\;|3\rangle\langle 1|\,, \qquad \mathsf{M}_2 \equiv \mathsf{M}(\omega_3, 0) = g\sqrt{(1-\lambda_A)\tau}\;|1\rangle\langle 3|\,, \tag{9.43}$$

$$\mathsf{M}_3 \equiv \mathsf{M}(0, -\omega_2) = g\sqrt{\lambda_B\tau}\;|2\rangle\langle 1|\,, \qquad \mathsf{M}_4 \equiv \mathsf{M}(0, +\omega_2) = g\sqrt{(1-\lambda_B)\tau}\;|1\rangle\langle 2|\,, \tag{9.44}$$

$$\mathsf{M}_0 = \mathbb{1}_S - i\tau\mathsf{H}_S - \frac{1}{2}\sum_{j=1}^{4}\mathsf{M}_j^\dagger\mathsf{M}_j. \tag{9.45}$$

That is, a jump from $1 \to 3$, M_1, in the system is associated with a decrease of $-\omega_3$ in the bath A's energy, while a jump $3 \to 1$, M_2, is associated to an increase $+\omega_3$ in the bath A's energy. Similarly changes $\mathsf{M}_3, \mathsf{M}_4$ in the system are associated with $-\omega_2, +\omega_2$ in the bath B, respectively. Further, note that the probability distribution associated to each of these processes writes $P_j = \mathrm{Tr}\big(\mathsf{M}_j\rho_S\mathsf{M}_j^\dagger\big)$, $j = 1,2,3,4$ and $P_0 = 1 - \sum_{j=1}^4 P_j$. Since P_j is of first order in τ, the QMSP (9.2) remains relevant in the limit $\tau \to 0$. Note that, in the TPM-CM perspective, we would have 16 possible trajectories $\gamma = (a, b, a', b')$, since each ancillae energy can assume two values. Yet, here we did not need to make reference to the γ-TPM protocol in the ancillae to establish the heat. We have in general 9 possibilities (q_A, q_B), but due to the fact that we work in infinitesimal τ, two-jump process are forbidden because they appear only as second order terms.

This restriction discards 4 realizations, and we are left precisely with the processes associated to the jump operators in Eqs. (9.43),(9.44) and (9.45). I used CMs here for convenience, but by no means this is necessary to construct the quantum jump unravelings. This highlights that, in spite of the precise way we construct the LME, we do not need to make explicit reference to it in applying the QMSP; it only depends on the channel generated in the system and on the heat outcomes.

With the Kraus components constructed and numerically solving for the steady-states for each choice of h, we can finally construct the QMSP of work for the SSDB amplifier. The results are plotted in Fig. 9.3.

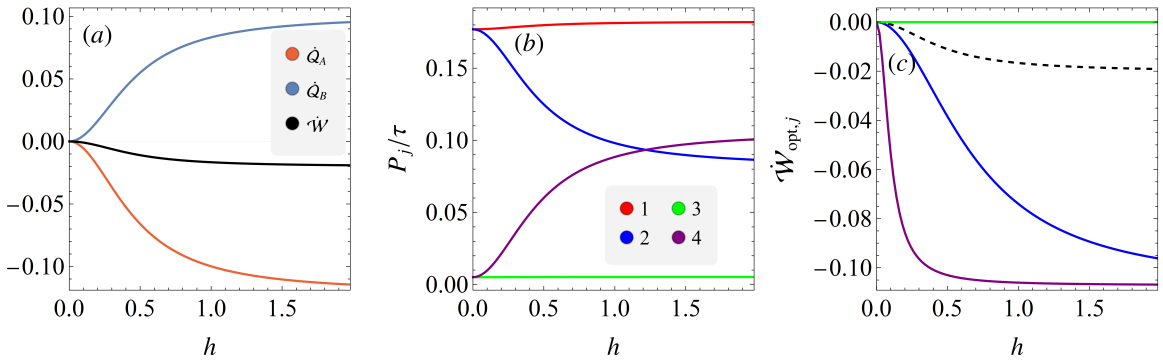

Figure 9.3: In these plots I set $T_A = 1.0, T_B = 0.2, \omega_3 = 1.2, \omega_2 = g = 1.0$. (a) The operation of the SSDB amplifier at the level of averages, the concerned quantities are rates. In (b) and (c) I concentrate in the trajectories with non-zero jumps in the baths ($j = 1, 2, 3, 4$). (b) Probability associated to each j normalized by τ, P_j/τ. (c) Work predictor associated to each trajectory. The predictor associated to 1 and 3 is identically zero for all h. The work-rate average is also reproduced for comparison (black-dashed line).

Figure 9.3 (a) represents the average operation of the engine in terms of heat and work rates. (b) and (c) represent the probabilities P_j and their associated predictors, respectively. We can see at (b) that the trajectories associated to jumps in the hot bath start with equal probabilities ($h = 0$) and as, h is turned on, the trajectory associated to the jump $3 \to 1$ (blue) has a smaller probability while its counterpart $1 \to 3$ (red) remains with the same probability. While the predictor of the red plot remains at zero, overlapping with the green curve, the blue curve starts to decrease. A similar behaviour is associated to the cold bath; while the probability associated to the upward jump $1 \to 2$ (green) is unaltered and its predictor is zero, the downward jump $2 \to 1$ (purple) increases its probability. In the steady-state, coherence emerges between the levels $|2\rangle$ and $|3\rangle$, making them less distinguishable in the *beginning* of the process; for this reason, they do not affect the processes $1 \to 2, 3$, but make the downwards transitions $2, 3 \to$

1 less distinguishable so that their probabilities tend to homogenize while the magnitudes of their associated work grow. Effectively, the uncertainty between $|2\rangle, |3\rangle$ creates a mismatch between the energy change in the system and the heat. Note that, for clarity, the no-transition probability and predictor were omitted, their only role is to drag the average value far below the stochastic realizations of the predictor, since its associated probability is high compared to any other processes.

9.4.2 Finite time SSDB amplifier

Finally, I consider the same parameter region of the LME scenario, but here I work with finite time collisions and set $\tau = 1.0$. Different from the last example, I start by considering the bath energy outcomes $\gamma = (a, b, a', b')$ of the ancillae to construct the QMSP (9.2) as a function of (q_A, q_B). In Fig.9.4 (a) the average behaviour of this engine is represented. In Fig.9.4 (b) we see the probabilities $P(q_A, q_B)$

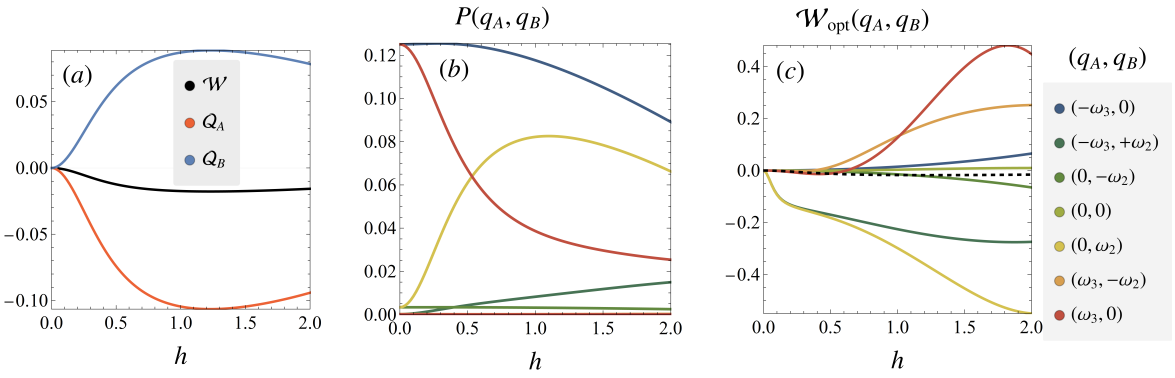

Figure 9.4: In these plots I set $T_A = 1.0, T_B = 0.2, \omega_3 = 1.2, \omega_2 = \tau = g = 1.0$. (a) SSDB amplifier at the level of averages. (b) Probabilities associated to each process, $P(q_A, q_B)$. If we concentrate in the red and yellow curves, these are the process most affected by coherence; their distinguishability varies as we increase h. The yellow curve has zero probability at $h = 0$ and is rendered possibile due to coherence between levels $|2\rangle$ and $|3\rangle$. For visualization purposes, I have removed $P(0, 0)$ which remains approximately between 0.5 and 0.8. (c) The QMSP, $\mathcal{W}_{\rm opt}(q_A, q_B)$. The dashed line represents the average work. If we again concentrate in the yellow curve, it is responsible for stochastic work extraction and supersedes in absolute value the red curve, which amounts to stochastic work consumption.

Figure 9.4 (b)/(c) immediately points out that in finite times have more allowed process than in the LME scenario. Now, although with small probabilities, $(\pm\omega_3, \mp\omega_3)$ may occur. Yet, the processes $(\pm\omega_3, \pm\omega_2)$ remain forbidden and are not represented in the plots. The reason is that they violate global energy conservation. Looking at Fig. 9.4(b)/(c) we note that there are similarities with the LME limit; the processes which are most affected by h are still $(\omega_3, 0)$ and

$(0, \omega_2)$, which are associated to downward jumps in system levels sharing coherence. Yet, at finite times we note that $(\omega_3, 0)$ is now positive and their counterparts, $(-\omega_3, 0)$ and $(0, -\omega_2)$, are now significantly affected in larger h regions too. Qualitatively, this happens because once we consider higher orders in τ the interaction which is initially only between a bath and a gap start to be influenced by other parts of the Hilbert space. Then, information has enough time to back-flow from the upper levels, and even in the processes which initially start from the ground state, coherence between the upper levels comes to be relevant[5].

[5]Roughly, we can see the $O(\tau)$ contributions of $e^{-i\tau \mathsf{H}}$ as linear contributions from sines and cosines, and once we consider $\tau \geq 1$, the oscillating contributions become prominent.

Chapter 10

Conclusion

In this dissertation I have investigated through the collisional model framework the role of fluctuations and coherence in quantum thermodynamics, with particular interest in autonomous heat engines. I have used, in this context, ideas from resource theory of coherence, and classified non-equilibrium steady-states accordingly (Chapters 3). I have then used this framework to revisit the heat engine of Scovil and Schulz-DuBois, a prototypical model to study heat and work in the quantum regime. Through the collisional model I have spotted the role of steady-state coherence and work in producing coherent light (Chapter 5). Subsequently, I have discussed some of the paradigms involving fluctuations of thermodynamic currents in the quantum regime. I have contributed to this topic in extending full counting statistics to collisional models, which generalize local master equation approaches (Chapter 7). Finally, I have discussed the problem of accounting for coherence in work distributions and the technique of quantum Bayesian networks (Chapter 8). Using this formalism, I have provided a technique to predict the unravelings of work in coherent systems based on measurements which do not destroy such quantum feature (Chapter 9).

The findings here presented are relevant in both theoretical and practical applications. In theory, the formalism of collisional models is useful to distinguish heat and work and amenable to computational techniques; thus, the extension of full counting techniques to this context is a desirable convenience to the quantum thermodynamics community. In practical applications, the control of fluctuations, be them quantum or classical, is crucial in engineering technologies. The quantum mean-square predictor of work provides a novel method to access work in the quantum realm. In incoherent scenarios, it can be used to provide minimal measurement protocols, while in the presence of coherence it allows one to include coherence in work statistics.

This result brings new insights to quantum thermodynamics, and provides a model to predict work based only on information which is, in principle, accessible to experiments. It thus also shows good prospects for future experimental investigations and applications in quantum technologies. Notably, this technique is also a modular contribution and is amenable to adaptions to probabilistic models for quantum systems other than the QBN scheme.

There are also directions of investigation which I still look forward, in continuation of the present work. For instance, the QMSP technique could be used at contexts broader than thermodynamics, such as metrology and adjusted to describe particular experiments; the combination of RT characterization of NESS, CMs and FCS formalisms could be used to study new quantum FTs and bounds on measurement precision (such as thermodynamic uncertainty relations [133]); in the direction of the latter, the characterization of the SSDB engine here presented could serve as a prototypical model. Moreover, the QBNs program discussed here is still an ongoing investigation, and also has room for theory and experiments.

All the developments presented in this dissertation were done in conjunction with my supervisor, Prof. Gabriel T. Landi, and supported by the Brazilian funding agency CAPES.

Appendix A

Mathematical identities

Backer-Campbell-Hausdorff formula

$$e^{xA}Be^{-xA} = B + x[A,B] + \frac{x^2}{2}[A,[A,B]] + ... + \frac{x^n}{n!}[A,...[A,B]]... \tag{A.1}$$

Dyson's commutator

Consider the commutator $e^{-tB}[A, e^{tB}]$, which I differentiate w.r.t. t

$$\frac{d}{dt}e^{-tB}[A,e^{tB}] = -e^{-tB}BAe^{tB} + BA + e^{-tB}ABe^{tB} - BA \tag{A.2}$$

$$= e^{-tB}[A,B]e^{tB} \tag{A.3}$$

$$= \frac{d}{dt}\int_0^t ds e^{-sB}[A,B]e^{sB}, \tag{A.4}$$

therefrom, the initial commutator and the integral coincide up to a constant

$$e^{-tB}[A,e^{tB}] = \int_0^t ds e^{-sB}[A,B]e^{sB} + K. \tag{A.5}$$

Setting $t = 0$, I conclude that $K = 0$ and we have the formula

$$[A, e^{tB}] = \int_0^t ds e^{(t-s)B}[A, B]e^{sB}. \tag{A.6}$$

Note that, since I differentiated w.r.t. t, if were $B(t)$ there would be extra terms due to the partial derivative $\partial_t B(t)$. Dyson's commutator follows by setting $t = 1$

$$[A, e^{B}] = \int_0^1 ds e^{(1-s)B}[A, B]e^{sB}. \tag{A.7}$$

Appendix B

Collisional model for the SSDB engine

In this Appendix I present the calculations and the operator algebra discussed in Chapter 4 and also a LME version of the model.

B.1 Operator algebra

Starting by the Hamiltonian

$$\mathsf{H}_S = \omega_3 |3\rangle\langle 3| + \omega_2 |2\rangle\langle 2| + (h |3\rangle\langle 2| + h^* |2\rangle\langle 3|), \tag{B.1}$$

I define $\mathsf{A} \equiv |1\rangle\langle 3|$, $\mathsf{B} \equiv |1\rangle\langle 2|$ and $\mathsf{C} \equiv |2\rangle\langle 3|$. Based on these three operators and their conjugates I introduce nine hermitian operators

$$\mathsf{N}_3 = \mathsf{A}^\dagger \mathsf{A} \tag{B.2}$$

$$\mathsf{A}_x = \mathsf{A}^\dagger + \mathsf{A} \tag{B.3}$$

$$\mathsf{A}_y = -i(\mathsf{A}^\dagger - \mathsf{A}) \tag{B.4}$$

$$\mathsf{N}_2 = \mathsf{B}^\dagger \mathsf{B}, \tag{B.5}$$

$$\mathsf{B}_x = \mathsf{B}^\dagger + \mathsf{B}, \tag{B.6}$$

$$\mathsf{B}_y = -i(\mathsf{B}^\dagger - \mathsf{B}) \tag{B.7}$$

$$\mathsf{C}^\dagger\mathsf{C} = \mathsf{N}_3 = \mathsf{A}^\dagger\mathsf{A}, \tag{B.8}$$

$$\mathsf{C}_x = \mathsf{C}^\dagger + \mathsf{C}, \tag{B.9}$$

$$\mathsf{C}_y = -i(\mathsf{C}^\dagger - \mathsf{C}), \tag{B.10}$$

and

$$\mathsf{N}_1 \equiv |1\rangle\langle 1| = \mathsf{B}\mathsf{B}^\dagger = \mathsf{A}\mathsf{A}^\dagger. \tag{B.11}$$

Moreover, note that

$$\mathsf{N}_2 = |2\rangle\langle 2| = \mathsf{C}\mathsf{C}^\dagger = \mathsf{B}^\dagger\mathsf{B}. \tag{B.12}$$

In this language, I rewrite

$$\mathsf{H}_S = \omega_3\mathsf{N}_3 + \omega_2\mathsf{N}_2 + (h^*\mathsf{C} + h\mathsf{C}^\dagger) \tag{B.13}$$

I can now establish their algebraic properties. First, observe that $\mathsf{A}, \mathsf{C}, \mathsf{B}$ are all nilpotent. Moreover, the following commutators give

$$\begin{aligned}[\mathsf{A}_x, \mathsf{A}_y] &= -i[|1\rangle\langle 3| + |3\rangle\langle 1|, |1\rangle\langle 3| - |3\rangle\langle 1|] = -i(-\mathsf{N}_1 + |3\rangle\langle 3| + |3\rangle\langle 3| - \mathsf{N}_1) \\ &= -2i(\mathsf{N}_3 - \mathsf{N}_1),\end{aligned} \tag{B.14}$$

$$[\mathsf{N}_3, \mathsf{A}_x] = [|3\rangle\langle 3|, |1\rangle\langle 3| + |3\rangle\langle 1|] = -|1\rangle\langle 3| + |3\rangle\langle 1| = i\mathsf{A}_y, \tag{B.15}$$

$$[\mathsf{N}_3, \mathsf{A}_y] = i[|3\rangle\langle 3|, |1\rangle\langle 3| - |3\rangle\langle 1|] = i(-|1\rangle\langle 3| - |3\rangle\langle 1|) = -i\mathsf{A}_x. \tag{B.16}$$

Similarly

$$[\mathsf{B}_x, \mathsf{B}_y] = -2i(\mathsf{N}_2 - \mathsf{N}_1) \tag{B.17}$$

$$[\mathsf{N}_2, \mathsf{B}_x] = i\mathsf{B}_y \tag{B.18}$$

$$[\mathsf{N}_2, \mathsf{B}_y] = -i\mathsf{B}_x \tag{B.19}$$

$$[\mathsf{C}_x, \mathsf{C}_y] = -2i(\mathsf{N}_3 - \mathsf{N}_2) \tag{B.20}$$

$$[\mathsf{N}_3, \mathsf{C}_x] = i\mathsf{C}_y \tag{B.21}$$

$$[\mathsf{N}_3, \mathsf{C}_y] = -i\mathsf{C}_x. \tag{B.22}$$

Note that for each letter these operators do not form Lie algebra. In fact, the letters are not independent and the cross-letter commutators which will be useful are

$$[\mathsf{N}_2, \mathsf{A}_{x/y}] = 0 = [\mathsf{N}_3, \mathsf{B}_{x/y}] \tag{B.23}$$

$$[\mathsf{N}_3, \mathsf{C}_x] = i\mathsf{C}_y \tag{B.24}$$

$$[\mathsf{N}_3, \mathsf{C}_y] = i\mathsf{C}_x \tag{B.25}$$

$$[\mathsf{N}_2, \mathsf{C}_y] = -i\mathsf{C}_x \tag{B.26}$$

$$[\mathsf{N}_2, \mathsf{C}_y] = -i\mathsf{C}_x \tag{B.27}$$

$$[\mathsf{C}_x, \mathsf{A}_x] = -i\mathsf{B}_y \tag{B.28}$$

$$[\mathsf{C}_x, \mathsf{A}_y] = i\mathsf{B}_x \tag{B.29}$$

$$[\mathsf{C}_x, \mathsf{B}_x] = -i\mathsf{A}_y \tag{B.30}$$

$$[\mathsf{C}_x, \mathsf{A}_y] = i\mathsf{A}_x \tag{B.31}$$

Finally, we are in position to introduce an interaction with the environment. We assume that these are qubits, with $\mathsf{H}_X = \omega_X \sigma_X^z/2$, and to achieve a quite general machine we have $X = A, B, C$. That is, three baths. Each one will be connected to a gap, represented by the letter operators within the system. That is

$$\mathsf{V}_A = g_A \left[\frac{1+\eta}{2} \sigma_A^x \mathsf{A}_x + \frac{1-\eta}{2} \sigma_A^y \mathsf{A}_y \right], \tag{B.32}$$

$$\mathsf{V}_B = g_B \left[\frac{1+\eta}{2} \sigma_B^x \mathsf{B}_x + \frac{1-\eta}{2} \sigma_B^y \mathsf{B}_y \right], \tag{B.33}$$

$$\mathsf{V}_C = g_C \left[\sigma_C^+ \mathsf{C} + \sigma_c^- \mathsf{C}^\dagger \right]. \tag{B.34}$$

have the full interaction $\mathsf{V} = \mathsf{V}_A + \mathsf{V}_B + \mathsf{V}_C$. The total Hamiltonian is then $\mathsf{H} = \mathsf{H}_0 + \mathsf{V}$, with $\mathsf{H}_0 = \mathsf{H}_A + \mathsf{H}_B + \mathsf{H}_C + \mathsf{H}_S$ and

$$\mathsf{H}_A = \frac{\omega_A}{2} \sigma_A^z \tag{B.35}$$

$$\mathsf{H}_B = \frac{\omega_B}{2} \sigma_B^z \tag{B.36}$$

$$\mathsf{H}_C = \omega_C a^\dagger a. \tag{B.37}$$

B.2 Conserved quantities

To understand the origins of the breakdown of local energy conservation, we shall compute the commutator $[\mathsf{H}_0, \mathsf{U}] = [\mathsf{H}_0, \mathsf{V}]$. For this sake we have

$$[\mathsf{H}_X, \mathsf{V}] = g_X[\mathsf{H}_X, \mathsf{V}_x] = ig_X\omega_X\left(\frac{1+\eta}{2}\sigma_X^y\mathsf{X}_x - \frac{1-\eta}{2}\sigma_X^x\mathsf{X}_y\right) \quad X = A, B \;\; \mathsf{X} = \mathsf{A}, \mathsf{B}. \tag{B.38}$$

and

$$[\mathsf{H}_C, \mathsf{V}_C] = \omega_C g_C(a^\dagger\mathsf{C} - a\mathsf{C}). \tag{B.39}$$

Now, to the commutators with the system's Hamiltonian

$$\begin{aligned}
[\mathsf{H}_S, \mathsf{V}_A] =& g_A\left[\omega_3\mathsf{N}_3 + h^*\mathsf{C} + h\mathsf{C}^\dagger, \frac{1+\eta}{2}\sigma_A^x\mathsf{A}_x + \frac{1-\eta}{2}\sigma_A^y\mathsf{A}_y\right] && \text{(B.40)}\\
=& ig_A\omega_3\left(\frac{1+\eta}{2}\sigma_A^x\mathsf{A}_y - \frac{1-\eta}{2}\sigma_A^y\mathsf{A}_x\right) \\
&+ g_A\frac{1+\eta}{2}\left(h^*\mathsf{B} - h\mathsf{B}^\dagger\right)\sigma_A^x - ig_A\frac{1-\eta}{2}\left(h^*\mathsf{B} + h\mathsf{B}^\dagger\right)\sigma_A^y, && \text{(B.41)}
\end{aligned}$$

where the latter derived commuation rules were used. Very similarly

$$\begin{aligned}
[\mathsf{H}_S, \mathsf{V}_B] =& \left[\omega_2\mathsf{N}_2 + h^*\mathsf{C} + h\mathsf{C}^\dagger, \frac{1+\eta}{2}\sigma_B^x\mathsf{B}_x + \frac{1-\eta}{2}\sigma_B^y\mathsf{B}_y\right] && \text{(B.42)}\\
=& g_B i\omega_2\left(\frac{1+\eta}{2}\sigma_B^x\mathsf{B}_y - \frac{1-\eta}{2}\sigma_B^y\mathsf{B}_x\right) && \text{(B.43)}\\
&- g_B\frac{1+\eta}{2}\left(h^*\mathsf{A} - h\mathsf{A}^\dagger\right)\sigma_B^x - ig_B\frac{1-\eta}{2}\left(h^*\mathsf{A} + h\mathsf{A}^\dagger\right)\sigma_B^y, && \text{(B.44)}
\end{aligned}$$

and we are left with

$$\begin{aligned}
[\mathsf{H}_S, \mathsf{V}_C] &= g_C\left[\omega_3\mathsf{N}_3 + \omega_2\mathsf{N}_2 + h^*\mathsf{C} + h\mathsf{C}^\dagger, a\mathsf{C}^\dagger + a^\dagger\mathsf{C}\right] && \text{(B.45)}\\
&= ig_C(\omega_3 - \omega_2)\left(a\mathsf{C}^\dagger - a^\dagger\mathsf{C}\right) + g_C(ha - h*a^\dagger)(\mathsf{N}_3 - \mathsf{N}_2)
\end{aligned}$$

We can now join everything to conclude

$$
\begin{aligned}
[\mathsf{H}_0, \mathsf{V}] = {} & ig_A \left[\left(\omega_3 \frac{1+\eta}{2} - \omega_A \frac{1-\eta}{2} \right) \sigma_A^x \mathsf{A}_y - \left(\omega_3 \frac{1-\eta}{2} - \omega_A \frac{1+\eta}{2} \right) \sigma_A^y \mathsf{A}_x \right] \\
& + ig_B \left[\left(\omega_2 \frac{1+\eta}{2} - \omega_B \frac{1-\eta}{2} \right) \sigma_B^x \mathsf{B}_y - \left(\omega_2 \frac{1-\eta}{2} - \omega_B \frac{1+\eta}{2} \right) \sigma_B^y \mathsf{B}_x \right] \\
& + ig_C(\omega_3 - \omega_2 - \omega_C) \left(a\mathsf{C}^\dagger - a^\dagger \mathsf{C} \right) \\
& + g_A \frac{1+\eta}{2} \left(h^* \mathsf{B} - h\mathsf{B}^\dagger \right) \sigma_A^x - ig_A \frac{1-\eta}{2} \left(h^* \mathsf{B} + h\mathsf{B}^\dagger \right) \sigma_A^y \\
& - g_B \frac{1+\eta}{2} \left(h^* \mathsf{A} - h\mathsf{A}^\dagger \right) \sigma_B^x - ig_B \frac{1-\eta}{2} \left(h^* \mathsf{A} + h\mathsf{A}^\dagger \right) \sigma_B^y \\
& + g_C(ha - h^* a^\dagger)(\mathsf{N}_3 - \mathsf{N}_2)
\end{aligned}
\tag{B.46}
$$

We can now analyze some cases of interest. Let $\eta = 0$ and we have the XX analog, that is, a quanta exchange interaction

$$
\begin{aligned}
[\mathsf{H}_0, \mathsf{V}] = {} & \frac{ig}{2} \left[(\omega_3 - \omega_A) \sigma_A^x \mathsf{A}_y - (\omega_3 - \omega_A) \sigma_A^y \mathsf{A}_x \right] \\
& + \frac{ig}{2} \left[(\omega_2 - \omega_B) \sigma_B^x \mathsf{B}_y - (\omega_2 - \omega_B) \sigma_B^y \mathsf{B}_x \right] \\
& + ig_C(\omega_3 - \omega_2 - \omega_C) \left(a\mathsf{C}^\dagger - a^\dagger \mathsf{C} \right) \\
& + g_A \frac{1}{2} \left(h^* \mathsf{B} - h\mathsf{B}^\dagger \right) \sigma_A^x - ig_A \frac{1}{2} \left(h^* \mathsf{B} + h\mathsf{B}^\dagger \right) \sigma_A^y \\
& - g_B \frac{1}{2} \left(h^* \mathsf{A} - h\mathsf{A}^\dagger \right) \sigma_B^x - ig_B \frac{1}{2} \left(h^* \mathsf{A} + h\mathsf{A}^\dagger \right) \sigma_B^y \\
& + g_C(ha - h^* a^\dagger)(\mathsf{N}_3 - \mathsf{N}_2)
\end{aligned}
\tag{B.47}
$$

This is zero only if the environments are resonant with the system's gaps and $h = h^* = 0$. Further, let me consider $\eta = h = h^* = 0$, in which case we can find a conserved quantity regardless of resonance conditions. For this, I consider the commutators:

$$[\mathsf{N}_1, \mathsf{V}_A] = g_A(\sigma_A^- \mathsf{A} - \sigma_A^- \mathsf{A}^\dagger), \tag{B.48}$$

$$[\mathsf{N}_1, \mathsf{V}_B] = g_B(\sigma_B^- \mathsf{B} - \sigma_B^- \mathsf{B}^\dagger), \tag{B.49}$$

$$[\mathsf{N}_1, \mathsf{V}_C] = 0, \tag{B.50}$$

$$[\mathsf{N}_3, \mathsf{V}_A] = -g_A(\sigma_A^- \mathsf{A} - \sigma_A^- \mathsf{A}^\dagger), \tag{B.51}$$

$$[\mathsf{N}_3, \mathsf{V}_C] = -g_C(a^\dagger \mathsf{C} - a\mathsf{C}^\dagger), \tag{B.52}$$

$$[\mathsf{N}_3, \mathsf{V}_B] = 0, \tag{B.53}$$

$$[\mathsf{N}_2, \mathsf{V}_B] = -g_B(\sigma_B^- \mathsf{B} - \sigma_B^- \mathsf{B}^\dagger), \tag{B.54}$$

$$[\mathsf{N}_2, \mathsf{V}_C] = +g_C(a^\dagger \mathsf{C} - a\mathsf{C}^\dagger), \tag{B.55}$$

$$[\mathsf{N}_2, \mathsf{V}_A] = 0, \tag{B.56}$$

$$\tag{B.57}$$

Noting that their sum is zero, we then have a conserved quantity

$$\Omega_S = \mathsf{N}_3 + \mathsf{N}_2 + \mathsf{N}_1 \tag{B.58}$$

which by its turn commutes with H_S. Yet, this quantity is trivial; since each N_i is a projector, it is just $\mathbb{1}_S$. We can yet construct a legit one which will be useful by considering together the commutators

$$[a^\dagger a, \mathsf{V}_C] = g_C(a^\dagger \mathsf{C} - a\mathsf{C}^\dagger), \tag{B.59}$$

$$[a^\dagger a, \mathsf{V}_B] = [a^\dagger a, \mathsf{V}_C] = 0, \tag{B.60}$$

$$[\sigma_X^z, \mathsf{V}_X] = 2g_X(\sigma_X^+ \mathsf{X}^\dagger - \sigma_X^- \mathsf{X}) \quad \mathsf{X} = \mathsf{A}, \mathsf{B} \quad X = A, B), \tag{B.61}$$

$$[\sigma_A^z, \mathsf{V}_B] = [\sigma_B^z, \mathsf{V}_A] = 0, \tag{B.62}$$

by means of which we realize that

$$\Omega_z = a^\dagger a + \sigma_A^z + \frac{\sigma_B^z}{2} + \mathsf{N}_3 - \mathsf{N}_1 \tag{B.63}$$

also satisfies $[\Omega_z, \mathsf{V}] = 0 = [\Omega_z, \mathsf{H}_S] = 0$.

B.3 LME limit for the SSDB amplifier

In this section I establish the LME limit within a a certain parameter region, for simplicity. The one of choice is that with only two baths exchange interactions and the h term (SSDB amplifier), *i.e.*,

$$\mathsf{H}_A = \frac{\omega_A}{2}\sigma_A^z, \tag{B.64}$$

$$\mathsf{H}_B = \frac{\omega_B}{2}\sigma_B^z, \tag{B.65}$$

$$\mathsf{H}_S = \omega_3\mathsf{N}_3 + \omega_2\mathsf{N}_2 + h(\mathsf{C} + \mathsf{C}^\dagger), \tag{B.66}$$

$$\mathcal{V}_A = \frac{g}{\sqrt{\tau}}\mathsf{V}_A = \frac{g}{\sqrt{\tau}}(\sigma_A^-\mathsf{A}^\dagger + \sigma_A^+\mathsf{A}), \tag{B.67}$$

$$\mathcal{V}_B = \frac{g}{\sqrt{\tau}}\mathsf{V}_B = \frac{g}{\sqrt{\tau}}(\sigma_B^-\mathsf{B}^\dagger + \sigma_B^+\mathsf{B}), \tag{B.68}$$

$$\mathsf{H} = \mathsf{H}_0 + \mathcal{V} = \mathsf{H}_0 + \frac{g}{\sqrt{\tau}}\mathsf{V}. \tag{B.69}$$

I now perform the same procedure presented in Section 3.3 of Chapter 3. That is, I compute lower orders of $\tau << 1$ in $\rho_S(\tau) = \mathrm{Tr}_{AB}\{\mathsf{U}_\tau\rho\mathsf{U}_\tau^\dagger\}$.

$$\rho_S(\tau) - \rho_S = -i\tau[\mathsf{H}_S, \rho_S] - \frac{\tau}{2}\,\mathrm{Tr}_{AB}\{[\mathsf{V},[\mathsf{V},\rho]]\} \tag{B.70}$$

Noting that $[\mathsf{V},[\mathsf{V},\rho]] = 2\mathsf{V}\rho\mathsf{V} - \{\mathsf{V}^2,\rho\}$, we now compute V^2

$$\begin{aligned}\mathsf{V}^2 = g^2(&\sigma_A^+\sigma_A^-\mathsf{A}\mathsf{A}^\dagger + \sigma_A^-\sigma_A^+\mathsf{A}^\dagger\mathsf{A} + \sigma_A^+\sigma_B^-\mathsf{A}\mathsf{B}^\dagger + \sigma_A^-\sigma_B^+\mathsf{A}^\dagger\mathsf{B}\\ &+ \sigma_B^+\sigma_A^-\mathsf{B}\mathsf{A}^\dagger + \sigma_B^-\sigma_A^+\mathsf{B}^\dagger\mathsf{A} + \sigma_B^+\sigma_B^-\mathsf{B}\mathsf{B}^\dagger + \sigma_B^-\sigma_B^+\mathsf{B}^\dagger\mathsf{B})\end{aligned} \tag{B.71}$$

We shall now exploit the fact that $\rho = \rho_A^{\mathrm{th}} \otimes \rho_B^{\mathrm{th}} \otimes \rho_S$; whenever we take the trace w.r.t. A or B terms such as $\mathrm{Tr}_{AB}\{\sigma_A^+\sigma_B^-\mathsf{A}\mathsf{B}^\dagger\rho\}$ vanish. Then, only few terms survive the trace and we find

$$\begin{aligned}\mathrm{Tr}_{AB}\{\mathsf{V}^2,\rho\} &= g^2(\mathrm{Tr}\left\{\sigma_A^-\sigma_A^+\rho_A^{\mathrm{th}}\right\}\{\mathsf{A}^\dagger\mathsf{A},\rho_S\} + \mathrm{Tr}\left\{\sigma_B^-\sigma_B^+\rho_B^{\mathrm{th}}\right\}\{\mathsf{B}^\dagger f,\rho_S\}\\ &\quad + \mathrm{Tr}\left\{\sigma_A^+\sigma_A^-\rho_A^{\mathrm{th}}\right\}\{\mathsf{A}\mathsf{A}^\dagger,\rho_S\} + \mathrm{Tr}\left\{\sigma_B^+\sigma_B^-\rho_B^{\mathrm{th}}\right\}\{\mathsf{B}\mathsf{B}^\dagger,\rho_S\})\\ &= g^2\left[(1-\lambda_A)\{\mathsf{A}^\dagger\mathsf{A},\rho_S\} + \lambda_A\{\mathsf{A}\mathsf{A}^\dagger,\rho_S\} + (1-\lambda_B)\{\mathsf{B}^\dagger f,\rho_S\} + \lambda_B\{\mathsf{B}\mathsf{B}^\dagger,\rho_S\}\right]\end{aligned}$$

in a similar fashion, we can compute

$$\mathrm{Tr}_{AB}\{\mathsf{V}\rho\mathsf{V}\} = g^2\left[\lambda_A\mathsf{A}^\dagger\rho_S\mathsf{A} + (1-\lambda_A)\mathsf{A}\rho_S\mathsf{A}^\dagger + (1-\lambda_B)\mathsf{B}\rho_S\mathsf{B}^\dagger + \lambda_B\mathsf{B}^\dagger\rho_S\mathsf{B}\right]. \tag{B.72}$$

Substituting in (B.70) dividing by τ and taking $\tau \to 0$ we establish the master equation in GKSL form

$$\dot{\rho}_S = -i[\mathsf{H}_S, \rho_S] + \mathcal{D}_A(\rho_S) + \mathcal{D}_B(\rho_S), \tag{B.73}$$

$$\mathcal{D}_A(\rho_S) = g^2\left[(1-\lambda_A)\left(\mathsf{A}\rho_S\mathsf{A}^\dagger - \frac{1}{2}\left\{\mathsf{A}^\dagger\mathsf{A}, \rho_S\right\}\right) + \lambda_A\left(\mathsf{A}^\dagger\rho_S\mathsf{A} - \frac{1}{2}\left\{\mathsf{A}\mathsf{A}^\dagger, \rho_S\right\}\right)\right], \tag{B.74}$$

$$\mathcal{D}_B(\rho_S) = g^2\left[(1-\lambda_B)\left(\mathsf{B}\rho_S\mathsf{B}^\dagger - \frac{1}{2}\left\{\mathsf{B}^\dagger\mathsf{B}, \rho_S\right\}\right) + \lambda_B\left(\mathsf{B}^\dagger\rho_S\mathsf{B} - \frac{1}{2}\left\{\mathsf{B}\mathsf{B}^\dagger, \rho_S\right\}\right)\right]. \tag{B.75}$$

Bibliography

[1] H. B. Callen, "Thermodynamics and an Introduction to Thermostatics," *Thermodynamics and and introduction to thermostatistics*, pp. 74–77, 1985.

[2] G. T. Landi and M. Paternostro, "Irreversible entropy production, from quantum to classical," *arXiv*, pp. 1–62, Sep. 2020, ISSN: 23318422. arXiv: 2009.07668.

[3] P. A. M. Dirac, *The Principles of Quantum Mechanics*. Clarendon Press, 1930.

[4] L. D. Landau and E. M. Lifshitz, *Statistical Physics*. Elsevier, 1980, p. 544, ISBN: 9780080570464. DOI: 10.1016/C2009-0-24487-4.

[5] S. Weinberg, *Lectures on Quantum Mechanics*, 2nd ed. Cambridge University Press, 2015. DOI: 10.1017/CBO9781316276105.

[6] J. Von Neumann and N. A. Wheeler, *Mathematical foundations of quantum mechanics; New ed.* Princeton, NJ: Princeton University Press, Mar. 2018. DOI: 0691178577.

[7] E. T. Jaynes, "Information theory and statistical mechanics," *Phys. Rev.*, vol. 106, pp. 620–630, 4 May 1957. DOI: 10.1103/PhysRev.106.620.

[8] ——, "Information theory and statistical mechanics. ii," *Phys. Rev.*, vol. 108, pp. 171–190, 2 Oct. 1957. DOI: 10.1103/PhysRev.108.171.

[9] V. Gorini, A. Kossakowski, and E. C. Sudarshan, "Completely positive dynamical semigroups of N-level systems," *Journal of Mathematical Physics*, vol. 17, no. 5, pp. 821–825, 1975, ISSN: 00222488. DOI: 10.1063/1.522979.

[10] G. Lindblad, "Completely positive maps and entropy inequalities," *Communications in Mathematical Physics*, vol. 40, no. 2, pp. 147–151, 1975, ISSN: 00103616. DOI: 10.1007/BF01609396.

[11] G. Lindblad, "On the generators of quantum dynamical semigroups," *Communications in Mathematical Physics*, vol. 48, no. 2, pp. 119–130, 1976, ISSN: 00103616. DOI: 10.1007/BF01608499.

[12] H. Spohn, "Entropy production for quantum dynamical semigroups," *Journal of Mathematical Physics*, vol. 19, no. 5, pp. 1227–1230, 1977, ISSN: 00222488. DOI: 10.1063/1.523789.

[13] F. Binder and L. A. Correa, *Fundamental Theories of Physics 195 Thermodynamics in the Quantum Regime*, ISBN: 9783319990453.

[14] N. Erez, G. Gordon, M. Nest, and G. Kurizki, "Thermodynamic control by frequent quantum measurements," *Nature*, vol. 452, no. 7188, pp. 724–727, Apr. 2008, ISSN: 0028-0836. DOI: 10.1038/nature06873.

[15] M. A. Ciampini, L. Mancino, A. Orieux, C. Vigliar, P. Mataloni, M. Paternostro, and M. Barbieri, "Experimental extractable work-based multipartite separability criteria," *npj Quantum Information*, vol. 3, no. 1, pp. 1–5, 2017, ISSN: 20566387. DOI: 10.1038/s41534-017-0011-9.

[16] S. An, J. N. Zhang, M. Um, D. Lv, Y. Lu, J. Zhang, Z. Q. Yin, H. T. Quan, and K. Kim, "Experimental test of the quantum Jarzynski equality with a trapped-ion system," *Nature Physics*, vol. 11, no. 2, pp. 193–199, 2015, ISSN: 17452481. DOI: 10.1038/nphys3197. arXiv: 1409.4485.

[17] F. Cerisola, Y. Margalit, S. MacHluf, A. J. Roncaglia, J. P. Paz, and R. Folman, "Using a quantum work meter to test non-equilibrium fluctuation theorems," *Nature Communications*, vol. 8, no. 1, pp. 1–6, 2017, ISSN: 20411723. DOI: 10.1038/s41467-017-01308-7. arXiv: 1706.07866.

[18] K. D. Wu, Z. Hou, G. Y. Xiang, C. F. Li, G. C. Guo, D. Dong, and F. Nori, "Detecting non-Markovianity via quantified coherence: theory and experiments," *npj Quantum Information*, vol. 6, no. 1, 2020, ISSN: 20566387. DOI: 10.1038/s41534-020-0283-3.

[19] A. Ronzani, B. Karimi, J. Senior, Y. C. Chang, J. T. Peltonen, C. D. Chen, and J. P. Pekola, "Tunable photonic heat transport in a quantum heat valve," *Nature Physics*, vol. 14, no. 10, pp. 991–995, 2018, ISSN: 17452481. DOI: 10.1038/s41567-018-0199-4. arXiv: 1801.09312.

[20] J. Kettler, N. Vaish, L. M. de Lépinay, B. Besga, P. L. de Assis, O. Bourgeois, A. Auffèves, M. Richard, J. Claudon, J. M. Gérard, B. Pigeau, O. Arcizet, P. Verlot, and J. P. Poizat, "Inducing micromechanical motion by optical excitation of a single quantum dot," *Nature Nanotechnology*, vol. 16, no. 3, pp. 283–287, 2021, ISSN: 17483395. DOI: 10.1038/s41565-020-00814-y.

[21] A. Bérut, A. Arakelyan, A. Petrosyan, S. Ciliberto, R. Dillenschneider, and E. Lutz, "Experimental verification of Landauer's principle linking information and thermodynamics," *Nature*, vol. 483, no. 7388, pp. 187–189, 2012, ISSN: 00280836. DOI: 10.1038/nature10872.

[22] C. K. Hu, A. C. Santos, J. M. Cui, Y. F. Huang, D. O. Soares-Pinto, M. S. Sarandy, C. F. Li, and G. C. Guo, "Quantum thermodynamics in adiabatic open systems and its trapped-ion experimental realization," *npj Quantum Information*, vol. 6, no. 1, pp. 1–11, 2020, ISSN: 20566387. DOI: 10.1038/s41534-020-00300-2. arXiv: 1902.01145.

[23] V. Cimini, S. Gherardini, M. Barbieri, I. Gianani, M. Sbroscia, L. Buffoni, M. Paternostro, and F. Caruso, "Experimental characterization of the energetics of quantum logic gates," *npj Quantum Information*, vol. 6, no. 1, pp. 1–8, 2020, ISSN: 20566387. DOI: 10.1038/s41534-020-00325-7. arXiv: 2001.11924.

[24] K. Y. Fong, H. K. Li, R. Zhao, S. Yang, Y. Wang, and X. Zhang, "Phonon heat transfer across a vacuum through quantum fluctuations," *Nature*, vol. 576, no. 7786, pp. 243–247, 2019, ISSN: 14764687. DOI: 10.1038/s41586-019-1800-4.

[25] A. Fornieri and F. Giazotto, "Towards phase-coherent caloritronics in superconducting circuits," *Nature Nanotechnology*, vol. 12, no. 10, pp. 944–952, 2017, ISSN: 17483395. DOI: 10.1038/nnano.2017.204. arXiv: 1610.01013.

[26] J. P. Pekola, P. Solinas, A. Shnirman, and D. V. Averin, "Calorimetric measurement of work in a quantum system," *New Journal of Physics*, vol. 15, 2013, ISSN: 13672630. DOI: 10.1088/1367-2630/15/11/115006.

[27] J. P. Pekola, "Towards quantum thermodynamics in electronic circuits," *Nature Physics*, vol. 11, no. 2, pp. 118–123, 2015, ISSN: 17452481. DOI: 10.1038/nphys3169.

[28] K. Micadei, J. P. Peterson, A. M. Souza, R. S. Sarthour, I. S. Oliveira, G. T. Landi, T. B. Batalhão, R. M. Serra, and E. Lutz, "Reversing the direction of heat flow using quantum correlations," *Nature Communications*, vol. 10, no. 1, pp. 3–8, 2019, ISSN: 20411723. DOI: 10.1038/s41467-019-10333-7. arXiv: 1711.03323.

[29] P. Strasberg, G. Schaller, and T. Brandes, "Quantum and information thermodynamics: A unifying framework based on repeated interactions," *Physical Review X*, vol. 7, no. 2, pp. 1–33, 2017, ISSN: 21603308. DOI: 10.1103/PhysRevX.7.021003. arXiv: 1610.01829.

[30] G. De Chiara, G. Landi, A. Hewgill, B. Reid, A. Ferraro, A. J. Roncaglia, and M. Antezza, "Reconciliation of quantum local master equations with thermodynamics," *New Journal of Physics*, vol. 20, no. 11, 2018, ISSN: 13672630. DOI: 10.1088/1367-2630/aaecee. arXiv: 1808.10450.

[31] M. Esposito, U. Harbola, and S. Mukamel, "Nonequilibrium fluctuations, fluctuation theorems, and counting statistics in quantum systems," *Reviews of Modern Physics*, vol. 81, no. 4, pp. 1665–1702, 2009, ISSN: 15390756. DOI: 10.1103/RevModPhys.81.1665. arXiv: 0811.3717.

[32] H. E. Scovil and E. O. Schulz-Dubois, "Three-level masers as heat engines," *Physical Review Letters*, vol. 2, no. 6, pp. 262–263, 1959, ISSN: 00319007. DOI: 10.1103/PhysRevLett.2.262.

[33] F. L. S. Rodrigues, G. De Chiara, M. Paternostro, and G. T. Landi, "Thermodynamics of weakly coherent collisional models," *Physical Review Letters*, vol. 123, no. 14, Jun. 2019, ISSN: 10797114. DOI: 10.1103/PhysRevLett.123.140601. arXiv: 1906.08203.

[34] A. Streltsov, G. Adesso, and M. B. Plenio, "Colloquium: Quantum coherence as a resource," *Reviews of Modern Physics*, vol. 89, no. 4, pp. 1–34, 2017, ISSN: 15390756. DOI: 10.1103/RevModPhys.89.041003. arXiv: arXiv:1609.02439v3.

[35] M. Lostaglio, "An introductory review of the resource theory approach to thermodynamics," *Reports on Progress in Physics*, vol. 82, no. 11, p. 114 001, Nov. 2019, ISSN: 0034-4885. DOI: 10.1088/1361-6633/ab46e5. arXiv: 1808.10450.

[36] T. Baumgratz, M. Cramer, and M. B. Plenio, "Quantifying coherence," *Physical Review Letters*, vol. 113, no. 14, pp. 1–5, 2014, ISSN: 10797114. DOI: 10.1103/PhysRevLett.113.140401. arXiv: 1311.0275.

[37] I. Marvian and R. W. Spekkens, "Modes of asymmetry: The application of harmonic analysis to symmetric quantum dynamics and quantum reference frames," *Physical Review A - Atomic, Molecular, and Optical Physics*, vol. 90, no. 6, pp. 1–23, 2014, ISSN: 10941622. DOI: 10.1103/PhysRevA.90.062110. arXiv: 1312.0680.

[38] D. J. Evans, E. G. D. Cohen, and G. P. Morriss, "Probability of second law violations in shearing steady states," *Physical Review Letters*, vol. 71, no. 15, pp. 2401–2404, Oct. 1993, ISSN: 0031-9007. DOI: 10.1103/PhysRevLett.71.2401.

[39] G. Gallavotti and E. G. Cohen, "Dynamical ensembles in nonequilibrium statistical mechanics," *Physical Review Letters*, vol. 74, no. 14, pp. 2694–2697, 1995, ISSN: 00319007. DOI: 10.1103/PhysRevLett.74.2694. arXiv: 9410007 [chao-dyn].

[40] C. Jarzynski, "C.Jarzynski;Phys.Rev.E 56,5018-5035(1997).pdf," *Pre*, vol. 56, no. 5, pp. 5018–5035, 1997.

[41] G. E. Crooks, "Journal of Statistical Physics, Volume 90, Numbers 5-6 - SpringerLink," *Journal of Statistical Physics*, vol. 90, pp. 1481–1487, 1998.

[42] M. Perarnau-Llobet, E. Bäumer, K. V. Hovhannisyan, M. Huber, and A. Acin, "No-Go Theorem for the Characterization of Work Fluctuations in Coherent Quantum Systems," *Physical Review Letters*, vol. 118, no. 7, pp. 1–6, 2017, ISSN: 10797114. DOI: 10.1103/PhysRevLett.118.070601. arXiv: 1606.08368.

[43] K. Micadei, G. T. Landi, and E. Lutz, "Quantum Fluctuation Theorems beyond Two-Point Measurements," *Physical Review Letters*, vol. 124, no. 9, p. 90 602, 2020, ISSN: 10797114. DOI: 10.1103/PhysRevLett.124.090602. arXiv: 1909.12189.

[44] P. J. Bickel and K. A. Doksum, "Mathematical Statistics: Basic Ideas and Selected Topics," vol. 1, no. 3, pp. 412–413, Aug. 1977, ISSN: 0040-1706.

[45] M. Janovitch and G. T. Landi, "Quantum mean-square predictors of work," Apr. 2021. arXiv: 2104.07132.

[46] I. C. M. Nielsen, *Quantum Computation and Quantum Information*. Cambridge, 2010.

[47] F. P. Heinz-Peter Breuer, *The Theory of Open Quantum Systems*. Oxford University Press, USA, 2002, ISBN: 0198520638,9780198520634.

[48] G. T. Landi, *Quantum Information and Quantum Noise*. 2018.

[49] M. Gross and S. Haroche, "Superradiance: An essay on the theory of collective spontaneous emission," *Physics Reports*, vol. 93, no. 5, pp. 301–396, 1982, ISSN: 03701573. DOI: 10.1016/0370-1573(82)90102-8.

[50] D. J. Wineland, J. J. Bollinger, W. M. Itano, F. L. Moore, and D. J. Heinzen, *Spin squeezing and reduced quantum noise in spectroscopy*, 1992. DOI: 10.1103/PhysRevA.46.R6797.

[51] M. Brune, E. Hagley, J. Dreyer, X. MaÎtre, A. Maali, C. Wunderlich, J. M. Raimond, and S. Haroche, "Observing the progressive decoherence of the "meter" in a quantum measurement," *Physical Review Letters*, vol. 77, no. 24, pp. 4887–4890, 1996, ISSN: 10797114. DOI: 10.1103/PhysRevLett.77.4887.

[52] S. Haroche, "Nobel Lecture: Controlling photons in a box and exploring the quantum to classical boundary," *Reviews of Modern Physics*, vol. 85, no. 3, pp. 1083–1102, 2013, ISSN: 00346861. DOI: 10.1103/RevModPhys.85.1083.

[53] L. Bruneau, A. Joye, and M. Merkli, "Repeated interactions in open quantum systems," *Journal of Mathematical Physics*, vol. 55, no. 7, pp. 1–68, 2014, ISSN: 00222488. DOI: 10.1063/1.4879240. arXiv: 1305.2472.

[54] B. Vacchini, "General structure of quantum collisional models," *International Journal of Quantum Information*, vol. 12, no. 2, 2014, ISSN: 02197499. DOI: 10.1142/S0219749914610115. arXiv: 1404.0635.

[55] N. K. Bernardes, A. R. Carvalho, C. H. Monken, and M. F. Santos, "Coarse graining a non-Markovian collisional model," *Physical Review A*, vol. 95, no. 3, pp. 1–6, 2017, ISSN: 24699934. DOI: 10.1103/PhysRevA.95.032117. arXiv: 1701.06419.

[56] S. Cusumano, V. Cavina, M. Keck, A. De Pasquale, and V. Giovannetti, "Entropy production and asymptotic factorization via thermalization: A collisional model approach," *Physical Review A*, vol. 98, no. 3, pp. 1–9, 2018, ISSN: 24699934. DOI: 10.1103/PhysRevA.98.032119. arXiv: 1807.04500.

[57] E. P. Hanson, A. Joye, Y. Pautrat, and R. Raquépas, *Landauer's Principle for Trajectories of Repeated Interaction Systems*, 7. 2018, vol. 19, pp. 1939–1991, ISBN: 0002301806. DOI: 10.1007/s00023-018-0679-1.

[58] S. Seah, S. Nimmrichter, D. Grimmer, J. P. Santos, V. Scarani, and G. T. Landi, "Collisional Quantum Thermometry," *Physical Review Letters*, vol. 123, no. 18, pp. 4–8, 2019, ISSN: 10797114. DOI: 10.1103/PhysRevLett.123.180602. arXiv: 1904.12551.

[59] S. Seah, S. Nimmrichter, and V. Scarani, "Nonequilibrium dynamics with finite-time repeated interactions," *Physical Review E*, vol. 99, no. 4, pp. 1–13, 2019, ISSN: 24700053. DOI: 10.1103/PhysRevE.99.042103. arXiv: 1809.04781.

[60] P. Strasberg, "Repeated Interactions and Quantum Stochastic Thermodynamics at Strong Coupling," *Physical Review Letters*, vol. 123, no. 18, p. 180 604, 2019, ISSN: 10797114. DOI: 10.1103/PhysRevLett.123.180604. arXiv: 1907.01804.

[61] D. Cilluffo and F. Ciccarello, "Quantum non-markovian collision models from colored-noise baths," *Springer Proceedings in Physics*, vol. 237, pp. 29–40, 2019, ISSN: 18674941. DOI: 10.1007/978-3-030-31146-9_3. arXiv: 1903.08700.

[62] L. H. Reis, S. H. Silva, and E. Pereira, "Beyond the Lindblad master equation: Heat, work, and energy currents in boundary-driven spin chains," *Physical Review E*, vol. 101, no. 6, 2020, ISSN: 24700053. DOI: 10.1103/PhysRevE.101.062107. arXiv: 2005.11755.

[63] J. Ehrich, M. Esposito, F. Barra, and J. M. Parrondo, "Micro-reversibility and thermalization with collisional baths," *Physica A: Statistical Mechanics and its Applications*, vol. 552, 2020, ISSN: 03784371. DOI: 10.1016/j.physa.2019.122108. arXiv: 1904.07931.

[64] G. de Chiara and M. Antezza, "Quantum machines powered by correlated baths," *arXiv*, pp. 1–9, 2020, ISSN: 23318422. DOI: 10.1103/physrevresearch.2.033315. arXiv: 2006.12848.

[65] M. Cattaneo, G. De Chiara, S. Maniscalco, R. Zambrini, and G. L. Giorgi, "Collision models can efficiently simulate any multipartite Markovian quantum dynamics," 2020. arXiv: 2010.13910.

[66] S. L. Jacob, M. Esposito, J. M. Parrondo, and F. Barra, "Thermalization induced by quantum scattering," *arXiv*, pp. 1–17, 2020, ISSN: 23318422. arXiv: 2012.01062.

[67] J. de Ramón and E. Martín-Martínez, "A non-perturbative analysis of spin-boson interactions using the Weyl relations," *arXiv*, pp. 1–20, 2020, ISSN: 23318422. arXiv: 2002.01994.

[68] J. F. Bougron and L. Bruneau, "Linear Response Theory and Entropic Fluctuations in Repeated Interaction Quantum Systems," *Journal of Statistical Physics*, vol. 181, no. 5, pp. 1636–1677, 2020, ISSN: 15729613. DOI: 10.1007/s10955-020-02640-x. arXiv: 2002.10989.

[69] O. A. Molitor and G. T. Landi, "Stroboscopic two-stroke quantum heat engines," *Physical Review A*, vol. 102, no. 4, pp. 1–11, 2020, ISSN: 24699934. DOI: 10.1103/PhysRevA.102.042217. arXiv: 2008.07512.

[70] S. Vriend, D. Grimmer, and E. Martín-Martínez, "The Unruh effect in slow motion," *arXiv*, pp. 1–13, 2020, ISSN: 23318422. arXiv: 2011.08223.

[71] I. Marvian and R. W. Spekkens, "Extending Noether's theorem by quantifying the asymmetry of quantum states," *Nature Communications*, vol. 5, no. 1, p. 3821, May 2014, ISSN: 2041-1723. DOI: 10.1038/ncomms4821.

[72] C. Sparaciari, J. Oppenheim, and T. Fritz, "A Resource Theory for Work and Heat," *Physical Review A*, vol. 96, no. 5, pp. 1–17, Jul. 2016, ISSN: 24699934. DOI: 10.1103/PhysRevA.96.052112. arXiv: 1607.01302.

[73] E. Chitambar and G. Gour, "Are Incoherent Operations Physically Consistent? – A Critical Examination of Incoherent Operations," pp. 1–25, 2016. DOI: 10.1103/PhysRevLett.117.030401;10.1103/PhysRevA.94.052336. arXiv: 1602.06969.

[74] J. Aberg, "Quantifying Superposition," 2006. arXiv: 0612146 [quant-ph].

[75] E. Chitambar and G. Gour, "Critical examination of incoherent operations and a physically consistent resource theory of quantum coherence," *Phys. Rev. Lett.*, vol. 117, p. 030 401, 3 Jul. 2016. DOI: 10.1103/PhysRevLett.117.030401.

[76] J. P. Santos, L. C. Céleri, G. T. Landi, and M. Paternostro, "The role of quantum coherence in non-equilibrium entropy production," *npj Quantum Information*, vol. 5, no. 1, pp. 1–8, 2019, ISSN: 20566387. DOI: 10.1038/s41534-019-0138-y. arXiv: 1707.08946.

[77] L. Boltzmann, "Weitere studien über das wärmegleichgewicht unter gasmolekülen," in *Kinetische Theorie II: Irreversible Prozesse Einführung und Originaltexte*. Wiesbaden: Vieweg+Teubner Verlag, 1970, pp. 115–225, ISBN: 978-3-322-84986-1. DOI: 10.1007/978-3-322-84986-1_3.

[78] P. Ehrenfest and T. Ehrenfest, *The conceptual foundations of the statistical approach in mechanics*. Mineola, NY: Dover, Feb. 2015, This Dover edition, first published by Dover Publications, Inc., in 1990 and brought back into print in 2015, is a reprint of the English translation by Michael J. Moravcsik published by The Cornell University Press, Ithaca, New York, in 1959. DOI: 0486662500.

[79] R. R. Camasca and G. T. Landi, "Memory kernel and divisibility of Gaussian Collisional Models," *arXiv*, pp. 1–18, 2020. arXiv: 2008.00765.

[80] M. Esposito, K. Lindenberg, and C. Van Den Broeck, "Entropy production as correlation between system and reservoir," *New Journal of Physics*, vol. 12, 2010, ISSN: 13672630. DOI: 10.1088/1367-2630/12/1/013013. arXiv: 0908.1125.

[81] G. Manzano, J. M. Horowitz, and J. M. R. Parrondo, "Quantum fluctuation theorems for arbitrary environments: adiabatic and non-adiabatic entropy production," *Physical Review X*, vol. 8, no. 3, pp. 1–25, Sep. 2017, ISSN: 21603308. DOI: 10.1103/PhysRevX.8.031037. arXiv: 1710.00054.

[82] P. Talkner, E. Lutz, and P. Hänggi, "Fluctuation theorems: Work is not an observable," *Physical Review E - Statistical, Nonlinear, and Soft Matter Physics*, vol. 75, no. 5, pp. 7–8, 2007, ISSN: 15502376. DOI: 10.1103/PhysRevE.75.050102. arXiv: 0703189 [cond-mat].

[83] R. P. Feynman, R. B. Leighton, and M. Sands, *The Feynman lectures on physics; New millennium ed.* New York, NY: Basic Books, 2010, Originally published 1963-1965.

[84] E. Geva and R. Kosloff, "The quantum heat engine and heat pump: An irreversible thermodynamic analysis of the three-level amplifier," *Journal of Chemical Physics*, vol. 104, no. 19, pp. 7681–7699, 1996, ISSN: 00219606. DOI: 10.1063/1.471453.

[85] E. Boukobza and D. J. Tannor, "Three-level systems as amplifiers and attenuators: A thermodynamic analysis," *Physical Review Letters*, vol. 98, no. 24, pp. 1–4, 2007, ISSN: 00319007. DOI: 10.1103/PhysRevLett.98.240601.

[86] S. W. Li, M. B. Kim, G. S. Agarwal, and M. O. Scully, "Quantum statistics of a single-atom Scovil-Schulz-DuBois heat engine," *Physical Review A*, vol. 96, no. 6, pp. 1–10, 2017, ISSN: 24699934. DOI: 10.1103/PhysRevA.96.063806. arXiv: 1710.00902.

[87] K. E. Dorfman, D. Xu, and J. Cao, "Efficiency at maximum power of a laser quantum heat engine enhanced by noise-induced coherence," *Physical Review E*, vol. 97, no. 4, 2018, ISSN: 24700053. DOI: 10.1103/PhysRevE.97.042120. arXiv: 1803.11314.

[88] H. M. Friedman, B. K. Agarwalla, and D. Segal, "Quantum energy exchange and refrigeration: A full-counting statistics approach," *New Journal of Physics*, vol. 20, no. 8, 2018, ISSN: 13672630. DOI: 10.1088/1367-2630/aad5fc.

[89] M. T. Mitchison, "Quantum thermal absorption machines: refrigerators, engines and clocks," *Contemporary Physics*, vol. 60, no. 2, pp. 164–187, 2019, ISSN: 13665812. DOI: 10.1080/00107514.2019.1631555. arXiv: 1902.02672.

[90] W. Niedenzu, M. Huber, and E. Boukobza, "Concepts of work in autonomous quantum heat engines," *Quantum*, vol. 3, pp. 1–13, 2019, ISSN: 2521327X. DOI: 10.22331/q-2019-10-14-195. arXiv: 1907.01353.

[91] J. Liu and D. Segal, "Coherences and the thermodynamic uncertainty relation: Insights from quantum absorption refrigerators," *arXiv*, pp. 1–14, 2020, ISSN: 23318422. DOI: 10.1103/physreve.103.032138. arXiv: 2011.14518.

[92] A. A. S. Kalaee and A. Wacker, "Positivity of entropy production for the three-level maser," *Physical Review A*, vol. 103, no. 1, 2021, ISSN: 24699934. DOI: 10.1103/PhysRevA.103.012202. arXiv: 2010.08934.

[93] D. Karevski, "Ising Quantum Chains," Nov. 2006. arXiv: 0611327 [cond-mat].

[94] F. Ciccarello, "Collision models in quantum optics," *arXiv*, 2017, ISSN: 23318422. DOI: 10.1515/qmetro-2017-0007. arXiv: 1712.04994.

[95] L. Levitov and G. Lesovik, *Charge-transport statistics in quantum conductors*, 1992.

[96] ——, "Charge distribution in quantum shot noise," *JETP letters*, vol. 58, no. 3, pp. 230–235, 1993, ISSN: 0021-3640.

[97] L. S. Levitov, H. Lee, and G. B. Lesovik, "Electron counting statistics and coherent states of electric current," *Journal of Mathematical Physics*, vol. 37, no. 10, pp. 4845–4866, Oct. 1996, ISSN: 00222488. DOI: 10.1063/1.531672. arXiv: 9607137 [cond-mat].

[98] Y. V. Nazarov and M. Kindermann, "Full counting statistics of a general quantum mechanical variable," *European Physical Journal B*, vol. 35, no. 3, pp. 413–420, Jul. 2001, ISSN: 14346028. DOI: 10.1140/epjb/e2003-00293-1. arXiv: 0107133 [cond-mat].

[99] Y. V. Nazarov, "Full counting statistics and field theory," *Annalen der Physik (Leipzig)*, vol. 16, no. 10-11, pp. 720–735, 2007, ISSN: 00033804. DOI: 10.1002/andp.200710259. arXiv: 0705.4083.

[100] A. Kamenev, *Field Theory of Non-Equilibrium Systems*. Cambridge University Press, 2011. DOI: 10.1017/CBO9781139003667.

[101] L. M. Sieberer, M. Buchhold, and S. Diehl, "Keldysh field theory for driven open quantum systems," *Reports on Progress in Physics*, vol. 79, no. 9, 2016, ISSN: 00344885. DOI: 10.1088/0034-4885/79/9/096001. arXiv: arXiv:1512.00637v2.

[102] M. F. Maghrebi and A. V. Gorshkov, "Nonequilibrium many-body steady states via Keldysh formalism," *Physical Review B*, vol. 93, no. 1, pp. 1–17, 2016, ISSN: 24699969. DOI: 10.1103/PhysRevB.93.014307. arXiv: 1507.01939.

[103] R. P. Feynman and F. L. Vernon, "The theory of a general quantum system interacting with a linear dissipative system," *Annals of Physics*, vol. 24, no. C, pp. 118–173, 1963, ISSN: 1096035X. DOI: 10.1016/0003-4916(63)90068-X.

[104] A. E. Allahverdyan and T. M. Nieuwenhuizen, "Fluctuations of work from quantum subensembles: The case against quantum work-fluctuation theorems," *Physical Review E - Statistical, Nonlinear, and Soft Matter Physics*, vol. 71, no. 6, pp. 1–30, 2005, ISSN: 15393755. DOI: 10.1103/PhysRevE.71.066102.

[105] P. Solinas and S. Gasparinetti, "Full distribution of work done on a quantum system for arbitrary initial states," *Physical Review E - Statistical, Nonlinear, and Soft Matter Physics*, vol. 92, no. 4, pp. 1–8, Apr. 2015, ISSN: 15502376. DOI: 10.1103/PhysRevE.92.042150. arXiv: 1504.01574.

[106] P. Solinas, H. J. Miller, and J. Anders, "Measurement-dependent corrections to work distributions arising from quantum coherences," *Physical Review A*, vol. 96, no. 5, pp. 1–9, 2017, ISSN: 24699934. DOI: 10.1103/PhysRevA.96.052115. arXiv: 1705.10296.

[107] P. P. Hofer, "Quasi-probability distributions for observables in dynamic systems," *Quantum*, vol. 1, p. 32, 2017, ISSN: 2521327X. DOI: 10.22331/q-2017-10-12-32. arXiv: 1702.00998.

[108] B. M. Xu, J. Zou, L. S. Guo, and X. M. Kong, "Effects of quantum coherence on work statistics," *Physical Review A*, vol. 97, no. 5, pp. 1–12, 2018, ISSN: 24699934. DOI: 10.1103/PhysRevA.97.052122. arXiv: 1707.09591.

[109] K. Funo and H. T. Quan, "Path Integral Approach to Quantum Thermodynamics," *Physical Review Letters*, vol. 121, no. 4, p. 40 602, 2018, ISSN: 10797114. DOI: 10.1103/PhysRevLett.121.040602. arXiv: 1708.05113.

[110] M. Campisi, P. Hänggi, and P. Talkner, "Colloquium : Quantum fluctuation relations: Foundations and applications," *Reviews of Modern Physics*, vol. 83, no. 3, pp. 771–791, Jul. 2011, ISSN: 0034-6861. DOI: 10.1103/RevModPhys.83.771.

[111] W. L. Ribeiro, G. T. Landi, and F. L. Semião, "Quantum thermodynamics and work fluctuations with applications to magnetic resonance," *American Journal of Physics*, vol. 84, no. 12, pp. 948–957, 2016, ISSN: 0002-9505. DOI: 10.1119/1.4964111. arXiv: 1601.01833.

[112] H. Tasaki, "Jarzynski Relations for Quantum Systems and Some Applications," 2000. arXiv: 0009244 [cond-mat].

[113] C. Jarzynski and D. K. Wójcik, "Classical and quantum fluctuation theorems for heat exchange," *Physical Review Letters*, vol. 92, no. 23, p. 230 602, Jun. 2004, ISSN: 00319007. DOI: 10.1103/PhysRevLett.92.230602. arXiv: 0404475 [cond-mat].

[114] U. Seifert, "Entropy Production along a Stochastic Trajectory and an Integral Fluctuation Theorem," *Physical Review Letters*, vol. 95, no. 4, p. 040 602, Jul. 2005, ISSN: 0031-9007. DOI: 10.1103/PhysRevLett.95.040602. arXiv: 0503686 [cond-mat].

[115] K. Saito and Y. Utsumi, "Symmetry in full counting statistics, fluctuation theorem, and relations among nonlinear transport coefficients in the presence of a magnetic field," *Physical Review B - Condensed Matter and Materials Physics*, vol. 78, no. 11, pp. 1–7, 2008, ISSN: 10980121. DOI: 10.1103/PhysRevB.78.115429. arXiv: 0709.4128.

[116] A. E. Rastegin, "Non-equilibrium equalities with unital quantum channels," *Journal of Statistical Mechanics: Theory and Experiment*, vol. 2013, no. 06, P06016, Jun. 2013, ISSN: 1742-5468. DOI: 10.1088/1742-5468/2013/06/P06016.

[117] á. M. Alhambra, L. Masanes, J. Oppenheim, and C. Perry, "Fluctuating Work: From Quantum Thermodynamical Identities to a Second Law Equality," *Physical Review X*, vol. 6, no. 4, p. 041 017, Oct. 2016, ISSN: 2160-3308. DOI: 10.1103/PhysRevX.6.041017.

[118] J. Åberg, "Fully Quantum Fluctuation Theorems," *Physical Review X*, vol. 8, no. 1, p. 11 019, 2018, ISSN: 21603308. DOI: 10.1103/PhysRevX.8.011019. arXiv: 1601.01302.

[119] H. Kwon and M. S. Kim, "Fluctuation Theorems for a Quantum Channel," *Physical Review X*, vol. 9, no. 3, p. 31 029, 2019, ISSN: 21603308. DOI: 10.1103/PhysRevX.9.031029. arXiv: 1810.03150.

[120] J. Santos, A. Timpanaro, and G. Landi, "Joint fluctuation theorems for sequential heat exchange," *Entropy*, vol. 22, no. 7, pp. 1–10, 2020, ISSN: 10994300. DOI: 10.3390/e22070763. arXiv: 2003.02150.

[121] A. Sone, Y.-X. Liu, and P. Cappellaro, "Quantum Jarzynski Equality in Open Quantum Systems from the One-Time Measurement Scheme," *Physical Review Letters*, vol. 125, no. 6, pp. 1–13, Feb. 2020, ISSN: 10797114. DOI: 10.1103/PhysRevLett.125.060602. arXiv: 2002.06332.

[122] A. Levy and M. Lostaglio, "A quasiprobability distribution for heat fluctuations in the quantum regime," *arXiv*, pp. 1–16, Sep. 2019, ISSN: 23318422. DOI: 10.1103/PRXQuantum.1.010309. arXiv: 1909.11116.

[123] D. Andrieux and P. Gaspard, "A fluctuation theorem for currents and non-linear response coefficients," *Journal of Statistical Mechanics: Theory and Experiment*, vol. 02006, no. 2, Apr. 2007, ISSN: 17425468. DOI: 10.1088/1742-5468/2007/02/P02006. arXiv: 0704.3318.

[124] F. Douarche, S. Ciliberto, A. Petrosyan, and I. Rabbiosi, "An experimental test of the jarzynski equality in a mechanical experiment," *Europhysics Letters (EPL)*, vol. 70, no. 5, pp. 593–599, Jun. 2005. DOI: 10.1209/epl/i2005-10024-4.

[125] T. B. Batalhão, A. M. Souza, L. Mazzola, R. Auccaise, R. S. Sarthour, I. S. Oliveira, J. Goold, G. De Chiara, M. Paternostro, and R. M. Serra, "Experimental Reconstruction of Work Distribution and Study of Fluctuation Relations in a Closed Quantum System," *Physical Review Letters*, vol. 113, no. 14, p. 140 601, Oct. 2014, ISSN: 0031-9007. DOI: 10.1103/PhysRevLett.113.140601.

[126] D. Collin, F. Ritort, C. Jarzynski, S. B. Smith, I. Tinoco, and C. Bustamante, "Verification of the Crooks fluctuation theorem and recovery of RNA folding free energies," *Nature*, vol. 437, no. 7056, pp. 231–234, 2005, ISSN: 00280836. DOI: 10.1038/nature04061.

[127] A. E. Allahverdyan, "Nonequilibrium quantum fluctuations of work," *Physical Review E - Statistical, Nonlinear, and Soft Matter Physics*, vol. 90, no. 3, p. 032 137, Sep. 2014, ISSN: 15502376. DOI: 10.1103/PhysRevE.90.032137. arXiv: 1404.4190.

[128] A. Engel and R. Nolte, "Jarzynski equation for a simple quantum system: Comparing two definitions of work," *Epl*, vol. 79, no. 1, 2007, ISSN: 12864854. DOI: 10.1209/0295-5075/79/10003. arXiv: 0612527 [cond-mat].

[129] A. J. Roncaglia, F. Cerisola, and J. P. Paz, "Work measurement as a generalized quantum measurement," *Physical Review Letters*, vol. 113, no. 25, pp. 1–4, 2014, ISSN: 10797114. DOI: 10.1103/PhysRevLett.113.250601. arXiv: 1409.3812.

[130] G. De Chiara, A. J. Roncaglia, and J. P. Paz, "Measuring work and heat in ultracold quantum gases," *New Journal of Physics*, vol. 17, 2015, ISSN: 13672630. DOI: 10.1088/1367-2630/17/3/035004. arXiv: 1412.6116.

[131] P. Talkner and P. Hänggi, "Aspects of quantum work," *Physical Review E*, vol. 93, no. 2, pp. 1–11, 2016, ISSN: 24700053. DOI: 10.1103/PhysRevE.93.022131.

[132] P. P. Hofer, M. Perarnau-Llobet, D. M. Miranda, G. Haack, R. Silva, J. B. Brask, and N. Brunner, "Markovian master equations for quantum thermal machines: local vs global approach," *arXiv*, 2017, ISSN: 23318422.

[133] A. M. Timpanaro, G. Guarnieri, J. Goold, and G. T. Landi, "Thermodynamic uncertainty relations from exchange fluctuation theorems," *Physical Review Letters*, vol. 123, no. 9, pp. 1–6, Apr. 2019, ISSN: 10797114. DOI: 10.1103/PhysRevLett.123.090604. arXiv: 1904.07574.

[134] A. Darwiche, *Modeling and Reasoning with Bayesian Networks*. Cambridge University Press, 2009. DOI: 10.1017/CBO9780511811357.

[135] C. Elouard, D. A. Herrera-Martí, M. Clusel, and A. Auffèves, "The role of quantum measurement in stochastic thermodynamics," *npj Quantum Information*, vol. 3, no. 1, pp. 1–9, 2017, ISSN: 20566387. DOI: 10.1038/s41534-017-0008-4. arXiv: 1607.02404.

[136] M. S. Leifer and R. W. Spekkens, "Towards a Formulation of Quantum Theory as a Causally Neutral Theory of Bayesian Inference," *Physical Review A - Atomic, Molecular, and Optical Physics*, vol. 88, no. 5, pp. 1–44, Jul. 2011, ISSN: 10502947. DOI: 10.1103/PhysRevA.88.052130. arXiv: 1107.5849.

[137] H. Margenau and R. N. Hill, "Correlation between Measurements in Quantum Theory:" *Progress of Theoretical Physics*, vol. 26, no. 5, pp. 722–738, Nov. 1961, ISSN: 0033-068X. DOI: 10.1143/PTP.26.722. eprint: https://academic.oup.com/ptp/article-pdf/26/5/722/5454875/26-5-722.pdf.

[138] B.-m. Xu, J. Zou, L.-s. Guo, and X.-m. Kong, "PHYSICAL REVIEW A 97 , 052122 (2018)," vol. 052122, pp. 1–12, 2018. DOI: 10.1103/PhysRevA.97.052122.

[139] H. J. Miller and J. Anders, "Time-reversal symmetric work distributions for closed quantum dynamics in the histories framework," *New Journal of Physics*, vol. 19, no. 6, 2017, ISSN: 13672630. DOI: 10.1088/1367-2630/aa703f. arXiv: 1610.04285.

[140] M. Lostaglio, "Quantum Fluctuation Theorems, Contextuality, and Work Quasiprobabilities," *Physical Review Letters*, vol. 120, no. 4, p. 40 602, 2018, ISSN: 10797114. DOI: 10.1103/PhysRevLett.120.040602. arXiv: 1705.05397.

[141] Y. Aharonov, D. Z. Albert, and L. Vaidman, "How the result of a measurement of a component of the spin of a spin- 1/2 particle can turn out to be 100," *Physical Review Letters*, vol. 60, no. 14, pp. 1351–1354, Apr. 1988, ISSN: 0031-9007. DOI: 10.1103/PhysRevLett.60.1351.

[142] N. Y. Halpern, B. Swingle, and J. Dressel, "The quasiprobability behind the out-of-time-ordered correlator," *Physical Review A*, vol. 97, no. 4, pp. 1–37, Apr. 2017, ISSN: 24699934. DOI: 10.1103/PhysRevA.97.042105. arXiv: 1704.01971.

[143] N. Yunger Halpern, A. Bartolotta, and J. Pollack, "Entropic uncertainty relations for quantum information scrambling," *Communications Physics*, vol. 2, no. 1, p. 92, Dec. 2019, ISSN: 2399-3650. DOI: 10.1038/s42005-019-0179-8. arXiv: 1806.04147.

[144] J. T. Monroe, N. Y. Halpern, T. Lee, and K. W. Murch, "Weak measurement of superconducting Qubit Reconciles incompatible operators," *arXiv*, pp. 1–12, 2020, ISSN: 23318422. DOI: 10.1103/physrevlett.126.100403. arXiv: 2008.09131.

[145] K. Micadei, J. P. S. Peterson, A. M. Souza, R. S. Sarthour, I. S. Oliveira, G. T. Landi, R. M. Serra, and E. Lutz, "Experimental validation of fully quantum fluctuation theorems," *arXiv*, pp. 1–7, Dec. 2020, ISSN: 23318422. arXiv: 2012.06294.

[146] K. Micadei, G. T. Landi, and E. Lutz, "Extracting Bayesian networks from multiple copies of a quantum system," vol. 2, no. 1, pp. 1–6, arXiv: 2103.14570v2.

[147] B. de Finetti, *Theory of Probability*, A. Machí and A. Smith, Eds., ser. Wiley Series in Probability and Statistics. Chichester, UK: John Wiley & Sons, Ltd, Feb. 2017, ISBN: 9781119286387. DOI: 10.1002/9781119286387.

[148] S. Deffner, J. P. Paz, and W. H. Zurek, "Quantum work and the thermodynamic cost of quantum measurements," *Physical Review E*, vol. 94, no. 1, pp. 1–5, 2016, ISSN: 24700053. DOI: 10.1103/PhysRevE.94.010103. arXiv: 1603.06509.

[149] M. H. Mohammady and A. Romito, "Conditional work statistics of quantum measurements," *Quantum*, vol. 3, p. 175, Sep. 2018, ISSN: 2521327X. DOI: 10.22331/q-2019-08-19-175. arXiv: 1809.09010.